The role of gliotransmitters in astrocyte-driven modulation of synaptic plasticity in the neocortex

by

Seyed Mohammed Ali Rasooli-Nejad

A thesis submitted for the degree of Doctor of Philosophy

University of Warwick, Systems Biology Doctoral Training Centre

July 2014

Contents

Tables

Figures

Boxes

Abbreviations

Δ^9-THC	Δ^9-Tetrahydrocannabinol
2-AG	2-arachidonoylglycerol
5'-AMP	5'-Adenosine Monophosphate
ABD	Agonist Binding Domain
ABS	Artola, Brocher and Singer
AEA	anandamide
AMPA	α-amino-3-hydroxy-5-methyl-4-isoxazole propionic acid receptors
AMPAR	AMPA receptors
Asc-1	Alanine-serine-cysteine transporter-1
ATP	Adenosine Triphosphate
BCM	Bienenstock, Cooper and Munro
CA	Cornu Ammonis
CaM	Calcium Calmodulin
CaMK-II	Calcium Kinase II
CNO	Clozapine-N-Oxide
CNS	Central Nervous System
CV	Coefficient of Variation
DAG	Diacylglycerol
DAAO	D-amino acid oxidase
DGL	Diacylglycerol Lipase
DHPG	3,5-dihydroxyphenylglycine

dnSNARE	Double Negative Soluble N-ethylmaleimide-sensitive factor attachment protein receptors
Dox	Doxycycline
DREADD	Designer Receptors Exclusively Activated by Designer Drugs
DSE	Depolarisation-induced suppression of excitation
DSI	Depolarisation-induced suppression of inhibition
EAAT	Excitatory Amino Acid Transporter
eCB	endocannabinoids
eCB-LTD	eCB mediated long-term depression
eCB-Rs	endocannabinoid receptors
eCB-STD	eCB-mediated short-term depression
EGFP	Enhanced Green Fluorescent Protein
EM	Expectation Maximisation
ER	Endoplasmic Reticulum
eEPSCs	evoked Excitatory Post-Synaptic Currents
fEPSPs	field Excitatory Post-Synaptic Potentials
GABA	γ-aminobutyric acid
$GABA_AR$	$GABA_A$ receptors
GATs	GABA Transporters
GFAP	Glial Fibrillary Acidic Protein
GFEC	GFAP-EGFP
GLAST	Glutamate/Aspartate Transporter
GLT	Glutamate Transporter-1
GluA	AMPAR subunit
GluN	NMDAR subunit

GlyT-1	Glycine Transporters
GPCRs	G-Protein Coupled Receptors
H_0	Null Hypothesis
H_1	Alternate Hypothesis
HFS	High Frequency Stimulation
hM3Dq	human M3 Muscuranic receptor
IP_3	Inositol 1,4,5-triphosphate
IP_3R2	IP_3 receptor type 2
IPSCs	Inhibitory Post-Synaptic Currents
IPSPs	Inhibitory Post-Synaptic Potentials
L	Log-likelihood
LTD	Long-Term Depression
LTP	Long-Term Potentiation
m	quantal content
mEPSCs	miniature Excitatory Post-Synaptic Currents
mGluR	metabotropic Glutamate Receptors
MRGA1	MAS-related G protein-coupled receptor member A1
n	number of release sites
NMDA	N-methyl-D-aspartate receptors
NMDAR	NMDAR receptors
NTD	N-terminal domain
p	probability of release
P2XRs	Ionotropic ATP Receptors
PAR	Protease Activated Receptors
PDF	Probability Density Function

PIP_2	Phosphatidylinositol 4,5-bisphosphate
PLC-β	Phospholipase C-β
q	quantal amplitude
ROI	Region of Interest
SD_{EPSC}	Standard Deviation of the EPSC amplitude Distribution
SD_{noise}	Standard Deviation of Baseline Noise Amplitude
SD_q^2	Quantal Variance
sEPSCs	Spontaneous Excitatory Post-Synaptic Currents
SICs	Slow Inward Currents
SNAP25	Synaptosomoal-Associated Protein 25 kDa
SON	Supra-Optic Nucleus
SR	Serine Racemase
STDP	Spike-Timing Dependent Protocol
SLMVs	Synaptic-like micro-vesicles
TBS	Theta Burst Stimulation
tetO	tet-operator
TM	Transmembrane Domain
tTA	tetracycline Transactivator
VAMPs	Vesicle Associated Membrane Protein 2
VGLUTs	Vesicular Glutamate Transporters
VNUT	Vesicular ATP transporter
VRACs	Volume Regulated Anion Channels
W	Wilks statistics
WT	Wild-Type

Acknowledgements

First and foremost I would like to thank my supervisor Dr Yuriy Pankratov for his continual support and guidance throughout my PhD. I would like to thank my PhD advisory committee members Dr Mark Wall, Professor Bruno Frenguelli and Dr Magnus Richardson. I would like to thank Dr Oleg Palygin for teaching me some of the scientific techniques and for helping me in the laboratory. I would also like to thank the Warwick Systems Biology DTC for giving me the opportunity to carry out this project. Finally, I would like to thank my parents for their support during my PhD.

Declaration

I, Seyed Mohammed Ali Rasooli-Nejad, hereby declare that all of the work in this thesis is my own unless otherwise stated. None of this work has been previously submitted for any degree at this or any other institution. All sources of information used in the preparation of this thesis are indicated by references.

The work presented (including data generated and data analysis) was carried out by me with the exception for data on Figures 3.1, 3.2 amd 5.1. I have included these figures in the introduction section of the results chapter and not in the results sections. For some of the Figures presented in the result sections, I collaborated with other colleagues for the generation of the data. These collaborative work have been clearly stated in the body of the text.

Abstract

Communication between neuronal and glial cells is important for many brain functions. Astrocytes can modulate synaptic strength by releasing gliotransmitters. The mechanisms underlying release of gliotransmitters remain uncertain with exocytosis being the most intriguing and debated pathway. Furthermore, the contribution of gliotransmitter release to synaptic transmission and plasticity is also debated. Therefore, the purpose of this project was to investigate whether astrocytes can release gliotransmitters via vesicular exocytosis and to investigate the role of this release in synaptic transmission and plasticity in the somatosensory cortex. To investigate this, the transgenic mice line called dnSNARE, where vesicular exocytosis of gliotransmitters is impaired specifically in astrocytes, were used in combination with electrophysiological and pharmacological approaches.

It was shown that cortical astrocytes can release ATP via calcium-dependent vesicular exocytosis. The released astrocytic ATP can bind to neuronal P2X receptors. This results in inhibition of GABAergic transmission. This in turn leads to increase in NMDAR activity during synaptic transmission and plasticity. It was shown that NMDAR-dependent LTP is modulated via vesicular exocytosis of ATP from astrocytes.

It was also shown that astrocytes can release glutamate and D-serine via vesicular exocytosis. However, release of D-serine was not required for LTP induction in the somatosensory cortex. Release of glutamate from astrocytes activated GluN2B-containing NMDARs on cortical neurones. These GluN2B-containing NMDARs contributed to LTP induction in the cortex.

The role of endocannabinoid signalling in synaptic transmission and plasticity was also investigated. It was shown that application of anandamide could result in calcium elevation in astrocytes by acting on CB1 receptors on these cells. This lead to vesicular exocytosis of ATP from astrocytes onto P2X receptors on neurones. This vesicular release of ATP from astrocytes contributed to LTP induction in the somatosensory cortex.

Chapter 1: Introduction: First part

Role of Astrocytes in Synaptic Transmission and Plasticity

1.1 An Introduction to astrocytes and tripartite synapse

The Central Nervous System (CNS) consists of two types of nerve cells: Neurones and Glial cells. Astrocytes are the main type of glial cells in CNS grey matter. In the grey matter, stellate protoplasmic astrocytes are characterised by irregular cell bodies, branched processes that are up to 50 μm long and very negative membrane potentials (Volterra and Meldolesi, 2005). They also have specific proteins for example Glial fibrillary acidic proteins (GFAP), which are intermediate filaments not present in neurones. Gap junctions couples neighbouring astrocytes to one another (Wallraff *et al.*, 2004). Astrocyte functions include role in neurogenesis (Seri *et al.*, 2001), providing a link between neurones and blood (Golgi, 1885, Andrienzen, 1893) and clearing the extracellular space of neuronal activity driven accumulation of K^+ (Walz, 2000) and glutamate (Bergles and Jahr, 1998, Hertz and Zielke, 2004); but because, unlike neurones, astrocytes do not generate action potentials it was previously thought that they do not actively contribute to synaptic transmission.

In 1990, it was shown that glutamate application resulted in oscillatory and propagating calcium waves in cultured astrocytes (Cornell-Bell *et al.*, 1990). This report suggested that astrocytes are not passive bystanders during synaptic transmission but are instead capable of sensing synaptic transmission. Furthermore, observation of intercellular calcium waves suggested that astrocytes are functionally interconnected. A few years later it was shown that astrocytes not only receive information from synaptic transmission but also contribute to neuronal synaptic transmission by releasing transmitters (Parpura *et*

al., 1994, Araque *et al.*, 1998, Araque *et al.*, 1999). Owing to these discoveries, astrocytes were considered active participants in information processing in the brain and for this reason the term "tripartite synapse" was coined in 1999 (Araque *et al.*, 1999). The idea behind the concept of tripartite synapse is the bidirectional communication between astrocytes and neurones involving pre-synaptic terminals, post-synaptic spines and astrocyte processes enwrapping these terminals and spines. The theory behind this concept is that neurotransmitters released from pre-synaptic neurones can activate receptors on astrocytes, thereby leading to release of more transmitters from astrocytes. These additional transmitters can then effect synaptic transmission by acting upon pre- and post-synaptic neurones. The transmitters released by astrocyte were termed gliotransmitters. The three major gliotransmitters are glutamate, Adenosine triphosphate (ATP) and D-serine. A single hippocampal astrocyte is in close proximity of approximately 100 neurones (Agulhon *et al.*, 2008) and can make contact with over 100,000 synapses (Bushong *et al.*, 2002). It has been shown that in the cortex, a single astrocyte can enwrap 4-8 neuronal somata and make contact with an estimated 300-600 neuronal dendrites (Halassa *et al.*, 2007). These reports suggest that gliotransmission from a single astrocyte can modulate the activity of groups of synapses confined within the boundaries of the astrocyte. The extent to which astrocytes contribute to synaptic transmission and their functional significance are still unknown despite the considerable progress in gliotransmission research over the last 10-15 years.

Disorders of the nervous system rise due to changes in synaptic transmission. Therefore, gliotransmission contribution to synaptic transmission implicates

astrocytes as a cause or mediatory factor in neurological disorders. In contrast to this, astrocytes could also be envisaged to have a protective role in disorders, preventing further damage rather than amplifying deleterious effects. Astrocytes have been implicated in Alzheimer's disease (Hartlage-Rubsamen *et al.*, 2003), Parkinson disease (Tsai and Coyle, 2002, Tuominen *et al.*, 2005) and epilepsy (Tian *et al.*, 2005), hence the reason for study of astrocytes.

1.2 Synaptic Plasticity

Acquiring and retrieving memory is part of the cognitive process of brain. Memory involves alterations in inhibitory and excitatory connections between neurones of brain structures such as cortex and hippocampus. It is believed that synaptic plasticity underlies memory formation (Martin *et al.*, 2000). Synaptic plasticity allows neurones to store information in response to experience. The term "Synaptic plasticity" refers to short and long term activity dependent changes in the strength of synaptic transmission. These changes in synaptic strength could be either structural changes or changes involving molecular mechanisms. The latter involves changes in neurotransmitter release and/or changes involving receptors that bind these transmitters. These changes can occur at pre-synaptic and post-synaptic levels. Long-term potentiation (LTP) refers to lasting changes that result in strengthening of synaptic transmission whilst Long term depression (LTD) refers to lasting changes that lead to weakening of synaptic transmission. There are different forms of experimentally induced LTP and LTD, depending on brain region and transmitter receptors involved.

Both hippocampus and cortex are involved in memory formation (Eichenbaum, 2000). Hippocampus is involved in formation of new memories, whilst the neocortex is involved in consolidation and long-term storage of memories. LTP and LTD have been induced in different regions of the hippocampus and cortex, including dentate gyrus (Bliss and Lomo, 1973), CA1 region (Dudek and Bear, 1992), visual cortex (Kirkwood and Bear, 1994) and somatosensory cortex (Castro-Alamancos *et al.*, 1995). However, most studies of gliotransmitter role in synaptic plasticity have concentrated on hippocampus with few studies in the cortex. For this reason, in my project, I investigated synaptic plasticity in the somatosensory cortex.

1.3 Ionotropic receptors in Long Term Potentiation

AMPAR Structure and Function: Two types of Ionotropic glutamate receptors are N-methyl-D-aspartate receptors (NMDARs) and α-amino-3-hydroxy-5-methyl-4-isoxazole propionic acid receptors (AMPARs). AMPARs are tetramers, which means that they are composed from four possible subunits (GluA1-4). Each subunit of AMPAR consists of four membrane domains (M1-4), an extracellular domain and a C-terminal intracellular domain (Mayer and Armstrong, 2004). The extracellular domain consists of an N-terminal domain (NTD) and an Agonist binding domain (ABD) (Stern-Bach *et al.*, 1994, Ayalon and Stern-Bach, 2001). As its name suggests, ABD is the site for glutamate binding. They are permeable to monovalent cations such as Na^+ and K^+ but are

not permeable to Ca^{2+} as the GluA2 subunit prevents calcium permeability (Hollmann and Heinemann, 1994) .

NMDAR Structure and Function: NMDARs are also tetrameric. They have three classes of subunit types: GluN1-3. There are eight different subunits for GluN1, four subunits for GluN2 (GluN2A-D) and two subunits for GluN3 (GluN3A-B) (Dingledine *et al.*, 1999). Co-expression of at least one GluN1 and one GluN2 are required for the channel to be functional (Dingledine *et al.*, 1999). Similar to AMPARs, each subunit consists of four membrane domains (M1-4), an extracellular domain and a C-terminal intracellular domain. Three of the membrane domains are transmembrane domains (TM1, 3 and 4), whilst M2 is a re-entrant pore loop (Mayer, 2006). The extracellular domain consists of an NTD and an ABD. Glycine and D-serine bind to the ABD of GluN1 and GluN3 (Yao and Mayer, 2006), whilst glutamate binds to ABD of GluN2 (Furukawa *et al.*, 2005).

NMDA receptors have slower kinetics than AMPA receptors. AMPARs have a rise time of 100-600 μs and a decay time of 2-3 ms (Colquhoun *et al.*, 1992), whilst NMDARs have a rise time of about 7ms and a decay time of 200 ms (Lester *et al.*, 1990). Unlike AMPARs, Mg^{2+} blocks current through NMDARs at resting membrane potentials (Mayer *et al.*, 1984). Furthermore, unlike majority of AMPARs, most NMDARs have high permeability to Ca^{2+} (Burnashev, 1996, Watanabe *et al.*, 2002). The high Ca^{2+} permeability, the blockage by Mg^{2+} at resting membrane potentials, and the slower kinetics of NMDA receptors are the

main properties of NMDARs that form the basis of the role in inducing a form of LTP that is called NMDAR-dependent LTP.

NMDAR-dependent LTP: Experimental stimulation of pre-synaptic neurones results in a transmembrane voltage response in the post-synaptic spine. This post-synaptic response is as a result of Na^+ influx through AMPARs (Figure 1.1: steps1-4). This leads to a small depolarisation of the post-synaptic spine. There is no ion flux through NMDARs because they are blocked by Mg^{2+} ion (Figure 1.1A). If the amplitude and frequency of pre-synaptic stimulation is constant (**baseline** stimulation), then the synaptic efficacy remains the same i.e. with each pre-synaptic stimulation, same size of AMPAR-mediated post-synaptic response is observed. However, there are experimental protocols that can have long-lasting changes on synaptic efficacy. These protocols involve activation of presynaptic neurones at a high frequency and include i) 100 Hz High frequency stimulation (HFS) (Bliss and Lomo, 1973) and Theta burst stimulation (TBS; see section 1.4 for details on this protocol). The high frequency of pre-synaptic neurone stimulation during these protocols leads to increase in Na^+ flux in post-synaptic neurone, hence leading to further depolarisation of the post-synaptic spine (Figure 1.1: step5). With more depolarisation, Mg^{2+} blockage of NMDARs is lowered (Mayer *et al.*, 1984). As NMDARs are permeable to divalent cations in addition to Na^+, their opening leads to Ca^{2+} entry and accumulation in the post-synaptic spine (Figure 1.1: step 6) (Burnashev, 1996, Watanabe *et al.*, 2002). Calcium can act as a second messenger to activate specific intracellular mechanisms. This involves activation of Calcium Calmodulin (CaM), which in turn activates α-calcium-Calmodulin-dependent protein kinase II (CaMK-II)

(Figure 1.1: step7) resulting in CaMK-II auto-phosphorylation on residue Thr^{286} (Malenka *et al.*, 1989, Silva *et al.*, 1992, Lisman *et al.*, 1997). This kinase phosphorylates post-synaptic AMPA receptors at the GluA1 subunit (Roche *et al.*, 1996, Barria *et al.*, 1997) and GluA2 subunit (Oh and Derkach, 2005) thus increasing AMPAR conductance (Figure 1.1: step8). It has also been shown that CaMKII could also be involved in trafficking of more AMPA receptors to the synaptic spine (Figure 1.1: step9) (Hayashi *et al.*, 2000). Thus, subsequent to delivery of HFS or TBS, when the frequency of presynaptic stimulation is returned to pre-induction frequency (baseline stimulation), the AMPAR conductance is larger in comparison to prior to TBS/HFS delivery (see Figure 1.1C). This means that after TBS/HFS delivery, synaptic efficacy increases. As this increase in synaptic efficacy is long-lasting, it is called **Long** term potentiation. Larger synaptic efficacy means that there is a higher probability of action potential generation in the post-synaptic neurone as a result of synaptic transmission. The **induction** of LTP occurs during the short period of HFS/TBS delivery, where NMDARs are open. As LTP induction requires activity of NMDARs, this LTP is called NMDAR-dependent LTP. During LTP induction, NMDARs act as coincident detectors, meaning that they are activated only when the pre-synaptic release of glutamate is coincident with post-synaptic depolarisation. It is their blockage by Mg^{2+} at resting potentials that allows them to be coincident detectors. Their other unique property, which is calcium permeability, results in LTP induction. The induction of NMDAR-dependent LTP during TBS/HFS leads to increase in AMPAR component on post-synaptic neurone, which is called the **expression** of NMDAR-dependent LTP.

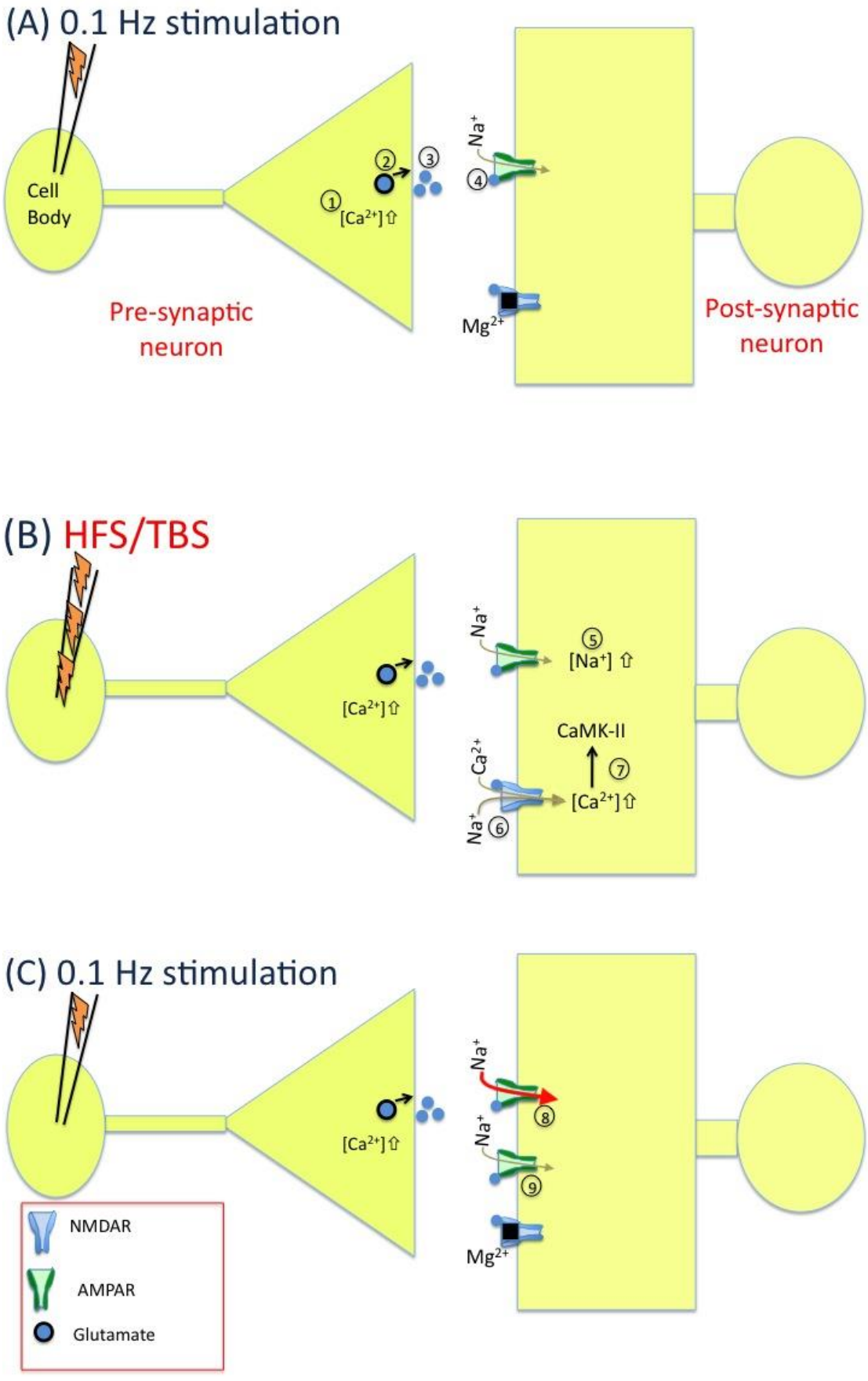

Figure 1.1. See next page for Figure legend.

Figure 1.1. Induction of NMDAR-dependent LTP. Stimulation of pre-synaptic neurone results in calcium entry into pre-synaptic terminals (1) through voltage-gated calcium channels. This triggers the fusion of vesicles to the membrane (2) and the subsequent release of neurotransmitters like glutamate from the terminal (3). Glutamate binding to AMPARs on the post-synaptic spine leads to the influx of sodium through these channels (4), hence causing depolarisation. Activation of pre-synaptic neurone at a higher frequency (B), leads to increase in sodium flux into post-synaptic spine (5). This leads to further depolarisation of the post-synaptic spine, which relieves the magnesium blockage of NMDARs, therefore allowing calcium entry through these receptors (6). Calcium elevation activates intracellular signalling involving CaMK-II (7). Activated CaMK-II then phosphorylates AMPARs. This means that following return of pre-synaptic stimulation to baseline (0.1 Hz) frequency (C), there is an increase in conductance of AMPARs (8) and/or increase in number of AMPARs present at posy-synaptic density (9). This results in a higher synaptic efficacy.

Induction thresholds for NMDAR-dependent LTD and LTP: LTD can be induced in the same hippocampal and cortical synapses where NMDAR-dependent LTP can be induced (Dudek and Bear, 1992, Kirkwood and Bear, 1994). Interestingly, this depression is also NMDAR dependent. Both NMDAR-dependent LTP and NMDAR-dependent LTD are as a result of Ca^{2+} entry through NMDA receptors. In both cases NMDAR opening leads to intracellular signalling. The difference between LTP and LTD induction lies in the magnitude and duration of Ca^{2+} entry, which in turn depends on the frequency of the stimulation protocol (Malenka and Bear, 2004). The magnitude of calcium entry determines the direction of plasticity. This means that there are thresholds for both LTP and LTD induction. These thresholds are dependent on calcium levels. However, calcium entry depends on opening of NMDARs. This means that these thresholds are also dependent on the degree of depolarisation. The thresholds for LTP and LTD can be represented by the Artola, Brocher and Singer (ABS) rule (Figure 1.2) (Artola and Singer, 1993), which is derived from the Bienenstock, Cooper and Munro (BCM) model (Bienenstock *et al.*, 1982). LTP is induced by high frequency stimulation, whilst LTD is induced by "low" frequency stimulation (LFS). This "low" frequency refers to the much lower frequency in comparison to HFS or TBS protocol, but the frequency of LFS is still higher than the frequency of baseline stimulation. With low frequency stimulation a moderate level of post-synaptic depolarisation is reached. This in turn leads to a moderate level of calcium elevation. If this calcium elevation reaches the first threshold (θ_D in Figure 1.2) then LTD is induced. During higher frequency of pre-synaptic stimulation, the magnitude of calcium elevation in post-synaptic neurone is higher in comparison to LTD induction. If this higher calcium

elevation crosses the second threshold (θ_P in Figure 1.2), then LTP is induced. LTP involves phosphorylation by kinases such as CaMK-II, which leads to increase in post-synaptic AMPAR component. In contrast, LTD involves AMPAR dephosphorylation by phosphotases such as calcineurin (Lee *et al.*, 1998) and endocytosis of AMPARs from the spine (Lu *et al.*, 2007).

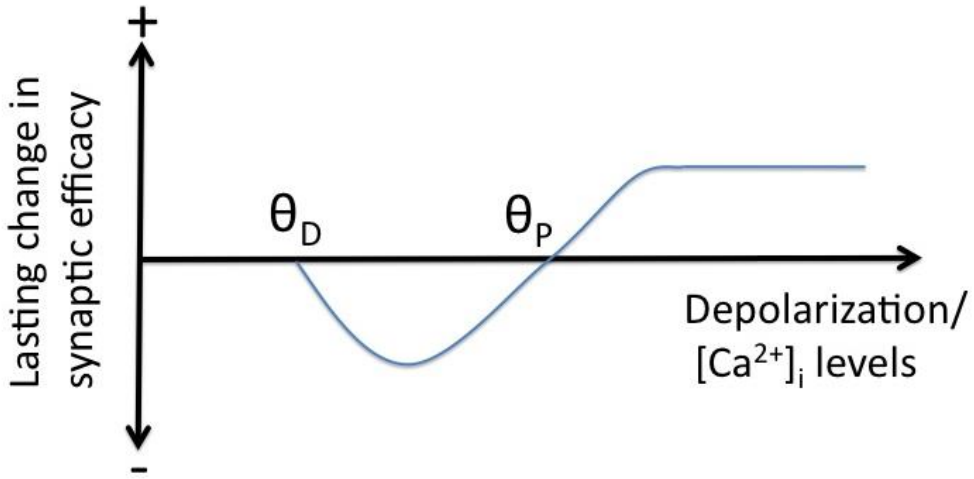

Figure 1.2. **Artola, Brocher and Singer (ABS) rule.** Θ_D is the LTD threshold and θ_P is the LTP threshold.

NMDA-dependent LTP and other forms of plasticity are phenomenon that are induced experimentally but the mechanism of their induction and expression are believed to have physiological basis and functional relevance (Martin *et al.*, 2000). In the next section I will give a brief history on experimental protocols used to successfully induce LTP in the cortex.

1.4 History of LTP protocol in the hippocampus and cortex

Theta rhythm is characterized by the approximately sinusoidal extracellular waves of 3-12Hz recorded from various brain regions using electroencephalography. Theta waves can be recorded during learning-related behaviours in animals such as when a rat is walking, running, exploring or sniffing (Macrides *et al.*, 1982). Classically, waves recorded from the brain with frequency in the 4-7 Hz range were categorised as theta waves but extracellular waves recorded from rat Hippocampus that are 3-12 Hz are also referred to as theta waves. It is believed that theta waves are due to synchronous oscillations of post-synaptic membrane potentials (Andersen, 1980, Buzsaki, 1986) but the neurones involved in the generation of these almost sinusoidal variations are not known. It is known that the Medial septum has a role in the mechanism of theta generation in the hippocampus (Green and Arduini, 1954). However, hippocampus preparation *in vitro* has also been shown to generate spontaneous theta rhythms independent of Medial septum and entorhinal cortex (Goutagny *et al.*, 2009).

Many researchers have tried to induce LTP in various brain regions including hippocampus by using different protocols for stimulation of afferent pathways, which may or may not mimic the natural bursting activity of neurones in physiological conditions. Tetanus stimulation (HFS) is the most popular protocol for LTP induction in the hippocampus. However, some researchers attempted to induce LTP using the theta wave frequency range (Theta burst stimulation), which they believed to be a more physiological LTP induction protocol. Work by Larson and co-workers (Larson *et al.*, 1986) was one of the studies that showed that burst stimulation with inter-burst frequency of 5 Hz (within theta frequency range) resulted in higher chance of LTP induction in the CA1 region of hippocampus compared to inter-burst frequencies that were out of the theta range. Two years later, another group (Pavlides *et al.*, 1988) showed that in Dentate Gyrus, tetanic burst stimulation applied coincidently at the peak of theta waves also induced LTP whilst stimulation at the trough or other phases of theta waves did not. All this indicated a link between theta wave and LTP. Stimulation at theta wave frequency was considered the optimal frequency for LTP induction in the hippocampus.

The reason that 5 Hz is the optimal frequency is due to the role played by γ-aminobutyric acid (GABA) receptors. As mentioned above, glutamate released from excitatory pre-synaptic terminals can depolarise post-synaptic pyramidal neurones. However, in addition to this effect, pre-synaptic glutamate release can also activate inhibitory interneurones. These neurones can in turn release GABA, which can bind to and activate post-synaptic $GABA_A$ receptors of pyramidal neurones. The influx of Cl^- ions through these receptors leads to generation of

inhibitory post-synaptic potentials (IPSPs) in the post-synaptic neurone. This decreases the degree of depolarisation in these cells, thus Mg^{2+} blockage of NMDARs is not relieved. However, interneurones contain $GABA_B$ autoreceptors, which means that they are receptors that can be activated by GABA released from their own cell. The activation of these $GABA_B$ receptors leads to the reduction of GABA released from interneurones (Davies *et al.*, 1990), hence decreasing inhibition of pyramidal cells. This effect was found to have a peak at 200 ms (Davies *et al.*, 1991). This means that during LTP experiments, burst delivery 200 ms after the previous burst leads to generation of smaller IPSPs in the pyramidal cell. This would lead to a larger depolarisation of these cells. Therefore, there is a higher probability that during stimulation, Mg^{2+} blockage of NMDARs is relieved, which would increase the chance of LTP induction.

LTP protocols have also been conducted in the neocortex. Studies from the late 80s and early 90s attempted to find the optimal protocol for LTP induction in the neocortex but the results where not successful. For example, one of the first attempts involved delivery of TBS to layer 6 of cortex whilst recording from layer 3. However, unlike in hippocampus, TBS did not induce LTP in the cortex (Komatsu *et al.*, 1988). The problem of LTP induction in the cortex was solved in 1993 by a group of researchers (Kirkwood *et al.*, 1993). These researchers stimulated layer 4 of neocortex rather than layer 6. They suggested that when recording from layer 2/3 in the cortex, stimulation of layer 6 leads to polysynaptic transmission whilst layer 4 stimulation involves monosynaptic transmission. During LTP induction in the CA1 region of hippocampus,

stimulation of Schaffer collaterals involves monosynaptic transmission; therefore stimulation of layer 4 of cortex should result in a higher chance of LTP induction in this brain region. Indeed, with layer 4 stimulation they found that TBS protocol could induce LTP in the visual cortex just as it did in the hippocampus. Two years later, when a different group applied the same protocol to a different region of the cortex, the somatosensory cortex, they also successfully induced LTP (Castro-Alamancos *et al.*, 1995).

1.5 Metabotropic glutamate receptors

In addition to ionotropic NMDARs and AMPARs, glutamate can also bind to metabotropic glutamate receptors (mGluRs). These receptors are of the C family of G-protein coupled receptors (GPCRs). Each mGluR is a dimmer with each subunit consisting of an extracellular glutamate-binding domain, a heptahelical transmembrane domain and an intracellular C-terminal domain, which couples with the heterotrimeric G-proteins (Pin *et al.*, 2003).

There are eight mGluR genes (mGluR1-8). These are grouped in three classes: I-III. Class I mGluRs (mGluR1 and mGluR5) are involved in increasing intracellular calcium concentration (Frenguelli *et al.*, 1993). After activation by glutamate, these receptors exert their effect via their coupling to G_q/G_{11}. This leads to Phospholipase Cβ activation, which in turn results into inositol 1,4,5-triphosphate (IP_3) generation, leading to Ca^{2+} release from endoplasmic reticulum (ER) (Yuzaki and Mikoshiba, 1992).

High expression of class I mGluRs has been detected in various brain regions including hippocampus and cortex (Baude *et al.*, 1993, Romano *et al.*, 1995). These receptors are mainly localised to peri-synaptic regions of post-synaptic neurones. They are also present on astrocytes.

1.6 Astrocyte activity during Glutamatergic Transmission

Calcium elevation in astrocytes: In order for astrocytes to contribute to synaptic transmission by gliotransmitter release they first need to "sense" synaptic transmission. They can sense synaptic transmission through intracellular calcium elevation as a result of activation of their receptors. It has been shown that metabotropic glutamate receptors are one type of receptors that result in calcium elevation in astrocytes. The presence of mGluR5 has been shown in acutely isolated astrocytes from rat hippocampus (Cai *et al.*, 2000). Furthermore, in brain slices from 2-3 weeks old rats, it has been shown that electrical stimulation of Schaffer collaterals fibres leads to Ca^{2+} elevation in microdomains of hippocampal astrocytes (Panatier *et al.*, 2011). This increase in astrocytic calcium levels was blocked by mGluR5 antagonists. This result suggested that glutamate release from pre-synaptic neurones as a result of electrical stimulation can spillover from synaptic cleft into extracellular space, where astrocyte microdomains are situated (Figure 1.3: steps 1-3). Glutamate in extracellular space can then bind to mGluRs present on astrocyte microdomains (Figure 1.3: step 5). This in turn leads to calcium elevations in these microdomains (Figure 1.3: step 7).

It has been shown that mGluR-dependent Ca^{2+} elevations in astrocytes can lead to the release of glutamate from these cells (Fellin *et al.*, 2004). This released glutamate activated NMDARs on neurones and resulted in appearance of atypically large NMDAR-mediated currents called Slow Inward Currents (SICs). It was shown that these SICs were due to activity of GluN2B-containing NMDARs. As GluN2B NMDARs are thought to be extra-synaptic (see a section below entitled "Role for Synaptic and extra-synaptic NMDAR receptors" for more detail on GluN2B NMDARs) it was postulated that glutamate from astrocytes can activate extra-synaptic NMDARs on post-synaptic pyramidal neurones (Figure 1.3: steps 8-10).

Taken together, the above studies suggested that astrocytic mGluR5 receptors are the main way for astrocytes to "sense" synaptic transmission. Following their activation as a result of calcium elevation, astrocytes contribute to synaptic transmission by releasing gliotransmitters such as glutamate.

The above reports support the general consensus that calcium elevation in astrocytes is as a result of activation of mGluR5 on these cells. However, a recent study in hippocampus and cortex showed that astrocytic mGluR5 is significantly expressed only in mice that are less than two weeks of age. Mice older than 2-weeks showed little mGluR5 expression in astrocytes (Sun *et al.*, 2013). Immunolabelling in adult mice showed that 70-80% immunoreactivity for mGluR5 was associated with neuronal post-synaptic spines and dendritic shafts, whilst only 5% immunoreactivity was associated with astrocytes. *In vitro* and *in vivo* application of mGluR5 agonists such as 3,5-dihydroxyphenylglycine

(DHPG), increased astrocytic calcium elevation in young (P12-P15) mice but failed to increase calcium elevation in adult mice. Interestingly, application of exogenous ATP in adult mice resulted in calcium elevation in astrocytes. Taken together, the authors suggested that mGluR-dependent calcium signalling in astrocytes is restricted to young mice. In adult mice, calcium signalling in astrocytes does not depend on mGluR5 and probably depends on other receptors such as ATP ionotropic and metabotropic receptors.

The above-mentioned study excludes the possibility of mGluR5-dependent activation of astrocytes in adult mice but it does not necessarily exclude the activation of astrocytic calcium signalling via glutamate. Ionotropic glutamate receptors on astrocytes can lead to calcium signalling in these cells. Electrophysiological recordings from acutely isolated cortical astrocytes and astrocytes in cortical slice preparations revealed differences in properties of NMDARs on astrocytes in comparison to their counterparts in neurones (Lalo *et al.*, 2006). Unlike neuronal NMDARs, Mg^{2+} does not block astrocytic NMDARs at resting membrane potentials (Figure 1.3: steps 2 and 6). It was suggested that as astrocytes are not as excitable as neurones (they depolarise only slightly) the Mg^{2+}/voltage-independence property of astrocytic NMDARs allows these receptors to be activated at resting membrane potentials. Subsequent research in cortical slices of adult (three months old) mice showed that activation of these astrocytic NMDARs via pharmacological agonists lead to calcium elevations in these cells (Palygin *et al.*, 2010). Furthermore, astrocytic calcium elevations as a result of electrical stimulation of neuronal afferents were also shown to be NMDAR-mediated. Taken together, these results suggested that NMDA

receptors provide another route for calcium entry into astrocytes (Figure 1.3: steps 6-7).

Pharmacological activation of calcium elevations in astrocytes: As mentioned above, calcium elevation in astrocytes leads to glutamate release from these cells. Therefore, in order to investigate the role of astrocytic glutamate release in synaptic transmission, researchers need to experimentally induce calcium elevations specifically in astrocytes. Researchers utilise different experimental methods to induce calcium elevations specifically in astrocytes. These methods include: uncaging of caged Ca^{2+} or IP_3 by photolysis (Araque *et al.*, 1998), mechanical or electrical stimulation of astrocytes (Jourdain *et al.*, 2007) and activation of metabotropic receptors on astrocytes. The latter method usually involves using DHPG to specifically activate class I metabotropic glutamate receptors (Fellin *et al.*, 2004). However, as mentioned above, these receptors are also present on neurones, hence DHPG application might not specifically activate astrocytes over neurones. Furthermore, as also mentioned above, expression of mGluR5 in astrocytes declines in rodents of above 2 weeks of age. Therefore, agonists of metabotropic glutamate receptors cannot be used to activate astrocytes in older animals. However, there exists another type of metabotropic receptors that show higher expression in astrocytes than in neurones and therefore can be used for calcium elevation specifically in astrocytes. These receptors will be introduced in the following section.

Protease Activated Receptor-1 mediated calcium elevations in astrocytes: Thrombin is a serine protease involved in blood coagulation and tissue repair.

Thrombin can also induce numerous cellular responses by acting as a signalling molecule (Wang and Reiser, 2003). It does this via proteolytic activation of certain G protein-coupled receptors called protease activated receptors (PARs) (Coughlin, 1994). These receptors have an extracellular N-terminal domain. Cleavage of this domain by serine proteases such as thrombin reveals a tethered ligand with a peptide sequence of SFLLRN. This ligand can then activate the receptor by binding to the second transmembrane loop of the receptor (Lerner *et al.*, 1996). This in turn leads to intracellular signal transduction. Synthetic peptides that mimic the action of the tethered ligand can directly activate PARs in the absence of proteolytic cleavage (Hollenberg *et al.*, 1997).

Protease-activated receptors have four members: PAR1-PAR4. These receptors are expressed in many different brain regions including hippocampus and cortex (Striggow *et al.*, 2001). It has been shown that in the human hippocampus and cortex, PAR1 localisation is predominant in astrocytes over neurones (Junge *et al.*, 2004). Like some other GPCRs such as mGluRs, PAR1 receptors are also coupled to G_q/G_{11} and PLC, meaning that their activation can lead to calcium elevation (Wang and Reiser, 2003). A study in CA1 region of hippocampus of brain slices from 2-3 weeks old mice has shown that application of exogenous synthetic PAR1 agonist (TFLLR) activates calcium elevations in astrocytes but not neurones (Lee *et al.*, 2007). This shows that TFLLR can be used to selectively activate astrocytes over neurones. Furthermore, the same study showed that PAR1 activation of cultured astrocytes resulted in a calcium dependent glutamate release from these cells. In contrast, TFLLR application to cultured neurones neither resulted in calcium elevations nor in glutamate release,

again suggesting the specificity of TFLLR/PAR1 for astrocytes. It was also shown that in hippocampal slices, application of PAR1 agonist could increase evoked NMDAR EPSCs but failed to increase the frequency and amplitude of miniature AMPAR EPSCs.

Another report provided further support to the above findings by showing that PAR1 agonist application to the CA1 region of hippocampus of 2-3 weeks old mice leads to calcium elevations specifically in astrocytes (Shigetomi *et al.*, 2008). This in turn lead to glutamate release from these cells, which lead to the appearance of NMDAR-mediated SICs in pyramidal neurons.

Taken together, these findings suggest that PAR-1 application can increase calcium elevations specifically in astrocytes, which in turn leads to glutamate from these cells. The released glutamate can enhance neuronal NMDARs but has no significant effect on neuronal AMPARs.

The above-mentioned studies investigated specific PAR1 activation of astrocytes only in young animals. However, a recent study of the CA3 region of hippocampus from 2 month old rats showed the localisation of PAR1 specifically on astrocytes (Shavit *et al.*, 2011). Interestingly, by using electron microscopy, it was also shown that the localisation of PAR1 receptors was mainly at astrocytic processes surrounding the synapse (Figure 1.3: step 11). This suggested that release of endogenous proteases during synaptic transmission could potentially activate PAR1 receptors on astrocytes. Even though proteases such as thrombin are, under physiological conditions, excluded from the brain by the blood brain

barrier, their expression has been shown in neurones and glial cells (Arai *et al.*, 2006) suggesting endogenous release of proteases in the brain. Taken together, the above results show that PAR1 agonists such as TFLLR can be used as a pharmacological tool to activate calcium elevations specifically in astrocytes and not neurones. This allows researchers to investigate the role of calcium mediated gliotransmitter release from astrocytes.

Effect of activation of astrocytic PAR1 on LTP: Glutamate released as a result of PAR1 activation of astrocytes can increase neuronal NMDAR activity. As NMDARs are involved in LTP induction, this suggests that PAR1 activation of astrocytes could have a potential role in synaptic plasticity. A group of researchers have attempted to investigate the role of PAR agonists on synaptic plasticity (Maggio *et al.*, 2008). They recorded fEPSPs from hippocampal slices (CA1 region) from 2 months old rats. They showed that in the absence of HFS delivery, 10 minutes application of thrombin, which is an agonist for PAR1, PAR3 and PAR4 receptors, resulted in an NMDAR dependent LTP. This thrombin induced LTP was blocked by specific PAR1 antagonist, suggesting that only PAR1 receptors (and not PAR3 or PAR4) are involved in LTP induction. As PAR1 are mainly localised on astrocytes, these results suggest that thrombin-induced LTP is as a result of PAR1 activation of calcium-dependent gliotransmitter release from astrocytes.

It was further shown that LTP could not be induced if only a small concentration of a specific PAR1 agonist (SFLLRN) was applied. HFS protocol can induce LTP because during the delivery of this protocol depolarisation of post-synaptic

neurone crosses the LTP threshold (Figure 1.2). An experimental protocol that fails to depolarise the post-synaptic neurone above the LTP threshold is referred to as the sub-threshold protocol. The sub-threshold cannot induce LTP. However, when small concentration of SFLLRN was applied before delivery of a sub-threshold stimulation protocol, LTP was induced. The size of this LTP was similar to LTP induced by threshold HFS protocol. This result suggested that application of PAR1 agonist could enhance the sub-threshold LTP protocol to the threshold level for LTP induction. As PAR1 are mainly localised on astrocytes, this enhancement of sub-threshold to threshold level can be attributed to PAR1 activation of gliotransmitter release from astrocytes.

Glutamate uptake by astrocytes: As mentioned above, calcium elevation in astrocytes can lead to glutamate release form these cells. However, one of the main functions of astrocytes is the clearance of glutamate spillover. Excitatory Amino Acid Transporters (EAATs) remove glutamate from the extracellular space and into the neurones or astrocytes preventing excitotoxicity (Verkhratsky and Kirchhoff, 2007). Two types of EAATs, Glutamate/Aspartate transporter (GLAST/EAAT1) and Glutamate transporter-1 (GLT1, EAAT2), are almost exclusively expressed in astrocytes (Figure 1.3: step 4) (Verkhratsky and Kirchhoff, 2007), with GLT1 accounting for 80% of glutamate uptake in the brain (D'Antoni *et al.*, 2008). Glutamate uptake by astrocytes prevents the spillover of this transmitter unto other synapses, thereby allowing for a spatially precise synaptic transmission. An interesting question that arises here is that if astrocytes are involved in clearance of glutamate from extracellular space, then what could be the function of glutamate released from these cells? Antibody

labelling has shown approximately six fold lower glutamate concentration in astrocytes than in neurones (Bramham *et al.*, 1990), suggesting that perhaps astrocytes do not contribute to glutamate release. For these reasons, contribution to synaptic transmission by glutamate released from astrocytes has been questioned (Nedergaard and Verkhratsky, 2012).

In summary, most glutamate that spills over into extra-synaptic space is removed by astrocytic EAATs (Figure 1.3: steps 1-4). Some of the extra-synaptic glutamate can activate ionotropic and metabotropic receptors on astrocytes, leading to calcium elevation in these cells (Figure 1.3: steps 5-7). Calcium elevation in astrocytes can result into gliotransmitter release. Experimental activation of calcium elevation in astrocytes shows glutamate release from these cells (Figure 1.3: steps 7-11). Glutamate release by astrocytes has been shown to enhance NMDAR activity of hippocampal neurones. The functional significance of this NMDAR enhancement is yet to be determined.

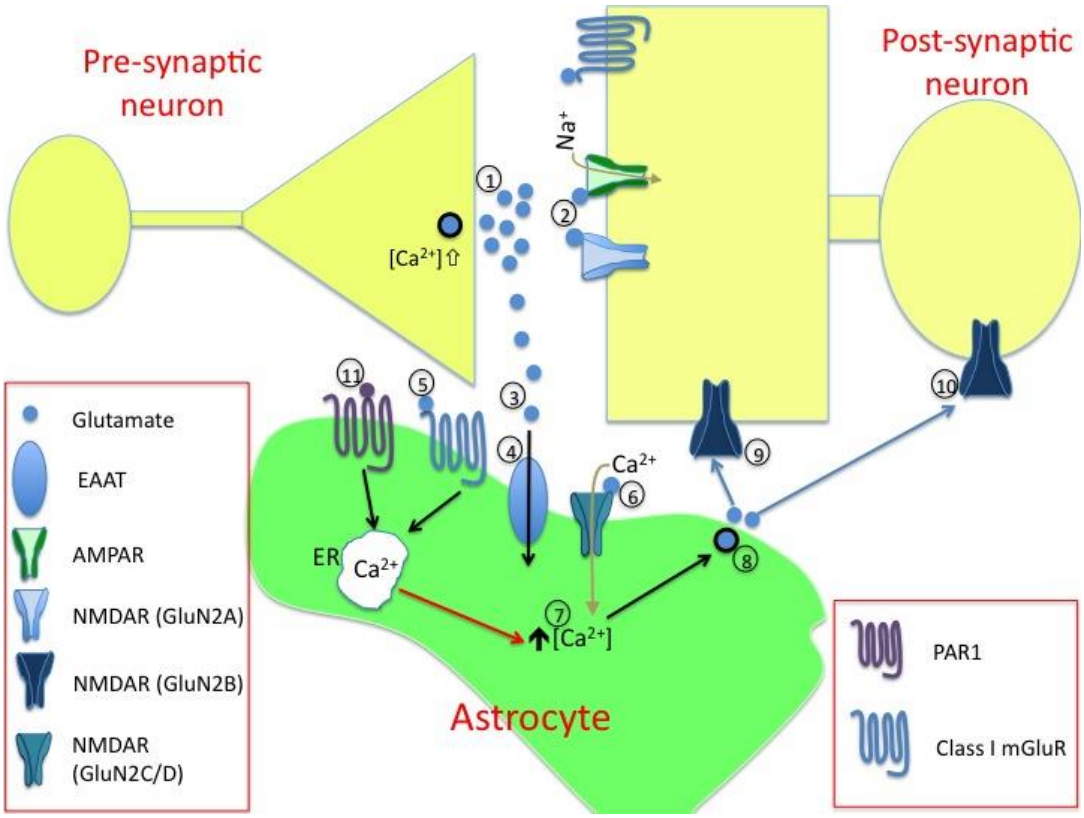

Figure 1.3. Astrocyte activity during glutamatergic transmission. Glutamate released from neuronal terminals (1) result in synaptic transmission by binding to post-synaptic receptors (2). Glutamate released during synaptic transmission spills over into extra-synaptic space (3). Most of the glutamate in the extra-synaptic space is removed by EAATs on astrocytes (4). Some of the spilled over glutamate activates metabotropic receptors (5) and ionotropic receptors (6) on astrocyte microdomains. Activation of these receptors is a means by which astrocytes "sense" synaptic transmission. This leads to elevation of astrocytic intracellular calcium concentration (7). Calcium elevation can result in release of glutamate from astrocytes (8). Astrocytic glutamate can enhance neuronal NMDAR activity by binding to extra-synaptic neuronal NMDARs. These extra-synaptic NMDARs are localised just outside the active zones (9) and at more distal regions such as dendritic shafts and soma (10). Extra-synaptic NMDARs are usually GluN2B containing receptors. Calcium elevation in astrocytes can be induced pharmacologically. PAR1 are localised mainly on astrocytes and not neurones (11). PAR1 activation with synthetic PAR1 agonists can lead to calcium elevations specifically in astrocyte. Note that astrocytic calcium elevation as a result of activation of metabotropic glutamate receptors only occurs in young animals that are less than three weeks old.

Glutamatergic transmission involves the binding of glutamate to AMPARs, NMDARs and mGluRs. However, NMDAR activity also requires the binding of co-agonists in addition to glutamate.

1.7 Role for NMDAR co-agonists glycine and D-serine

The opening of NMDA receptors requires the binding of two agonists. Sole binding of Glutamate to GluN2 subunits of NMDARs either fails to open the receptor or will only gate the channel to sub-conductance level (Banke and Traynelis, 2003). The GluN1 subunit of NMDAR provides a binding site for D-serine or glycine. Binding of either of these NMDAR co-agonists, together with glutamate binding to GluN2 subunit, leads to a complete opening of the NMDAR channel (Banke and Traynelis, 2003). As NMDARs are pivotal for induction of synaptic plasticity, the role for these co-agonists could potentially be crucial in induction of NMDAR-dependent LTP.

Glycine release and uptake: It has been shown that glycine is present in neuronal synaptic vesicles of rat cortex (Martineau *et al.*, 2013) thereby suggesting that neurones are the source of glycine release in the cortex (Figure 1.4: step 1). Glycine transporters (GlyT-1) are present on both neurones and astrocytes. These Na^+ dependent transporters can rapidly transport glycine into neurones and astrocytes (Figure 1.4: steps 6-7) (Bergeron *et al.*, 1998, Cubelos *et al.*, 2005). It has been suggested that this rapid uptake of glycine by GlyT-1 prevents saturation of NMDARs, and enables D-serine to act as the primary co-

agonist for modulating NMDAR activity in cortex and hippocampus (Fossat *et al.*, 2011, Henneberger *et al.*, 2013).

D-serine release: Staining experiments have shown that in rat hippocampus and cortex, D-serine is mainly localised to astrocytes (Schell *et al.*, 1997, Fossat *et al.*, 2011, Martineau *et al.*, 2013). These staining experiments showed that pattern of distribution for D-serine was similar to pattern of distribution for NMDARs, suggesting that astrocytic D-serine was localised in close vicinity of NMDA receptors (Schell *et al.*, 1997). This finding indicates that D-serine release from astrocytes can modulate NMDAR activity. Studies in astrocyte cultures have suggested that the release of D-serine from astrocytes is vesicular and calcium dependent (Figure 1.4: step 2) (Bezzi *et al.*, 2004, Mothet *et al.*, 2005).

Due to the predominant astrocytic localisation of D-serine, it was previously thought that D-serine was only released via astrocytes and not neurones. However, evidence has been provided for neuronal localisation of D-serine in the hippocampus (Ehmsen *et al.*, 2013) and cortex (Kartvelishvily *et al.*, 2006). In a study from 2006, immunostaining of rat cortical slices suggested that D-serine was mainly localised to neurones (Kartvelishvily *et al.*, 2006). The same study provided evidence of D-serine release from cortical neuronal cultures. D-serine release remained unaffected, when mechanism of neurotransmitter uptake into synaptic vesicles was blocked. This suggested that release of D-serine from cultured neurones is through a non-vesicular pathway. In a later study, the same group corroborated their findings in cultured neurones by providing evidence for

calcium independent non-vesicular D-serine release from neurones in cortical slices of adult (2 months old) rats (Rosenberg *et al.*, 2010). Recently, it has been shown that this neuronal non-vesicular D-serine release is carried out by transporters called alanine-serine-cysteine transporter-1 (Asc-1) (Figure 1.4: step 3) (Rosenberg *et al.*, 2013).

The studies described above suggest that D-serine can be released by both neurones and astrocytes. However, D-serine production depends solely on astrocytes. The first step of D-serine synthesis involves production of L-serine from glucose. This first step takes place in astrocytes and not neurones. Serine Racemase (SR) converts L-serine to D-serine. Both astrocytes and neurones express SR (Miya *et al.*, 2008, Martineau *et al.*, 2013) thereby suggesting that both cells are capable of converting L-serine to D-serine. In a model proposed by Herman Wolosker (Wolosker, 2011), it was suggested that astrocytes release L-serine into extracellular space where it is taken up by neurones through Asc-1 transporters. Neurones can then convert L-serine to D-serine. Subsequently, neurones can use Asc-1 transporters to release D-serine into extracellular space.

D-serine is considered to be the primary co-agonist that modulates NMDAR activity. This is important because the degree of NMDAR activity determines whether LTP or LTD is induced. Furthermore, D-serine has been implicated in neurological disorders with NMDAR hypo-activity or NMDAR-mediated excitotoxicity (Katsuki *et al.*, 2004, Van Horn *et al.*, 2013) again suggesting the importance of D-serine release in modulation of NMDAR activity. For these

reasons, researchers are investigating the role of D-serine on synaptic transmission and plasticity.

As mentioned above, astrocytic calcium-dependent vesicular release is a main source of D-serine. Therefore, the contribution of astrocytic vesicular release of D-serine on NMDAR activity is of interest. If this contribution is found to be significant, then one can envision astrocytic D-serine release as a possible therapeutic target in neurological disorders.

D-serine role in synaptic transmission and plasticity: Some researchers have attempted to elucidate the role of D-serine in synaptic transmission and plasticity. One group, whom worked on the Schaffer collaterals of CA1 region of hippocampus (Henneberger *et al.*, 2010), showed that chelating Ca^{2+} concentration in astrocytes (hence, theoretically, blocking calcium-dependent gliotransmitter release) significantly reduced the extent of LTP. This drop in potentiation was rescued when exogenous D-serine was applied to the brain slice. This finding suggested a major role in LTP induction for D-serine released by hippocampal astrocytes.

A different study in the Supra-optic nucleus (SON) of the hypothalamus also showed the importance of D-serine in LTP induction (Panatier *et al.*, 2006). In this study, a pairing protocol induced LTP in the SON of virgin rats. However, addition of D-amino acid oxidase (DAAO), which breaks down D-serine but not glycine, induced LTD rather than the usual LTP. In lactating rats, where astrocyte coverage is drastically reduced during lactation, the pairing protocol

(without DAAO) induced LTD. However, when exogenous D-serine was applied to brain slices from lactating rats, the pairing protocol lead to LTP induction. From these outcomes the authors concluded that D-serine release from astrocytes has a major role in LTP induction. This work was an inspiration for the same group to investigate the effect of D-serine in a different area of brain: the prefrontal cortex (Fossat *et al.*, 2011). They showed that exogenous D-serine increased the amplitude of evoked NMDAR mediated EPSC. Surprisingly, glycine did not increase the amplitude of NMDAR-mediated EPSC. They attributed the lack of enhancing effect of glycine on rapid glycine uptake via glycine transporters (see above). They used the outcome of their results to reinforce the argument on the major role of D-serine (rather than glycine) in synaptic transmission.

In a recent study by the same group, it was shown that in the CA1 region of rat hippocampus, endogenous D-serine acts on synaptic NMDARs whilst endogenous glycine acts on extra-synaptic GluN2B-containing NMDARs (Figure 1.4: steps 4-5) (Papouin *et al.*, 2012). It was also shown that application of exogenous DAAO significantly decreased the extent of LTP. Application of D-serine alongside DAAO restored the size of LTP. These results suggested that endogenously released D-serine not only enhances synaptic NMDAR transmission but that this enhancement contributes to the extent of LTP in the hippocampus. In contrast, it was shown that endogenous glycine and GluN2B containing NMDARs did not contribute to LTP induction and LTP extent. The authors did not investigate the source of D-serine (neuronal or astrocytic) in this study.

The above results implicate D-serine release in LTP induction. However, not all studies are in agreement about the requirement of D-serine in LTP induction. In one study on 3-4 weeks old rats (Kang *et al.*, 2013) and another study in 2-3 months old rats (Rosenberg *et al.*, 2013), DAAO application failed to change LTP extent in the CA1 region of hippocampus. These results suggest that endogenous D-serine is not required for LTP induction.

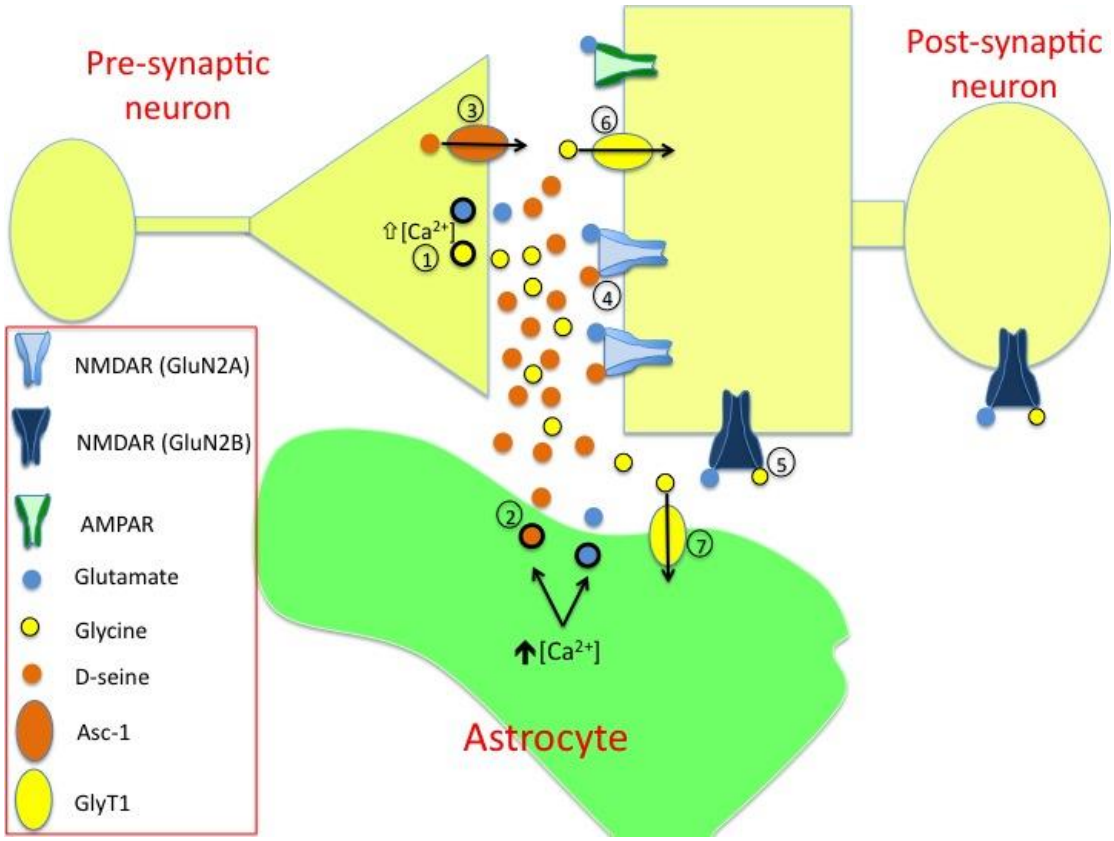

Figure 1.4. Glycine and D-serine release in the tripartite synapse. Neurones can release glutamate and glycine through calcium dependent vesicular release (1). D-serine is released via calcium dependent vesicle release from astrocytes (2). D-serine can also be released by neurones via a non-vesicular pathway involving Asc-1 transporters (3). A study in the hippocampus has shown that D-serine mainly acts on synaptic NMDARs (4) whilst glycine mainly acts on extra-synaptic NMDARs (5). It has been suggested that synaptic NMDAR modulation mainly depends on D-serine release because extracellular glycine is rapidly transported into astrocytes and neurones via GlyT-1 (6 and 7).

Decline in memory and cognitive function is generally linked to impaired synaptic plasticity. For example, aged rats show impaired LTP and learning (Clayton *et al.*, 2002). Implication of NMDARs in LTP means that these receptors could be possible therapeutic targets for cognitive impairment. Broad NMDAR agonists and antagonists are not used for neurological disorders because of the adverse side effects of these pharmacological agents. Therefore, therapeutic targeting of specific NMDARs according to their subunit composition and localisation would be a better strategy. For this reason it is important to investigate the function, properties and localisation of different NMDAR subtypes. One of the studies mentioned above showed that LTP induction did not depend on extra-synaptic NMDA receptors (Papouin *et al.*, 2012). However, the scientific literature on the contribution of synaptic GluN2A-containing NMDARs and extra-synaptic GluN2B-containing NMDARs in synaptic plasticity is controversial due to seemingly contradictory results from different labs.

1.8 Role for Synaptic and extra-synaptic NMDA receptors

For most NMDARs, there exists at least one GluN1 subunit and one GluN2 subunit. Usually two of each of these subunits exists and the NMDAR is called the di-heterometic GluN1/GluN2 containing receptor. It has been shown that at start of development (up to one to two weeks of age) in the hippocampus and cortex, the GluN2B subtype is abundant whilst GluN2A is relatively rare. As development progresses towards maturity (post one to two weeks postnatal), the number of GluN2A subunits increases whilst number of GluN2B subunits

decreases (Sans *et al.*, 2000, Erisir and Harris, 2003, Liu *et al.*, 2004). In mature hippocampus and cortex, GluN2A subunit is the predominant GluN2 subunit whilst GluN2B subunit is the second most abundant GluN2 subunit (Monyer *et al.*, 1994), suggesting that both subunits have important roles in NMDAR-dependent transmission and plasticity.

Synaptic NMDARs refer to receptors at the active zone of the synapse. Extra-synaptic zone refers to parts of the neurone that does not contain active zones. The term Peri-synaptic zone usually refers to the extra-synaptic area about 100 nm around the synapse (Petralia, 2012). The extra-synaptic area (excluding the peri-synaptic area) includes the soma and dendritic shaft. Extra-synaptic sites are mainly in contact with adjacent non-synaptic processes of glial cells and axons/dendrites of neighbouring neurones (Petralia *et al.*, 2010). It is believed that in mature neurones, synaptic NMDARs mainly consist of GluN2A subunits whilst extra-synaptic NMDARs mainly consist of GluN2B subunits (Tovar and Westbrook, 1999, Valtschanoff *et al.*, 1999, Groc *et al.*, 2004, Groc *et al.*, 2006, Petralia *et al.*, 2010, Papouin *et al.*, 2012).

GluN2B-containing NMDA receptors have lower peak currents and slower rise and decay times compared to GluN2A containing NMDA receptors (Monyer *et al.*, 1994, Erreger *et al.*, 2005). A study in the granule cells of dentate gyrus showed that miniature NMDAR EPSCs had faster kinetics than evoked (by afferent stimulation) EPSCs (Dalby and Mody, 2003). This suggested that miniature NMDAR EPSCs consist of fast synaptic GluN2A containing NMDAR activity, whilst evoked EPSCs consist of a combination of fast synaptic NMDAR

activity and slower extra-synaptic GluN2B-containing NMDAR activity. This also suggests that when afferent fibres are not active (no action potentials) spontaneous release of glutamate only activates synaptic NMDARs. Release as a result of spontaneous activity is not sufficient enough for glutamate spillover to extra-synaptic regions (Figure 1.5A). Therefore, extra-synaptic NMDARs are not activated during spontaneous glutamate release. However, during evoked recordings, where afferent fibres are stimulated, extra-synaptic NMDARs are activated along with synaptic NMDARs (Figure 1.5B). This activation of extra-synaptic receptors could be due to glutamate spillover as a result of more synaptic glutamate release (Figure 1.5B: step 6) (Rusakov and Kullmann, 1998). Alternatively, as mentioned in an earlier section, extra-synaptic GluN2B containing receptors can be activated by glutamate release from astrocytes (Figure 1.5B: steps 7-10) (Fellin *et al.*, 2004).

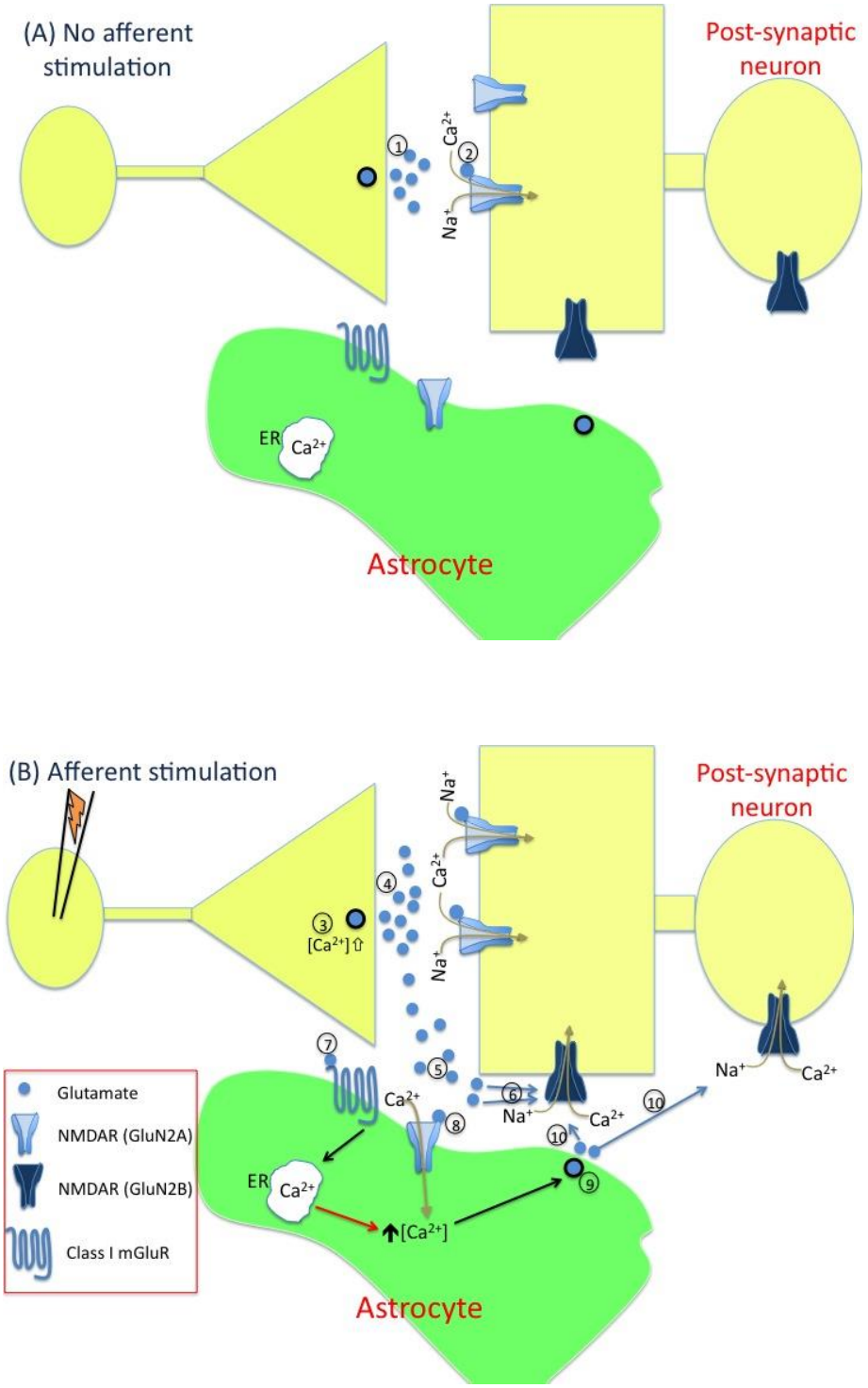

Figure 1.5. See next page for Figure legend.

Figure 1.5. Synaptic and extra-synaptic NMDAR mediated transmission. (A) When afferent fibres are not stimulated there is spontaneous vesicular release of glutamate from nerve terminals (1). This spontaneous glutamate release activates synaptic NMDARs on post-synaptic neurones (2). There is no glutamate spillover. Therefore, extra-synaptic GluN2B containing NMDARs are not activated. **(B)** Afferent fibre stimulation leads to opening of voltage gated calcium channels at nerve terminals. This leads to calcium elevations at nerve terminals (3), which in turn results in increase in vesicular release of glutamate (4). Due to this increase in glutamate release, some of the glutamate spillover into extra-synaptic space (5). Spilled over glutamate can activate extra-synaptic GluN2B containing receptors directly (6). Alternatively, spilled over glutamate can activate calcium elevations in astrocytes by binding to astrocytic NMDARs (7) and mGluRs (8). This in turn leads to glutamate release from astrocytes (9), which can activate extra-synaptic GluN2B containing NMDARs (10). AMPARs are not shown in this schematic representation because during NMDAR EPSC recordings they are blocked by AMPAR antagonists. During these recordings, NMDARs are not blocked by magnesium because NMDAR EPSC are usually recorded at depolarised potentials or in the absence of extracellular Mg^{2+}. Note that for simplicity, glycine and D-serine release are not shown on this schematic representation.

Contribution of synaptic and extra-synaptic NMDA receptors to synaptic plasticity: As the number of GluN2B containing NMDARs decrease and the number of GluN2A containing NMDARs increase with development, one would expect that synaptic GluN2A containing NMDARs to be the main subtype needed for LTP induction. Indeed, many studies implicate the importance of GluN2A containing NMDA receptors in LTP induction. In a study in CA1 region of hippocampus in 9-10 weeks old mice, GluN2A KO resulted in a significant reduction in HFS-induced LTP, suggesting the importance of GluN2A subtype in LTP induction (Sakimura *et al.*, 1995). In another study in CA1 region of hippocampus, from 4 week old mice, application of GluN2B antagonist Ifenprodil failed to block HFS-induced LTP whilst application of GluN2A antagonist NVP-AAM077 managed to block LTP (Liu *et al.*, 2004). Furthermore, a more recent study showed that application of GluN2B antagonist did not have an effect on HFS induced LTP in the CA1 region of hippocampus of 2-3 months old rats (Papouin *et al.*, 2012).

In contrast, there are other studies that show that NMDAR-induced LTP also depends upon the activation of extra-synaptic GluN2B-containing NMDA receptors. A study showed that over-expression of GluN2B receptors lead to enhancement of HFS-induced LTP in the CA1 region of hippocampus of 2-3 months old rats, suggesting that GluN2B receptors are involved in modulating the extent of LTP (Wang *et al.*, 2009). A study in the prefrontal cortex of 6-to-8 weeks old mice showed that both GluN2A and GluN2B containing NMDA receptors were required for TBS-induced LTP induction (Zhao *et al.*, 2005). Another study in the CA1 region of hippocampus of 2 months old rats showed

that Ifenprodil application significantly reduced the extent of HFS-induced LTP (Maggio *et al.*, 2008).

Taken together, it is likely that both GluN2B and GluN2A containing NMDARs contribute to LTP induction in the hippocampus and prefrontal cortex.

Glutamatergic transmission is not the only form of synaptic transmission. Synaptic transmission also involves GABAergic and purinergic transmission. Both GABAergic and purinergic transmission can modulate glutamatergic transmission. Therefore, in the following sections I will introduce GABAergic and purinergic transmission.

1.9 GABAergic transmission

$GABA_A$ receptor structure: GABA is an inhibitory neurotransmitter released by interneurones via vesicular exocytosis. The ionotropic receptors for GABA are the pentameric $GABA_A$ receptors ($GABA_ARs$). Each $GABA_A$ subunit consists of an extracellular N-terminal domain, followed by four transmembrane domains and ending with an extracellular C-terminal domain (Sigel and Steinmann, 2012). There exist 8 different $GABA_A$ subunit classes (α, β, γ, ρ, ε, θ, π, δ) and a total of 19 different $GABA_A$ subunits (Sigel and Steinmann, 2012). As a result of the large number of $GABA_A$ subunits, there exist a large number of $GABA_AR$ subtypes. The most abundant $GABA_AR$ in the brain consists of $\alpha1$, $\beta2$, $\gamma2$ subunits (Sieghart and Sperk, 2002).

Phasic and tonic Inhibition: Post-synaptic $GABA_A$Rs are exposed to a transient but high concentration of GABA following the release of this transmitter from pre-synaptic interneurones (Figure 1.6: step 1). Binding of GABA to $GABA_A$Rs opens these receptors, allowing Cl^- influx into the post-synaptic neurone (Figure 1.6: step 2). This anion conductance is called an Inhibitory Post-Synaptic Current (IPSC) and leads to hyper-polarisation of the post-synaptic neurone (Figure 1.6: step 3) (Edwards *et al.*, 1990). IPSCs are rapid and short-term events and underlie what is known as "phasic inhibition".

Phasic inhibition is due to fast synaptic release of GABA onto $GABA_A$Rs that mainly have synaptic localisation. However, $GABA_A$Rs also exist on extra-synaptic sites. These extra-synaptic $GABA_A$Rs are present on soma and axons of neurones. Low ambient concentrations of GABA in extra-cellular space can open these receptors leading to a temporally longer period of inhibition in comparison to phasic inhibition. This persistent inhibitory action of GABAergic transmission is called "tonic inhibition". Phasic transmission is temporally specific as it occurs only during firing of interneurones. It is also spatially specific because it takes place only at specific inhibitory synapses where GABA is released. In contrast, tonic inhibition is due to a persistent inhibition by ambient GABA concentrations; therefore it is not temporally specific. Furthermore, tonic inhibition does not involve activation of specific GABAergic synapses, but involves activation of extra-synaptic $GABA_A$Rs of many neighbouring neurones. Therefore, tonic inhibition has lower spatial specificity compared to phasic inhibition. The existence of tonic inhibition has been shown in different regions

of the brain including hippocampus and cortex (Bai *et al.*, 2001, Yamada *et al.*, 2007).

The overall conductance (charge transfer) during tonic inhibition is higher than in phasic inhibition. This is because tonic inhibition involves a continuous and persistent activation of extra-synaptic $GABA_A$Rs. Furthermore, as tonic inhibition involves the activity of $GABA_A$Rs on many neighbouring neurones, there is a larger number of $GABA_A$Rs recruited during tonic inhibition than in phasic inhibition. During phasic inhibition, only a small number of $GABA_A$Rs are open. These $GABA_A$Rs are mainly localised to synaptic/active sites. As these receptors are situated very close to GABA release terminals (Figure 1.6: step 2), their opening leads to appearance of IPSCs during voltage-clamp recordings. However, extra-synaptic $GABA_A$Rs can also be recruited during synaptic transmission. This happens for extra-synaptic $GABA_A$Rs that are close to site of synaptic release, where they can be activated by spillover of GABA from synaptic cleft during fast synaptic transmission (Figure 1.6: steps 4-5). This activation of extra-synaptic $GABA_A$Rs also leads to appearance of IPSCs during patch clamp recordings. However, during tonic inhibition, extra-cellular ambient GABA is, temporally and spatially, far away from their release sites (Figure 1.6: step 6). Hence, their binding to extra-synaptic $GABA_A$Rs does not lead to appearance of IPSCs. Instead, in a voltage clamp recording, this tonic inhibition of extra-synaptic receptors are associated with the holding current that is required to clamp the neurones at a given membrane potential. The larger the tonic $GABA_A$R activity, the larger the size of the holding current.

As a result of its high temporal and spatial specificity, phasic inhibition is involved in the generation of rhythmic activities in neuronal networks by synchronising the activity of a large number of pyramidal neurones (Cobb *et al.*, 1995). Furthermore, phasic inhibition also has a role in TBS-induced LTP (see section 1.4). Tonic inhibition on the other hand puts a persistent threshold on excitation of neurones (Figure 1.6: step 7).

Tonic inhibition could also have a role in modulating the threshold of synaptic plasticity. Studies in hippocampus have shown that some subtypes of $GABA_A$Rs are predominantly present on extra-synaptic sites. These include δ and α5 containing $GABA_A$Rs (Brunig *et al.*, 2002, Wei *et al.*, 2003). It has been shown that these receptors are involved in tonic inhibition (Stell *et al.*, 2003, Caraiscos *et al.*, 2004) suggesting that tonic inhibition mainly involves extra-synaptic receptors. Another study has shown that these extra-synaptic $GABA_A$Rs could also be involved in synaptic plasticity, learning and memory (Dawson *et al.*, 2006). They showed that in the CA1 region of hippocampus of 6-9 months old mice antagonism of α5 containing extra-synaptic $GABA_A$Rs not only decreased tonic inhibition but also increased the extent of HFS-induced LTP in comparison to control conditions. Furthermore, in vivo investigation showed that antagonism of α5 containing extra-synaptic $GABA_A$Rs lead to improvement in learning and memory tasks. These results implied that modulation of tonic inhibition by extrasynaptic $GABA_A$Rs could have a role in modulating NMDAR-dependent LTP. These results suggest that in the investigation of excitatory synaptic plasticity such as NMDAR-dependent LTP of glutamatergic synapses, one must

keep in mind the potential modulating roles played by $GABA_A$Rs and inhibitory transmission.

Extracellular GABA concentration does not solely depend on release of GABA. It is also regulated by GABA transporters (GATs) (Chen *et al.*, 2004). These transporters actively remove GABA from the extracellular space. The three types of GATs are numbered GAT1-3. GAT1 is localised to neurones (Guastella *et al.*, 1990) whilst GAT3 is mainly localised to glial cells (Figure 1.6: steps 7-8) (Borden *et al.*, 1992). By maintaining extracellular GABA concentrations, GATs indirectly control tonic inhibition. This control of tonic inhibition has been shown for both GAT1 and GAT3 (Overstreet *et al.*, 2000, Shigetomi *et al.*, 2012).

In summary, phasic and tonic inhibition depend on release of GABA, uptake of GABA and localisation of post-synaptic $GABA_A$Rs. The control of inhibition through these factors could have a modulatory role in glutamatergic synaptic plasticity.

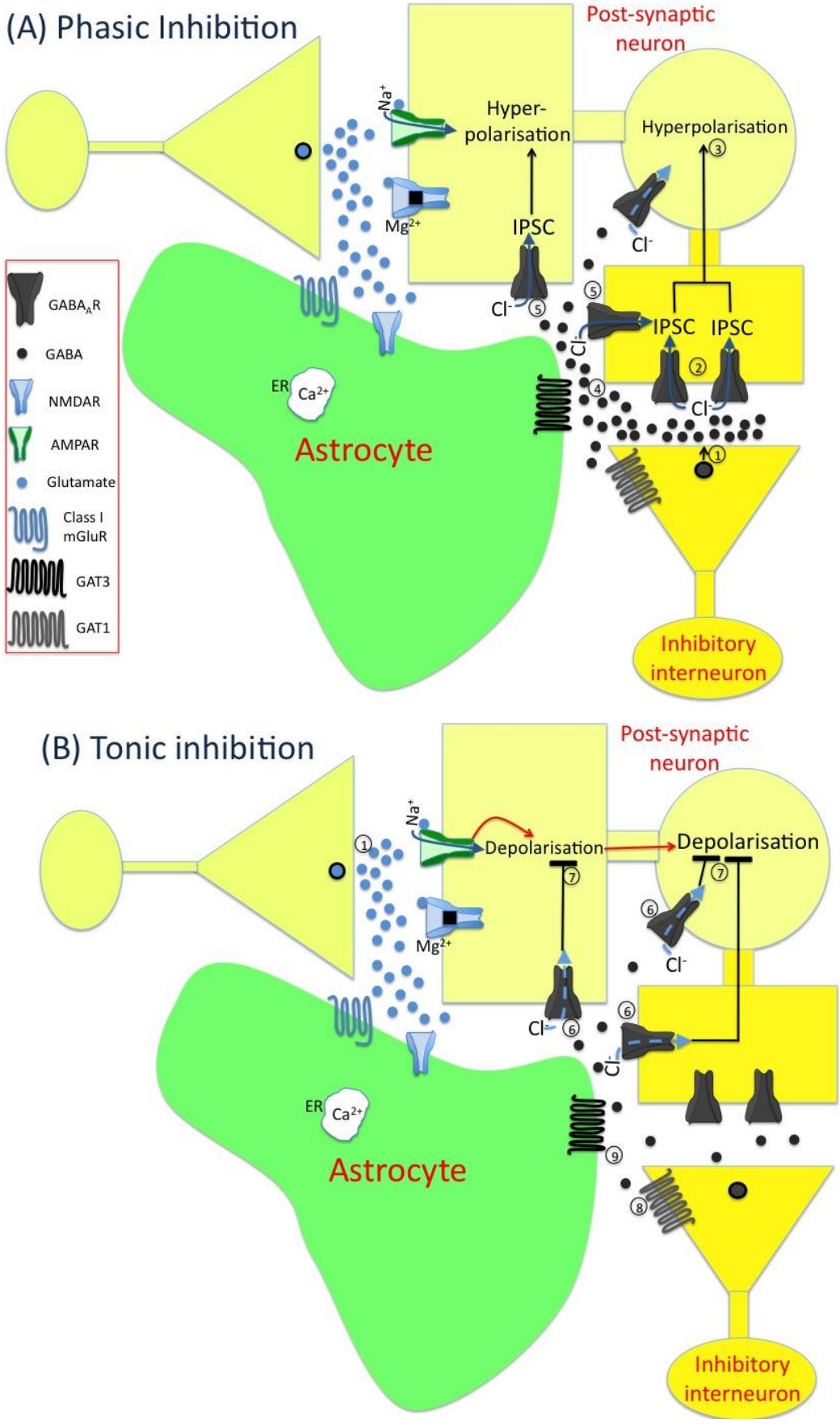
(A) Phasic Inhibition
Post-synaptic neuron
Hyper-polarisation
Hyperpolarisation
IPSC
IPSC
IPSC
Astrocyte
Inhibitory interneuron
GABA$_A$R
GABA
NMDAR
AMPAR
Glutamate
Class I mGluR
GAT3
GAT1
(B) Tonic inhibition
Post-synaptic neuron
Depolarisation
Depolarisation
Astrocyte
Inhibitory interneuron

Figure 1.6. Phasic and tonic inhibition. (A) During phasic inhibition there is a transient release of high amount of GABA into the synaptic cleft (1). Activation of synaptic $GABA_ARs$ by GABA leads to Cl^- entry into the post-synaptic neurone (2). This rapid and short-term $GABA_AR$ transmission is called IPSC (thick blue arrows), which leads to temporally and spatially specific hyper-polarisation (3). During fast phasic transmission there will be spillover of GABA onto extra-synaptic space (4). Binding of spilled over GABA to extra-synaptic $GABA_ARs$ also leads to generation of fast GABAergic currents (5). **(B)** During tonic inhibition there is no synaptic release of GABA. However, low ambient concentrations of GABA are present in the extracellular space. Ambient GABA molecules continuously activate extra-synaptic $GABA_ARs$, leading to tonic inhibition (6). This tonic inhibition is persistent and slow (dashed blue lines) because GABA molecules are temporally and spatially far away from their release sites. Tonic inhibition is involved in maintaining a persistent threshold on post-synaptic excitation (7). Tonic inhibition also involves extra-synaptic $GABA_ARs$ on neighbouring neurones, which are not shown on this diagram. Neuronal GAT1 (8) and astrocytic GAT3 (9) are involved in actively removing GABA from the extra-cellular space.

1.10 Purinergic transmission

Structure and localisation of P2X receptors: It was first in 1972 that Geoffrey Burnstock introduced the concept of ATP as a neurotransmitter (Burnstock, 1972). Both neurones and astrocytes can release ATP. Neuronal and astrocytic ATP release is either via exocytosis (Pankratov *et al.*, 2006) or down a concentration gradient through plasmalemmal channels (Cotrina *et al.*, 1998). ATP can be released at the same hippocampal and cortical nerve terminals where glutamate is released (Figure 1.7: part 1) (Pankratov *et al.*, 2006, Pankratov *et al.*, 2007). Subsequent to release, ATP binds ATP receptors on neurones and astrocytes. Ionotropic ATP receptors are called P2X receptors whilst metabotropic ATP receptors are called P2Y receptors. There exists seven subunit isoforms for P2X receptors: P2X1-7 (Khakh *et al.*, 2001). P2X receptors (P2XRs) can exist either as homomeric or heteromeric assembly of P2X subunits. Heteromeric assemblies include P2X1/P2X2, P2X1/P2X4, P2X1/P2X5, P2X2/P2X3, P2X2/P2X6 and P2X4/P2X6 receptors (North, 2002). Homomeric P2X2 receptors, homomeric P2X4 receptors and P2X4/P2X6 heteromeric receptors are the most abundant P2XR subtype in the CNS system (Illes and Alexandre Ribeiro, 2004). High expression of P2X2 and P2X4 receptors has been shown in the hippocampus and cortex of adult rats (Le *et al.*, 1998, Xiang *et al.*, 1998). Most subtypes of P2X receptors are activated by low micromolar concentrations. Ionotropic P2X receptors are different in structure to NMDARs and AMPARs. NMDARs and AMPARs are tetrameric receptors but P2X receptors are trimeric (they are made up of three P2X subunits) (Erb *et al.*, 2006). Each P2X subunit has an intracellular N-terminal domain, an extracellular ATP

binding domain and an intracellular C-terminal domain (Khakh *et al.*, 2001). This means that each subunit has two transmembrane domains. Therefore, each P2X receptor contains six transmembrane domains. These transmembrane domains contribute to the function of the receptor pore (Egan *et al.*, 2006). P2X receptors are permeable to both monovalent and divalent cations. For most P2X receptor subtypes calcium permeability is higher than monovalent cation permeability (Egan *et al.,* 2006). Their calcium conductance is not as high as NMDARs but they are not blocked by magnesium at membrane potentials below -40mV (Pankratov *et al.,* 2009). In fact, P2XR Ca^{2+} influx is higher at less depolarised membrane potentials (Pankratov *et al.*, 1999).

It has been shown that P2X receptors are expressed at low levels on neurones and that they are mainly present on peri- and extra-synaptic regions (Figure 1.7: part 5) (Le *et al.*, 1998). Support for this finding comes from electrophysiological recordings where neuronal P2X receptors only contribute 5-15% to the amplitude of cortical evoked EPSC currents (Pankratov *et al.*, 2003). Furthermore, electron microscopy has shown that P2X2 and P2X4 containing P2XRs are mainly situated at peri-synaptic sites in the CA1 region of rat hippocampus (Rubio and Soto, 2001). Due to the relative paucity of P2XRs on post-synaptic neurones in comparison to glutamatergic ionotropic receptors, it has been suggested that ion entry through P2X receptors does not contribute to depolarisation of the post-synaptic neurone. However, P2XRs can contribute to synaptic transmission and plasticity by activation of downstream intracellular signalling as a result of calcium entry (Khakh and North, 2012).

In a study in the cortex, it was shown that acutely isolated astrocytes express functional P2X1/P2X5 heteromeric receptors in adult mice but not other P2X subunits (Lalo *et al.*, 2008). The P2X1/P2X5 heteromeric receptors are unique in comparison to other P2X receptors because they are activated by nanomolar ATP concentrations. This high sensitivity of P2X1/P2X5 heteromeric receptors suggests that astrocytic P2XRs can detect extremely low levels of extra-cellular ATP. It has been shown that application of exogenous P2X receptor agonist to isolated cortical astrocytes can lead to fast calcium elevation in these cells (Palygin *et al.*, 2010). Furthermore, calcium elevation as a result of cortical neuronal afferent stimulation was partially blocked by P2X receptor antagonist. This suggested that ionotropic P2X receptors are also involved in astrocytic calcium elevation in addition to mGluRs and NMDARs (Figure 1.7: part 2). Taken together, these studies show the presence of P2X receptors on cortical astrocytes and their possible role in contributing to fast calcium rise in astrocytes.

The role of purinergic signalling in synaptic transmission and plasticity: Application of exogenous ATP to brain slices can induce LTP. It has been shown that 10 minutes application of 10 μM exogenous ATP to hippocampal slices from guinea pigs (Fujii, 2004) and rats (Ievglevskyi *et al.*, 2012) can induce LTP. This LTP is induced without any TBS or HFS protocol and is solely as a result of ATP application. Interestingly, during ATP application there is a depression of evoked potentials and LTP is only **expressed** subsequent to ATP washout. This potentiation is called ATP-induced LTP to distinguish it from NMDAR dependent LTP, which is induced via high frequency stimulation protocols. However, ATP-induced LTP is also NMDAR dependent as application of

NMDAR antagonists blocks LTP induction (Fujii, 2004). It was shown that ATP-induced LTP does not depend on P2X or P2Y receptors but is dependent on plasma membrane associated ecto-protein kinases (Fujii, 2004). As a result, it was suggested that extracellular ATP could act as a phosphate donor for phosphorylation of NMDARs via these ecto-protein kinases (Figure 1.7: part 4). This phosphorylation can theoretically result into large Ca^{2+} influx into the NMDARs, thereby leading to LTP.

It is believed that ATP binding to P2X receptors can contribute to NMDAR-dependent LTP. In brain slices from 19-21 days old rats, high frequency stimulation of hippocampal Schaffer collaterals for 1 second induces LTP, whereas stimulation for 0.2 sec (a sub-threshold protocol) induces short-term potentiation. Inhibition of P2X receptors by the broad antagonist Pyridoxalphosphate-6-azophenyl-2',4'-disulfonic acid (PPADS) during sub-threshold protocol led to LTP induction (Pankratov *et al.*, 2002). This suggested that antagonising P2X receptors reduces the LTP threshold. The same study also showed that in hippocampal pyramidal neurones, activation of P2X receptors by exogenous and endogenous ATP resulted in a reduction in the NMDAR response (Pankratov *et al.*, 2002). Therefore, the authors suggested that activation of P2X receptors by ATP results in inhibition of NMDAR activity (Figure 1.7: part 6), which in turn increases the threshold for LTP induction.

In contrast to the above report, a study using P2X4 KO mice showed that in the CA1 region of hippocampus from 3-4 weeks old mice, extent of LTP was significantly lower compared to WT mice (Baxter *et al.*, 2011). Furthermore, in

P2X4 KO mice, facilitation of NMDAR EPSC via pharmacological NMDA application was lower in comparison to WT mice. These data suggested that P2X4 receptors significantly contribute to the size of LTP by increasing NMDAR activity. This finding suggests that P2X receptor activity can enhance NMDAR activity and so it seems to be contradicting the above-mentioned report where blocking P2XRs via PPADS application lead to LTP induction during the sub-threshold (0.2 Hz) protocol. These contradictory results suggest that role of P2XRs in modulating NMDAR activity and LTP is rather complex. However, it must be noted that PPADS does not block P2X4 receptors. Therefore, these seemingly contradictory results might be due to the specific roles played by different P2XR subtypes.

Another group also showed the involvement of activation of P2XRs on enhancing glutamatergic synaptic efficacy. In this study in the hypothalamus, activation of P2X receptors by astrocytic ATP led to insertion of AMPARs on post-synaptic neurones (Figure 1.7: parts 7-9) (Gordon *et al.*, 2005). This report also points to another important finding about purinergic transmission: the source of ATP that is involved in modulation of synaptic transmission is astrocytic.

Interestingly, the same researchers who showed that ATP activation of P2X receptors led to attenuation of NMDAR activity have also shown that ATP activation of P2X receptors can lead to attenuation of $GABA_A$ receptor activity. They showed that calcium elevation in astrocytes via application of PAR-1 agonist results in ATP release from these cells (Figure 1.7: parts 10-11). The released ATP then activates neuronal P2XRs and leads to intracellular signalling

(Figure 1.7: part 12). This P2XR-mediated intracellular signalling in turn leads to decrease in amplitude of $GABA_AR$-mediated currents on cortical neurones (Figure 1.7: part 13) (Lalo *et al.*, 2009).

A further complexity in the role of purinergic transmission is the rapid (~200 ms) hydrolysis of ATP to Adenosine (Dunwiddie *et al.*, 1997). Adenosine role has been attributed to the regulation of sleep (Schmitt *et al.*, 2012). Extracellular ATP is broken down via dephosphorylation by ecto-nucleotidases to 5'-Adenosine Monophosphate (5'-AMP) and subsequently to adenosine via 5'-nucleotidase (Zimmermann and Braun, 1999). Alternatively, Adenosine can be released into the extracellular space directly from neurones via facilitated diffusion (Wall and Dale, 2013). There exists four different types of receptors for adenosine (Olah and Stiles, 1995). All these receptors are G-protein coupled metabotropic receptors with seven transmembrane domains and are called A1, $A2_a$, $A2_b$ and A3 receptors. The A1 receptors are the most abundant adenosine receptors and are distributed throughout the brain with particularly high density in hippocampus and cortex (Fastbom *et al.*, 1987). Binding of adenosine to A1 receptors results in inhibition of neurotransmitter release (Proctor and Dunwiddie, 1987). This tonic suppression of neurotransmitter release by A1 receptors is prominent for excitatory glutamatergic transmission (Dunwiddie and Hoffer, 1980).

A study has shown that astrocytic vesicular release contributes to adenosine-mediated tonic suppression. They showed this by developing the transgenic mouse line called dominant negative soluble N-ethylmaleimide-sensitive factor

attachment protein receptors (dnSNAREs) mouse (Pascual *et al.*, 2005). In this transgenic mouse, the cytosolic portion of the SNARE domain of synaptobrevin 2 is expressed selectively in astrocytes. This selectively prevents vesicular release from astrocytes but not neurones (see Chapter 2 for more details). In the CA1 region of the hippocampus of dnSNARE mice, baseline evoked fEPSPs were larger in comparison to baseline evoked fEPSP from WT mice (Pascual *et al.*, 2005). Application of A1 receptor agonist to dnSNARE slices resulted in a decrease in the baseline fEPSP. These results suggested that in dnSNARE mice, impairment of astrocytic vesicular release results in less ATP release and hence less extracellular adenosine availability. This means that in hippocampal slices of dnSNARE mice, there is less tonic suppression of glutamatergic transmission via A1 receptors, hence resulting in a larger baseline fEPSP. Application of PPADS did not alter baseline fEPSP in WT and dnSNARE mice, thereby indicating that P2XRs do not contribute to baseline glutamatergic activity. The same study also showed that the size of HFS-induced LTP was less in dnSNARE mice compared to WT mice. The authors attributed the decrease in LTP size in dnSNARE mice to the larger baseline fEPSP in these mice. They suggested that as a result of larger baseline fEPSP, there is less extent for fEPSP size to increase by during LTP induction. Taken together, the authors concluded that the release of ATP from astrocytes and its subsequent rapid breakdown to adenosine persistently suppresses tonic excitatory synaptic transmission (Figure 1.7: steps 14-16). This suppression provides control over extent of LTP magnitude and threshold. Even before this study, it was already known that A1 receptors tonically inhibit glutamatergic transmission, thereby modulating LTP threshold. The originality

of this report resides in the fact that a major source of this extracellular adenosine is shown to be as a result of vesicular release from astrocytes.

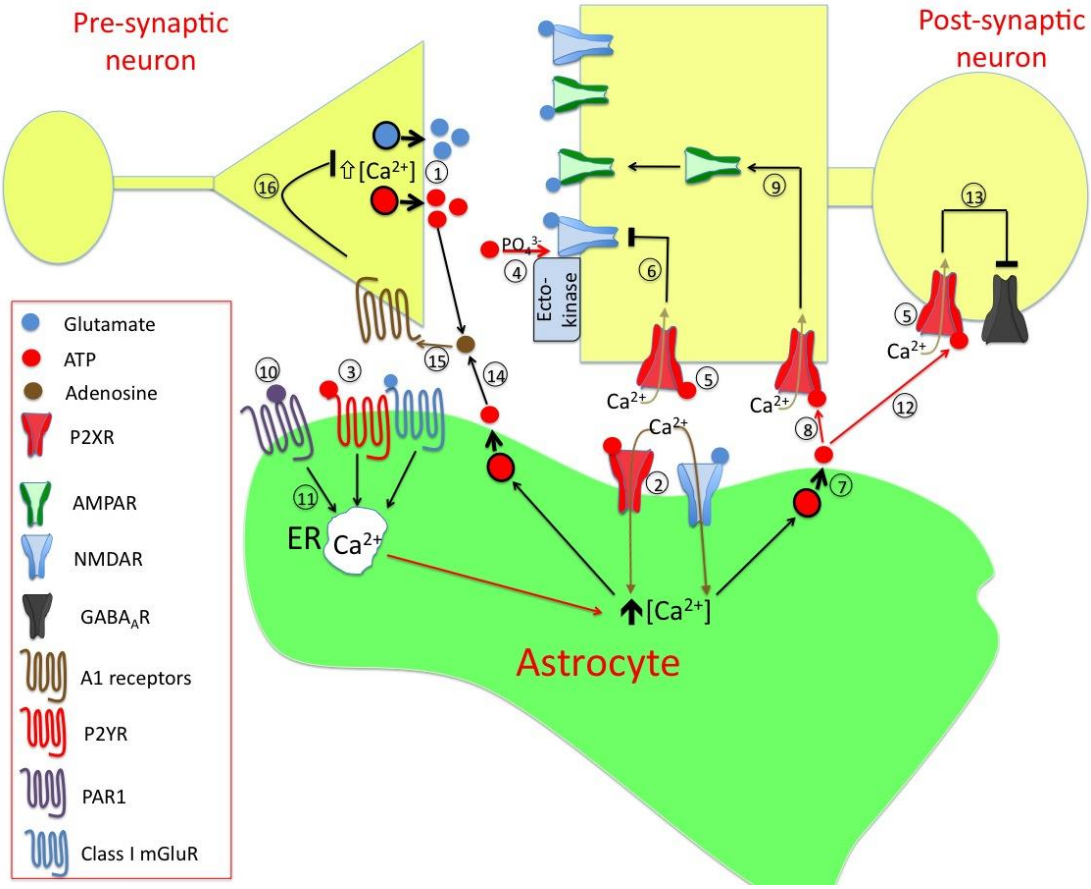

Figure 1.7. Different roles for purinergic signalling in synaptic transmission. ATP can be released from the same nerve terminals where glutamate is release (1). This ATP release can activate ionotropic P2X receptors (2) and metabotropic P2Y (3) receptors on astrocytes, thereby leading to calcium elevation in these cells. Extracellular ATP can enhance NMDAR activity by acting as a phosphate donor for phosphorylation by ecto-protein kinases (4). Neuronal P2X receptors are mainly localised to extra-synaptic regions (5). Activation of these extra-synaptic P2XRs by endogenously released ATP can inhibit NMDAR activity via P2XR triggered intracellular signalling involving phosphotases (6). ATP can also be released from astrocytes (7). This astrocytic ATP release can activate neuronal P2XRs (8). This in turn leads to AMPAR insertion on post-synaptic neurone (9). Astrocytic ATP release can also indirectly inhibit $GABA_AR$s. Activation of PAR1 receptors on astrocytes (10) leads to calcium elevation in these cells (11). This in turn leads to ATP release from astrocytes. The released ATP can then bind to extra-synaptic neuronal P2X receptors (12). This triggers activation of protein kinase C, which results in inhibition of neuronal $GABA_AR$s (13). Extracellular ATP released by neurones and astrocytes can be rapidly broken down to adenosine (14). Adenosine can then bind to A1 receptors on pre-synaptic neurones (15) leading to a persistent tonic suppression of calcium dependent neurotransmitter release (16).

1.11 Mechanisms of gliotransmitter release from astrocytes

Astrocytes can release gliotransmitters such as Glutamate, ATP and D-serine. The contribution of these gliotransmitters to synaptic transmission and plasticity has been discussed above. Another area of tripartite research involves the investigation of mechanisms by which gliotransmitters are released from astrocytes. This area of research is rather controversial because different studies have suggested different mechanisms of gliotransmitter release. The release mechanism that is mostly under investigation, and for that reason is mostly debated, is calcium dependent vesicular exocytosis.

Evidence in support of calcium dependent exocytosis of gliotransmitter release from astrocytes comes in four different forms:

(1) Evidence for presence of vesicles in astrocytes: The presence of Synaptic-like micro-vesicles (SLMVs) has been shown in astrocytes of brain slice preparations (Bezzi *et al.*, 2004, Jourdain *et al.*, 2007, Bergersen *et al.*, 2012). These vesicles are about 30-40 nm in diameter, which is similar to the size of synaptic vesicles (Bergersen *et al.*, 2012, Martineau *et al.*, 2013). In addition to SLMVs, presence of larger vesicles of approximately 300 nm has been shown in cultured and acutely isolated astrocytes (Chen *et al.*, 2005).

Unlike neurones, astrocytes lack active zones. However, many studies have shown that astrocytic Ca^{2+} oscillations that occur either spontaneously or in response to neuronal stimulation are usually restricted to certain regions of

astrocytes (Aguado *et al.*, 2002, Nett *et al.*, 2002, Hirase *et al.*, 2004, Panatier *et al.*, 2011). These regions, which are called astrocyte microdomains, are believed to surround the synaptic cleft. These extra-synaptic microdomains contain small SLMV groups just beneath the astrocytic cell membrane (Bezzi *et al.*, 2004). Imaging via electron microscopy has shown that these SLMV containing microdomains are opposite neuronal terminals and dendrites, thereby suggesting that these microdomains are exocytotic domains that can respond and modulate synaptic transmission (Bezzi *et al.*, 2004).

Taken together, evidence for presence of vesicles in astrocytes suggests that these cells can utilise vesicles for exocytosis. However, in situ studies have shown that astrocyte SLMVs to be seven to nine fold less dense compared to their synaptic counterparts (Bezzi *et al.*, 2004, Jourdain *et al.*, 2007, Martineau *et al.*, 2013). Due to the paucity of SLMVs compared to neuronal vesicles, the level of contribution of exocytotic mechanism to gliotransmitter release has been debated.

(2) Evidence for presence of proteins involved in exocytosis in astrocytes: Neuronal vesicular exocytosis involves the presence of certain proteins involved in the exocytosis mechanism. Neurotransmitter transporters such as the Vesicular glutamate transporters (VGLUTs) and Vesicular ATP transporter (VNUT) are involved in transporting neurotransmitters into vesicles ready for exocytosis. Vesicular exocytosis requires the formation of a functional complex between vesicular and membrane proteins called SNAREs. Vesicle associated membrane protein 2 (VAMP2), which is also called synaptobrevin 2, is, as the name

suggests, a vesicular SNARE. VAMP2 binds to two SNAREs on the plasma membrane. These are the syntaxins and SNAP25 (synaptosomoal-associated protein 25 kDa) (Jahn and Scheller, 2006). This binding is crucial for exocytosis. Synaptotagmin is another vesicular SNARE. Binding of Ca^{2+} to synaptotagmin catalyses exocytosis (Ushkaryov *et al.*, 1992).

The presence of some (but not all) of these analogous proteins has been found in astrocyte cultures. These include VGLUTs, VNUT, VAMP2, VAMP3 (cellubrevin), syntaxin, SNAP23, synaptotagmin 4 and synaptotagmin 11 (Parpura *et al.*, 1995, Maienschein *et al.*, 1999, Zhang *et al.*, 2004, Cahoy *et al.*, 2008, Oya *et al.*, 2013). However, some have argued that these findings could be due to artefacts of cell cultures (Fiacco *et al.*, 2009, Hamilton and Attwell, 2010). Therefore, there have also been attempts to demonstrate the presence of these proteins in brain slices. The presence of VGLUT1/2 and VAMP3 has been shown in astrocytic SLMVs in slices of rat hippocampus (Bezzi *et al.*, 2004). Furthermore, astrocytic VAMP2 expression has also been shown in rat cortical slices (Martineau *et al.*, 2013). In contrast, there are reports that have failed to confirm the presence of some of these proteins. For example, Immunostaining and western blotting failed to demonstrate astrocytic VGLUT1/2 expression in both culture preparations and hippocampal/cortical slices from mice (Li *et al.*, 2013). Therefore, the presence of vesicular exocytosis in astrocytes remains controversial.

(3) Evidence for localisation of gliotransmitters in astrocytic vesicles: Evidence for localisation of glutamate and D-serine in astrocytic vesicles of

cortical slices from 1-month-old rats has also been provided (Bergersen *et al.*, 2012, Martineau *et al.*, 2013). Evidence suggesting presence of ATP in astrocytic vesicles has been provided for astrocyte cultures (Pangrsic *et al.*, 2007). In this study, fusion of astrocytic vesicles resulted in the release of ATP suggesting that astrocytes are capable of exocytotic ATP release.

(4) Evidence for exocytosis of gliotransmitters as a result of calcium elevation: Tetanus toxin can cleave VAMP2, thereby preventing fusion of vesicles and exocytosis. Pharmacological agonists like DHPG and NMDA can elevate calcium levels in astrocytes, thereby leading to gliotransmitter release. Use of these agonists with and without tetanus toxin has allowed researchers to investigate whether calcium dependent gliotransmitter release occurs through exocytosis. Researchers utilised this pharmacological approach and showed that calcium-dependent release of glutamate (Araque *et al.*, 2000, Bezzi *et al.*, 2004) and D-serine (Bezzi *et al.*, 2004, Mothet *et al.*, 2005) occurs via exocytosis in astrocyte cultures.

Calcium-dependent exocytosis of ATP has also been shown in astrocyte cultures (Coco *et al.*, 2003). However, this study showed that ATP release from astrocyte culture was only partially blocked by tetanus toxin. This result suggested that release of ATP through VAMP2-dependent exocytosis only partially contributes to ATP release from astrocytes. It was shown that ATP is mainly stored in secretory granules, which are VAMP-independent. The authors suggested that calcium dependent ATP release from astrocytes could occur via both vesicles and secretory granules.

The evidences for presence of exocytosis in astrocytes are all from studies in culture preparations. However, there have also been attempts by some studies to provide evidence for exocytosis of gliotransmitters in slice preparations. For example, in a recent study in the CA1 region of hippocampus (Kang *et al.*, 2013), clamping astrocytic Ca^{2+} at a high concentration of 100-150nM resulted in an increase in neuronal NMDAR fEPSP. However, when DAAO and a SR inhibitor where added to the patch clamp pipette, NMDAR fEPSP did not increase. This result suggested that astrocytes could enhance neuronal NMDAR activity by releasing D-serine via a calcium dependent mechanism. Furthermore, addition of a tetanus toxin to the patch pipette blocked the increase NMDAR fEPSP. This suggested that the calcium dependent release of D-serine from astrocytes was via a vesicular mechanism.

As mentioned in a previous section, evidence for glutamate release as a result of astrocytic calcium elevation has been provided in brain slice preparations (Fellin *et al.*, 2004). However, it is yet to be determined whether this calcium dependent glutamate release from astrocytes in slice preparation is via an exocytosis mechanism.

An indirect evidence for exocytosis of ATP from astrocytes in brain slice preparations has been provided (Pascual *et al.*, 2005). This evidence comes from the previously mentioned study that used the transgenic mice line called dnSNARE (see section 'The role of purinergic signalling in synaptic transmission and plasticity'). It was shown in this study that in dnSNARE mice, there is a lower level of adenosine-mediated tonic suppression of

neurotransmitter release. It was suggested that this is as a result of less extracellular adenosine concentrations in dnSNARE mice compared to WT mice. As adenosine concentration depends on release and breakdown of ATP, the authors suggested that impairment of VAMP-dependent exocytosis of ATP in dnSNARE mice is the reason for lower level of adenosine-mediated tonic suppression in these mice. Therefore, this study provides indirect evidence for ATP release via exocytotic mechanism from astrocytes. A more direct evidence for calcium-dependent exocytosis of ATP from astrocytes remains to be affirmed.

Gliotransmitter release via other mechanisms: As mentioned above, the density of astrocytic SLMVs is much less than synaptic vesicles. Therefore, it has been suggested that other mechanisms of gliotransmitter release could be involved in astrocytes. Studies in cultured hippocampal astrocytes have shown evidence for release of gliotransmitters via Ca^{2+} dependent exocytosis from lysosomes (Li *et al.*, 2008, Liu *et al.*, 2011). It was shown that lysosomes and SLMVs co-exist in cultured astrocytes (Liu *et al.*, 2011). Non-exocytotic mechanisms have also been suggested. One such mechanism is via P2X7 receptors. The P2X7 receptor is unusual compared to other P2X receptors because of formation of a large pore after its activation. It has been proposed that ATP and glutamate might be released from astrocytes in this manner (Suadicani *et al.*, 2006, Hamilton *et al.*, 2008). However, release through P2X7 receptors takes place only in pathological conditions and not physiological conditions. Another mechanism proposed is the release of ATP and glutamate through connexin hemichannels (Contreras *et al.*, 2002, Stout *et al.*, 2002, Ye *et al.*,

2003). A possible mechanism is via Volume regulated anion channels (VRACs). This has been shown to occur during pathological conditions such as ischemia (Phillis *et al.*, 1997) and involves the release of amino acids such as glutamate from astrocytes in response to their swelling as a result of ion and water entry. However, it has been suggested that this mechanism could also occur under physiological conditions as a result of mild swelling induced by glutamate and K^+ uptake by astrocytes (Crepel *et al.*, 1998, Amzica and Neckelmann, 1999, Kimelberg, 2004). A recent study has shown that calcium elevations in cultured astrocytes as a result of TFLLR application results in glutamate release not by vesicular exocytosis but via bestrophin-1 channels (Woo *et al.*, 2012). Therefore, calcium-dependent gliotransmitter release does not necessarily mean that the release mechanism is exocytotic. Furthermore, not every astrocytic calcium elevation leads to gliotransmitter release.

There exists an important study (Agulhon *et al.*, 2010) where Ca^{2+} levels were specifically increased in hippocampal astrocytes (and not neurones) by using an RF (Arg-Phe) amide in slices of transgenic mouse line that expressed MAS-related G protein-coupled receptor member A1 (MRGA1) specifically in astrocytes. Subsequent to this astrocyte-specific calcium elevation, no changes on short or long term plasticity where seen. Furthermore, in the same study, prevention of astrocytic Ca^{2+} oscillations via IP_3 receptor type 2 (IP_3R2) knockout mice (IP_3R2 is specific to astrocytes) did not alter short or long term potentiation. The authors concluded that either calcium dependent gliotransmitter release is not involved in synaptic plasticity or that Ca^{2+} elevations are not the sole trigger for gliotransmitter release. The conclusion from this report was

important because it indicated that in addition to calcium elevation, other intracellular signalling pathways might also be required for vesicular and non-vesicular release of gliotransmitters. An example supporting this idea is the generation of SICs via activation of astrocytes using PAR1 agonist but not by activation of astrocytic $P2Y_1$ receptors (Shigetomi *et al.*, 2008). Activation of both PAR-1 and $P2Y_1$ receptors results in calcium elevation in astrocytes but only PAR1 activation leads to generation of SICs.

In summary, astrocytic gliotransmitter release can involve a multitude of possible mechanisms, some of which might or might not have physiological relevance. Most of these mechanisms are dependent on elevations of astrocytic calcium levels. However, not every calcium elevation will have the same outcome. Furthermore, it is likely that different mechanisms of gliotransmitter release will have different effects on synaptic transmission. Therefore, in the investigation of role for gliotransmitter release in synaptic transmission and plasticity, one must take into account the mechanisms by which gliotransmitters are released.

1.12 Project Objectives and hypothesis

The purpose of this project was to investigate the role of gliotransmitter release in synaptic plasticity during LTP induction. Given that the cortex is involved in memory and cognition, my aim in this project was to investigate gliotransmitter role in synaptic plasticity in the cortex. Furthermore, given that calcium-dependent exocytosis of gliotransmitters is the mechanism of release that has been mostly debated my aim was to investigate the role for gliotransmitter

release mediated via calcium-dependent vesicular exocytosis. For this purpose, I used the pharmacological agent PAR1 agonist and the transgenic dnSNARE mice. I will separate this general aim into different specific objectives:

Role for astrocytic D-serine: Role for astrocytic D-serine release in LTP induction has been shown in hippocampus and hypothalamus (Panatier *et al.*, 2006, Henneberger *et al.*, 2010) but not in the cortex. In this project, I have attempted to investigate whether vesicular release of D-serine from astrocytes is also important in LTP induction in the somatosensory cortex.

Role for astrocytic glutamate: Evidence for glutamate release as a result of astrocytic calcium elevation has been shown in brain slices (Fellin *et al.*, 2004). However, there is still no evidence from brain slices showing whether this astrocytic glutamate release is via vesicular exocytosis. Furthermore, the functional significance of this astrocytic glutamate release in synaptic transmission and plasticity has not been shown. It has been shown that glutamate release from astrocytes can activate neuronal extra-synaptic GluN2B-containing NMDARs (Fellin *et al.*, 2004) but whether these receptors are involved in LTP induction is controversial (see section 1.8). Therefore, one of my aims was to investigate whether glutamate is released from astrocytes unto neurones via calcium-dependent vesicular exocytosis. My other aim was to investigate whether extra-synaptic GluN2B-containing NMDA receptors are involved in LTP induction in the somatosensory cortex.

Role for ATP release: It has been shown that tonic extracellular adenosine levels depend on vesicular exocytosis from astrocytes (Pascual *et al.*, 2005). As adenosine levels depend on ATP breakdown, this suggests that astrocytes release ATP via vesicular exocytosis. However, as yet, there is no direct evidence for calcium-dependent exocytosis of ATP from astrocytes. As mentioned above, it has been shown that ATP is involved in modulation of synaptic transmission by modulating the activity of other receptors such as NMDARs and $GABA_A$Rs (Lalo *et al.*, 2009, Baxter *et al.*, 2011). Therefore, my aim was to provide evidence for calcium dependent exocytosis of ATP from astrocytes and to investigate the role of this astrocytic ATP release in modulation of synaptic transmission and plasticity.

My first hypothesis was that astrocytes release gliotransmitters via calcium-dependent vesicular exocytosis. My second hypothesis was that calcium-dependent exocytosis of ATP, glutamate and D-serine from astrocytes can positively modulate synaptic transmission and LTP induction in the somatosensorycortex.

Chapter 2: Materials and Methods

2.1 Animals

Experiments were performed in somatosensory cortex of dnSNARE transgenic mice (Zhang *et al.*, 2004), their WT littermates and transgenic mice expressing enhanced green fluorescent protein (EGFP) under the control of the glial fibrillary acidic protein (GFAP) promoter (Nolte *et al.*, 2001). Mice were 1 to 3 months old.

Generation of transgenic dnSNARE mice as a tool for investigating vesicular exocytosis by astrocytes: As was mentioned in the introduction, there is mounting evidence that astrocytes can release gliotransmitters via SNARE protein dependent mechanisms. One of the proteins involved in this exocytosis mechanism is VAMP2. Astrocytic expression of VAMP2 and cellubrevin has been shown in brain slices (Bezzi *et al.*, 2004, Wilhelm *et al.*, 2004, Martineau *et al.*, 2013). In 2005, dnSNARE mice were generated by a group of researchers (Pascual *et al.*, 2005). Here, I will give a brief explanation on how these researchers generated this transgenic mice line. It has been shown that expression of an exogenous SNARE domain prevents the formation of endogenous SNARE complex (Hua and Scheller, 2001); hence preventing vesicular-mediated exocytosis. For this purpose, the cytosolic portion of VAMP2 (amino acids 1 to 96) was selectively expressed in astrocytes in order to block gliotransmission (Pascual *et al.*, 2005). Two lines of transgenic mice were developed. The first transgenic line (GFAP-tTA mouse) contained the 2kB human GFAP promoter followed by tTA (tetracycline transactivator) gene. GFAP is an intermediate filament expressed specifically by astrocytes and not neurons. In GFAP-positive

astrocytes of GFAP-tTA mice, GFAP promoter derives the expression of tTA. The second transgenic mice line was the tet-operator (*tetO*) transgenic mice line, which contained three constructs. Each construct contained the *tetO* responsive element promoter. For the first construct, *lacZ* sequence was downstream of *tetO* whilst the second construct contained EGFP domain and the third construct contained the dnSNARE domain. The three constructs were co-injected into C57/CH3 hybrid zygotes. The *tetO* transgenic mice were mated with GFAP-tTA transgenic mice. This crossing yielded mice lines that express SNARE, *LacZ* and EGFP in GFAP-positive astrocytes and not in neurones. The *LacZ* and EGFP are the reporters of the dnSNARE expression. *LacZ* was only expressed in astrocytes suggesting that dnSNARE domain is selectively expressed in astrocytes. Astrocytes that show EGFP expression are highly likely to express the SNARE domain of VAMP2, which blocks gliotransmission. Expression of the SNARE domain of VAMP2 during development might have detrimental effects. To prevent this, doxycycline (Dox) is supplied to mice drinking water (25μg/ml) until 3 weeks of age. Doxycycline is then removed from drinking water. 4 weeks subsequent to the removal of Dox, electrophysiological experiments are performed. Doxycyline binding to tTA prevents the binding of tTA to *tet*O, hence suppressing expression of transgenes. The crossed transgenic mice line was called dnSNARE mice.

2.2 Drugs

Tables 2.1a, 2.1b and 2.1c show the list of pharmacological agents used in this project

Name	Abbreviation	Function	Company
Thr-Phe-Leu-Leu-Arg-NH2	TFLLR-NH2	PAR-1 selective agonist	Tocris Bioscience (Bristol, UK)
Anandamide	AEA	Endogenous cannabinoid receptor agonist	Tocris Bioscience (Bristol, UK)
N-(piperidin-1-yl)-5-(4-iodophenyl)-1-(2,4-dichlorophenyl)-4-methyl-1H-pyrazole-3-carboxamide	AM251	CB1 receptor antagonist	Tocris Bioscience (Bristol, UK)
Adenosine-5'-(γ-thio)-triphosphate tetralithium salt	ATPγS	Non-hydrolysable P2 receptor agonist	Tocris Bioscience (Bristol, UK)
6,7-dinitroquinoxaline-2,3-dione	DNQX	Selective AMPA antagonist	Tocris Bioscience (Bristol, UK)
threo Ifenprodil hemitartate	Ifenprodil	GluN2B subunit- selective NMDAR antagonist	Tocris Bioscience (Bristol, UK)
D-serine	D-serine	Glycine agonist at the NMDAR	Tocris Bioscience (Bristol, UK)
5-(3-bromophenyl)-1,3-dihydro-2H-benzofuro[3,2-e]-1,4-diazepin-2-one	5-BDBD	P2X4 receptor antagonist	Tocris Bioscience (Bristol, UK)
2-amino-5-phosphonovaleric acid (D-AP-5)	D-AP5	Competitive NMDAR glutamate site antagonist	Abcam biochemicals (Bristol UK)
DL-2-Amino-5-phosphonopentanoic acid	DL-AP5	Competitive NMDAR glutamate site antagonist	Abcam biochemicals (Bristol UK)
4-[[4-Formyl-5-hydroxy-6-methyl-3-[(phosphonooxy)methyl]-2-pyridinyl]azo]-1,3-benzenedisulfonic acid tetrasodium salt	PPADS	P2 receptor antagonist	Abcam biochemicals (Bristol UK)
2-(3-Carboxypropyl)-3-amino-6-(4 methoxyphenyl) pyridazinium bromide	Gabazine	Competitive selective $GABA_A$ receptor antagonist	Abcam biochemicals (Bristol UK)
Tetrodotoxin	TTX	Selective inhibitor of Na^+ channel conductance	Tocris Bioscience (Bristol, UK)
Sodium Fluoroacetate	FAC	Disrupts the Krebs cycle	Sigma-Aldrich biochemicals (Dorset, UK)

Table 2.1a

Name	Abbreviation	Function	Company
Picrotoxin	PTX	$GABA_A$ receptor antagonist	Sigma-Aldrich biochemicals (Dorset, UK)
6-Cyano-7-nitroquinoxaline-2,3-dione, FG-9065	CNQX	Competitive AMPA/kainate glutamate receptor antagonist	Sigma-Aldrich biochemicals (Dorset, UK)
L-Glutamic acid	Glutamate	Agonist for different glutamate receptors	Sigma-Aldrich biochemicals (Dorset, UK)
8,8'-[Carbonylbis(imino-4,1-phenylenecarbonylimino-4,1-phenylenecarbonylimino)]bis-1,3,5-naphthalenetrisulfonic acid hexasodium salt	NF279	P2X1-3 receptor antagonist	Tocris Bioscience (Bristol, UK)
R-(R*,S*)]-6-(5,6,7,8-Tetrahydro-6-methyl-1,3-dioxolo[4,5-g]isoquinolin-5-yl)furo[3,4-e]-1,3-benzodioxol-8(6H)-one	Bicuculline	$GABA_A$ antagonist	Tocris Bioscience (Bristol, UK)
(S)-1-[2-[Tris(4-methoxyphenyl)methoxy]ethyl]-3-piperidinecarboxylic acid	(S)-SNAP5114	GABA transporter inhibitor, showing selectivity for GAT2 and GAT3	Sigma-Aldrich biochemicals (Dorset, UK)
6-Methyl-2-(phenylethynyl)pyridine hydrochloride	MPEP	Highly selective mGluR5 metabotropic glutamate receptor antagonist	Sigma-Aldrich biochemicals (Dorset, UK)
2R*,3S*)-1-(Phenanthrenyl-3-carbonyl)piperazine-2,3-dicarboxylic acid	UBP141	GluN2C/GluN2D subunit selective NMDAR antagonist	Abcam biochemicals (Bristol UK)

Table 2.1b

Name	Abbreviation	Function	Company
Magnesium chloride Calcium chloride Sodium chloride Potassium chloride Sodium bicarbonate Casium Chloride Sodium dihydrogen monophosphate Glucose Guanosine triphosphate Magnesium Adenosine triphosphate Ethylene glycol-bis(β-aminoethyl ether)-N,N,N′,N′-tetraacetic acid tetrasodium salt 4-(2-Hydroxyethyl)piperazine-1-ethanesulfonic acid, N-(2-Hydroxyethyl)piperazine-N′-(2-ethanesulfonic acid)	$MgCl_2$ $CaCl_2$ NaCl KCl $NaHCO_3$ CsCl NaH_2PO_4 $C_6H_{12}O_6$ GTP MgATP EGTA HEPES	Salts for Krebs and intracellular solution	Sigma-Aldrich biochemicals (Dorset, UK)
Bis[2-(acetyloxymethoxy)-2-oxoethyl]-[2-[2-[2-[bis[2-(acetyloxymethoxy)-2-oxoethyl]amino]-5-methylphenoxy]ethoxy]-4-[3,6-bis(dimethylamino)xanthen-9-ylidene]cyclohexa-2,5-dien-1-ylidene]azanium bromide	Rhod-2 AM	Cell permeable fluorescent Ca^{2+} indicator	Abcam biochemicals (Bristol UK)
Glycine, N-[4-[6-[(acetyloxy)methoxy]-2,7-difluoro-3-oxo-3H-xanthen-9-yl]-2-[2-[2-[bis[2-[(acetyloxy)methoxy]-2-oxoethyl]amino]-5-methylphenoxy]ethoxy]phenyl]-N-[2-[(acetyloxy)methoxy]-2-oxoethyl]-,(acetyloxy)methyl ester	Fluo-4 AM	Fluorescent calcium indicator	Sigma-Aldrich biochemicals (Dorset, UK)
Fura 2 acetoxymethyl ester	Fura-2 AM	Fluorescent calcium indicator	Abcam biochemicals (Bristol UK)

Table 2.1c

2.3 Cortical Slice Preparation

Cervical dislocation was carried out on mice prior to decapitation in accordance with United Kingdom legislation. After decapitation, brains were rapidly dissected on ice-cold physiological saline **cutting** solution containing (in mM): 130 NaCl, 2.7 KCl, 3 $MgCl_2$, 0.5 $CaCl_2$, 18 $NaHCO_3$, 1 NaH_2PO_4, 15 glucose and pH 7.4 gassed with 95% O_2 to 5% CO_2. Dissected brain was glued to a vibratome chamber containing the cutting solution. Coronal cortical slices (300 μm thick) were cut using a vibrating slicer (Manual advance vibroslice, World Precision Instrument, USA) at 4°C. Cortical slices were then incubated in a chamber containing the **incubating** solution at room temperature for 2-6 hours prior to field EPSP or whole cell voltage clamp recording. The incubating solution was same as the cutting solution except that the incubating solution contained (in mM) 1 $MgCl_2$ and 2.5 $CaCl_2$.

2.4 Electrophysiological recordings

Whole-cell voltage-clamp recordings: Whole-cell voltage-clamp recordings from layer 2/3 pyramidal neurones were made with patch pipettes (5-10 MΩ) filled with intracellular solution (in mM): 5 NaCl, 5 $MgCl_2$, 10 HEPES, 0.5 GTP, 5 MgATP, 10 EGTA, 1 $CaCl_2$, 110 CsCl with a pH of 7.33. Slices were perfused with physiological saline at a rate of 1.5-2.5 ml/min. The physiological saline used for perfusion was the same as the incubating solution. The patch pipettes were thin walled glass microelectrode (World Precision Instruments, USA). Evoked and spontaneous currents were recorded using an AxoPatch200B

patch-clamp amplifier (Axon Instruments, USA) filtered at 2 kHz and digitized at 5 kHz. Experiments were controlled by PCI-6229 data acquisition board (National Instruments, USA) and WinFluor software (Strathclyde Electrophysiology Software, UK). Series resistances were 5-12 MΩ and input resistances were 500-1100 MΩ; both varied by less than 20% in the cells accepted for analysis.

For activation of synaptic inputs and fEPSPs, layer 4 of cortex was stimulated using a concentric bipolar microelectrode with 127 μm thick core diameter and 4 μm thick tip diameter (World Precision Instruments, USA). A constant current stimulator isolator (A.M.P.I ISO-Flex, IBIS Instrumentation Canada Inc) was used for evoking synaptic currents. Stimulus duration was 300 μs.

During spontaneous EPSC recordings, in order to trigger synaptically driven astroglial Ca^{2+} transients, High Frequency Stimulation (HFS) consisting of 5 pulses at 100 Hz was delivered to EPSC recordings. This HFS was repeated twice with an interval of 200 ms.

Field EPSP recordings: Slices were perfused with physiological saline as above. Thin walled glass microelectrode (World Precision Instruments, USA) was placed at layer II/III of the cortex. The pipette was filled with the same physiological saline used for perfusion of brain slices. Pipette resistances were 1-2 MΩ.

For induction of synaptic plasticity, HFS was repeated 10 times with 200 ms interval. This 10× repetition of HFS was called Theta Burst stimulation (TBS). Each HFS consists of 5 pulses; therefore each **sequence** of TBS consists of total of 50 pulses. One, two, three or five sequences of TBS were delivered in an attempt to induce synaptic plasticity. Each sequence was delivered once every ten seconds. Prior to TBS protocol or drug application, at least 10 minutes of steady baseline field EPSP (fEPSPs) were recorded. Baseline fEPSP were obtained at 0.1 Hz (every 10 sec) using a stimulation intensity that produced approximately 30-50% of maximal response.

Input-output protocol: Input refers to stimulating amplitude in mAs. **Output** refers to the size of the recorded fEPSP. Stimulus amplitude was increased from 0 mA to 1.4 mA in steps of 0.1 mA whilst recording fEPSPs.

Paired pulse protocol: Two simulating pulses were delivered with time intervals of either 50 ms or 200 ms, whilst recording fEPSPs. For each experiment, each paired pulse protocol was repeated 10 times. Paired pulse ratio (PPR) was calculated each time by dividing the fEPSP slope of the second pulse by the fEPSP slope of the first pulse. The average of the 10 PPRs was then taken as the PPR value for that paired pulse protocol in that experiment e.g. PPR during baseline (control) in WT mice.

2.5 Fluorescent calcium imaging in astrocytes

To monitor the cytoplasmic-free Ca^{2+}concentraton $[Ca^{2+}]_i$, cortical astrocytes were loaded by 40 min incubation with Fura-2AM. For fura-2 excitation, cells were alternately illuminated at wavelengths of 340±5 nm and 380±5 nm using the OptoScan monochromator (Cairn, Faversham, UK). Fluorescent images were recorded using Olympus BX51 microscope equipped with UMPLFL20x/NA0.95 objective and 2× intermediate magnification and Andor iXon885 EMCCD camera; exposure time was 35 ms at 2×2 binning; experiments were controlled by WinFluor software. The $[Ca^{2+}]_i$ levels were expressed as F_{340}/F_{380} ratio averaged over the whole-cell image.

To investigate the Ca^{2+} signaling activated by PAR-1 receptor agonist, cortical neurons and astrocytes of WT and dnSNARE mice were loaded with 50 μM Fluo-4. Whole-cell voltage-clamp recordings were used to confirm the identification of neurons and astrocytes and verify the lack of changes in the basic electrophysiological properties of the dnSNARE astrocytes. The Fluo-4 fluorescence signal was excited at 488±10 nm and measured at 530±20 nm; the fluorescent images were recorded and analyzed as described above.

Astrocytes were identified by their morphology under DIC observation and EGFP fluorescence (astrocytes from dn-SNARE and GFAP-EGFP mice).

To investigate astrocytic Ca^{2+} signalling during application of AEA and AM251 to cortical slices, multi-photon fluorescent Ca^{2+}-imaging was used. Astrocytes of

neocortical slices were loaded by 30 min incubation with 1 μM of Rhod-2AM at 33˚C. Multi-photon imaging of neurones and astrocytes was performed using Zeiss LSM-7MP multi-photon microscope coupled with the SpectraPhysics MaiTai pulsing laser; experiments were controlled by ZEN LSM software (Carl Zeiss, Germany). Images were further analyzed offline using ZEN LSM (Carl Zeiss) and ImageJ (NIH) software. The [Ca^{2+}] levels were expressed as ΔF/F ratio averaged over region of interest (ROI). For analysis of spontaneous Ca^{2+} transients in astrocytes, three ROIs located at branches and one ROI located at soma were chosen. Overall Ca^{2+} response to agonists of eCB agonist or synaptic stimulation was quantified using ROI covering the whole cell image.

2.6 Vibro-dissociation technique to acutely isolate neurons and astrocytes

Neurones and astrocytes were acutely isolated using the modified "vibrating ball" technique (Vorobjev, 1991, Lalo *et al.*, 2006). The glass ball (200 μm diameter) was moved slowly some 10–50 μm above the slice surface, while vibrating at 100 Hz (lateral displacements 20–30 μm). This technique preserves the function of membrane proteins and therefore is devoid of many artifacts of enzymatic cell isolation and culturing procedures. The composition of external solution for all isolated cell experiments was (mM) 135 NaCl, 2.7 KCl, 2.5 $CaCl_2$, 1 $MgCl_2$, 10 HEPES, 1 NaH_2PO_4, 15 glucose, pH adjusted with NaOH to 7.3.

2.7 Data Analysis

Field EPSP slope: Extracellular field recordings consisted of an artefact, a pre-synaptic component and fEPSP (Figure 2.1). Please refer to section 3.2 on how these components were distinguished from one another. The **slope** of the fEPSP was taken for analysis (Figure 2.1).

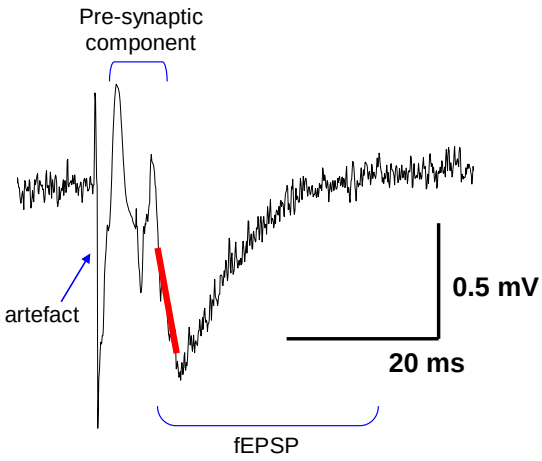

Figure 2.1. Example of an extracellular field recording. The artefact, pre-synaptic component and fEPSP have been highlighted. The red line shows where the slope of fEPSP was taken. This fEPSP slope was taken for analysis.

Forty to sixty minutes post TBS can be taken as a measure of **early** LTP/LTD phase. For each recording, an average fEPSP slope was taken from fEPSPs recorded from 40-60 minutes post TBS delivery. This average fEPSP slope was calculated for all the recordings in each experimental protocol e.g. for TBSx5 delivery to WT mice where n=15, 15 average fEPSP slopes were obtained. Then

the average of these 15 average fEPSPs was taken as the measure of the size of synaptic plasticity for that protocol. This average was calculated for all protocols. These pooled values were then represented as bar-charts (e.g. see Figure 3.3). Average time-courses were also created for fEPSP slopes for each protocol. These are shown alongside their corresponding bar-charts.

Evoked EPSCs: Due to the background noise in the recordings, it is not possible to know the precise value of EPSC amplitude. To be able to obtain consistent values for EPSC amplitudes across the whole recording, each EPSC in the recording had to be fitted with a model curve. Each EPSC was fitted with a model curve with a single exponential rise and decay phases. This was done using a software designed by Yuriy Pankratov (Pankratov and Krishtal, 2003). The offset, rise time and decay time for the model were estimated from the noisy EPSC. These estimates were used to fit a model curve to the EPSC. The parameters of each model curve were reasonably restricted by the range of 1-3 of the initial values. The software used minimal-square root procedure to determine the amplitude of the model curve. The rise time, decay time and offset were optimised by the gradient method to minimise the mean-square error (Pankratov and Krishtal, 2003). The mean square error of the fit was usually 5-20% of the EPSC amplitude. The rise time, decay time and amplitude of the fitted curve were taken for each EPSC.

Spontaneous EPSCs: The software designed by Yuriy Pankratov was used for automatically detecting spontaneous events from the recordings (Pankratov and Krishtal, 2003). The software automatically detected spontaneous EPSCs with

amplitude higher than 2xSD of baseline noise. Subsequent to this initial detection, every single spontaneous event was analysed within the 140 ms time window (40 ms before and 100 ms after peak). This analysis involved the same model fitting procedure as used for evoked EPSC explained above. If the mean square error of the fit exceeded 20%, then that spontaneous current was removed from the analysis.

Quantal Analysis: The software designed by Yuriy Pankratov was used for the following analysis (Pankratov and Krishtal, 2003). The Probability Density Function (PDF) was obtained from the EPSC amplitude distribution of the recording. This was done by convolving each peak measurement (x_i) with a normal distribution $G(0, \sigma)$. The PDF of the peak EPSC was obtained from:

$$P(x) = \frac{1}{N} \sum_{i=1}^{N} G(x_i, \sigma)$$

Where N is the sample size. The optimal width of Gaussian Kernel σ was chosen as 0.2-0.3 SD_{noise}. The SD_{noise} was the standard deviation of the baseline noise amplitude. Such a value is not too small and therefore avoids false peaks. It is also not too large as to obscure the quantal features of PDF.

Discrete peaks in the PDF suggest the presence of quantal release of transmitters. In an ideal situation, if there is no noise to the recording and there is no quantal variance, then the distance between successive peaks would be uniform and would represent the quantal amplitude. Due to the high quantal variance at central synapses, the peaks of the PDF are not resolved uniformly. Therefore, quantal binomial model of release must be fitted to the data to be able to

determine whether the peaks in the amplitude distribution correspond to quantal peaks. For this purpose, two models were fitted to the amplitude distribution. The null hypothesis (H_0) model was a non-quantal unimodal model. The unimodal model means that either 1) the peaks of the amplitude distribution are not quantal peaks (that they are peaks that appear randomly) and so the model is a continuous model or 2) that the amplitude distribution has quantal peaks but the quantal variance (SD_q^2) and/or the SD_{noise} is too large as to obscure the peaks. The unimodal model was a normal distribution with mean (μ) and standard deviation (SD_{EPSC}) of the amplitude distribution. The quantal binomial model was also fitted to the amplitude distribution. This was the alternative hypothesis (H_1). The PDF obtained above was used to estimate the parameters of this model. The distance between the peaks was taken as the preliminary estimate for quantal amplitude (q). The number of apparent peaks was taken as preliminary estimate for the maximal number of quanta/number of release sites (n). The mean quantal content (m) was estimated as either μ/q or as $1/CV^2$. CV is Coefficient of Variation and equals SD_{EPSC}/μ. The probability of release (p), which was assumed to be uniform for all release sites, was estimated as m/n.

The quantal binomial model had the following equation (Redman, 1990):

$$S(x) = \sum_{j=0}^{n} \frac{F_j}{\sqrt{2\pi((SD_{noise})^2 + j(SD_q)^2)}} \exp[-(jx)^2 / 2((SD_{noise})^2 + j(SD_q)^2)$$

where x is the current amplitude and (j) is the number of quantal releases e.g. j=0 means there was no quantal release (response failure). F_j is the probability of release for (j) quantal releases. It is represented by

$$F_j = \binom{n}{j} p^j (1 - p)^{n-j}$$

Both models were optimally fitted to the data using likelihood maximization technique of Expectation maximisation (EM) (Stricker and Redman, 1994), which adjusted the values of the estimated parameters to maximise the log-likelihoods for the best fit to the data. This gave log-likelihood estimates, L_0 and L_1, for each model. L_0 is the log-likelihood of the optimal fit to the unimodal model (H_0) and L_1 is the log-likelihood of the optimal fit to the binomial model (H_1). To compare the fit of the two models (to see whether log likelihood of L_1 is significantly higher than L_0), Wilks statistics (W) was performed

$$W \equiv -2(L_0 - L_1)$$

The distribution of W was assumed to be asymptotically distributed as a χ^2 random variable. The Wilks statistics for the fit of the two models was located on the χ^2 distribution. The binomial model was accepted if the unimodal model could be rejected at significance level $\alpha \leq 0.05$.

All data are presented as mean±SD unless stated otherwise.

Chapter 3: Results 1

Role for calcium dependent gliotransmitter release in synaptic transmission and plasticity.

3.1. Introduction

Previous studies investigating gliotransmitter role in synaptic transmission and plasticity have been carried out in the hippocampus (Pascual *et al.*, 2005, Henneberger *et al.*, 2010) with no report on gliotransmitter role during LTP induction in the cortex. Gliotransmitters can be released via different mechanisms. Calcium-dependent vesicular exocytosis is one possible mechanism of gliotrasnmitter release. Therefore, in this chapter my aim was to investigate the role of calcium dependent exocytosis of different gliotransmitters (glutamate, ATP and D-serine) during synaptic transmission and plasticity in the cortex.

To investigate the role of vesicular gliotransmitters in synaptic transmission and plasticity, the transgenic mice line dnSNARE were used. In dnSNARE mice vesicular release is specifically impaired in astrocytes and not neurones. Researchers who engineered these transgenic mice showed that in the CA1 region of the hippocampus the size of LTP is significantly reduced in these mice compared with recordings from wild-type (WT) mice (Pascual *et al.*, 2005). They attributed this attenuation of LTP to reduced tonic extracellular adenosine levels in dnSNARE mice. They suggested that as vesicular ATP release from astrocytes is impaired in dnSNARE mice, there is less extracellular ATP available to be broken down to adenosine. Therefore, tonic adenosine levels are reduced, resulting in a decrease in tonic suppression of glutamatergic transmission. This leads to a higher baseline glutamatergic transmission. The authors suggested that higher baseline glutamatergic transmission means that during LTP induction there is less extent for potentiation of glutamatergic

transmission, hence resulting in a lower LTP size in dnSNARE mice. Taken together, these results suggested that vesicular release of ATP from astrocytes is involved in LTP modulation in the hippocampus. However, astrocytic vesicular release also involves the release of glutamate and D-serine. Theoretically, release of these gliotransmitters is also impaired in dnSNARE mice. Despite the availability of these mice for 9 years there has not been any investigation in the role of astrocytic glutamate and D-serine (glutamatergic) release using these mice. Therefore, in this project, dnSNARE mice were used to investigate the role of astrocytic release of both purinergic and glutamatergic gliotransmitters during synaptic transmission and plasticity in the somatosensory cortex.

Some of the results in this chapter are based on the previous findings by my colleagues. For this reason, I will introduce these previous findings prior to proceeding to presenting the results obtained in my project.

Evidence for exocytosis of ATP from astrocytes has been provided in culture preparations by previous studies (Coco *et al.*, 2003, Pangrsic *et al.*, 2007). In slice preparations, only indirect evidence has been provided for vesicular exocytosis of ATP from hippocampal astrocytes (Pascual *et al.*, 2005). This indirect evidence was provided by researchers who engineered the dnSNARE mice. As mentioned above, these researchers showed that adenosine-mediated tonic suppression of neurotransmitter release depends on vesicular exocytosis from astrocytes. As adenosine levels depend on ATP breakdown, it was suggested that astrocytes release ATP via vesicular exocytosis. There is yet to be

a report showing direct evidence for calcium-dependent exocytosis of ATP from astrocytes in **slice** preparations.

To investigate whether astrocytes vesicularly release ATP, one must be able to specifically activate release from astrocytes in cortical slices. This would ensure that the evidence for ATP release in the cortex is specifically attributed to an astrocyte release. It has been shown that in hippocampal slices, PAR-1 agonist application can result in G-protein coupled calcium elevations specifically in astrocytes and not neurones (Lee *et al.*, 2007, Shigetomi *et al.*, 2008). It has also been shown that this specific calcium elevation in astrocytes results in glutamate release from these cells. Therefore, PAR-1 agonists can be used for specific activation of gliotransmitter release from astrocytes. My colleagues performed calcium imaging to investigate whether similar to hippocampal astrocytes, astrocytes in the somatosensory cortex also show specific calcium elevations in response to PAR-1 agonist application. For this purpose, pyramidal neurones and astrocytes in layer 2/3 of somatosensory cortex were patch clamped. Calcium indicator Fluo-4 (50 µM) was loaded in the patch pipette to allow for calcium imaging. The membrane holding voltage was set at -40 mV for patched pyramidal neurones and -80 mV for patched astrocytes. Figure 3.1A shows a gradient contrast image of a cortical pyramidal neurone of dnSNARE mice. The electrophysiological characterisation (using different holding voltages) of this neurone is shown below the image. As can be seen, there is a fast voltage-gated Na^+ current, which indicates that the patched cell was a neurone and not an astrocyte. As shown on Figure 3.1B-D, application of L-glutamate (100 µM) resulted in calcium elevation in the neurones. In contrast, there was no neuronal

calcium elevation with application of TFLLR (30 µM). This was the case for both WT and dnSNARE mice (Figure 3.1D). My colleagues repeated the same procedure was for patch-clamped astrocytes. Figure 3.1E represents a gradient contrast image and an Enhanced Green Fluorescence Protein (EGFP) fluorescent image of a cortical astrocyte from dnSNARE mice. Its electrophysiological characterisation is shown below the images. The large K^+ current and lack of Na^+ current shows that the patched cell is an astrocyte and not a neurone. As shown on Figure 3.1F-H, application of TFLLR resulted in calcium elevation in astrocytes from both WT and dnSNARE mice. This result showed that in the somatosensory cortex, PAR-1 agonist application specifically activates calcium elevations in astrocytes and not neurones. Therefore, PAR-1 agonist can be used as a pharmacological agent for the specific activation of astrocytes.

To investigate whether astrocytes vesicularly release ATP in the cortex, neurones in layer 2/3 of cortex were voltage clamped at membrane potential of -80 mV. P2XR- mediated miniature currents were recorded under tetrodotoxin (1 µM TTX) and antagonists of NMDARs (30 µM D-APV), AMPARs (50 µM CNQX) and $GABA_A$Rs (100 µM picrotoxin) (Figure 3.2). Theoretically, calcium elevation should result in vesicular release from astrocytes. To specifically activate calcium elevation in astrocytes, PAR-1 agonist TFLLR (10 µM) was exogenously applied to cortical slices following 10 minutes of baseline P2XR-mediated miniature EPSC (mEPSC) recordings. As shown on Figures 3.2A and 3.2D, application of TFLLR resulted in a significant increase in P2XR-mediated mEPSCs (increase of 72±21%, n=17). This result suggests that activation of calcium elevation in astrocytes can lead to release of ATP from these cells.

Intracellular calcium elevation can result into vesicular release of transmitters. To show that the release is indeed vesicular, the above-mentioned protocol was repeated in dnSNARE mice. In dnSNARE mice, vesicular release from astrocytes is impaired. Therefore, if astrocytic ATP release is via vesicular exocytosis, then in dnSNARE mice there should be no increase in the frequency of P2XR-mediated mEPSCs. As shown on Figures 3.2B and 3.2E, application of TFLLR failed to increase the frequency of P2XR-mediated mEPSCs. This result provided the first direct evidence that ATP release from cortical astrocytes in slice preparation is via vesicular exocytosis.

As shown on Figure 3.2A, application of PPADS (10 μM), which is a P2XR antagonist, decreased the frequency of P2XR-mediated mEPSCs. With PPADS application, the average decrease in P2XR-mediated mEPSCs frequency was 45±16% (n=7). This provides evidence that the mEPSCs recorded were indeed P2XR-mediated. The reason that not all P2XR-mediated mEPSCs were abolished following application of PPADS is probably because PPADS does not block P2X4 containing receptors. However, P2X4 containing receptors could potentially contribute to purinergic signalling in the cortex (Baxter *et al.*, 2011). Therefore, my colleagues repeated the above protocol with TFLLR in previously characterised P2X4 KO mice (Sim *et al.*, 2006). As shown on Figures 3.2C and 3.2F, application of TFLLR also increased the frequency of P2XR-mediated mEPSCs in P2X4 KO mice but this increase was only 28±15% (n=12), which was significantly lower than in WT mice ($p<0.005$). This result suggests that

P2X4 containing receptors are also activated following release of ATP from astrocytes.

Further analysis of P2XR-mediated mEPSCs revealed that in WT mice, mEPSCs showed bimodal amplitude distributions (Figure 3.2G). The amplitude distributions had peak times at 3.1±0.9 pA and 5.7±1.6 pA whilst the decay time distributions had peaks at 9.1±0.9 ms and 15.3±1.8 ms (n=14). The mEPSCs with slower amplitudes had longer decay times whilst the mEPSCs with larger amplitude had faster decay times (see Figure 3.2A for some example mEPSCs). Application of TFLLR selectively increased the probability of detection of smaller and slower mEPSCs in all 14 neurones tested. In contrast, P2XR-mediated mEPSCs recorded from dnSNARE mice did not show two peaks in the distributions of amplitude or decay times (Figure 3.2H). The P2XR-mediated mEPSCs showed only a unimodal distribution, with peak corresponding to large and fast mEPSCs. Application of TFLLR failed to change the amplitude and decay times of these mEPSCs.

Taken together, these results showed that P2XR-mediated mEPSCs have two distinct populations, which differ by their amplitudes and decay times. The larger and faster mEPSCs are present in both WT and dnSNARE mice. This suggested that these larger and faster mEPSCs have neuronal origin. In contrast, the population of mEPSCs that show slower decay times and smaller amplitudes, are only present in WT mice. Furthermore, the increase in frequency of P2XR-mediated mEPSCs as a result of TFLLR application is due to increase in the frequency of these smaller and slower mEPSCs in WT mice. This suggested that

the smaller and slower mEPSCs are due to vesicular exocytosis of ATP from astrocytes.

The results obtained by my colleagues (Figures 3.1 and 3.2) have been published (Lalo *et al.*, 2014). In the same paper further proof for ATP release from astrocytes was provided by using ATP biosensors. It was shown that application of TFLLR onto WT cortical slices resulted in a significant increase in extracellular ATP concentration. This increase was impaired in cortical slices from dnSNARE mice, again suggesting that ATP can be released specifically by astrocytes via vesicular exocytosis following TFLLR application. Please see Figure S10 in the paper for more details.

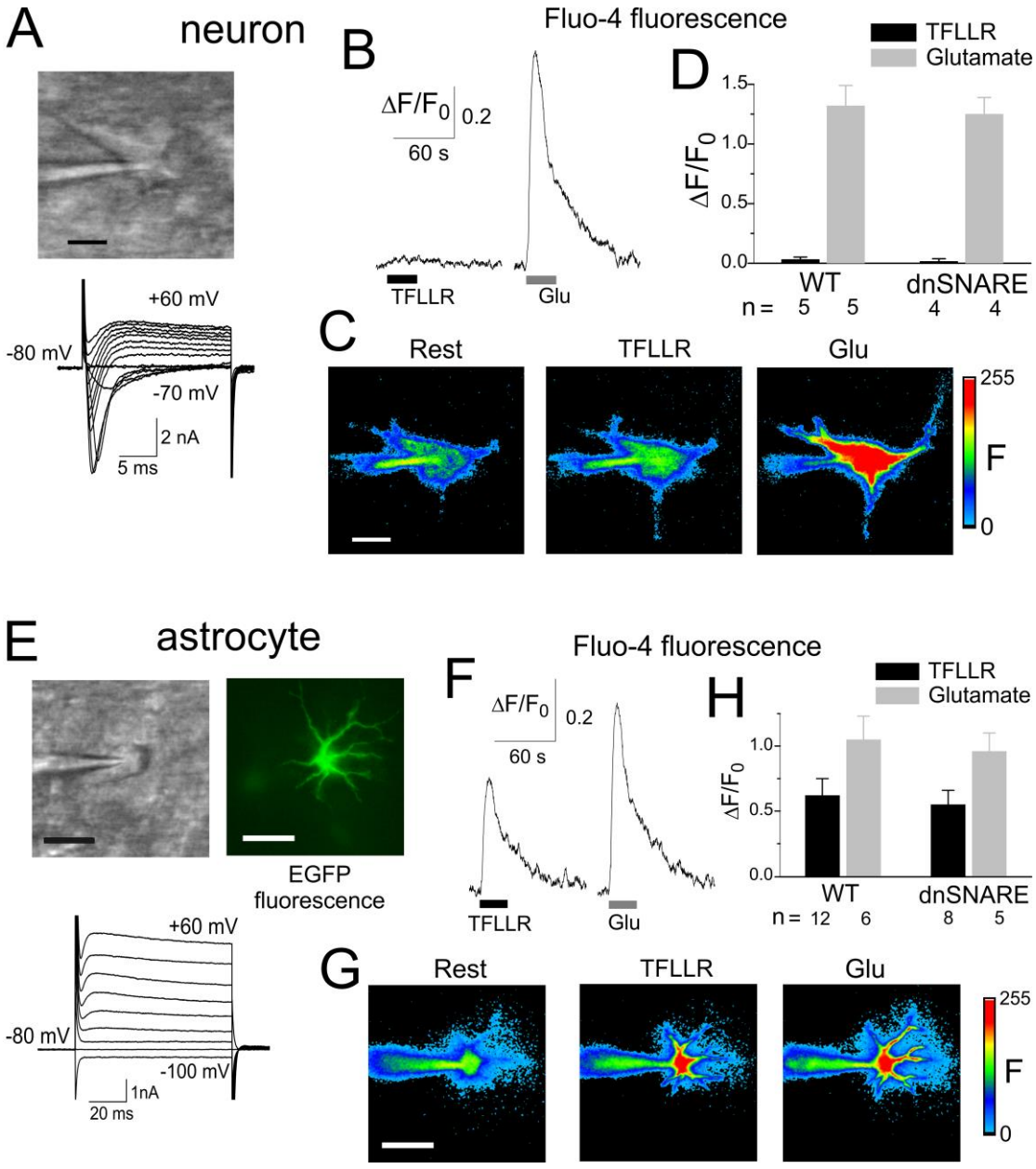

Figure 3.1. Differential action of PAR-1 agonist in the pyramidal neurones and astrocytes of somatosensory cortex. Pyramidal neurones (A-C) and astrocytes (E-G) of layer2/3 of somatosensory cortex of WT and dnSNARE mice were loaded with Ca^{2+} indicator Fluo-4 via patch pipette. Calcium signals were evoked in neurones and astrocytes by a 30-s long rapid application of 30 μM TFLLR and 100 μM L-glutamate to slices. The membrane holding voltage was -40 mV for neurones and -80 mV for astrocytes. **A** represents gradient contrast image and electrophysiological characterisation of neurones of dnSNARE mice. **B** shows Ca^{2+} transients evoked in a neurone of dnSNARE mouse by application of TFLLR and L-glutamate. **C** shows representative pseudo-colour fluorescent images recorded at rest and at the peak of calcium elevation. **D** shows the pooled data of peak calcium elevation. The difference between TFLLR and glutamate was statistically significant (p=0.004, one-way ANOVA). **E** represents gradient contrast image, EGFP fluorescent image and electrophysiological characterisation of astrocytes of dnSNARE mice. **F** shows Ca^{2+} transients evoked in an astrocyte of dnSNARE mouse by application of TFLLR and L-glutamate. **G** shows representative pseudo-colour fluorescent images recorded at rest and at the peak of calcium elevation. **H** shows the pooled data of peak calcium elevation.

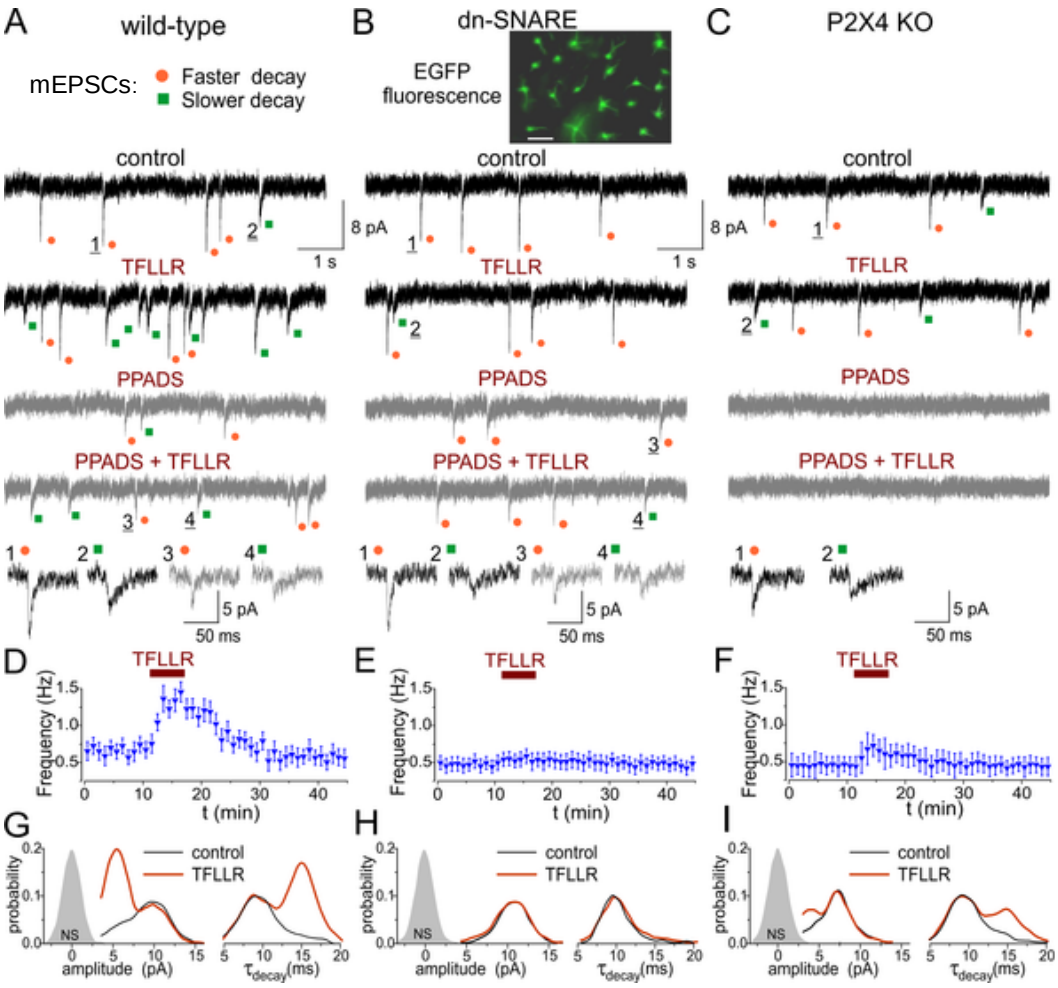

Figure 3.2. Quantal release of ATP from astrocytes in slice preparations. P2XR-mediated mEPSCs were recorded in the presence of TTX (1 μM), CNQX (50 μM) and D-APV (30 μM) and picrotoxin (100 μM) at -80 mV holding voltage. **A-C** show representative transmembrane currents in different experimental conditions. Orange dots represent currents with larger amplitude and kinetics whilst green dots represent currents with smaller amplitude and kinetics. **D-F** show time-courses for change in frequency during application of TFLLR. Each dot represents the frequency calculated for a 1 minute window. For Wt mice n=14, for dnSNARE mice n=18 and for P2X KO mice n=12. **G-H** show the amplitude and decay time distributions for P2XR-mediated mEPSCs before after TFLLR application. Shaded area show the amplitude distribution of background noise. **B** also shows and EGFP fluorescence image from dnSNARE mice. Scale bar is 20 μm.

3.2. Distinguishing the fEPSP from the artefact and pre-synaptic component of the cortical field recording

On way to investigate synaptic transmission and plasticity is to record fEPSPs. To record fEPSPs in the somatosensory cortex, the field-recording pipette was placed in layer 2/3 of cortex whilst layer 4 of cortex was stimulated using a bipolar electrode. These recordings were carried out at a frequency of 0.1 Hz. As can be seen from Figure 3.1, the recorded signal has a complex shape with different components. Experiments were carried out to distinguish between the artefact, pre-synaptic component and fEPSP. Tetrodotoxin (TTX) blocks voltage gated Sodium channels, hence preventing synaptic transmission. Therefore, application of TTX should remove both the pre-synaptic volley and the fEPSP, enabling one to distinguish the stimulus artefact from the rest of the recorded signal. Figure 3.1A shows the effect of TTX (1 μM) application on the recorded signal. As can be seen from this figure, TTX application removed all the components of the recorded signal with the exception of the artefact, which has been highlighted in the figure.

After distinguishing the stimulus artefact, the aim was to distinguish the fEPSP from the rest of the recorded signal. fEPSP is a post-synaptic component. Three experiments were carried out to distinguish the fEPSP from the pre-synaptic component of the signal. One experiment involved application of AMPA receptor antagonist DNQX. fEPSP is as a result of glutamatergic transmission. As glutamatergic transmission involves the opening of AMPA receptors, the post-synaptic component of the recorded signal should be blocked by AMPA

receptor antagonists leaving the pre-synaptic component unchanged. Figure 3.1B shows the effect of DNQX (30 µM) application on the recorded signal. The part of the signal that has disappeared after DNQX application is the AMPAR component of the signal. This is the fEPSP of the signal and has been highlighted as the post-synaptic component on the figure. DNQX application did not block the other components of the recorded signal. This has been highlighted as the pre-synaptic component of the signal.

The other two experiments involved the decrease in pre-synaptic release. Lowering of calcium levels can lead to decrease in pre-synaptic release. Increase in Magnesium concentration can also result in decrease in pre-synaptic release by blocking Calcium channels (Lansman *et al.*, 1986). Therefore, concentrations of Mg^{2+} and Ca^{2+} of the Krebs solution were altered to see the effect on pre-synaptic component and fEPSP. Under control conditions, Krebs contains 1 mM Mg^{2+} and 2.5 mM Ca^{2+}. Change of calcium concentration from 2.5 to 0 mM resulted in decrease in pre-synaptic component and disappearance of the post-synaptic component (Figure 3.3C). Increase of Magnesium concentration from 1 mM to 4 mM also decreased both the pre-synaptic and post-synaptic components (Figure 3.3D).

Taken together, these results distinguish the fEPSP from the artefact and pre-synaptic component of the recorded signal. For subsequent field recordings, the fEPSP component distinguished here is used for investigating synaptic transmission and plasticity.

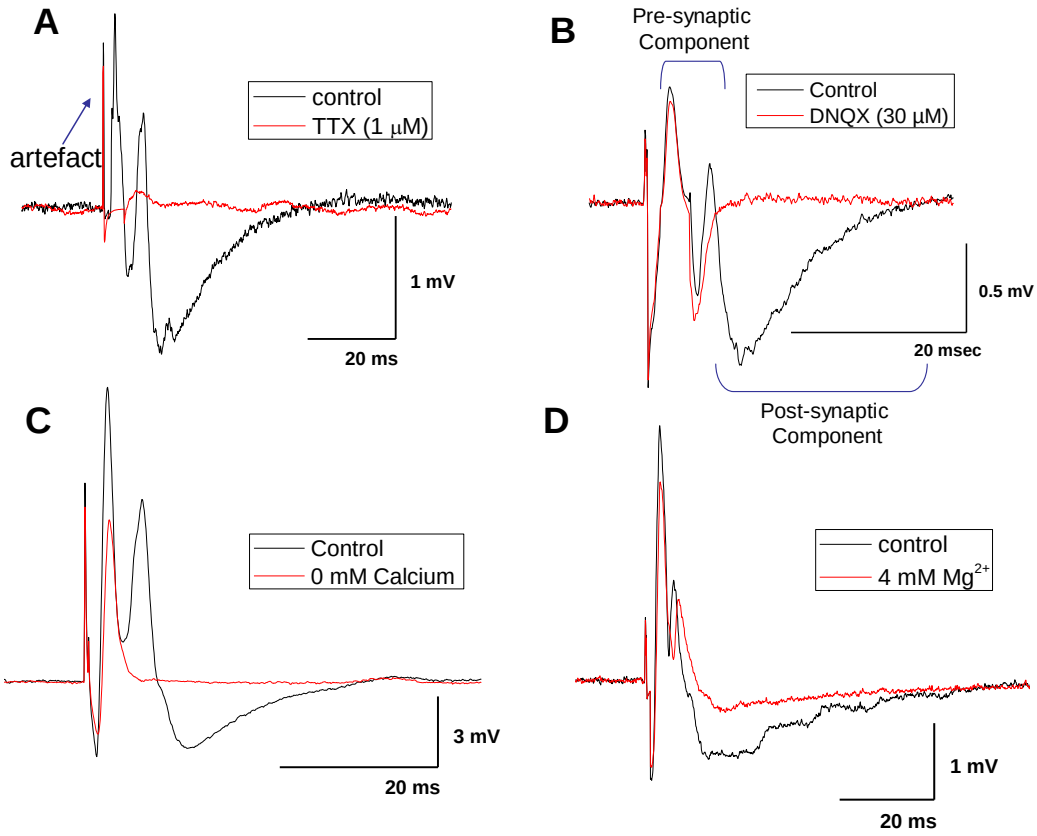

Figure 3.3. Separation of artefact, pre-synaptic component and post-synaptic component of fEPSP. A. 10 minutes application of TTX (1 μM) to fEPSP recording. **B.**. 15 min application of DNQX (30 μM) to fEPSP recording **C.** 10 minute application of 0 mM Ca^{2+} to fEPSP recording. **D.**. 20 minute application of 4 mM Mg^{2+} to fEPSP recording. Control fEPSPs (black) were recorded in 1 mM Mg^{2+} and 2.5 mM Ca^{2+}. Following ten minute baseline recording, the condition was changed (Red). WT mice were used for all the above recordings.

3.3. Stronger stimulation amplitude is required to reach 50% of maximum fEPSP response in cortical slices of dnSNARE mice compared to cortical slices of WT mice

Researchers who developed the dnSNARE mice have shown that in CA1 region of hippocampus, baseline glutamatergic transmission is higher in dnSNARE slices in comparison with control slices (Pascual *et al.*, 2005). They attributed this to lower tonic adenosine levels in dnSNARE mice. The authors suggested that due to impairment of vesicular release from astrocytes in dnSNARE mice, there is a decrease in extracellular ATP. As adenosine levels depend on ATP breakdown, tonic adenosine levels are also reduced, resulting in decrease in tonic suppression of glutamatergic transmission. This leads to a higher baseline glutamatergic transmission. They showed this by recording fEPEPs from CA1 region of hippocampus and changing the stimulus strength at regular intervals. This protocol is called the input-output protocol, where input refers to stimulus strength and output refers to fEPSP size. They showed that fEPSP was larger in dnSNARE mice than in WT mice for the same stimulus strength. To see whether this is the case in the somatosensory cortex, I also performed the input-output protocol in both WT and dnSNARE mice.

For input-output protocol, different stimulus amplitudes were delivered whilst recording fEPSPs at a frequency of 0.1 Hz (Figure 3.4). For stimulus strengths between 0.45 mA to 1.0 mA, fEPSP was significantly larger in WT mice compared to dnSNARE mice ($p<0.01$; two sample independent t-test; n=15 for dnSNARE mice and n=21 for WT mice). The stimulation strength required to

reach 50% of maximum fEPSP response in cortical slices of WT mice is 0.5 pA whilst the stimulation strength required to reach 50% of fEPSP max in dnSNARE mice is 0.7 pA. These results suggest that in dnSNARE mice, larger stimulus strength is required to reach the same level of synaptic transmission as in WT mice. This means that baseline synaptic transmission is larger in cortex of WT mice compared to dnSNARE mice. This result is in contrast to the above-mentioned study in the CA1 region of hippocampus, where baseline synaptic transmission was higher in dnSNARE mice than in WT mice. These results from cortical slices suggest that impairment of vesicular gliotransmitter release from astrocytes results in decrease in baseline glutamatergic transmission in the somatosensory cortex.

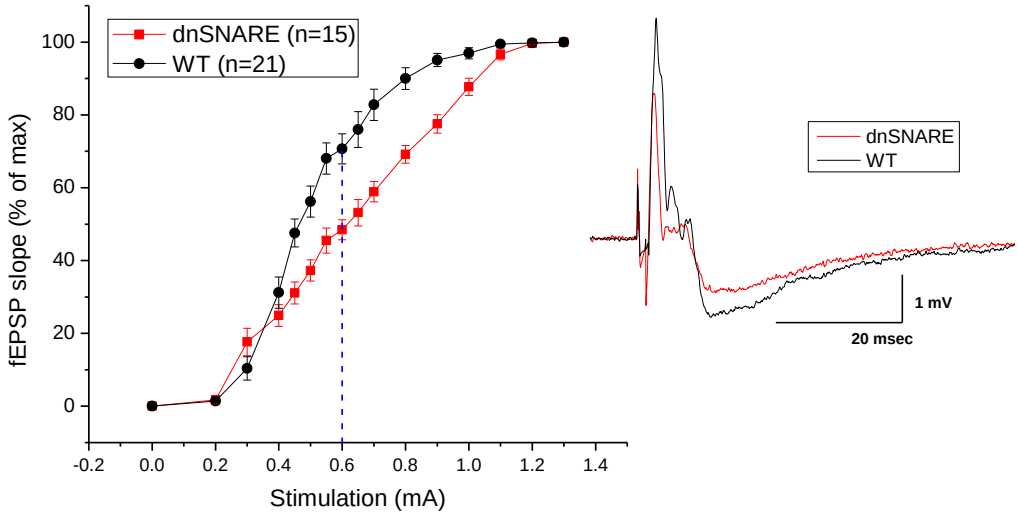

Figure 3.4. Input-output dependence for WT and dnSNARE mice. For stimulus strengths between 0.45 mA to 1.0 mA, fEPSP was significantly larger in cortical slices of WT mice compared to dnSNARE mice ($p<0.01$; 2 sample independent t-test). For the remaining stimulus strengths, there was no statistically significant difference between WT and dnSNARE mice ($p<0.05$). Example fEPSPs from WT and dnSNARE mice are shown on the right of the figure. These examples are from stimulus strength 0.6 mA (dashed blue line). At 0.6 mA, fEPSP is larger for WT mouse than in dnSNARE mouse.

3.4. Vesicular release of gliotransmitters contributes to TBS-induced LTP in the cortex

It has been shown that in the CA1 region of the hippocampus, LTP size is lower in dnSNARE mice compared to WT mice (Pascual *et al.*, 2005). My objective was to investigate whether this was the case in the somatosensory cortex. It has been shown previously that 4-6 trains of TBS application can induce LTP in the cortex (Kirkwood *et al.*, 1993). I used TBSx5 protocol to induce LTP in the somatosensory cortex. As can be seen from Figure 3.5A, delivery of TBSx5 to the somatosensory cortex results in LTP induction. The average percentage change in fEPSP 40-60 minutes post TBS application was +58±7.54% (n=15, Figure 3.5B). TBSx5 was also delivered to cortical slices from dnSNARE mice. In agreement with the abovementioned study of LTP in hippocampus of dnSNARE mice (Pascual *et al.*, 2005), my results showed a significant drop in LTP size in dnSNARE mice (+11±10.1%, n=14) compared to WT mice ($p<0.01$, two sample independent t-test; Figure 3.5A-B). These results show that vesicular gliotrasnmitter release contributes to LTP induction in the somatosensory cortex.

I obtained the data on Figure 3.5 by a joint effort with Dr Oleg Palygin and Dr Jemma Andrew.

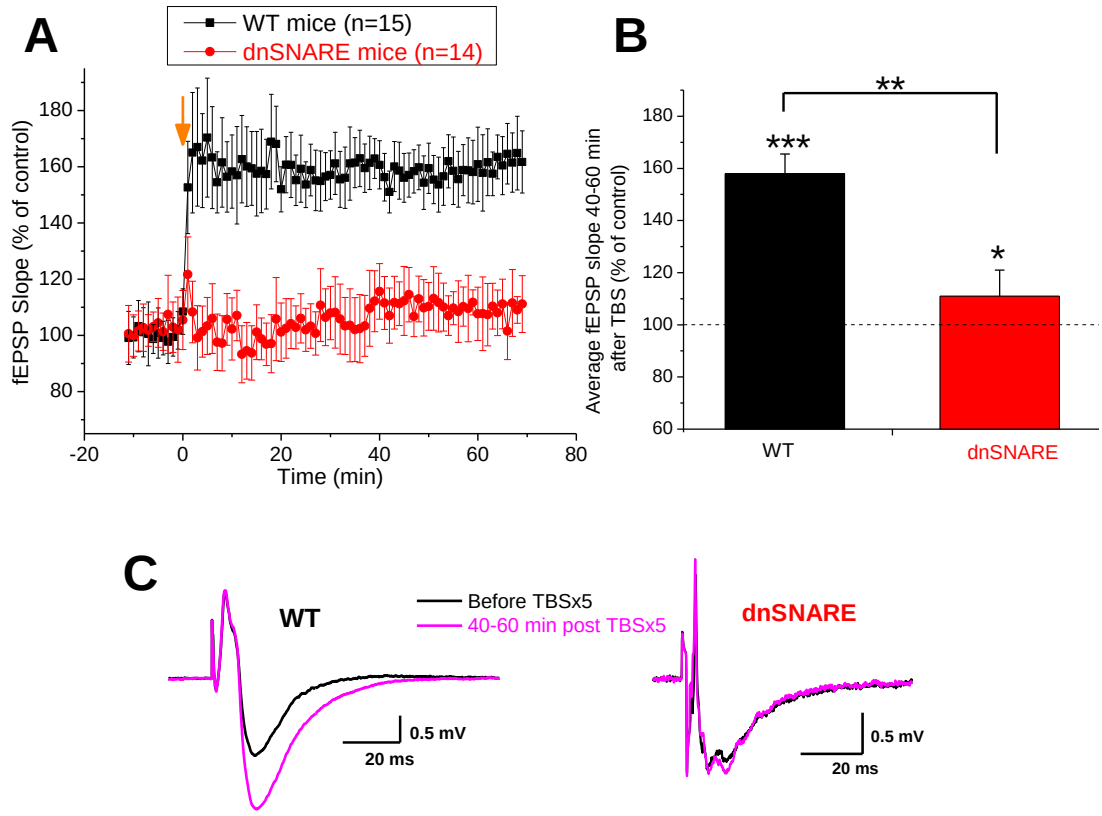

Figure 3.5. Vesicular release of gliotransmitters contributes to TBS induced LTP in the cortex. A shows the average time-courses for LTP recordings in WT and dnSNARE mice. Orange arrow shows position of TBS application. **B** represents the average % increase in fEPSP 40-60 minutes post TBS delivery. Two sample independent t-test was performed between WT and dnSNARE data. Paired t-test was performed for average % change in fEPSP from baseline. $p<0.05$, *; $p<0.01$, **; $p<0.001$, ***. **C** shows example fEPSPs before and after TBSx5 delivery.

3.5. TBSx5-induced LTP in the cortex is an NMDAR dependent form of LTP

It has been shown that TBS-induced LTP is NMDAR-dependent in the hippocampus (Malenka *et al.*, 1989), visual cortex (Kirkwood *et al.*, 1993) and somatosensory cortex (Castro-Alamancos *et al.*, 1995). NMDARs are usually not open at resting membrane potentials as they are blocked by Mg^{2+}. However, high frequency activity of pre-synaptic neurones during TBS delivery can result in depolarisation of post-synaptic neurones thereby leading to opening of post-synaptic NMDARs. The opening of these NMDARs leads to calcium entry into the post-synaptic neurones thereby leading to LTP. To show that my LTP recordings in WT mice were also NMDAR-dependent, the TBSx5 protocol was carried out in the presence of DL-AP5, which is an antagonist of NMDA receptors. After 10 minutes of baseline recordings, DL-AP5 was applied onto the slice. DL-AP5 application did not decrease the size of fEPSP (Figure 3.6). This was as expected because it was shown above that fEPSP consisted of AMPA receptor activity (Figure 3.4B). Following 5 minutes of DL-AP5 application, TBSx5 protocol was applied. As can be seen from Figure 3.6, LTP induction was prevented with DL-AP5 application. This result confirms that TBS-induced LTP in the cortex is an NMDAR-dependent LTP.

The flow-chart on Box 3.1 shows the summary of results that have been shown thus far. I have shown that astrocytic release of gliotransmitters via vesicular exocytosis is required for LTP induction. Gliotransmitters can be divided into two groups: purinergic and glutamatergic. In the following sections I will

investigate the role of these gliotransmitters in synaptic transmission and plasticity.

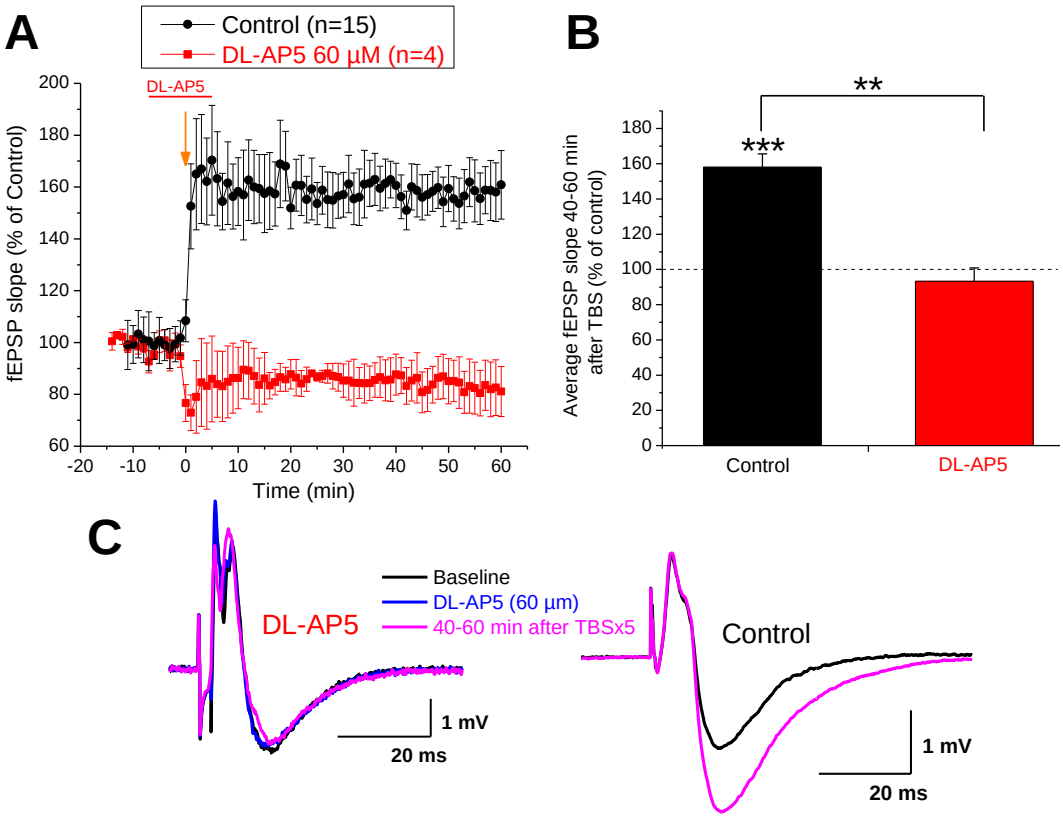

Figure 3.6. TBSx5-induced LTP in the cortex is NMDAR dependent. A shows the average time-courses. These recordings were performed in WT mice. For the DL-AP5 recordings, DL-AP5 was applied 5 minute prior to TBS and washed out 5 minutes post TBS. Orange arrow shows position of TBS application. **B** represents the average % increase in fEPSP 40-60 minutes post TBS delivery. Two sample independent t-test was performed between TBSx5 and TBSx5+DL-AP5 data. Paired t-test was performed for average % change in fEPSP from baseline. $p<0.05$, *; $p<0.01$, **; $p<0.001$, ***. **C** shows example fEPSPs before and after TBSx5 delivery.

Box 3.1.

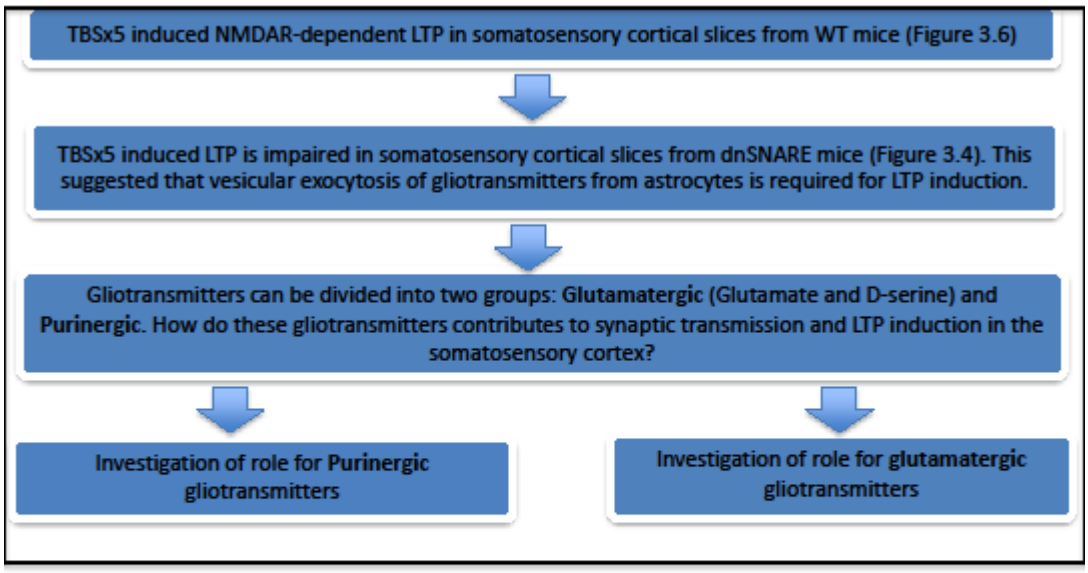
TBSx5 induced NMDAR-dependent LTP in somatosensory cortical slices from WT mice (Figure 3.6)
TBSx5 induced LTP is impaired in somatosensory cortical slices from dnSNARE mice (Figure 3.4). This suggested that vesicular exocytosis of gliotransmitters from astrocytes is required for LTP induction.
Gliotransmitters can be divided into two groups: Glutamatergic (Glutamate and D-serine) and Purinergic. How do these gliotransmitters contributes to synaptic transmission and LTP induction in the somatosensory cortex?
Investigation of role for Purinergic gliotransmitters
Investigation of role for glutamatergic gliotransmitters

3.6. Exogenous ATP, but not exogenous D-serine, can rescue LTP during TBSx5 protocol in cortical slices from dnSNARE mice

As was shown in section 3.4, vesicular release from astrocytes significantly contributes to LTP induction. This suggests that gliotransmitters released from astrocytes could have a role in synaptic plasticity in the cortex. But which one of the gliotransmitters is involved in LTP induction? D-serine has been implicated in modulation of LTP. In a study in the CA1 region of hippocampus, BAPTA was used to chelate Ca^{2+} levels in astrocytes; hence blocking calcium dependent gliotransmitter release (Henneberger *et al.*, 2010). This resulted in a significant reduction in LTP size. This drop in potentiation was rescued when exogenous D-serine was applied to the brain slice. This report suggested a major role in LTP induction for D-serine released by hippocampal astrocytes.

To investigate whether D-serine is also involved in LTP induction in the somatosensory cortex, exogenous D-serine (10 μM) was applied during TBSx5 protocol in dnSNARE cortical slices. Surprisingly, D-serine did not rescue LTP in dnSNARE mice (Figure 3.7). These results suggest that in the somatosensory cortex, vesicular release of D-serine from astrocytes does not contribute to LTP induction.

If D-serine is not the gliotransmitter involved in LTP induction in the somatosensory cortex, then which gliotransmitter contributes to LTP induction? ATP is another gliotransmitter released by astrocytes. One of my aims in this project was to investigate the role of vesicular release of ATP from astrocytes.

ATP can modulate synaptic transmission by modulating the activity of other receptors such as NMDARs and $GABA_A$Rs (Lalo, Andrew et al. 2009; Baxter, Choi et al. 2011). As TBS-induced LTP is NMDAR dependent, ATP release could potentially modulate synaptic plasticity. To investigate this, exogenous ATPγS was applied to dnSNARE cortical slices during TBSx5 protocol. ATPγS is a non-hydrolysable from of ATP, which means that it is not broken down to adenosine. Therefore, application of ATPγS ensures that only the effects of ATP, and not adenosine, are investigated. As shown on Figure 3.7, application of exogenous ATPγS (20 μM) to dnSNARE slices significantly increased the extent of TBSx5-induced LTP compared to control recordings ($p<0.001$, two sample t-test). With ATPγS application, the average increase in fEPSP 40-60 minutes post TBSx5 was +40.54±9.66% (n=6).

Taken together, these results suggest that ATP could be the gliotransmitter that contributes to LTP induction in the somatosensory cortex. Researchers who engineered the dnSNARE mice also showed that ATP release from astrocytes is involved in LTP induction in the hippocampus. However, they attributed this effect to breakdown of ATP to adenosine. Here, I have shown that ATP itself could have a potential role in LTP induction in the somatosensory cortex.

I obtained the data shown on Figure 3.7 in collaboration with Dr Oleg Palygin and Dr Jemma Andrew.

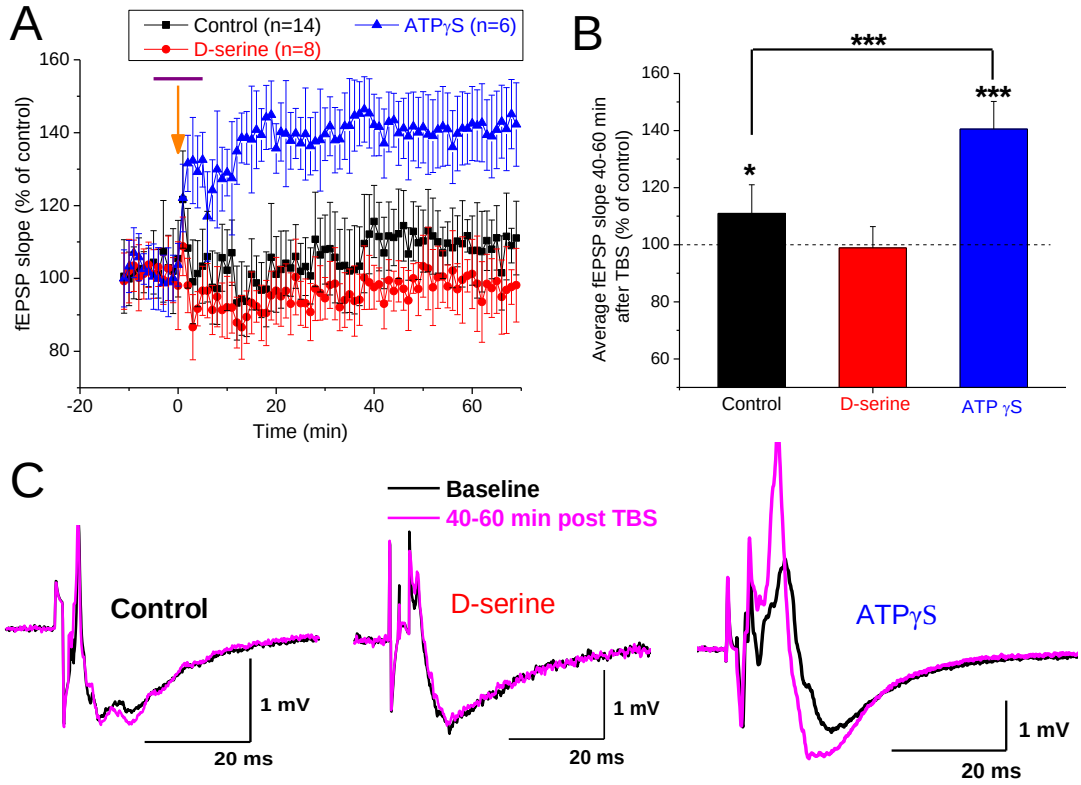

Figure 3.7. Exogenous ATP, but not exogenous D-serine, can rescue LTP during TBSx5 protocol in cortical slices from dnSNARE mice. These recordings were performed in dnSNARE mice. **A** shows the average time-courses. Orange arrow shows position of TBS application. 10 minutes of baseline fEPSP recordings were made before TBS application. Purple bar represents the time-span (5 minutes prior and 5 minutes post TBS) that exogenous ATPγS (20μM) or D-serine (10μM) was applied. **B** represents the average % increase in fEPSP 40-60 minutes post TBS delivery. The average % change in fEPSP for the dnSNARE recordings was +11±10.1%. The average % change in fEPSP for the D-serine recordings was -1.11±7.46%. The average % change in fEPSP for the ATPγS recordings was +40.54±9.66%. Paired t-test was performed for average % change in fEPSP from baseline. Two sample independent t-tests were performed between control and D-serine/ATPγS experiments. $p<0.05$, *; $p<0.01$, **; $p<0.001$, ***. **C** shows example fEPSPs before and after TBSx5 delivery.

3.7. ATP-induced LTP is impaired in cortical slices from dnSNARE mice

As was shown in the previous section, application of exogenous ATPγS can rescue LTP during TBSx5 in dnSNARE mice. This suggested that astrocytic ATP contributes to TBS-induced LTP in the somatosensory cortex. However, it is known that application of exogenous ATP alone, without delivery of HFS or TBS protocol, can induce LTP in WT hippocampal slices from guinea pigs (Fujii, 2004) and rats (Ievglevskyi *et al.*, 2012). This is called ATP-induced LTP. This LTP is only expressed after ATP has been washed out of the slice.

The above-mentioned reports showed ATP-induced LTP in WT slices. However, it is possible that ATP application alone can also induce LTP in dnSNARE cortical slices. If this is the case, it might mean that the LTP rescued via ATPγS application during TBSx5 in dnSNARE mice (shown on Figure 3.7) is not really a rescue of TBSx5-induced LTP but that it is solely dependent on exogenous ATP application i.e. it can be induced in both dnSNARE mice and WT mice in the absence of TBS protocol delivery. Therefore, to investigate whether this is the case in cortical slices, I decided to apply ATPγS in the absence of TBS protocol. As shown on Figure 3.8A, 10 minutes application of exogenous ATPγS (20μM) to WT cortical slices resulted in a significant LTP induction ($p<0.001$). In agreement with the above-mentioned reports in CA1 region of hippocampus, during ATPγS application there was a drop in fEPSP; LTP was only expressed following ATPγS washout. The average increase in fEPSP 40-60 minutes post ATPγS washout was +38±5.84% (n=14; Figure 3.8D). To my knowledge this is

the first time that evidence for ATP-induced LTP has been provided in the somatosensory cortex.

Application of ATPγS to dnSNARE cortical slices resulted in a small non-significant LTP ($p<0.05$; Figure 3.8). The average increase in fEPSP following ATPγS washout was +9.09±5.27% (n=6; Figure 3.8D). There was a significant difference in average change in fEPSP between ATPγS application in WT and dnSNARE mice ($p<0.05$; Figure 3.8D). These results suggest that ATP-induced LTP is impaired in dnSNARE cortical slices. This is in contrast to ATPγS application to dnSNARE cortical slices during TBSx5 delivery where there was a significant LTP. To highlight the difference between ATPγS application in dnSNARE mice when TBSx5 is delivered and when TBSx5 is not delivered, the average time-courses of these two data are shown on Figure 3.7C. There was a significant difference in fEPSP change 40-60 minutes post ATPγS washout between data with TBSx5 and data without TBSx5 (Figure 3.8D).

Taken together, these results suggest that in dnSNARE mice, both TBSx5 induced LTP and ATP-induced LTP are impaired. In dnSNARE mice, LTP is induced only when both protocols are applied together. This is in contrast to WT cortical slices, where separate application of either TBSx5 or ATPγS, induces a large LTP.

Even though in WT slices, ATP-induced LTP does not require HFS or TBS protocol, it is, however, an NMDAR-dependent form of LTP. The mechanism for ATP-induced LTP has been attributed to modulation of post-synaptic

NMDARs via ATP (Fujii, 2004). It has been suggested that ATP can act as a phosphate doner for phosphorylation of NMDARs via plasma membrane associated ecto-protein kinases. This means that ATP can indirectly modulate NMDAR activity thereby leading to Ca^{2+} influx and LTP. In contrast to the results from Fujii, another report suggested that ATP-induced LTP in rat hippoampus is dependent on both P2X and P2Y receptors (Ievglevskyi *et al.*, 2012). Both these reports used exogenous ATP to induce LTP. However, I used ATPγS to induce LTP. As ATPγS is a non-hydrolysable form of ATP, my results suggest that ATP can induce LTP without acting as a phosphate donor. Therefore, it is likely that ATP-induced LTP is mediated via action of P2X and P2Y receptors.

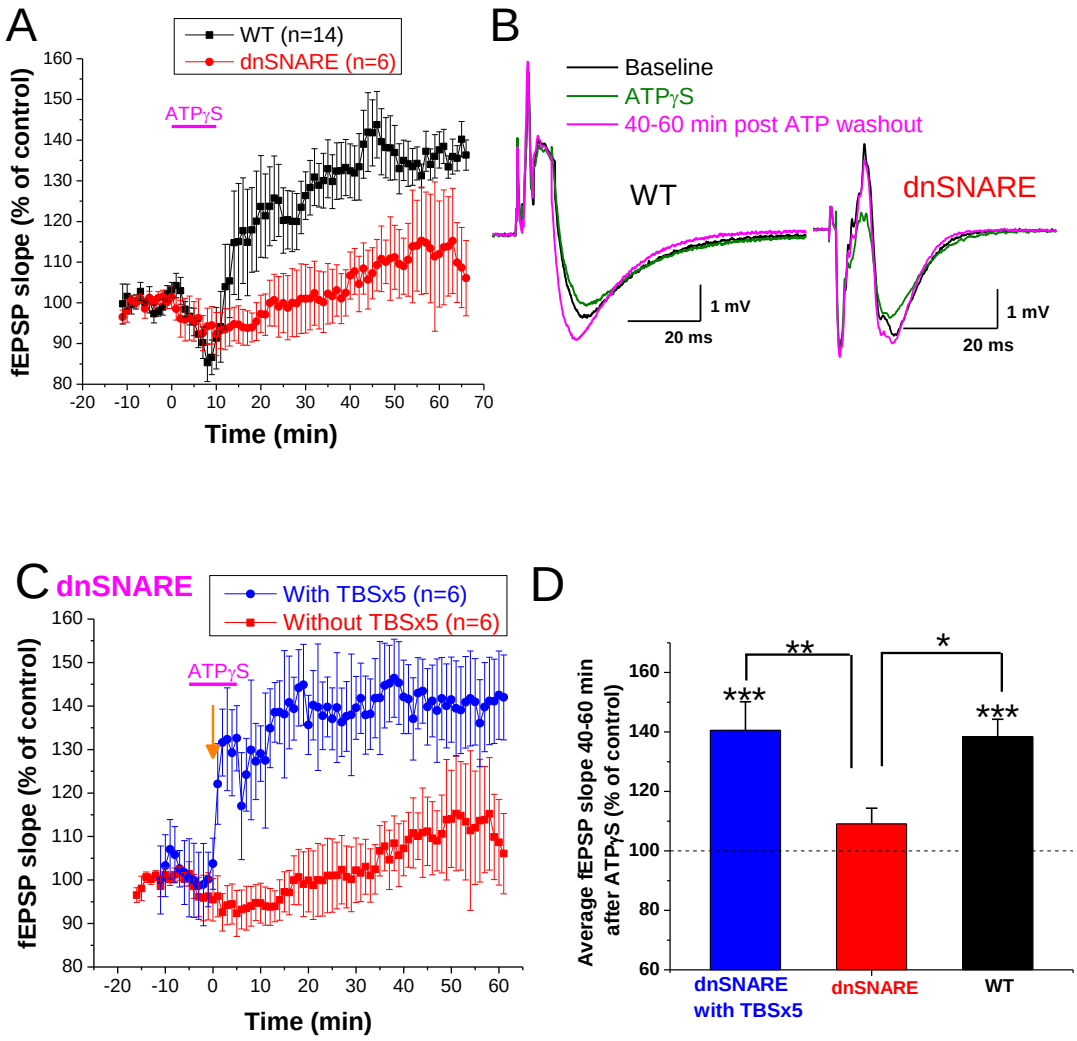

Figure 3.8. ATP-induced LTP is impaired in cortical slices from dnSNARE mice. 10 minutes of baseline fEPSP recordings were made before ATPγS (20μM) application. **A** shows the average time-courses for ATPγS (20μM) application in WT and dnSNARE mice. No TBSx5 protocol was delivered in either case. Purple bar represents the time-span (10 minutes) of exogenous ATPγS (20μM) application. **B** shows example fEPSPs before and after ATPγS application. **C** shows the average time-courses for ATPγS application in dnSNARE mice with and without TBSx5 delivery. Orange arrow shows position of TBSx5 delivery. **D** represents the average % increase in fEPSP 40-60 minutes post ATPγS application. The average % change in fEPSP for ATPγS application in dnSNARE mice with TBSx5 delivery was +40.54±9.66%. The average % change in fEPSP for ATPγS application without TBSx5 delivery in dnSNARE mice was +9.09±5.27%. The average % change in fEPSP for ATPγS application with TBSx5 delivery in WT mice was +38±5.84%. Paired t-test was performed for average % change in fEPSP from baseline. Two sample independent t-tests were performed between each two sets of data. $p<0.05$, *; $p<0.01$, **; $p<0.001$, ***.

Box 3.2.

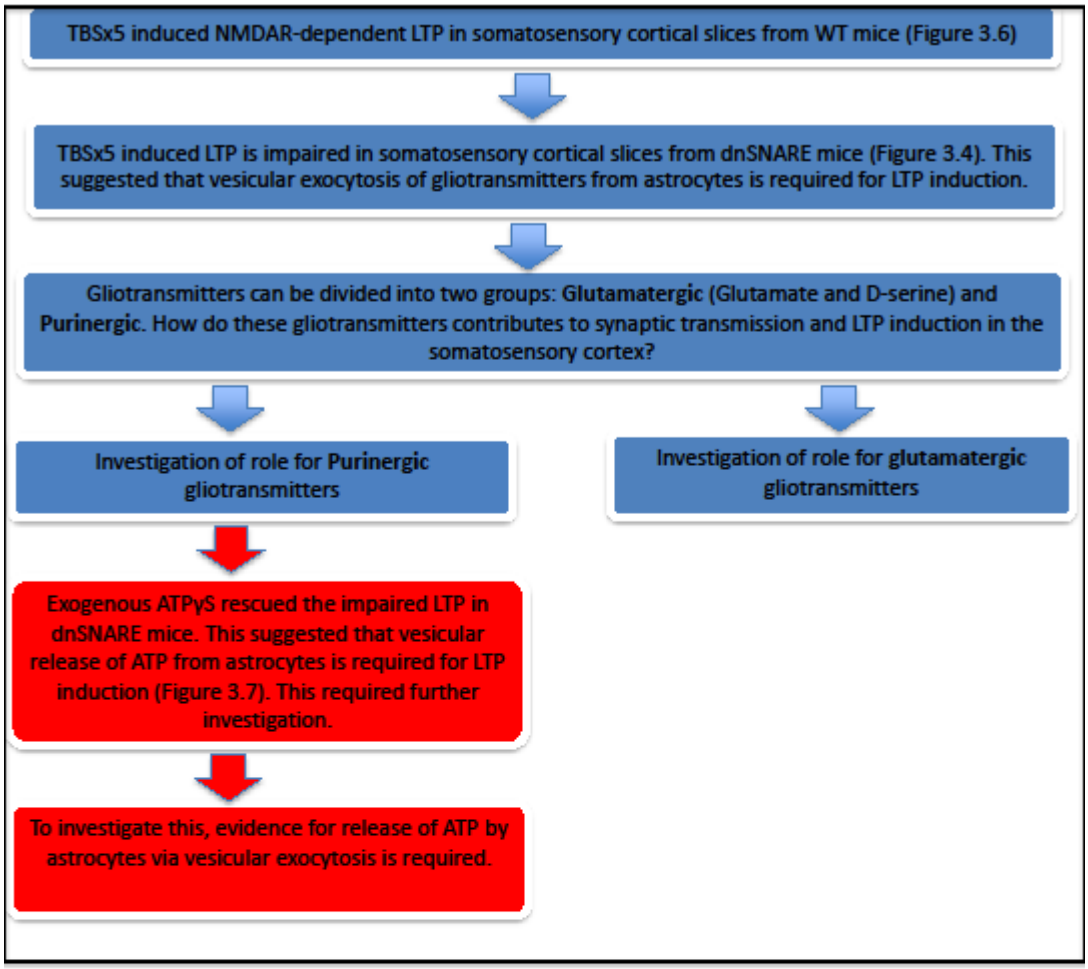
TBSx5 induced NMDAR-dependent LTP in somatosensory cortical slices from WT mice (Figure 3.6)
TBSx5 induced LTP is impaired in somatosensory cortical slices from dnSNARE mice (Figure 3.4). This suggested that vesicular exocytosis of gliotransmitters from astrocytes is required for LTP induction.
Gliotransmitters can be divided into two groups: Glutamatergic (Glutamate and D-serine) and Purinergic. How do these gliotransmitters contributes to synaptic transmission and LTP induction in the somatosensory cortex?
Investigation of role for Purinergic gliotransmitters
Investigation of role for glutamatergic gliotransmitters
Exogenous ATPγS rescued the impaired LTP in dnSNARE mice. This suggested that vesicular release of ATP from astrocytes is required for LTP induction (Figure 3.7). This required further investigation.
To investigate this, evidence for release of ATP by astrocytes via vesicular exocytosis is required.

3.8. Neuronal activity causes vesicular release of ATP from cortical astrocytes in slice preparations

It was shown in section 3.6 that application of exogenous ATPγS can rescue TBSx5-induced LTP in the somatosensory cortex. As a result of this finding it was suggested that astrocytes contribute to LTP induction via release of ATP. Therefore, the next aim of this project was to investigate whether ATP release from astrocytes contributes to synaptic transmission and plasticity. To investigate this, first evidence for ATP release from cortical astrocytes must be provided (see Box 3.2).

Evidence for vesicular release of ATP from astrocytes as a result of pharmacological activation of these cells via TFLLR was provided by my colleagues (see Section 3.1). In this section, the idea was to provide evidence for vesicular release of ATP from astrocytes as a result of activation of these cells via neuronal activity. It has been shown by several studies that neuronal activity can activate calcium elevations in astrocytes via activation of ionotropic and metabotropic receptors on these cells (Palygin *et al.*, 2010, Panatier *et al.*, 2011). As was shown in the previous section, calcium elevation in astrocytes via TFLLR application resulted in release of ATP from these cells. The objective in this section was to see whether calcium elevation in astrocytes as a result of **neuronal activity** could cause the vesicular release of ATP from these cells. For this purpose, neuronal P2XR-mediated currents were recorded in the presence of picrotoxin (100 µM) and CNQX (50 µM) at -80 mV holding voltage. Following 5 minutes of baseline P2XR-mediated spontaneous EPSC (sEPSC) recordings,

an episode of HFS was delivered to the afferent neuronal fibres. The HFS consisted of 5 pulses of 100 Hz stimulation, repeated two times with 200 ms (theta frequency) interval. As shown on Figures 3.9A and 3.9C, delivery of HFS resulted in a 2-fold elevation in the frequency of P2XR-mediated sEPSCs in WT mice. This suggests that following HFS delivery to afferent fibres, there is an increase in ATP release. This ATP release could be as a result of neuronal and astrocytic release. To see whether astrocytic vesicular exocytosis contributes to HFS-induced increase in sEPSCs, the same protocol was repeated in cortical slices from dnSNARE mice. In contrast to WT mice, there was only a modest transient increase in the frequency of P2XR-mediated sEPSCs in dnSNARE mice (Figures 3.9B and 3.9D).

Further analysis of P2XR-mediated sEPSCs was carried out. In WT mice, the average baseline sEPSC amplitude was 8.6±2.4 pA and the average sEPSC decay time was 9.9±2.5 ms (n=6). During the first 30 seconds after HFS delivery, the average amplitude increased to 12.4±4.2 pA and the decay time also increased to 11.2±2.3 ms (Figures 3.9C and 3.9E). One to three minutes post HFS, the average frequency of sEPSCs remained larger than baseline frequency; however the average amplitude decreased below baseline values (Figure 3.9C). This is as a result of increase in population of sEPSCs with lower amplitudes (5.5±1.3 pA) and slower decay times (15.4±2.2 ms) 1-3 minutes post HFS delivery (Figures 3.9E and 3.9G). As the number of these low amplitude sEPSCs increases, the overall average amplitude of sEPSCs (6.86±1.6 pA) drops below baseline. Therefore, as was the case with P2XR-mediated mEPSCs recorded by my colleagues (see Figure 3.2), there exist two distinct populations of purinergic

sEPSCs. One population ("slow" sEPSCs) has smaller amplitude and slower decay times whilst another population ("fast" sEPSCs) has larger amplitudes and faster decay times (Figures 3.9E and 3.9G). Thirty seconds post HFS delivery results in appearance of sEPSCs with large amplitudes (19.6±2.7 pA) and fast decay times (9.2±2.5 ms). The amplitude of these large currents corresponded to double of unitary amplitude of the "fast" purinergic sEPSCs. This suggests that there is an increase in the frequency of these "fast" sEPSCs 30 seconds post HFS delivery. However, 1-3 minutes post HFS delivery shows an increase in the frequency of "slow" sEPSCs.

As was shown on Figure 3.2, TFLLR application resulted in increase in frequency of population of P2XR-mediated mEPSCs that had small amplitudes and slow decay times. It was shown that these mEPSCs were due to vesicular release from astrocytes. As HFS delivery in WT mice also results in increase in these "slow" sEPSCs, one can suggest that these "slow" sEPSCs are due to release of ATP from astrocytes subsequent to activation of these cells via HFS delivery to neuronal afferents. Indeed, as shown on Figure 3.9D, there was no significant increase in frequency of sEPSCs following 1-3 minutes post HFS delivery to neuronal afferents in dnSNARE mice. HFS delivery to dnSNARE mice only resulted in increase in frequency of "fast" sEPSCs 30 seconds post HFS (Figures 3.9D and 3.9F). In dnSNARE mice there was a selective loss of the population of "slow" sEPSCs (Figure 3.9H) again suggesting that these "slow" EPSCs are as a result of astrocytic release.

Taken together, these data suggest that “fast” P2XR-mediated EPSCs are as a result of neuronal release of ATP whilst “slow” P2XR-mediated EPSCs are as a result of calcium dependent vesicular release of ATP from astrocytes. This ATP release from astrocytes can be triggered both pharmacologically (TFLLR application) and by activation of neuronal afferents. These data provide first ever direct evidence for vesicular release of ATP from astrocytes in cortical slices.

The data presented in Figure 3.9 was obtained by a joint effort with Dr Yuriy Pankratov.

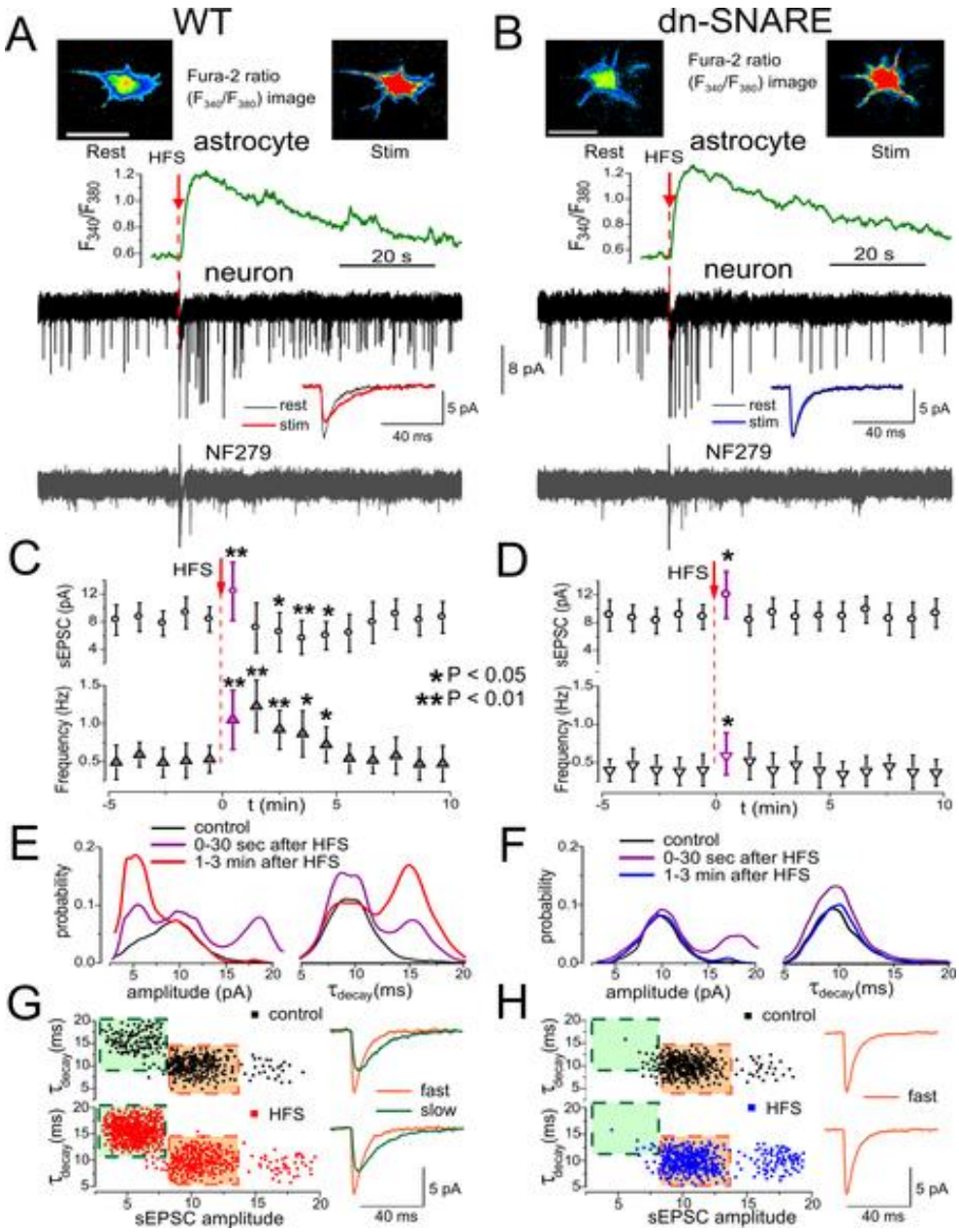

Figure 3.9. Neuronal activity causes vesicular release of ATP from cortical astrocytes in slice preparations. **A** and **B** show calcium imaging of astrocytes of layer2/3 of somatosensory cortex of both WT and dnSNARE mice. Scale bar is 10 μm. **A** and **B** also show voltage-clamp recordings of membrane currents in pyramidal neurones in the presence of picrotoxin (100 μM) and CNQX (50 μM) at -80 mV holding voltage. The P2X antagonist NF279 (3 μM) inhibited the sEPSCs, thereby suggesting that sEPSCs were indeed P2XR-mediated. Inlays show the average waveform (20 events) of spontaneous sEPSCs recorded before (rest) and 1 min after HFS (stim). **C** and **D** show the time-courses for amplitude and frequency of sEPSCs before and after HFS delivery. Each dot shows the average amplitude and frequency of spontaneous currents recorded in a 1 minute time window in the pyramidal neurones of WT and dnSNARE mice. **E** and **F** show the amplitude and decay time distributions of sEPSCs recorded before, immediately after (0-30 seconds), and 1-3 minutes after HFS (n=6). **G** and **H** represent the plot of decay time of sEPSCs against amplitude of sEPSCs. The corresponding waveforms (average of 20 traces) are shown in the inlay.

Box 3.3.

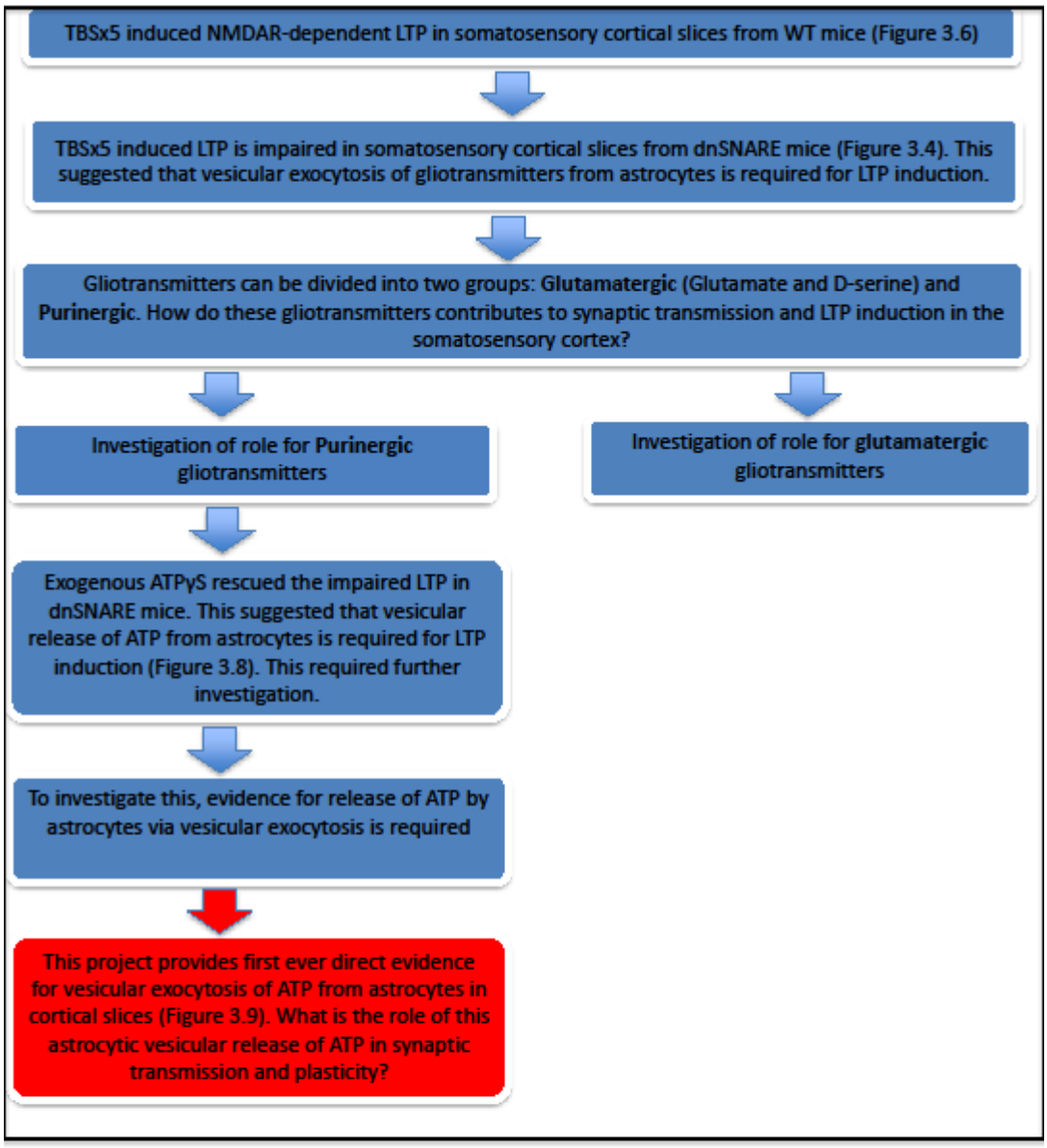
TBSx5 induced NMDAR-dependent LTP in somatosensory cortical slices from WT mice (Figure 3.6)
TBSx5 induced LTP is impaired in somatosensory cortical slices from dnSNARE mice (Figure 3.4). This suggested that vesicular exocytosis of gliotransmitters from astrocytes is required for LTP induction.
Gliotransmitters can be divided into two groups: Glutamatergic (Glutamate and D-serine) and Purinergic. How do these gliotransmitters contributes to synaptic transmission and LTP induction in the somatosensory cortex?
Investigation of role for Purinergic gliotransmitters
Investigation of role for glutamatergic gliotransmitters
Exogenous ATPγS rescued the impaired LTP in dnSNARE mice. This suggested that vesicular release of ATP from astrocytes is required for LTP induction (Figure 3.8). This required further investigation.
To investigate this, evidence for release of ATP by astrocytes via vesicular exocytosis is required
This project provides first ever direct evidence for vesicular exocytosis of ATP from astrocytes in cortical slices (Figure 3.9). What is the role of this astrocytic vesicular release of ATP in synaptic transmission and plasticity?

3.9. Role for astroglial ATP release: modulation of post-synaptic $GABA_A$ receptors in neocortical neurones

It was shown in section 3.8 that astrocytes are capable of calcium dependent vesicular release of ATP in the somatosensory cortex. The next objective was to investigate the role of astrocytic ATP release in synaptic transmission and plasticity (Box 3.3). As was shown in section 3.6, application of exogenous ATP can rescue TBSx5-induced LTP in dnSNARE mice, thereby indicating that astrocytic ATP release contributes to LTP induction. What is the mechanism whereby ATP release from astrocytes can contribute to LTP induction? As was discussed in section 3.7, the mechanisms for both TBS-induced LTP and ATP-induced LTP are NMDAR dependent. Therefore, theoretically, if ATP is to have a role in LTP induction then release of ATP from astrocytes must somehow modulate NMDAR activity. As mentioned above, application of ATPγS, which is a non-hydrolysable analogue of ATP, lead to ATP-induced LTP, thereby suggesting that ATP can indirectly modulate NMDARs by acting via its ionotropic or metabotropic receptors.

It has been shown previously by my colleagues that application of ATP analogues can decrease the amplitude of miniature IPSCs in cortical slices (Lalo, Andrew et al. 2009). Furthermore, it was also shown that in cortical slices, activation of astrocytes via TFLLR application results in increase in frequency of P2XR-mediated mEPSCs. This lead to P2XR-mediated intracellular signalling, which in turn resulted in decrease in amplitude of evoked and miniature $GABA_A$ receptor-mediated IPSCs. My colleagues have shown recently that the P2XR-

mediated inhibition of $GABA_A$ receptor activity as a result of application of TFLLR is absent in dnSNARE mice (Lalo, U. Palygin. 2014) (Please refer to Figure 6 of this paper). These results show that activation of P2XRs via astrocytic ATP can indirectly inhibit post-synaptic $GABA_A$ receptors in cortical neurones.

$GABA_A$-mediated IPSCs are rapid and short-term events and underlie what is known as phasic inhibition. Phasic inhibition is due to fast synaptic release of GABA onto $GABA_A$Rs that mainly have synaptic localisation. However, $GABA_A$Rs also exist on extra-synaptic sites. Low ambient concentrations of GABA in extra-cellular space can open these receptors leading to a temporally longer period of inhibition in comparison to phasic inhibition. This persistent inhibitory action of GABAergic transmission is called "tonic" inhibition. Tonic inhibition does not result into appearance of IPSCs. Instead, in a voltage clamp recording, tonic inhibition is associated with the holding current that is required to clamp neurones at a given membrane potential. The larger the tonic $GABA_A$R activity, the larger the size of the holding current. If ATP released from astrocytes can inhibit GABAergic phasic inhibition, then it is possible that it can also inhibit tonic inhibition. To investigate this, pyramidal neurones from layer 2/3 of somatosensory cortex were voltage clamped at holding potential of -80 mV under CNQX (50 µM) and D-APV (30 µM). Tonic inhibition was assessed by the change in the whole-cell holding current under action of $GABA_A$R antagonist bicuculline (50 µM).

As shown on Figure 3.10A, application of bicuculline to WT mice showed a tonic current of 39.9±8.3 pA (n=20). Application of tonic current to dnSNARE cortical slices, showed a tonic current of 76.9±15.1 pA (n=10), which was almost two times higher than in WT mice (Figure 3.10B). There was a significant difference in the average amplitude of tonic current between WT and dnSNARE mice ($p<0.01$). This shows that in dnSNARE mice there is less inhibition of extra-synaptic $GABA_A$Rs. This suggests that vesicular exocytosis from astrocytes is involved in the inhibition of tonic GABAergic activity. As was mentioned above, ATP release from astrocytes can inhibit phasic GABAergic activity. Therefore, it is possible that inhibition of tonic GABAergic activity is also as a result of ATP release from astrocytes. To investigate this, TFLLR was applied prior to bicuculline application to both WT and dnSNARE mice (Figure 3.10A-B). Application of TFLLR to WT cortical slices resulted in a marked upward shift in the holding current; the rest of the holding current was efficiently diminished by bicuculline. The average amplitude of tonic current subsequent to TFLLR application was 12.6±6.8 pA (n=14), which showed a decrease of 68±14% in amplitude in comparison to control/without TFLLR (Figure 3.10C). In contrast, application of TFLLR did not have a significant effect on tonic current in cortical slices from dnSNARE mice. In dnSNARE mice, the average amplitude of tonic current recorded under the action of TFLLR was 72.2±9.1 pA (n=7), which did not show a significant change in comparison to control (Figure 3.10C). In WT mice, the down-regulation of tonic current following TFLLR application was considerably attenuated by application of PPADS (10 μM). As TFLLR results in gliotransmitter release specifically from astrocytes, these result again show that vesicular release from astrocytes can inhibit tonic GABAergic

activity. Furthermore, as PPADS prevents this TFLLR inhibition of tonic GABAergic activity, these results suggest that it is the vesicular release of ATP that is involved in inhibition of tonic GABAergic transmission.

The above-mentioned results suggest that calcium-dependent vesicular release of ATP from astrocytes can inhibit both phasic and tonic GABAergic inhibition. However, in a recent study in the hippocampus, it has been shown that spontaneous calcium elevations in astrcoytes can modulate both phasic and tonic inhibition via GAT3 GABA transporters (Shigetomi *et al.*, 2012). GABA transporters can control extracellular GABA concentrations, thus controlling GABAergic tonic inhibition. This report showed that chelation of astrocytic calcium, and thereby preventing calcium oscillation in astrocytes, resulted in decrease in activity of GAT3 transporters. This lead to increase in extracellular GABA concentrations, which resulted in increase in GABAergic tonic inhibition. Phasic inhibition however decreased (IPSC amplitude decreased). The authors attributed the decrease in phasic inhibition to $GABA_AR$ desensitisation as a result of the increase in extracellular GABA concentrations. In summary, this report provided evidence that astrocytic calcium elevation is required for GAT3 control of GABAergic transmission in the hippocampus. Therefore, it is possible that in my experiments (Figure 3.10B), the larger tonic inhibition in dnSNARE mice compared to WT mice can be attributed to decrease in GAT3 activity in dnSNARE mice. However, this is unlikely for two reasons: first, calcium elevation is not impaired in dnSNARE mice (Figure 3.1), therefore, GAT3 activity should not be impaired; second, my results and those of my colleagues show decrease in **both** phasic and tonic inhibition.

To provide further support that GAT3 activity in astrocytes is not altered in dnSNARE mice, inhibitor of GAT3 (30 μM of (S)-SNAP5114) was applied to both WT and dnSNARE mice during IPSC recordings (Figure 3.11). Application of (S)-SNAP5114 to WT mice resulted in a significant increase in tonic inhibition and a significant decrease in the amplitude of phasic IPSCs. Application of (S)-SNAP5114 to dnSNARE mice also resulted in a significant increase in tonic inhibition and a significant decrease in the amplitude of phasic IPSCs. There was no significant difference in change in tonic and phasic inhibition between WT and dnSNARE mice (Figure 3.11, $p<0.05$, two sample t-test). As the effect of inhibition of GAT3 is simi;ar between WT and dnSNARE mice, these data suggest that the increase in tonic inhibition in dnSNARE mice is not as a result of alteration in GAT3 activity in these mice but as a result of impairment of vesicular release of ATP.

The results shown on Figures 3.9, 3.10 and 3.11 have been published (Lalo, U. Palygin O. et al. 2014).

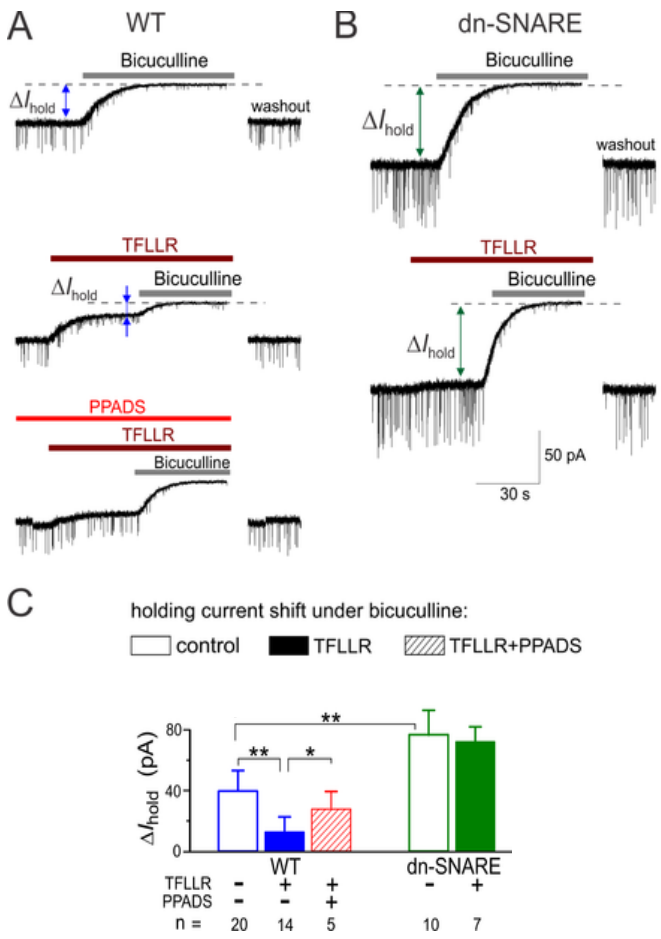

Figure 3.10. Exocytosis of ATP from astrocytes down-regulates the tonic inhibitory synaptic signalling. A and **B** show example IPSC recordings at -80 mV under the presence of CNQX (50 μM) and D-APV (30 μM). Tonic $GABA_AR$-mediated signalling was evaluated by upward shift in the whole-cell holding current (ΔI_{hold}) caused by application of bicuculline (50 μM) to layer 2/3 pyramidal neurones in brain slices of WT and dnSNARE mice. **C** shows bar-charts representing the average amplitude of tonic $GABA_AR$-mediated current measured in different conditions. Two sample independent t-tests were performed between each two sets of data. $p<0.05$, *; $p<0.01$, **.

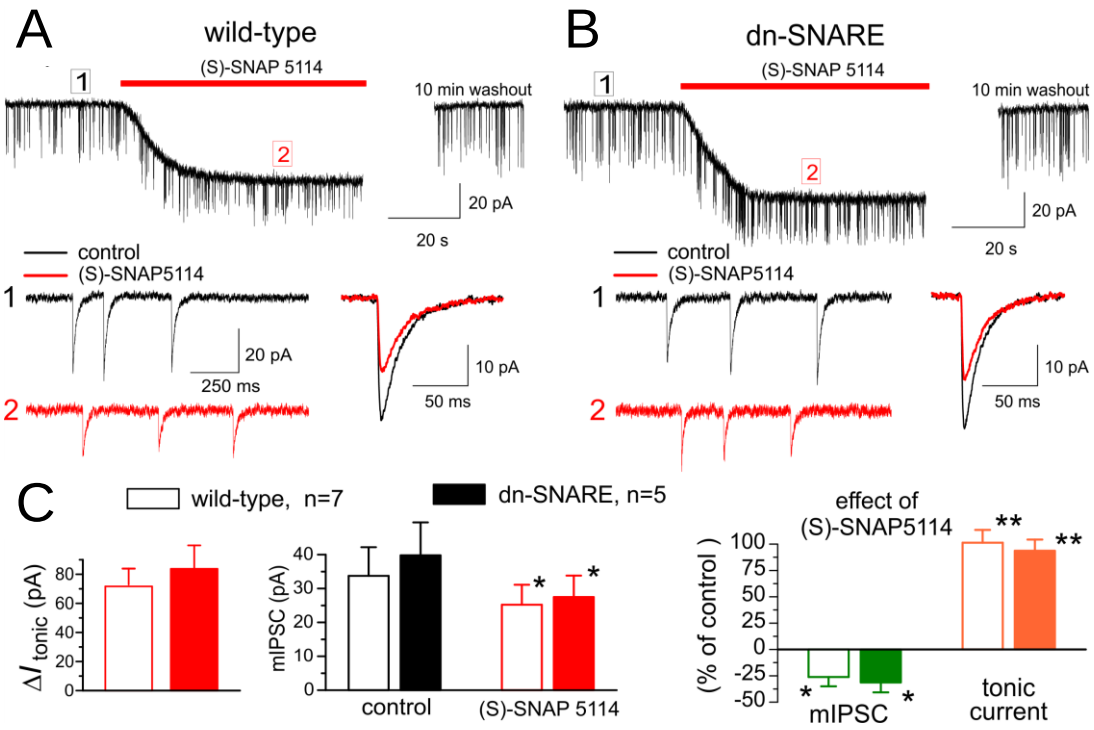

Figure 3.11. Inhibition of GABA GAT3 transporters decreased the GABAergic mIPSCs and increased the tonic current in neurones of WT and dnSNARE mice. A and **B** show GABAergic IPSC recordings in WT and dnSNARE mice under CNQX (50 μM), D-APV (30 μM) and PPADS (10 μM) at -80 mV holding voltage. Examples of mIPSCs, recorded at moments indicated, and average waveforms of phasic GABAergic current (average of 25 mIPSCs) are shown in the inlays below. **C** shows bar-charts that represent the average change for effect on phasic and tonic inhibition by (S)-SNAP5114 (30 μM). Paired t-test was perfomed for each data. Two sample independent t-tests were performed between each two sets of data. $p<0.05$, *; $p<0.01$, **.

3.10. ATP-mediated inhibition of GABAergic transmission leads to increase in NMDAR activity, thereby contributing to LTP induction

The findings in the previous section showed that astrocytic ATP can indirectly inhibit both phasic and tonic GABAergic transmission by acting on neuronal P2X receptors. Theoretically, inhibition of GABAergic transmission should increase excitability and result into higher chance of LTP induction. For example, it has been shown that in the CA1 region of hippocampus, inhibition of extra-synaptic $GABA_A$Rs not only decrease tonic inhibition but also increase the extent of HFS-induced LTP in comparison to control conditions (Dawson *et al.*, 2006). Therefore, it is possible that ATP can contribute to LTP induction by increasing excitation through inhibition of GABAergic transmission. This increase in excitation could, theoretically, lead to increase in NMDAR activity. This could be the case for ATP-induced LTP, where ATP is applied exogenously, and TBS-induced LTP, where ATP is released by astrocytes.

To investigate whether NMDAR activity increases as a result of inhibition of GABAergic transmission, the NMDAR component of fEPSP was investigated. As was shown on Figure 3.3B, application of DNQX completely abolished the fEPSP suggesting that fEPSP consists of AMPAR activity. If inhibition of GABAergic transmission results in NMDAR activity, then one would expect the appearance of an NMDAR component in the fEPSP following inhibition of GABAergic transmission. To investigate whether fEPSP consists of an NMDAR component, D-serine and D-AP5 were applied to fEPSP recordings.

Application of D-serine (10 µM) to fEPSP recordings resulted in a slight non-significant increase of +3.79±3.01% in fEPSP with respect to baseline recording ($p<0.05$, paired t-test; n=5; see Figure 3.12A, E and F). Following D-serine application, D-AP5 was applied on top of D-serine (Figure 3.12A). Application of D-AP5 (30 µM) resulted in a slight non-significant decrease of -4.74±3.76% in fEPSP (this time the % decrease is with respect to D-serine application and not baseline; see Figure 3.12A, E and F). These results show that, as expected, fEPSPs do not have a significant NMDAR component and therefore mainly consist of AMPAR activity as was shown on Figure 3.3B.

The above result shows that in control conditions, fEPSPs do not have a significant NMDAR component. To show that inhibition of GABAergic transmission results in appearance of NMDAR component in fEPSP recordings, the $GABA_A$ receptor antagonist, Gabazine (150 nM), was applied. Application of Gabazine resulted in an increase in fEPSP (Figure 3.12B and F). To see whether this increase is as a result of NMDAR activity, exogenous D-serine and D-AP5 were applied on top of Gabazine application (Figure 3.12B). Application of D-serine increased the fEPSP slope further (Figure 3.12B and F). The average increase in fEPSP with Gabazine and D-serine application was 34.01±9.76% with respect to baseline (n=4; see Figure 3.12E). This increase was statistically significant ($p<0.01$, paired t-test). Application of D-AP5 subsequent to D-serine resulted in significant drop of -48.58±13.94% in fEPSP ($p<0.01$, paired t-test; see Figure 3.12B, E and F). This result shows that blocking of $GABA_A$ receptors

leads to an increase in NMDAR component of fEPSP, thereby showing that inhibition of GABAergic transmission can increase NMDAR activity.

To see whether ATP also results in appearance of an NMDAR component in the fEPSP, ATPγS (20 μM) was applied to fEPSP recordings prior to application of D-serine and D-AP5. However, as ATPγS application results in depression of fEPSP and as it is only after washout that LTP is expressed (see Figure3.8A), D-serine and D-AP5 were applied 20 minutes after washout of ATPγS (Figure 3.12C). As expected, washout of ATPγS resulted in an increase in fEPSP. Application of D-serine subsequent to ATPγS washout resulted in a further increase in fEPSP (Figure 3.12C and F). The average increase in fEPSP following ATPγS washout and D-serine application was +18.74±8.19% (n=7, Figure 3.12E). This increase was statistically significant ($p<0.05$, paired t-test). Subsequent application of D-AP5 resulted in a significant decrease in fEPSP of -37.48±16.38% ($p<0.01$; see Figure 3.12C, E and F). These results suggest that ATP can increase the NMDAR component of fEPSP. As was mentioned in section 3.7, work by other researchers has shown that ATP can increase NMDAR activity by acting as a phosphate donor (Fujii, 2004). However, here I have shown that ATPγS, which is a non-hydrolysable form of ATP, can also lead to increase in NMDAR activity. This suggests that the increase in NMDAR activity following ATPγS application is via a mechanism other than phosphate donation. As ATP can result in inhibition of GABAergic transmission and as inhibition of GABAergic transmission via Gabazine application results in increase in NMDAR activity, I suggest that the possible mechanism for increase

in NMDAR activity following ATPγS application is through the ATP/P2XR-mediated inhibition of GABAergic transmission.

As was discussed in sections 3.8 and 3.9, PAR-1 agonist can result in calcium dependent vesicular release of ATP specifically from astrocytes. This ATP release can then activate P2XRs on neurones, which in turn can lead to inhibition of GABAergic phasic and tonic inhibition. In the current section I have provided evidence for appearance of NMDAR activity following application of Gabazine or ATPγS. As application of PAR-1 agonist can lead to both the release of ATP and the inhibition of GABAergic transmission then it is possible that PAR-1 agonist application can also lead to the appearance of NMDAR activity. To investigate this, TFLLR (10 µM) was applied to cortical slices during fEPSP recordings. Application of TFLLR resulted in an increase in fEPSP (Figure 3.12D-F). To see whether this increase was due to NMDAR activity, D-serine and D-AP5 were applied subsequent to TFLLR application (Figure 3.12D). D-serine application increased fEPSP even further. The average increase in fEPSP as a result of TFLLR and D-serine application was +17.01±4.62% (n=7; see Figure 3.12E). Application of D-AP5 resulted in a significant decrease of -28.34±7.70% in fEPSP (n=7, $p<0.05$, paired t-test; see Figure 3.12E). This result suggests that application of PAR-1 agonist can result in appearance of NMDAR activity. As PAR-1 agonist results in vesicular release of ATP specifically from astrocytes, these results suggest that ATP release from astrocytes can lead to a significant increase in NMDAR activity.

To investigate that the TFLLR mediated increase in NMDAR activity is indeed due to vesicular release from astrocytes, TFLLR was also applied to cortical slices from dnSNARE mice. In contrast to WT mice, TFLLR application to dnSNARE mice did not result in a significant increase in fEPSP (Figure 3.12D and F). Application of D-serine on top of TFLLR also failed to significantly increase fEPSP. The average increase in fEPSP following TFLLR and D-serine application was +2.65±2.81% (n=7). Application of D-AP5 resulted in a small non-significant drop in fEPSP of -3.58±3.32% (n=7, $p<0.05$, paired t-test, see Figure 3.12E). These results show that TFLLR mediated increase in NMDAR activity is dependent on vesicular release from astrocytes. As TFLLR application result in vesicular release of ATP from astrocytes (see Figure 3.2), this data suggest that TFLLR mediated vesicular release of ATP from astrocytes can lead to NMDAR activity.

As was shown on Figure 3.7A, application of ATPγS during the delivery of TBSx5 can rescue LTP in dnSNARE mice. If, as suggested above, the mechanism of ATP mediated increase in NMDAR activity is via inhibition of GABAergic transmission, then the rescue of LTP via application of exogenous ATPγS in dnSNARE mice is also as a result of inhibition of GABAergic transmission. To investigate whether in dnSNARE mice, inhibition of GABAergic transmission can also rescue LTP, Gabazine was applied to dnSNARE cortical slices prior to delivery of TBSx5. Gabazine (150 nM) was applied to dnSNARE mice 10-20 minutes before start of baseline fEPSP recording. Delivery of TBSx5 to Gabazine treated slices from dnSNARE mice resulted in a significant increase in the extent of LTP compared to control

($p<0.01$, two-sample t-test; see Figure 3.13). With Gabazine application, the average increase in fEPSP 40-60 minutes post TBSx5 was +35.47±9.23% (n=10). This result shows that inhibition of $GABA_A$ receptors can rescue LTP in dnSNARE mice. This suggests that the mechanism of rescue of LTP in dnSNARE mice via ATPγS application could involve the inhibition of GABAergic transmission.

Taken together, the results in this section suggest that vesicular release of ATP from astrocytes can lead to increase in NMDAR activity during synaptic transmission. ATP results in this increase by decreasing GABAergic transmission. Therefore, it is possible that during TBS protocol, release of ATP from astrocytes can inhibit GABAergic transmission, hence leading to increase in NMDAR activity and LTP induction.

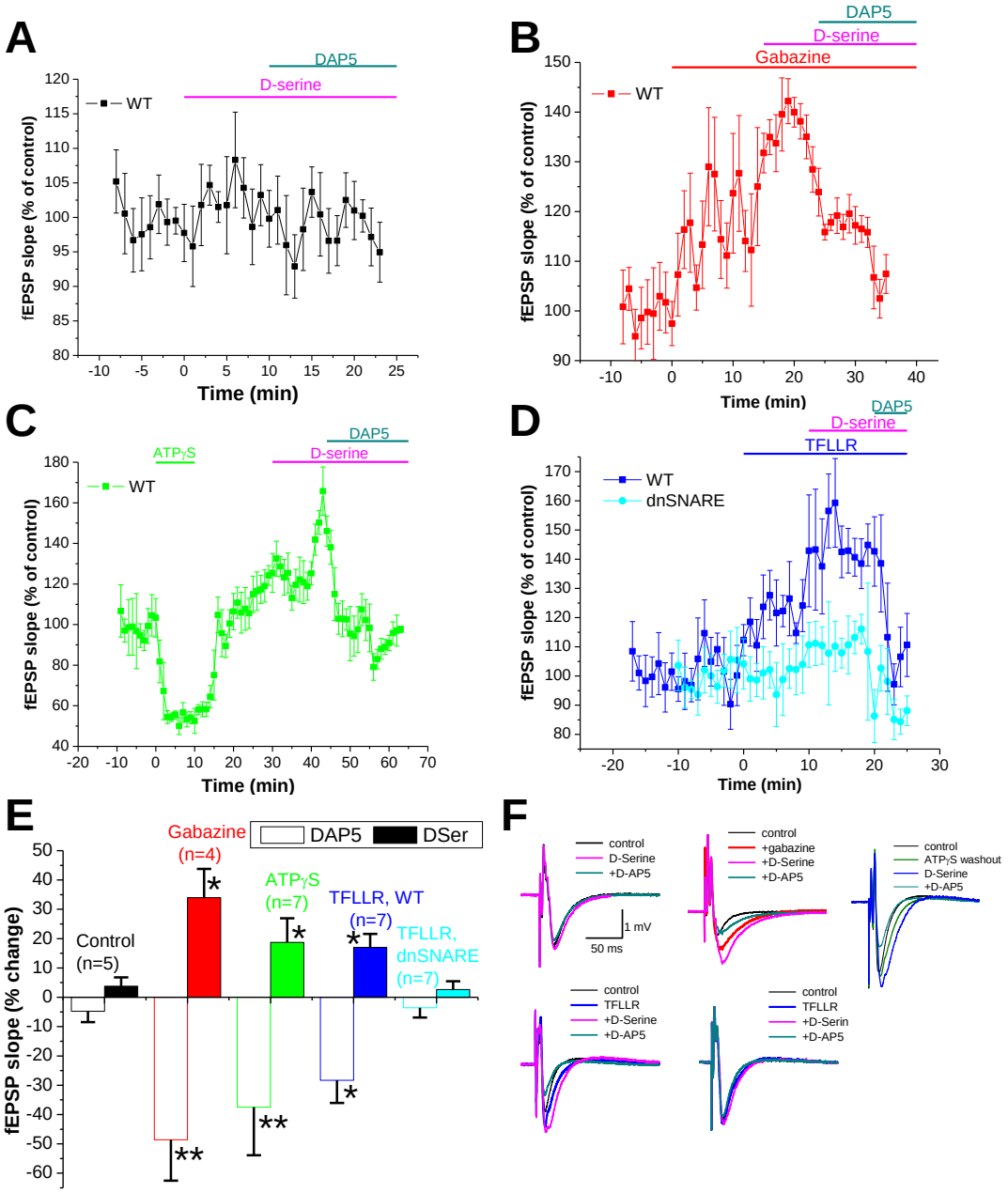

Figure 3.12. Application of ATPγS, Gabazine and TFLLR can increase the NMDAR component of fEPSP. A-D show time-courses of fEPSP recordings during application of different pharmacological agents. Each time-course is from a single experiment. Each dot shows the average fEPSP slope of fEPSPs recorded in a 1 minute time window. Bar-charts (**E**) represent the average % change in fEPSP across several experiments. Paired t-test was performed for average % change in fEPSP from baseline. $p<0.05$, *; $p<0.01$, **. **F** shows example fEPSPs corresponding to time-courses and bar-charts shown in **A-E**. In **A**, exogenous D-serine (10 μM) was applied after 10 minutes of stable baseline recording. Subsequently, D-AP5 (30 μM) was applied after 10 minutes of D-serine application. In **B**, Gabazine (150 nM) was applied for 15 minutes. Subsequently, D-serine was applied for 10 minutes followed by D-AP5. In **C**, ATPγS (20μM) was applied for 10 minutes. It was then washed out for 20 minutes, followed by application of D-serine and then D-AP. In **D**, which shows to time-courses (one for WT and one for dnSNARE mice), TFLLR (10 μM) was applied for 10 minutes. This was followed by 10 minutes application of D-serine and then D-AP5.

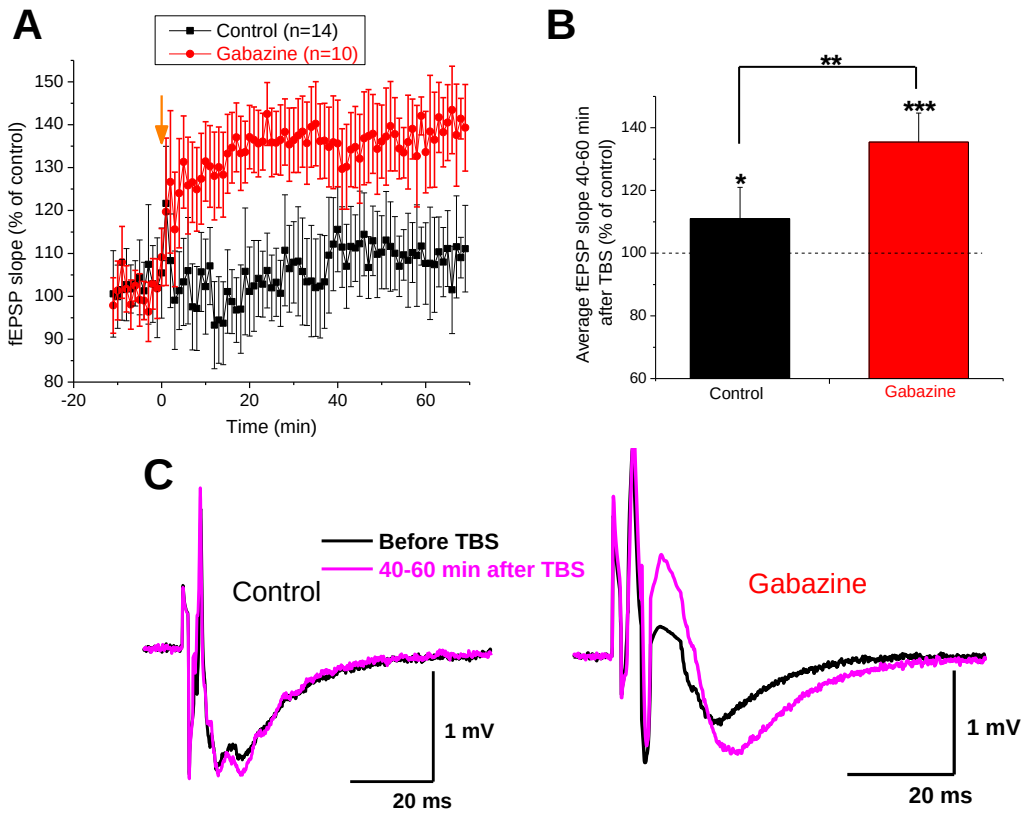

Figure 3.13. Inhibition of $GABA_A$ receptors can rescue LTP during TBSx5 in dnSNARE mice. These recordings were performed in dnSNARE mice. **A** shows the average time-courses. Gabazine (150 nM) was applied 10-20 minutes prior to start of recording. Orange arrow shows position of TBS application. 10 minutes of baseline fEPSP recordings were made before TBS application. **B** represents the average % increase in fEPSP 40-60 minutes post TBSx5 delivery. The average % change in fEPSP for control dnSNARE recordings was +11±10.1%. The average % change in fEPSP for Gabazine-treated dnSNARE slices was +35.47±9.23%. Paired t-test was performed for average % change in fEPSP from baseline. Two sample independent t-tests were performed between control and Gabazine-treated experiments. $p<0.05$, *; $p<0.01$, **; $p<0.001$, ***. **C** shows example fEPSPs before and after TBSx5 delivery.

3.11. Activation of astrocytic vesicular release with TFLLR can contribute to TBS-induced LTP.

A sub-threshold stimulation protocol is a stimulation protocol that usually fails to depolarise the post-synaptic neurone above the LTP threshold. A group of researchers have shown that application of small concentration of PAR-1 agonist to CA1 region of hippocampus of 2 months old mice can result in LTP induction with a sub-threshold HFS protocol (Maggio *et al.*, 2008). Therefore, I decided to investigate whether in the somatosensory cortex, application of PAR-1 agonist can also induce LTP with a sub-threshold protocol. This will provide further evidence that vesicular release from astrocytes can contribute to LTP induction. For this purpose, I had to first find a suitable TBS sub-threshold protocol.

As was shown on Figure 3.5, delivery of TBSx5 can result in the induction of LTP. It is known that four to six trains of TBS can induce LTP in the cortex (Kirkwood *et al.*, 1993). Therefore, to find a suitable sub-threshold protocol, I decided to lower the number of trains of TBS to 1-3 trains. Delivery of TBSx1 induced a non-significant increase of +6.17±3.64% in fEPSP 40-60 minutes post TBS (n=6, $p<0.05$, paired t-test; see Figure 3.14). Interestingly, delivery of TBSx2 induced a slight, though significant, decrease of -15±6.56% in fEPSP 40-60 minutes post TBS (n=7, $p<0.05$, paired t-test; see Figure 3.14). In contrast to TBSx2, delivery of TBSx3 induced a significant potentiation of 19.83±8.84% 40-60 minutes post TBS (n=12, $p<0.05$, paired t-test; see Figure 3.14).

The above results can be explained using the Artola, Brocher and Singer (ABS) rule. The ABS rule suggests that with moderate level of post-synaptic depolarisation, a moderate level of calcium elevation is reached. If the level of depolarisation/calcium elevation reaches a first threshold, then LTD is induced. With higher stimulation, post-synaptic depolarisation is increased further. If post-synaptic depolarisation reaches a second threshold, then LTP is induced. For a graphic representation of the ABS rule please refer to Figure 1. Using the ABS rule one can suggest that during TBSx1, post-synaptic depolarisation does not reach the first threshold, therefore there is no long term plasticity. During TBSx2, post-synaptic depolarisation crosses the first threshold leading to LTD. Addition of an extra train of TBS increases post-synaptic depolarisation above the second threshold, leading to LTP. Addition of more trains of TBS, as in TBSx5, results in a further increase in post-synaptic depolarisation, hence leading to a larger extent of LTP. This can be seen on Figure 3.14, where TBSx5 shows a larger potentiation in comparison to TBSx3.

Impairment of TBSx5-induced LTP in dnSNARE mice suggested that LTP induction with TBSx5 requires vesicular release from astrocytes. As LTP induction requires vesicular release from astrocytes, one can suggest that the reason that with sub-threshold TBS protocol LTP is not induced is because during this protocol astrocytes are activated to a lesser extent. This in turn would suggest that the degree of astrocytic vesicular release would positively contribute to post-synaptic depolarisation. Therefore, a sub-threshold protocol like TBSx2 induces LTD and not LTP because it has less vesicular release from astrocytes in comparison to TBSx5. This means that if during TBSx2, astrocytes are further

activated by applying the PAR-1 agonist TFLLR, then the second threshold of the ABS rule might be reached and thereby LTP might be induced. To test this hypothesis, TFLLR (10 µM) was applied during TBSx2 delivery to cortical slices from WT mice. Application of TFLLR during TBSx2 reversed the direction of plasticity from LTD to LTP (Figure 3.15). Application of TFLLR during TBSx2 showed a small but significant LTP with an average fEPSP of +18.07±7.30% 40-50 minutes post TBS ($n=14$, $p<0.05$, paired t-test; see Figure 3.15B). There was a statistically significant difference between TBSx2 under control conditions and TBSx2 under TFLLR ($p<0.05$, two sample independent t-test; see Figure 3.15B). As PAR-1 agonist results in vesicular release specifically from astrocytes, the results from Figure 3.15 provide further evidence that vesicular release from astrocytes is required for LTP induction.

Astrocytes can release D-serine, ATP and glutamate. As was shown on Figure 3.7, exogenous ATP could rescue LTP in dnSNARE mice but exogenous D-serine failed to do so. This suggested that it was the vesicular release of ATP from astrocytes that was required for LTP induction in the cortex and not the astrocytic release of D-serine. To provide further evidence that D-serine is not required for LTP induction, TBSx2 protocol was delivered during D-serine application. In contrast to TFLLR, application of D-serine (10 µM) during TBSx2 did not change the direction of synaptic plasticity from LTD to LTP. D-serine application during TBSx2 induced an LTD comparable to that of TBSx2 delivery under control conditions (Figure 3.15). With TBSx2 delivery during D-serine application, a significant LTD was induced with an average % decrease in fEPSP of -16.5±5.72% 40-50 minutes post TBSx2 ($n=7$, $p<0.05$, paired t-test;

see Figure 3.15B). There was no statistically significant difference between TBSx2 under control and TBSx2 under D-serine ($p<0.05$, two sample independent t-test). In contrast, there was a significant difference between TBSx2 under D-serine and TBSx2 under PAR-1 agonist ($p<0.01$, two sample t-test; see Figure 3.15B). These data provide further evidence that in the somatosensory cortex, D-serine does not contribute to LTP induction.

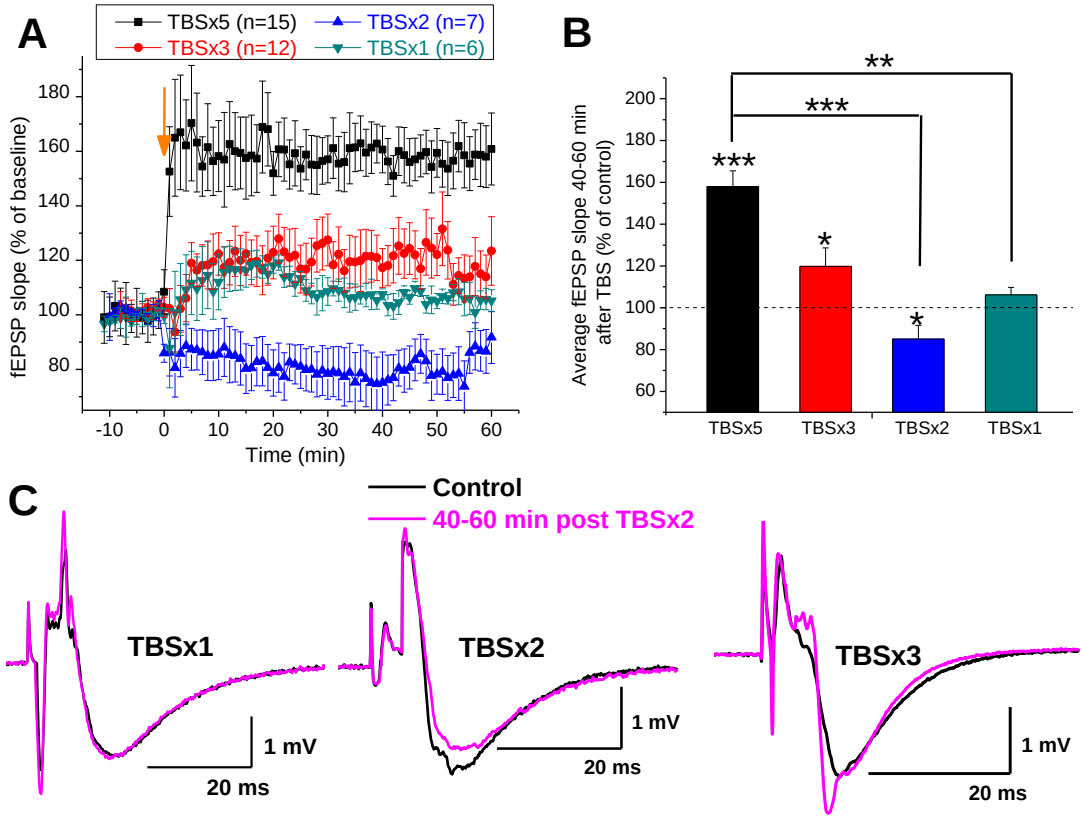

Figure 3.14. Sub-threshold protocols of LTP induction. These recordings were performed in WT mice. **A** shows the average time-courses for fEPSP recordings for different numbers of TBS delivery. Orange arrow shows position of TBS delivery. 10 minutes of baseline fEPSP recordings were made before TBS delivery. **B** represents the average % change in fEPSP 40-60 minutes post TBS delivery. The average % increase in fEPSP 40-60 minutes post TBSx5 was +58±7.54%. The average % increase in fEPSP 40-60 minutes post TBSx3 was +19.83±8.84%. The average % decrease in fEPSP 40-60 minutes post TBSx2 was -15±6.56%. The average % increase in fEPSP 40-60 minutes post TBSx1 was +6.17±3.64%. Two sample independent t-test was performed, in turn, between TBSx5 and each of the sub-threshold protocols. Paired t-test was performed for average % change in fEPSP from baseline. $p<0.05$, *; $p<0.01$, **; $p<0.001$, ***. **C** shows example fEPSPs before and after TBSx2 delivery.

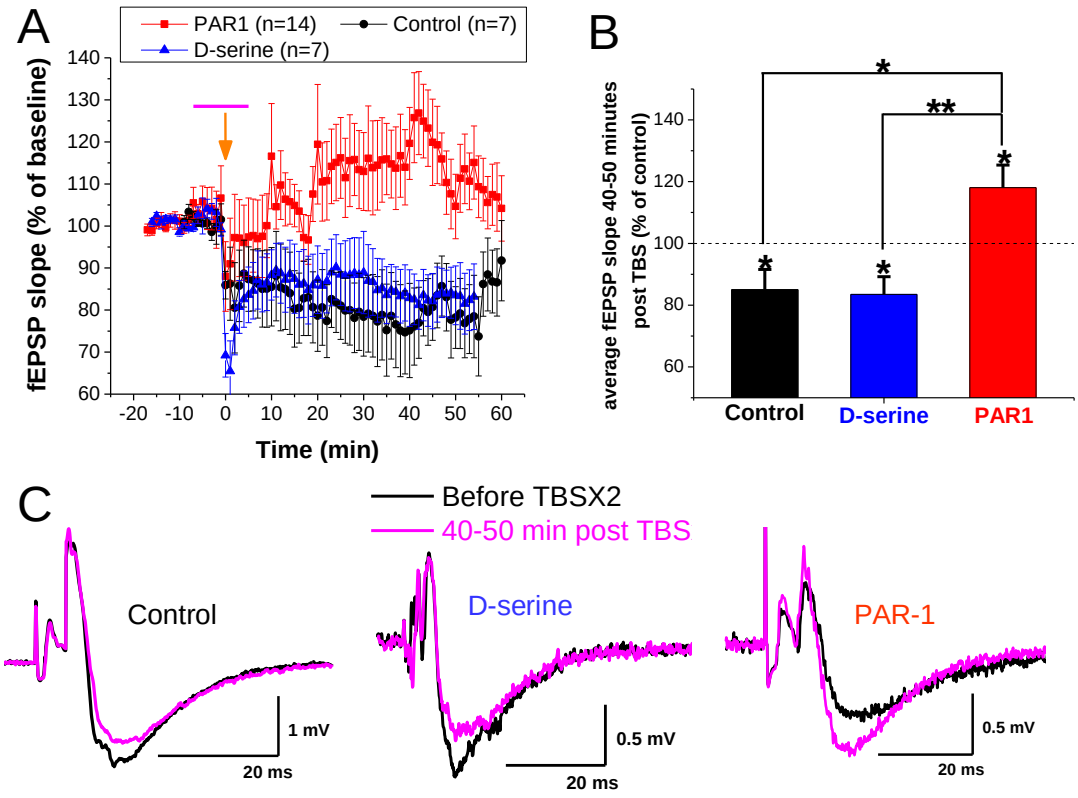

Figure 3.15. Application of PAR-1 agonist during TBSx2 reverses the direction of plasticity from LTD to LTP. These recordings were performed in WT mice. **A** shows the average time-courses for fEPSP recordings with TBSx2 protocol. Orange arrow shows position of TBSx2 delivery. 10 minutes of baseline fEPSP recordings were made before TBS delivery. Purple bar shows the time-span of D-serine (10 μM) or PAR1 agonist (10 μM TFLLR) application (each was applied 5 minute prior to TBSx2 and washed out 5 minutes post TBSx2). **B** represents the average % change in fEPSP 40-50 minutes post TBSx2 delivery. The average % decrease in fEPSP was -15±6.56% for TBSx2 protocol under control conditions. The average % decrease in fEPSP was -16.5±5.72% for TBSx2 protocol under D-serine application. The average % increase in fEPSP was +18.07±7.30% for TBSx2 protocol under TFLLR application. Two sample independent t-test was performed between each two pairs of data. Paired t-test was performed for average % change in fEPSP from baseline. $p<0.05$, *; $p<0.01$, **. **C** shows example fEPSPs before and after TBSx2 delivery.

The above finding showed that D-serine release is not required for LTP induction. This suggests that the rescue of LTP with TFLLR application during TBSx2 is not dependent on vesicular release of D-serine from astrocytes. In contrast, it was suggested that ATP release from astrocytes could contribute to LTP induction in the somatosensory cortex. It was shown in the previous sections that TFLLR activation of astrocytes can result in release of ATP from these cells. The released ATP then acts on P2X receptors on post-synaptic neurones, leading to inhibition of GABAergic transmission and increase in NMDAR activity. These findings suggest that the rescue of LTP with TFLLR application during TBSx2 could be as a result of TFLLR-mediated activation of astrocytic ATP release onto neuronal P2XRs. To investigate whether this rescue of LTP is dependent on the TFLLR-mediated increase in P2XR activity, P2XR antagonists PPADS (10 μM) and 5-BDBD (5 μM) were applied along with TFLLR during delivery of TBSx2 protocol. Inhibition of P2X receptors during TBSx2 prevented the TFLLR-mediated induction of LTP. Instead a significant LTD was induced ($p<0.05$, paired t-test; see Figure 3.16). The size of this LTD 40-50 minutes post TBS delivery was -28±10.56% (n=12). There was a statistically significant difference between the data for TBSx2 delivery under PPADS, 5-BDBD and TFLLR and the data for TBSx2 delivery under TFLLR but with no P2XR antagonists ($p<0.01$, two sample t-test; see Figure 3.16B). In contrast, the size of LTD with TBSx2 delivery under PPADS, 5-BDBD and TFLLR was similar to size of LTD when TBSx2 was applied under no pharmacological agent (control). There was no statistically significant difference between these two data ($p<0.05$, two sample t-test; see Figure 3.16B).

These results show that rescue of LTP with TFLLR during TBSx2 application is dependent on P2XRs. As TFLLR results in vesicular release of ATP from astrocytes, these findings suggest that astrocytic ATP can contribute to LTP induction by acting on neuronal P2XRs.

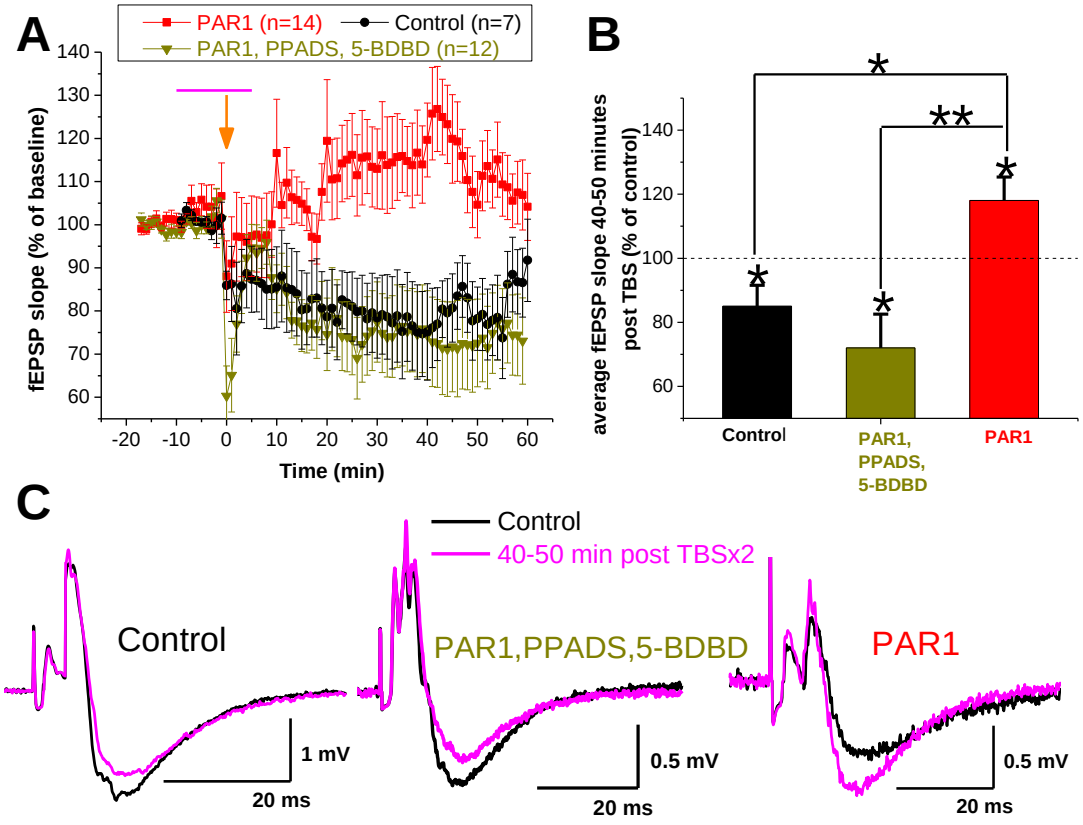

Figure 3.16. PAR-1 agonist rescue of LTP during TBSx2 is P2XR dependent. These recordings were performed in WT mice. **A** shows the average time-courses for fEPSP recordings with TBSx2 protocol. Orange arrow shows position of TBSx2 delivery. 10 minutes of baseline fEPSP recordings were made before drug application. Purple bar shows the time-span of application of PAR1 agonist (10 µM TFLLR), PPADS (10 µM) and 5-BDBD (5 µM). **B** represents the average % change in fEPSP 40-50 minutes post TBSx2 delivery. The average % decrease in fEPSP was -15±6.56% for TBSx2 protocol under control conditions. The average % decrease in fEPSP was -28±10.56% for TBSx2 protocol under TFLLR, PPADS and 5-BDBDB. The average % increase in fEPSP was +18.07±7.30% for TBSx2 protocol under TFLLR application. Two sample independent t-test was performed between each two pairs of data. Paired t-test was performed for average % change in fEPSP from baseline. $p<0.05$, *; $p<0.01$, **. **C** shows example fEPSPs before and after TBSx2 delivery.

According to the ABS rule, increase in post-synaptic depolarisation results in increase in calcium entry into post-synaptic neurone. If this calcium elevation reaches the first threshold then LTD is induced; if it reaches the second threshold then LTP is induced. As was shown previously, TBSx5-induced LTP is NMDAR-dependent (Figure 3.6). This suggests that during TBSx5-induced LTP, opening of NMDARs results in calcium elevation above the LTP threshold in post-synaptic neurones. To investigate whether the LTD induced via TBSx2 is also dependent on NMDARs, TBSx2 protocol was carried out in the presence of DL-AP5. Application of DL-AP5 (60 µM) during TBSx2 also resulted in LTD induction with an average fEPSP of -19.58±2.36% 40-60 minutes post TBS delivery (n=12, see Figure 3.17). There was no significant difference in the size of LTD between TBSx2 during control conditions and TBSx2 during DL-AP5 application ($p<0.05$, two sample independent t-test; see Figure 3.17B). This result suggests that the LTD induced with the sub-threshold TBSx2 protocol does not dependent on NMDA receptors.

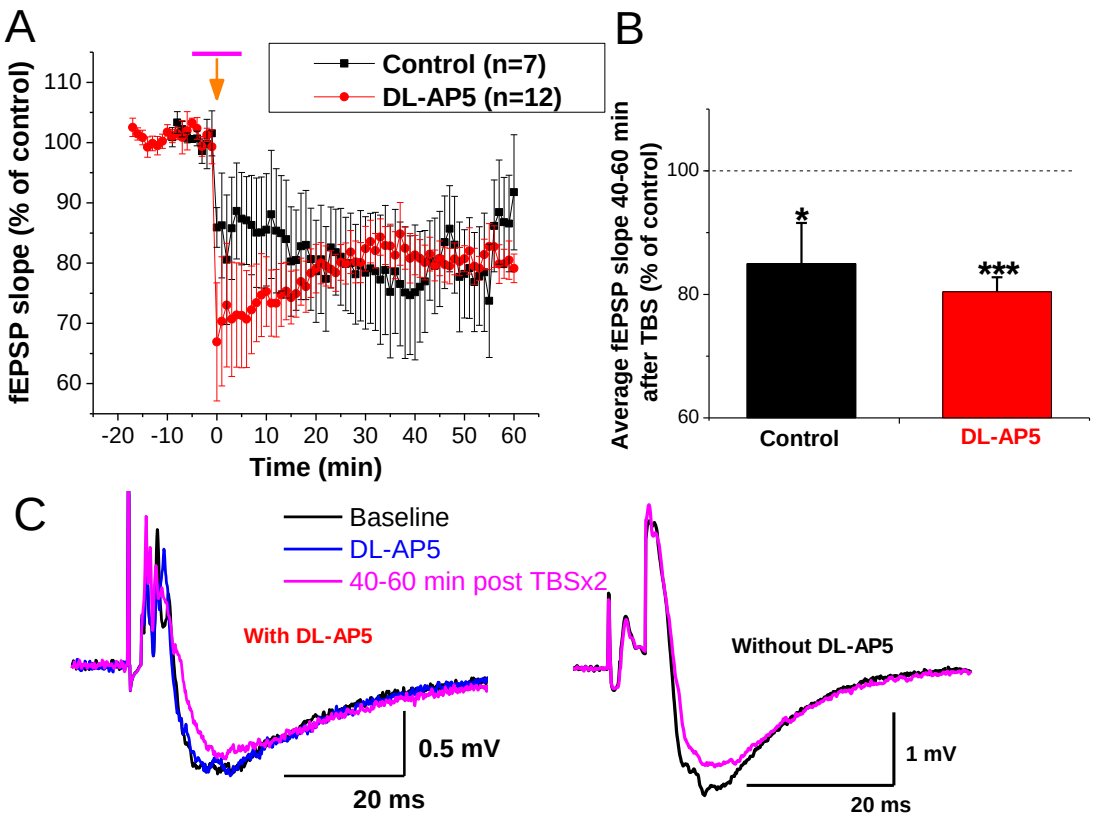

Figure 3.17. TBSx2-induced LTD is not NMDAR dependent. These recordings were performed in WT mice. **A** shows the average time-courses for fEPSP recordings. Purple bar shows the time-span of DL-AP5 application. DL-AP5 was applied 5 minute prior to TBS and washed out 5 minutes post TBS. Orange arrow shows position of TBS application. **B** represents the average % change in fEPSP 40-60 minutes post TBS delivery. For the DL-AP5 (60 µM) recordings, the average % decrease in fEPSP was -19.58±2.36%. For control recordings (without DL-AP5), the average % decrease in fEPSP was -15±6.56%. Two sample independent t-test was performed between TBSx2 and TBSx2+DL-AP5 data. Paired t-test was performed for average % change in fEPSP from baseline. $p<0.05$, *; $p<0.01$, **; $p<0.001$, ***. **C** shows example fEPSPs before and after TBSx5 delivery.

As was shown above, application of TFLLR could reverse the direction of TBSx2 plasticity from LTD to LTP. This suggested that increase in vesicular release from astrocytes can increase depolarisaion of post-synaptic neurones above the second threshold of ABS rule, thereby leading to LTP induction. If increase in astrocytic vesicular release can increase post-synaptic depolarisation, then it suggests that the size of LTP in an above threshold protocol like TBSx3 should also increase with TFLLR application. As can be seen from Figure 3.14, the size of LTP with TBSx3 is lower in comparison to the size of LTP with TBSx5. Application of TFLLR during TBSx3 should theoretically increase release from astrocytes further, thereby leading to increase in depolarisation of post-synaptic neurones and larger LTP size. To investigate whether this is the case, TBSx3 was delivered during TFLLR application. Application of TFLLR during TBSx3 resulted in an LTP of 35.14±8.39% (n=7; see Figure 3.18). This was larger than the 19.83±8.84% LTP size induced with TBSx3 delivered in the absence of TFLLR. However, there was no statistically significant difference between the two data ($p<0.05$, two sample t-test; see Figure 3.18). These results show that application of PAR1 agonist during TBSx3 can increase LTP size. This again suggests that activation of vesicular release from astrocytes can contribute to induction of LTP.

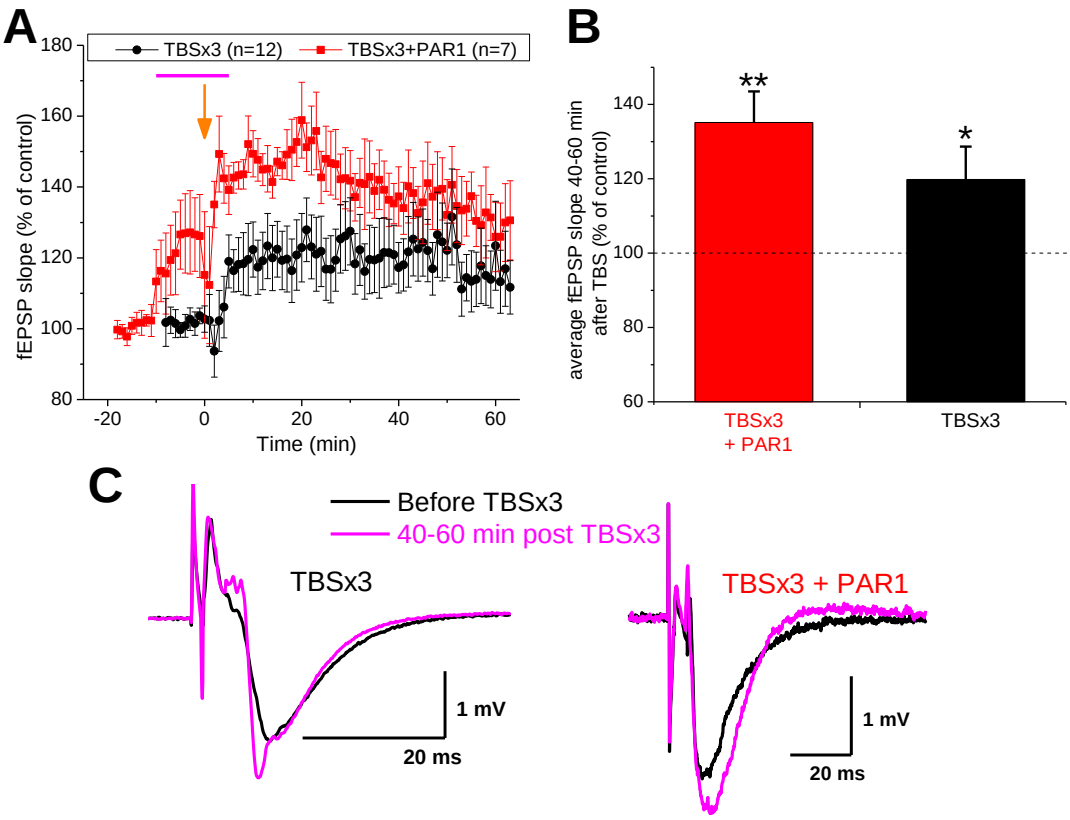

Figure 3.18. Application of PAR-1 agonist during TBSx3 increases the extent of LTP. These recordings were performed in WT mice. **A** shows the average time-courses for fEPSP recordings. Orange arrow shows position of TBSx3 delivery. 10 minutes of baseline fEPSP recordings were made before TBSx3 delivery. Purple bar shows the time-span of PAR1 agonist (10 μM TFLLR) application. **B** represents the average % increase in fEPSP 40-60 minutes post TBSx3 delivery. The average % increase in fEPSP was 19.83±8.84% for TBSx3 protocol under control application. The average % increase in fEPSP was 35.14±8.39% for TBSx3 protocol under TFLLR application. Two sample independent t-test was performed between the two sets of data. Paired t-test was performed for average % change in fEPSP from baseline. $p<0.05$, *; $p<0.01$, **. **C** shows example fEPSPs before and after TBSx3 delivery.

As was shown in section 3.10, application of TFLLR results in the appearance of an NMDAR component in the fEPSP. It was suggested that the TFLLR-mediated activation of astrocytic vesicular release of ATP results in the activation of P2XRs on post-synaptic neurones. This then leads to inhibition of GABAergic transmission, which leads to activation of post-synaptic NMDARs. This increase in NMDAR opening results in a larger fEPSP. In the current section it was shown that TFLLR application could change the direction of TBSx2 induced synaptic plasticity from LTD to LTP (Figure 3.15). Furthermore, TFLLR application increased the extent of TBSx3 induced LTP (Figure 3.18). These results suggested that TFLLR activation of astrocytes can contribute to TBS-induced LTP. As mentioned above, fEPSP size increases during the application of TFLLR (see Figures 3.12, 3.15A and 3.18A) and this increase is as a result of increase in NMDAR component. This suggests that the LTP induced via TFLLR application during TBSx2 protocol might be solely as a result of TFLLR i.e. that TFLLR by itself (without TBS delivery) induces LTP because of an increase in NMDAR component of fEPSP. Indeed, a study performed in the CA1 region of the hippocampus showed that in the absence of TBS or HFS protocol, application of thrombin, which is an agonist for PAR1, PAR3 and PAR4 receptors, for only 10 minutes was enough to induce a long-lasting LTP (Maggio *et al.*, 2008). To investigate whether this is the case in the somatosensory cortex, TFLLR was applied for ten minutes in the absence of TBS delivery. The fEPSP recording was continued for 50 minutes after TFLLR washout. Similar to Figure 3.12, application of TFLLR resulted in a significant increase in fEPSP ($p<0.05$, paired t-test; Figure 3.19A-B). The average increase was 16±11.81% following 5-10 minutes of TFLLR application (n=6; see Figure 3.19B). However, washout of

TFLLR resulted in a gradual decline in fEPSP. Thirty to forty minutes after TFLLR application, the average size of fEPSP was now only 6.75±3.60% with respect to baseline recording (n=6; see Figure 3.19B). These results show that in the somatosensory cortex, TFLLR application increases the fEPSP but that this increase in fEPSP is not an LTP because washout of TFLLR decreases fEPSP back to baseline value. This in turn suggests that the change of LTD to LTP with TFLLR application during TBSx2 is as a result of a long-term change in synaptic transmission.

The above results showed that application of TFLLR can lead to an increase in fEPSP (Figure 3.12 and 3.19). This increase was due to an increase in NMDAR activity. Is this increase due to pre or post-synaptic changes? It was shown that application of TFLLR results in inhibition of post-synaptic GABAergic currents. Please refer back to section 3.9 and the paper published by my laboratory (Lalo, U. Palygin O. et al. 2014). It was also shown that inhibition of $GABA_A$ receptors could lead to increase in NMDAR activity (Figure 3.12). This suggested that application of TFLLR could increase NMDAR activity by inhibiting post-synaptic GABAergic transmission. This in turn suggests that the increase in NMDAR activity should be as a result of effect on post-synaptic sites. To provide further evidence that the increase in NMDAR activity via TFLLR occurs at post-synaptic sites, paired pulse protocol was carried out before and after TFLLR application. Delivery of the second pulse 50 ms after the first pulse resulted in the facilitation of the second fEPSP (Figure 3.19C). The average paired pulse ratio (PPR) of this facilitation was 1.51±0.12 (n=6; see Figure 3.19C-D). Application of TFLLR increases the size of fEPSP (Figure 3.19A and

C). If paired pulse ratio changes following this increase, then it would indicate that the increase in NMDAR component following TFLLR application is as a result of pre-synaptic changes. However, if paired pulse ratio does not change, then it would suggest that the increase in fEPSP is as a result of post-synaptic changes. As expected, delivery of paired pulse protocol during TFLLR protocol failed to significantly change the PPR ($p<0.05$, paired t-test; see Figure 3.19C-D). Paired pulse ratio during TFLLR application was 1.40±0.11 (n=6). Washout of TFLLR also did not have a significant effect on PPR. These results provide further support that the increase in NMDAR component of fEPSP following TFLLR application is as a result of post-synaptic increase in NMDAR activity.

Taken together, the results in this section show that in the somatosensory cortex, the increase in fEPSP mediated by TFLLR application is not an LTP. However, if TFLLR is applied to sub-threshold TBS protocols, then LTP can be induced or its size increased. This suggests that activation of astrocytic vesicular release with TFLLR application can contribute to TBS-induced LTP.

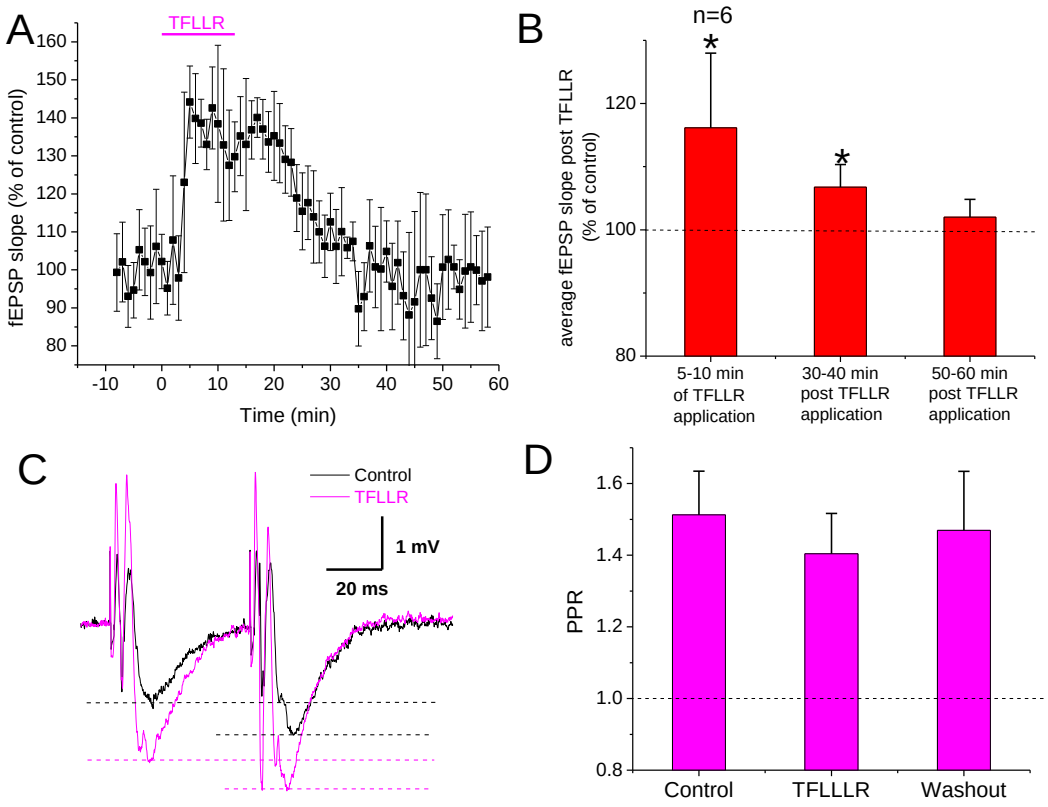

Figure 3.19. Application of PAR-1 agonist neither leads to LTP nor does it change the PPR. These recordings were performed in WT mice. **A** shows the time-course for fEPSP recordings before and after TFLLR application. Purple bar shows the time-span of TFLLR (10 μM) application. The time-course is from a single experiment. Each dot shows the average fEPSP slope of fEPSPs recorded in a 1 minute time window. **B** shows the average % change in fEPSP across several experiments following TFLLR application. The average % change in fEPSP 5-10 minutes post PAR-1 application was +16±11.81%. The average % change in fEPSP 30-40 minutes post PAR-1 application was 6.75±3.60%. The average % change in fEPSP 40-60 minutes post PAR-1 agonist application was 2±2.83%. Paired t-test was performed for average % change in fEPSP from baseline. $p<0.05$, *. **C** shows example fEPSP traces. Increase in slope and amplitude of fEPSP can be seen following TFLLR application. This example also shows the fEPSP as a result of second pulse. There was a 50 ms time interval between the two pulses. **D** shows the average PPR across the six recordings from **B**. Paired pulse protocol was carried out under control conditions, 5 minutes after TFLLR application, and 20 minutes after TFLLR washout. Two sample independent t-tests were performed between each two sets of data. There was no significant difference between any two sets of data ($p<0.05$).

Box 3.4.

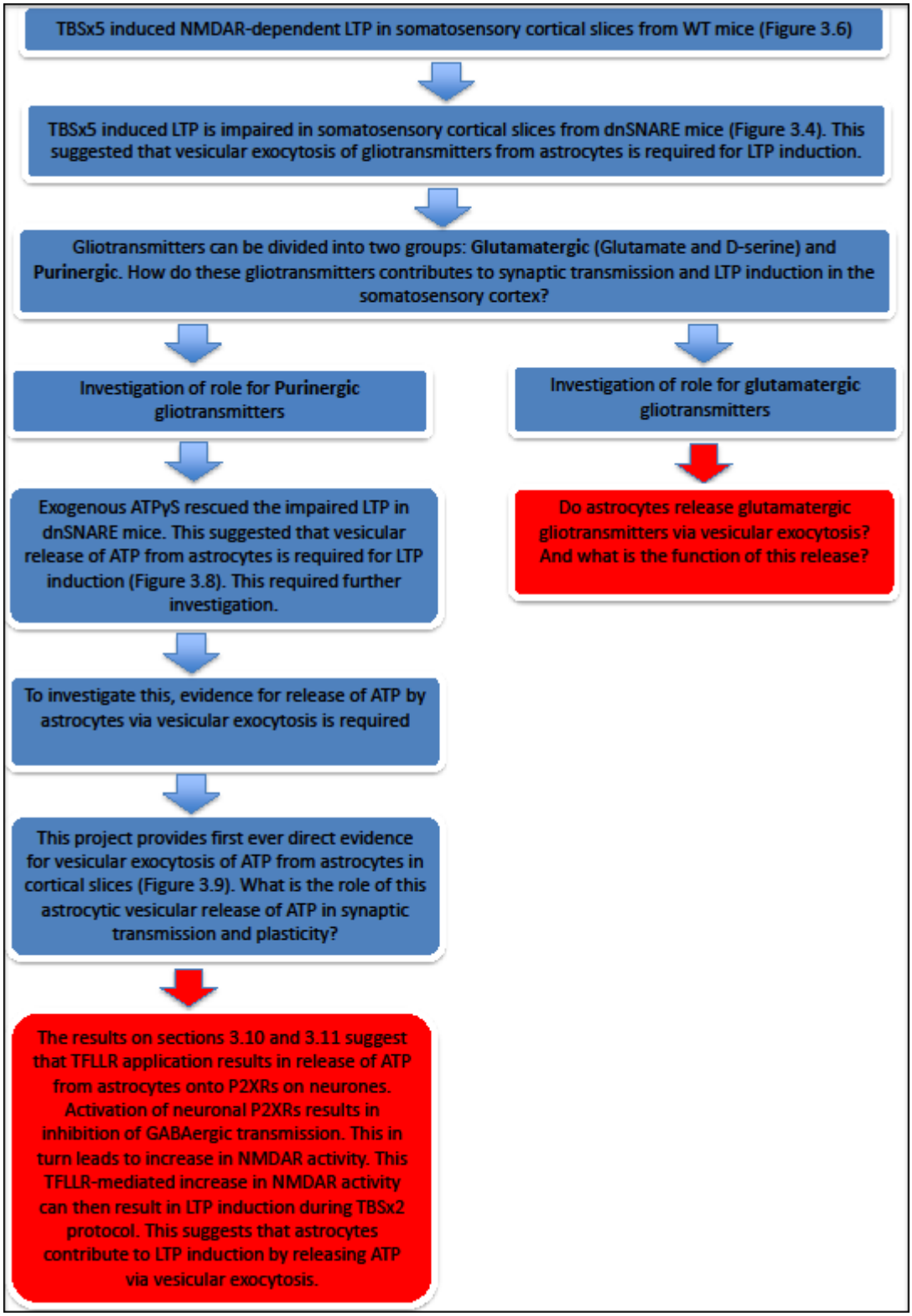
TBSx5 induced NMDAR-dependent LTP in somatosensory cortical slices from WT mice (Figure 3.6)
TBSx5 induced LTP is impaired in somatosensory cortical slices from dnSNARE mice (Figure 3.4). This suggested that vesicular exocytosis of gliotransmitters from astrocytes is required for LTP induction.
Gliotransmitters can be divided into two groups: Glutamatergic (Glutamate and D-serine) and Purinergic. How do these gliotransmitters contributes to synaptic transmission and LTP induction in the somatosensory cortex?
Investigation of role for Purinergic gliotransmitters
Investigation of role for glutamatergic gliotransmitters
Exogenous ATPγS rescued the impaired LTP in dnSNARE mice. This suggested that vesicular release of ATP from astrocytes is required for LTP induction (Figure 3.8). This required further investigation.
Do astrocytes release glutamatergic gliotransmitters via vesicular exocytosis? And what is the function of this release?
To investigate this, evidence for release of ATP by astrocytes via vesicular exocytosis is required
This project provides first ever direct evidence for vesicular exocytosis of ATP from astrocytes in cortical slices (Figure 3.9). What is the role of this astrocytic vesicular release of ATP in synaptic transmission and plasticity?
The results on sections 3.10 and 3.11 suggest that TFLLR application results in release of ATP from astrocytes onto P2XRs on neurones. Activation of neuronal P2XRs results in inhibition of GABAergic transmission. This in turn leads to increase in NMDAR activity. This TFLLR-mediated increase in NMDAR activity can then result in LTP induction during TBSx2 protocol. This suggests that astrocytes contribute to LTP induction by releasing ATP via vesicular exocytosis.

3.12. Application of PAR-1 agonist results in the astrocytic vesicular release of glutamatergic gliotransmitters onto extra-synaptic NMDARs

For summary of results thus far please refer to Box 3.4. Sections 3.7 to 3.12 show that in the somatosensory cortex, application of PAR-1 agonist can result in the vesicular release of ATP from astrocytes. This ATP release can activate P2XRs on neurones. Activation of P2XRs on neurones leads to the inhibition of post-synaptic GABAergic transmission (Lalo *et al.*, 2014). This in turn leads to an increase in post-synaptic NMDAR activity. If this PAR-1 agonist mediated increase in NMDAR activity occurs during the delivery of TBS protocols, then it can contribute to LTP induction. What these results suggest is that vesicular release of ATP from astrocytes can contribute to LTP induction. However, astrocytes can also release D-serine and glutamate. Therefore it would be interesting to know what roles these gliotransmitters play in synaptic transmission and plasticity. For this purpose, in this section and the following section of this chapter, the role of glutamatergic transmission in the context of tripartite synapse will be investigated.

Studies from other labs have provided evidence for vesicular exocytosis of glutamate from astrocytes in culture preparations (Araque *et al.*, 2000, Bezzi *et al.*, 2004). In hippocampal brain slice preparations, evidence for glutamate release has also been shown (Fellin *et al.*, 2004). However, whether in brain slice preparations release of glutamate occurs via vesicular exocytosis remains to be determined. Evidence for astrocytic release of D-serine via vesicular exocytosis

has been provided in both culture preparations (Bezzi *et al.*, 2004, Mothet *et al.*, 2005) and hippocampal slice preparations (Kang *et al.*, 2013). Therefore, in this project, the aim was to provide evidence for vesicular exocytosis of glutamate and D-serine from astrocytes in the somatosensory cortex.

To investigate whether D-serine and glutamate are released via vesicular exocytosis from astrocytes, my colleagues used microelectrode biosensors to measure the concentration of glutamate and D-serine in cortical slices (unpublished data). They showed that application of TFLLR (10 µM) to WT mice resulted in a robust increase in the extracellular concentrations of both D-serine and glutamate. In contrast, application of TFLLR to dnSNARE cortical slices did not result in increase in either D-serine or glutamate concentrations. These results suggested that TFLLR application can result in vesicular release of glutamate and D-serine specifically from astrocytes, thereby providing evidence that cortical astrocytes are capable of releasing D-serine and glutamate via vesicular exocytosis.

The biosensor data indicate that glutamate and D-serine can be released from astrocytes by vesicular exocytosis. If this were the case then one would expect an increase in glutamatergic transmission following the astrocytic release of glutamate and D-serine. To investigate this notion, neurones in layer 2/3 of the cortex were voltage clamped at membrane potential of -40mV. NMDAR-mediated spontaneous EPSCs were recorded under antagonists of $GABA_A$ receptors (100 µM Picrotoxin), AMPA receptors (30 µM DNQX) and P2X receptors (10 µM PPADS and 5 µM 5-BDBD). To specifically activate vesicular

release from astrocytes, TFLLR (10 µM) was applied to cortical slices following 10 minutes of baseline NMDAR-mediated spontaneous EPSC recordings (NMDAR sEPSCs). Application of TFLLR significantly increased the frequency of NMDAR sEPSCs ($p<0.01$, paired t-test; see Figures 3.20A and 3.20E). The frequency of NMDAR sEPSCs was 0.32±0.36 Hz during baseline recordings (n=13). This frequency increased to 0.87±0.39 Hz during TFLLR application (n=13). In contrast, TFLLR application did not significantly alter the average amplitude of NMDAR sEPSCs ($p<0.05$, paired t-test; see Figure 3.20E). The average NMDAR sEPSC was 5.58±0.32 pA during baseline conditions (n=13). TFLLR application decreased the average amplitude of NMDAR sEPSCs to 4.78±0.48 pA (n=13). To investigate whether the increase in frequency of NMDAR sEPSCs were as a result of vesicular release from astrcoytes, TFLLR was applied to cortical slices from dnSNARE mice. Application of TFLLR to dnSNARE mice had no significant effect on the frequency and amplitude of NMDAR sEPSCs ($p<0.05$, paired t-test; see Figures 3.20B and 3.20E). During baseline recordings in dnSNARE mice, the average amplitude of NMDAR sEPSCs was 6.09±0.42 pA and the average frequency was 0.29±0.22 Hz (n=6). With TFLLR application the average amplitude was 5.98±0.39 pA and the average frequency was 0.32±0.25 Hz. Taken together, these results suggest that application of TFLLR results in vesicular release of glutamatergic gliotransmitters from astrocytes. This vesicular release results in increase in frequency of NMDAR sEPSCs on neurones.

Further analysis of NMDAR sEPSCs revealed that in WT mice, sEPSCs showed a bimodal amplitude and decay distributions (Figure 3.20C). The sEPSCs with

slower amplitudes had longer decay times whilst the sEPSCs with larger amplitudes had faster decay times. Application of TFLLR selectively increased the probability of the detection of smaller and slower sEPSCs (Figures 3.20C and 3.20E). Application of TFLLR to dnSNARE mice did not increase the number of these slow sEPSCs (Figures 3.20B and 3.20D). This suggests that vesicular release from astrocytes results in increase in frequency of these "slow" NMDAR-mediated sEPSCs. This TFLLR-mediated increase in frequency of "slow" NMDAR sEPSCs is similar to the increase in frequency of "slow" P2XR-mediated sEPSCs following TFLLR application (Figure 3.2). Together, these results suggest that astrocytes, in addition to releasing purinergic gliotransmitters via vesicular exocytosis, are also capable of releasing glutamatergic gliotransmitters via vesicular exocytosis.

It has been shown that GluN2B-containing NMDARs have lower peak currents and slower decay times compared to GluN2A-containing NMDARs (Monyer *et al.*, 1994, Erreger *et al.*, 2005). Furthermore, it has been shown that release of glutamate from hippocampal astrocytes can activate GluN2B containing NMDARs (Fellin *et al.*, 2004). These reports suggest that the slow sEPSCs that appear following TFLLR application in my recordings could be due to activation of GluN2B containing NMDARs. To investigate this, Ifenprodil (10μM), which is an antagonist of GluN2B containing NMDARs, was applied to cortical slices subsequent to TFLLR application. Application of Ifenprodil resulted in a significant decrease in the average frequency of NMDAR sEPSCs ($p<0.01$, paired t-test) by inhibiting the slow sEPSCs (Figures 3.20A, 3.20C and 3.20F). In contrast, Ifenprodil application resulted in a significant increase in the average

amplitude of sEPSCs ($p<0.05$, paired t-test; Figure 3.20F). As ifenprodil inhibits GluN2B-containing NMDARs, the ratio of large NMDAR sEPSCs to GluN2B-mediated slow sEPSCs will increase; hence resulting in an increase in the average amplitude of NMDAR sEPSCs. Application of Ifenprodil during control conditions (without TFLLR) did not significantly alter the average amplitude and average frequency of sEPSCs (Figure 3.20F), suggesting that GluN2B-containing NMDA receptors are not activated under baseline spontaneous recordings where astrocytic release is not activated.

Taken together, these results show that the slow sEPSCs were due to GluN2B containing NMDARs. It is believed that in adult mice, synaptic NMDARs mainly consist of GluN2A subunits whilst extra-synaptic NMDARs mainly consist of GluN2B subunits (Tovar and Westbrook, 1999, Papouin *et al.*, 2012). Based on this, one can suggest that the results in this section show that activation of astrocytes can lead to vesicular release of glutamatergic gliotransmitters from these cells. These glutamatergic gliotransmitters can then activate extra-synaptic GluN2B containing NMDARs.

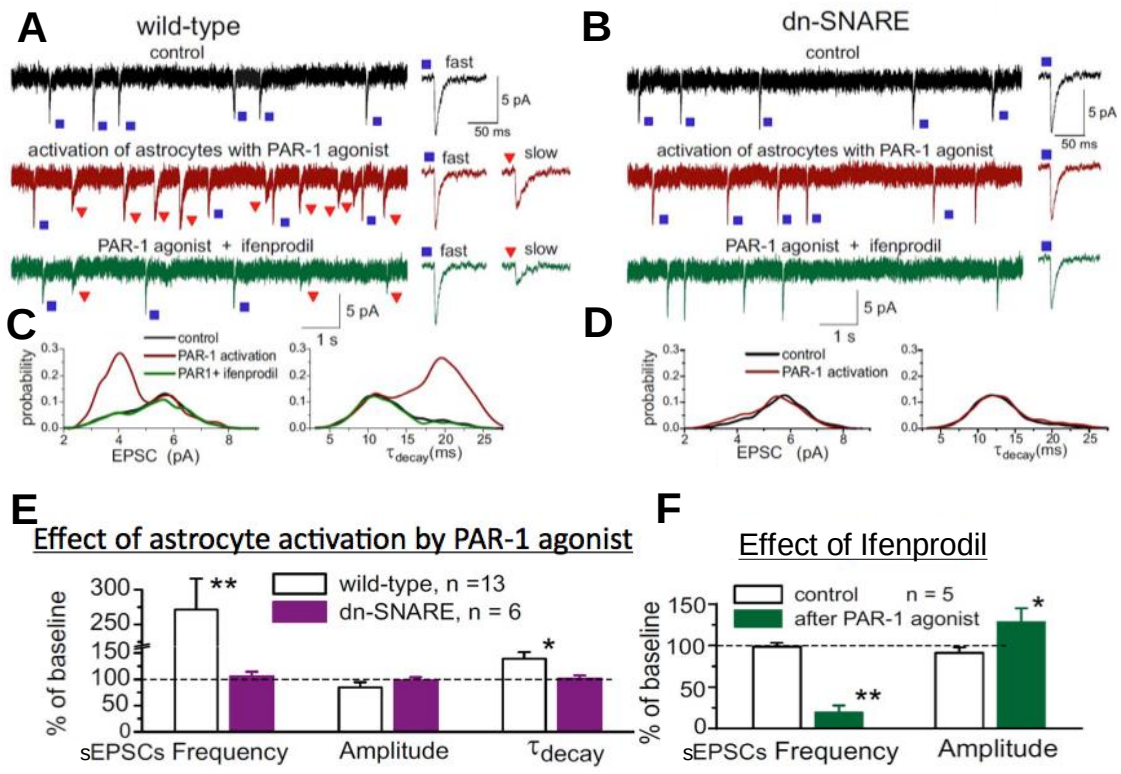

Figure 3.20. Activation of vesicular release from astrocytes via PAR-1 agonist leads to the appearance of small amplitude GluN2B-dependent NMDAR sEPSCs. A and **B** show example NMDAR sEPSC recordings from one WT mouse and one dnSNARE mouse. NMDA sEPSCs were recorded at -40 mV holding voltage under Picrotoxin (100 μM), DNQX (30 μM), 5-BDBD (10 μM) and PPADS (10 μM). The effect on sEPSCs following PAR-1 agonist (10 μM TFLLR) and Ifenprodil (10 μM) application are shown. **C** and **D** show the probability density functions for the examples shown in **A** and **B**. Bar-charts shown in **E** represent the average % change in the frequency, amplitude and decay time of control NMDAR sEPSCs following application of PAR-1 agonist. Bar-charts shown in **F** represent the average % change in amplitude and frequency of NMDAR sEPSCs following application of Ifenprodil in WT cortical slices. Ifenprodil was applied either on control conditions or on TFLLR treated slices. Paired t-test was performed for average % change in sEPSCs from baseline. $p<0.05$, *; $p<0.01$, **.

The above results show that TFLLR can lead to vesicular exocytosis of glutamatergic gliotransmitters specifically from astrocytes. This release was indicated by the increase in frequency of NMDAR sEPSCs. TFLLR-mediated release of glutamatergic gliotransmitters involves the release of both glutamate and D-serine, as was suggested by the above-mentioned biosensor experiments carried out by my colleagues. Are both D-serine and glutamate release from astrocytes contributing to increase in frequency of NMDAR sEPSCs? To investigate the effect of D-serine on NMDAR sEPSCs, exogenous D-serine was applied to cortical slices from WT mice. The effect of exogenous D-serine on NMDAR sEPSCs can then be compared to effect of TFLLR on NMDAR sEPSCs, thereby enabling one to suggest what effect, if any, does TFLLR-mediated release of D-serine from astrocytes has on NMDAR activity. Same as in Figure 3.20, sEPSCs were recorded at -40mV in the presence of PPADS (5 µM), 5-BDBD (5 µM), DNQX (30 µM) and picrotoxin (100 µM). Application of exogenous D-serine significantly increased both the average amplitude and average frequency of NMDAR sEPSCs with respect to control ($p<0.05$, paired t-test; see Figure 3.21A-C). This result is in contrast to TFLLR application (Figure 3.20), where there was only an increase in the average frequency of sEPSCs and not in the average amplitude. Furthermore, the increase in frequency with TFLLR was much larger than the increase in frequency with D-serine. With TFLLR the increase in the average frequency was 172% whilst the increase in the average frequency with D-serine was only 20% (see Figures 3.20E and 3.21B).

Further analysis of NMDAR sEPSCs revealed that unlike TFLLR application, application of D-serine showed no increase in the "slow" NMDAR sEPSCs. As can be seen from Figure 3.21D, there were two peaks on the amplitude probability distribution functions, labeled (**a**) and (**b**). These peaks were similar in sEPSC amplitude to the two peaks in the bimodal distribution shown on Figure 3.20C. However, in the example shown on Figure 3.21D, the second peak (**b**) is split in to two more peaks. Application of D-serine did not increase the probability of the first peak (**a**) (Figure 3.21D) but shifted the probability density function to the right. Furthermore, there was no appearance of a second "slower" peak in the decay time probability distribution function following D-serine application. These results show that application of exogenous D-serine increases the amplitude of NMDAR sEPSCs and does not lead to the appearance of the "slow" NMDAR sEPSCs. This is in contrast to TFLLR application, where there was no increase in amplitude but a large increase in frequency of "slow" NMDAR sEPSCs. This suggests that the TFLLR-mediated increase in "slow" extra-synaptic NMDAR sEPSCs is not mediated via astrocytic D-serine release and it might be mediated via astrocytic release of glutamate. Support for this notion comes from the report that in the hippocampus, D-serine only activates synaptic NMDARs and not the extra-synaptic GluN2B-containing NMDARs (Papouin, Ladepeche et al. 2012). It is possible that the D-serine released via TFLLR activation of astrocytes does not increase the average amplitude of NMDAR sEPSCs because the large increase in frequency of small GluN2B-mediated sEPSCs occludes the effect of D-serine on synaptic NMDARs. Indeed, when exogenous D-serine was applied to TFLLR treated slices, there was no change in either the average amplitude or the average frequency of NMDAR

sEPSCs (Figure 3.21B-C). Application of D-AP5 removed all the NMDAR sEPSCs, thereby showing that the sEPSCs were indeed mediated by activity of NMDARs (Figure 3.21A).

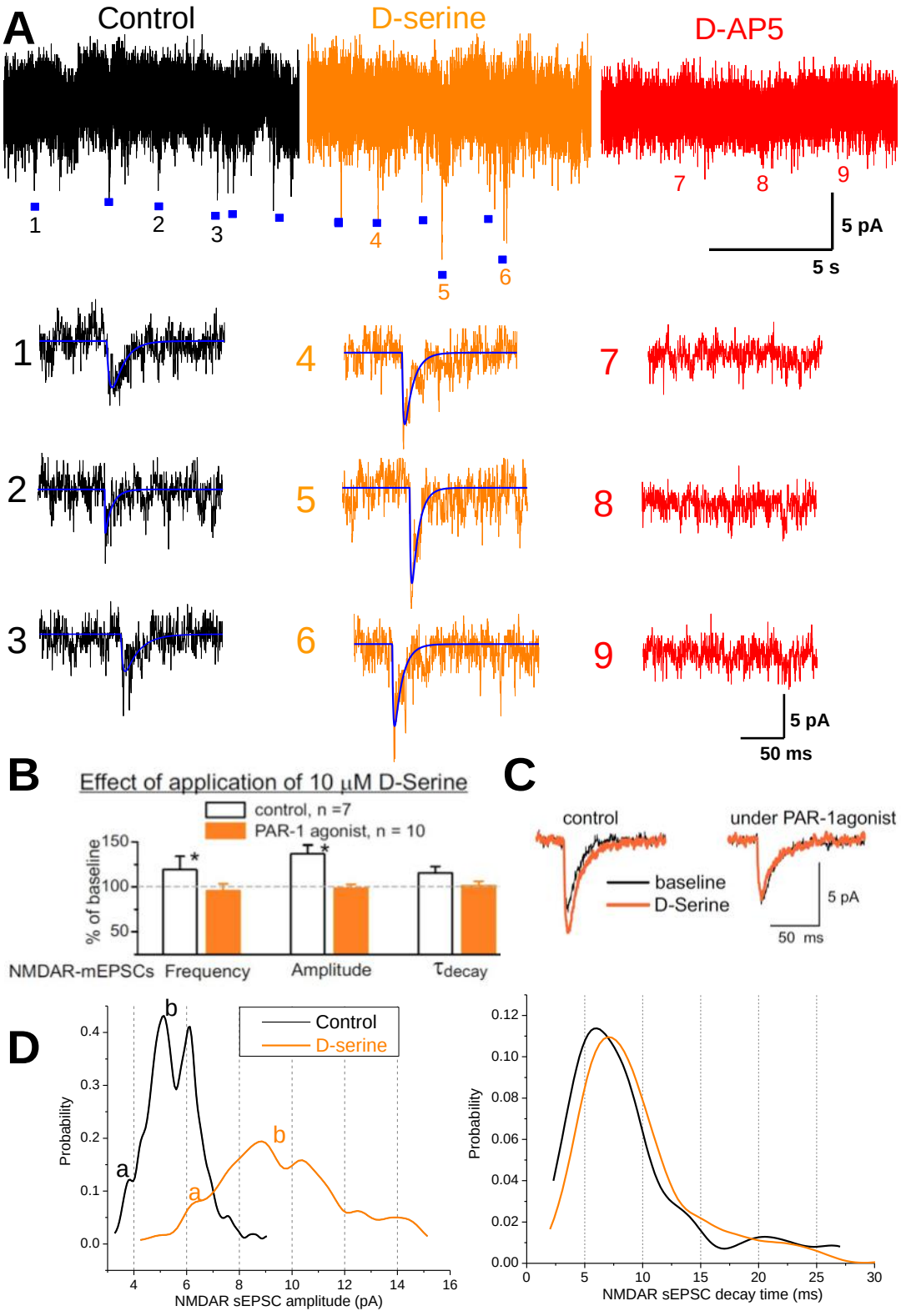

Figure 3.21. see next page for Figure legend.

Figure 3.21. Exogenous D-serine can increase the amplitude and frequency of NMDAR sEPSCs in control/baseline conditions but not in PAR-1 agonist treated slices. These recordings were performed in WT mice. **A** shows example traces for NMDAR sEPSC recordings under control, D-serine (10 μM) and D-AP5 (30 μM). The blue lines show the curves that were fitted on the sEPSCs. NMDAR sEPSCs were recorded at -40 mV holding voltage under Picrotoxin (100 μM), DNQX (30 μM), 5-BDBD (10 μM) and PPADS (10 μM). **B** shows bar-charts representing the average % change in the amplitude and frequency of NMDAR sEPSCs under control and PAR-1 (10 μM TFLLR) treated slices. In control conditions, the average amplitude of NMDAR sEPSC was 5.70±1.23 pA and the average frequency was 0.33±0.13 Hz. Under PAR-1 agonist, the average amplitude was 4.78±0.48 pA and the average frequency was 0.87±0.39 Hz. Paired t-test was performed for each data in comparison to control ($p<0.05$,*). **C** shows NMDAR sEPSC examples before and after D-serine application. Each of these examples are the average of twenty sEPSCs. **D** shows probability distribution functions for before and after D-serine application for one example recording.

Other labs have reported that D-serine application on hippocampal slices does not lead to change in the amplitude of evoked NMDAR EPSC (NMDAR eEPSC) (Fellin *et al.*, 2009, Deng *et al.*, 2011). In these reports, NMDAR eEPSCs were evoked using afferent stimulation. These results are in contrast to my spontaneous NMDAR mediated EPSC recordings in the somatosensory cortex, where D-serine application increases both the amplitude and frequency of NMDAR sEPSCs. One possibility that can explain the difference between my results and those from other labs is that it is possible that during evoked recordings, D-serine/glycine levels are saturated. To investigate this, D-serine and TFLLR were applied to slices from somatosensory cortex during recording of NMDAR eEPSCs. This experiment also allows one to investigate what are the effects of D-serine and TFLLR application on NMDARs when afferent neurons are persistently activated.

NMDAR eEPSCs were recorded under PPADS (10 μM), 5-BDBD (5 μM) picrotoxin (10 μM) and DNQX (30 μM). Baseline eESPCs were set at 20-30% of maximal response. Application of exogenous D-serine, subsequent to 5-10 minutes of baseline evoked EPSC recordings, significantly increased the evoked current by an average size of +106.75±5.74% ($p<0.001$, paired t-test, n=4; see Figure 3.22A). This showed that NMDA receptors are not saturated with respect to D-serine/glycine levels. Application of TFLLR also significantly increased the eEPSC amplitude by +27.94±25.33% ($p<0.05$, paired t-test, n=7; see Figure 3.22A). However, the increase in eEPSC amplitude with TFLLR was significantly smaller than the increase with D-serine application ($p<0.001$, two sample independent t-test; see Figure 3.22A).

Similar to spontaneous NMDAR EPSC recordings shown on Figure 3.21B-C, exogenous D-serine was applied subsequent to 10 minutes of TFLLR application to see whether D-serine could further increase the NMDAR EPSC after the initial rise due to TFLLR application. In contrast to spontaneous NMDAR EPSCs, application of D-serine resulted in a significant further increase of +47.15±30.65% in the amplitude of evoked NMDAR EPSCs. This increase was statistically significant ($p<0.05$, paired t-test, n=7; see Figure 3.22A). The overall change in eEPSC amplitude following application of TFLLR **and** D-serine with respect to baseline was +86.83±40.40%. There was no statistically significant difference between the increase in eEPSC amplitude when both TFLLR and D-serine where applied and when only D-serine was applied ($p<0.05$, two sample independent t-test). Application of D-AP5 completely abolished the NMDAR EPSC, thereby showing that the evoked EPSC was indeed mediated by NMDAR activity (Figure 3.22A).

Increase in eEPSC amplitude could be either due to pre-synaptic or post-synaptic changes. Further analysis of NMDAR eEPSC were carried out to investigate whether the increase in amplitude following D-serine and TFLLR application were due to pre-synaptic or post synaptic effects. Figure 3.22B shows the amplitude probability distribution functions (PDFs) for baseline (control) NMDAR eEPSC recordings and for eEPSCs recordings during application of exogenous D-serine. Binomial models of release were fitted to the data. These models are shown as grey lines on the pdfs on Figure 3.22B. The parameters for binomial models are also given on Figure 3.22B. Application of exogenous D-

serine increased the quantal amplitude from 2.01 pA to 5.07 pA, suggesting increase in **post-synaptic** NMDAR activity. The pre-synaptic parameters of the model, which are probability of release (p), number of release sites (n) and the average number of quanta (m), showed slight decrease.

Figure 3.22C shows amplitude PDFs for baseline NMDAR eEPSC recordings and for eEPSC recordings following application of TFLLR. Binomial model of release could be fitted for baseline recordings as shown on Figure 3.22C. However, binomial model could not be fitted for NMDAR eEPSCs recorded under TFLLR application (unimodal model could not be rejected). This was the case for all 7 NMDAR eEPSC recordings under TFLLR. Therefore, it is not possible to determine from these evoked EPSC recordings whether TFLLR application results in increase in eEPSC amplitude as a result of increase in release probability or as a result of an effect on post-synaptic receptors. However, as was shown on Figure 3.20, TFLLR application resulted in a significant increase in frequency of spontaneous NMDAR EPSCs, suggesting that the effect of TFLLR on NMDAR activity is due to increase in release probability and not as a result of a post-synaptic effect.

Figure 3.22C also shows the amplitude pdf for eEPSC recordings during D-serine application on top of TFLLR-treated cortical slices. Binomial model of release could be fitted to this data. The quantal amplitude of this model was 5.41 pA, which is larger than the 1.85 pA quantal amplitude of baseline recording. In contrast, there was no change in probability of release (p) and in number of

release sites (n). These results again suggest that D-serine increases NMDAR EPSCs by increasing the opening of post-synaptic NMDARs.

Taken together, the results in this section show that TFLLR can result in the release of glutamate and D-serine specifically from astrocytes. This release of glutamatergic gliotransmitters from astrocytes activates extra-synaptic GluN2B containing NMDA receptors on neurons. It was also suggested that application of exogenous D-serine can increase the amplitude of NMDAR eEPSCs by acting on post-synaptic NMDARs. As exogenous D-serine results in an increase in the amplitude of post-synaptic NMDARs whilst TFLLR does not increase the amplitude of NMDAR EPSCs but increases the frequency, one can suggest that the astrocytic release of D-serine following TFLLR application does not have a similar effect to exogenous D-serine application.

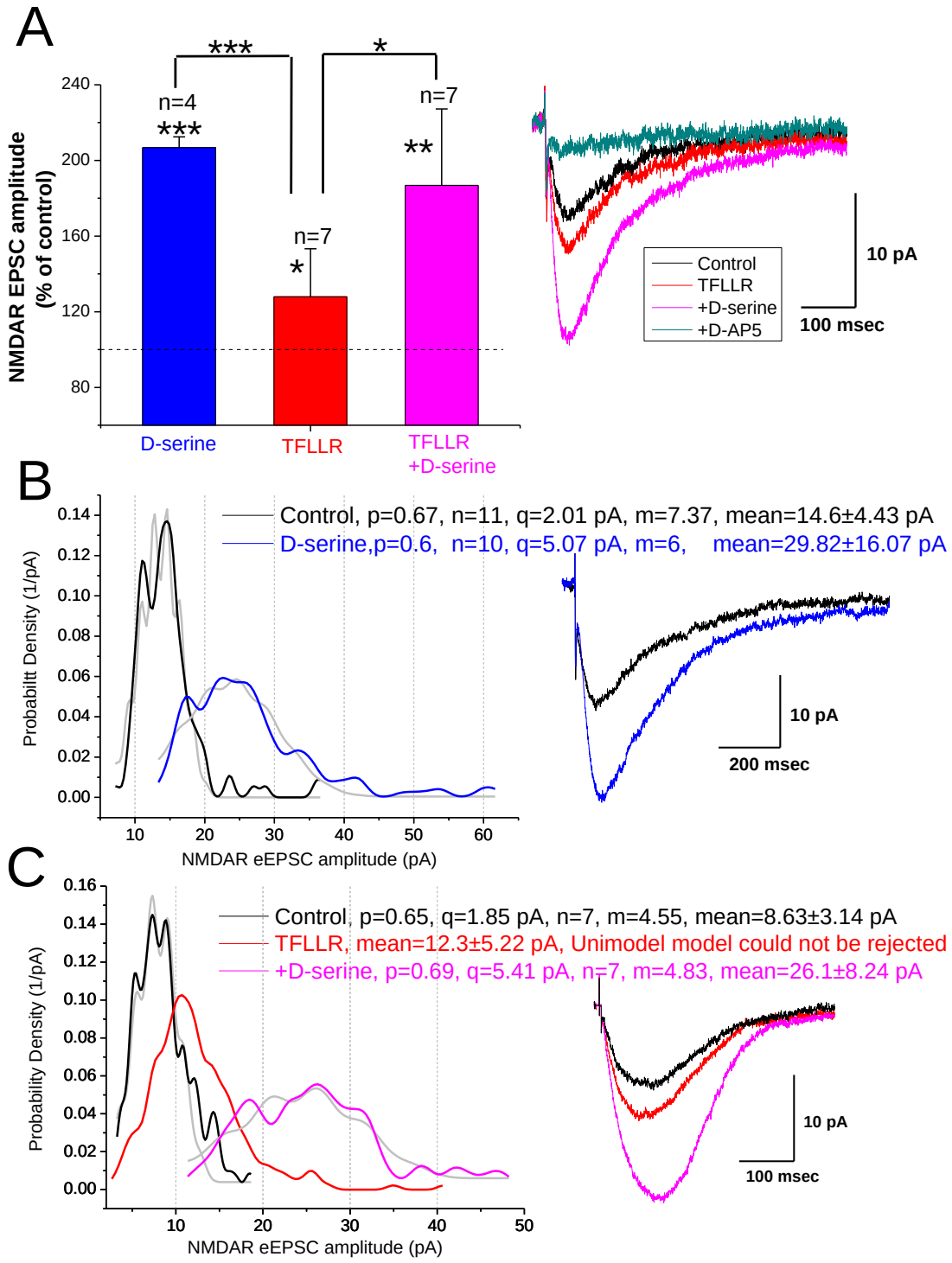

Figure 3.22. For Figure legend please see next page.

Figure 3.22. Exogenous D-serine and PAR-1 agonist can increase the amplitude of evoked NMDAR EPSCs. These recording were performed in WT mice. NMDAR eEPSCs were recorded at -40 mV holding voltage under Picrotoxin (100 μM), DNQX (30 μM), 5-BDBD (5 μM) and PPADS (10 μM). Examples of NMDAR eEPSCs are shown to the right hand side of the figure. **A** shows bar-charts representing the average % increase in eEPSC amplitude following D-serine (10 μM) and TFLLR (10 μM) application. Paired t-test was performed for each data in comparison to control. Paired t-test was also performed between TFLLR data and D-serine+TFLLR agonist data. Two sample t-test was performed between control and TFLLR agonist data. Two sample t-test was also carried out between control and D-serine+TFLLR agonist data. $p<0.05$ (*), $p<0.01$ (**), $p<0.001$ (***). **B** shows Probability distribution functions before and after D-serine application for one example recording. **C** shows probability distribution functions for control recordings, subsequent to TFLLR application, and after D-serine application on top of TFLLR. Model parameters are quantal amplitude (q), number of release sites (n), probability of release (p) and average number of quanta released (m).

Box 3.5.


TBSx5 induces NMDAR-dependent LTP in somatosensory cortical slices from WT mice (Figure 3.6)
TBSx5 induced LTP is impaired in somatosensory cortical slices from dnSNARE mice (Figure 3.4). This suggested that vesicular exocytosis of gliotransmitters from astrocytes is required for LTP induction.
Gliotransmitters can be divided into two groups: Glutamatergic (Glutamate and D-serine) and Purinergic. How do these gliotransmitters contributes to synaptic transmission and LTP induction in the somatosensory cortex?
Investigation of role for Purinergic gliotransmitters
Exogenous ATPγS rescued the impaired LTP in dnSNARE mice. This suggested that vesicular release of ATP from astrocytes is required for LTP induction (Figure 3.8). This required further investigation.
To investigate this, evidence for release of ATP by astrocytes via vesicular exocytosis is required
This project provides first ever direct evidence for vesicular exocytosis of ATP from astrocytes in cortical slices (Figure 3.9). What is the role of this astrocytic vesicular release of ATP in synaptic transmission and plasticity?
The results on sections 3.10 and 3.11 suggested that TFLLR application results in release of ATP from astrocytes onto P2XRs on neurones. Activation of neuronal P2XRs results in inhibition of GABAergic transmission. This in turn leads to increase in NMDAR activity. This TFLLR-mediated increase in NMDAR activity can then result in LTP induction during TBSx2 protocol. This suggests that astrocytes contribute to LTP induction by releasing ATP via vesicular exocytosis.
Investigation of role for glutamatergic gliotransmitters
Do astrocytes release glutamatergic gliotransmitters via vesicular exocytosis? And what is the function of this release?
Application of TFLLR results in the astrocytic release of D-serine and glutamate.
TFLLR-mediated release of glutamatergic gliotransmitters from astrocytes results in the activation of extra-synaptic Glun2B containing NMDARs. What is the role of these GluN2B containing NMDARs in synaptic plasticity?
Exogenous D-serine fails to rescue the impaired LTP in dnSNARE mice. This suggests that vesicular release of D-serine from astrocytes is not required for LTP induction (Figure 3.7).

3.13. GluN2B-containing NMDA receptors contribute to LTP induction in the somatosensory cortex

Please refer to Box 3.5 for summary of results thus far. It was suggested in the previous sections that vesicular release of ATP from astrocytes could contribute to LTP induction. However, it was also shown that astrocytes can release glutamatergic gliotransmitters onto extra-synaptic GluN2B containing NMDARs. Do these GluN2B containing NMDARs also contribute to LTP induction? Reports from the literature show contrasting results. Two studies have shown that application of GluN2B antagonist to hippocampal slices does not have an effect on LTP induction (Liu *et al.*, 2004, Papouin *et al.*, 2012). In contrast to these two reports, another study in the hippocampus showed that application of Ifenprodil significantly reduced the extent of HFS-induced LTP (Maggio *et al.*, 2008). Another study in the prefrontal cortex showed that GluN2B-containing receptors are required for TBS-induced LTP (Zhao *et al.*, 2005).

To investigate whether GluN2B-containing NMDARs contribute to LTP induction in the somatosensory cortex, TBSx5 protocol was repeated in Ifenprodil-treated WT cortical slices. Application of Ifenprodil (10 μM) resulted in a significant reduction in the extent of LTP (Figure 3.23). In Ifenprodil treated slices the average size of fEPSP 40-60 minutes post TBSx5 application was +21±7.83% (n=8), whilst in control slices the average size of fEPSP was +58±7.54% (n=15). There was a significant difference between these two sets of data ($p<0.05$, two sample independent t-test; see Figure 3.23B). These results

suggest that GluN2B containing NMDARs contribute to LTP induction in the somatosensory cortex.

TBSx2 induced LTD is changed into LTP induction via application of TFLLR (Figure 3.15). This LTP induction was attributed to TFLLR-mediated ATP release from astrocytes. However, TFLLR also results in the astrocytic release of glutamatergic gliotransmitters, which activate GluN2B-containing NMDARs on neurons. Does this TFLLR-mediated astrocytic release of glutamatergic gliotransmitters contribute to change of LTD to LTP during TBSx2? To investigate this, TBSx2 protocol was carried out in Ifenprodil and TFLLR treated slices. Delivery of TBSx2 protocol under ifenprodil and TFLLR did not result in a significant LTP ($p<0.05$, paired t-test; see Figure 3.24). However, there was no significant difference in the average fEPSP attained 40-50 minutes post TBS between TBSx2 delivery under both ifenprodil and TFLLR and TBSx2 delivery under TFLLR only ($p<0.05$, two sample t-test; see Figure 3.24B). There was however a significant difference in the average fEPSP attained 40-50 minutes post TBS between the TBSx2 delivery under TFLLR and Ifenprodil and TBSx2 induced LTD in control conditions ($p<0.05$, two sample independent t-test; see Figure 3.24B). This implies that GluN2B-containing NMDARs do not contribute to TFLLR-mediated reversal of TBSx2 induced LTD to LTP. In contrast, inhibition of P2XRs completely reversed the TFLLR-mediated TBSx2 induced LTP to LTD (Figure 3.15). Therefore, one can suggest that P2XRs play a more important role in this TFLLR-mediated LTP induction than GluN2B-containing NMDARs.

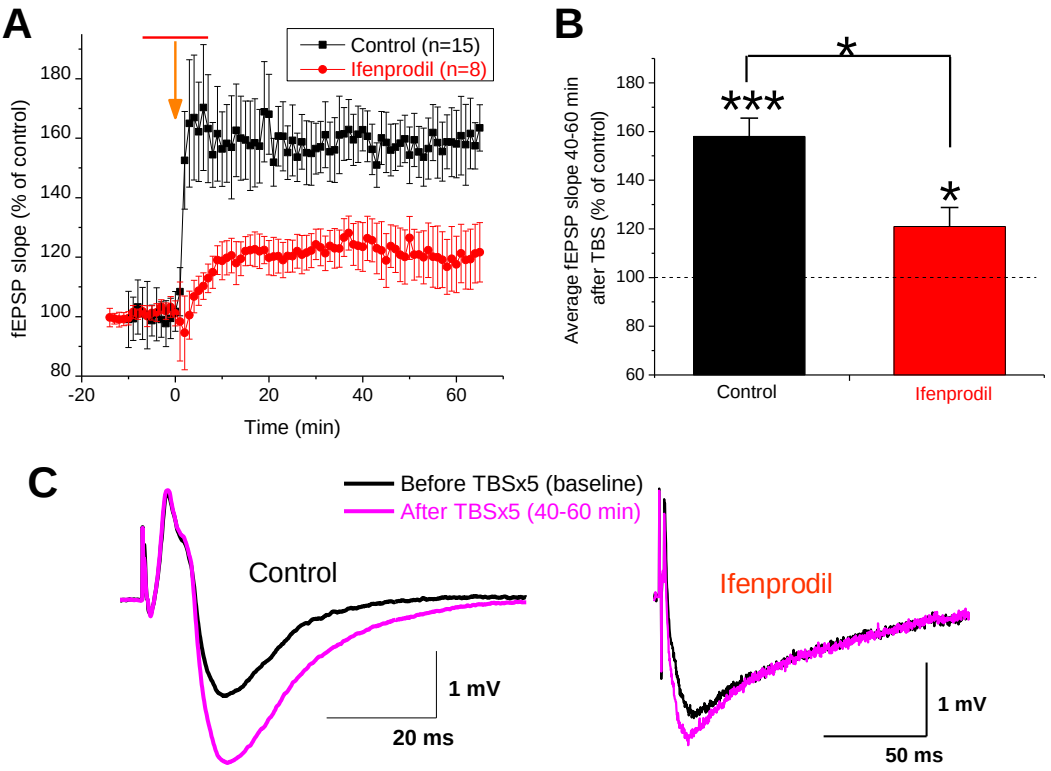

Figure 3.23. Inhibition of GluN2B-containing NMDARs decreases the size of TBSx5 induced LTP. These recordings were performed in WT mice. **A** shows the average time-courses for TBSx5 delivery under control and under Ifenprodil. Orange arrow shows position of TBSx5 delivery. Red bar shows the time-span of Ifenprodil (10 μM) application. **B** shows bar-charts representing the average % increase in fEPSP 40-60 minutes post TBSx5 delivery. Two sample independent t-test was performed between control and ifenprodil data. Paired t-test was performed for average % change in fEPSP from baseline. $p<0.05$, *; $p<0.01$, **; $p<0.001$, ***. **C** shows example fEPSPs before and after TBSx5 delivery.

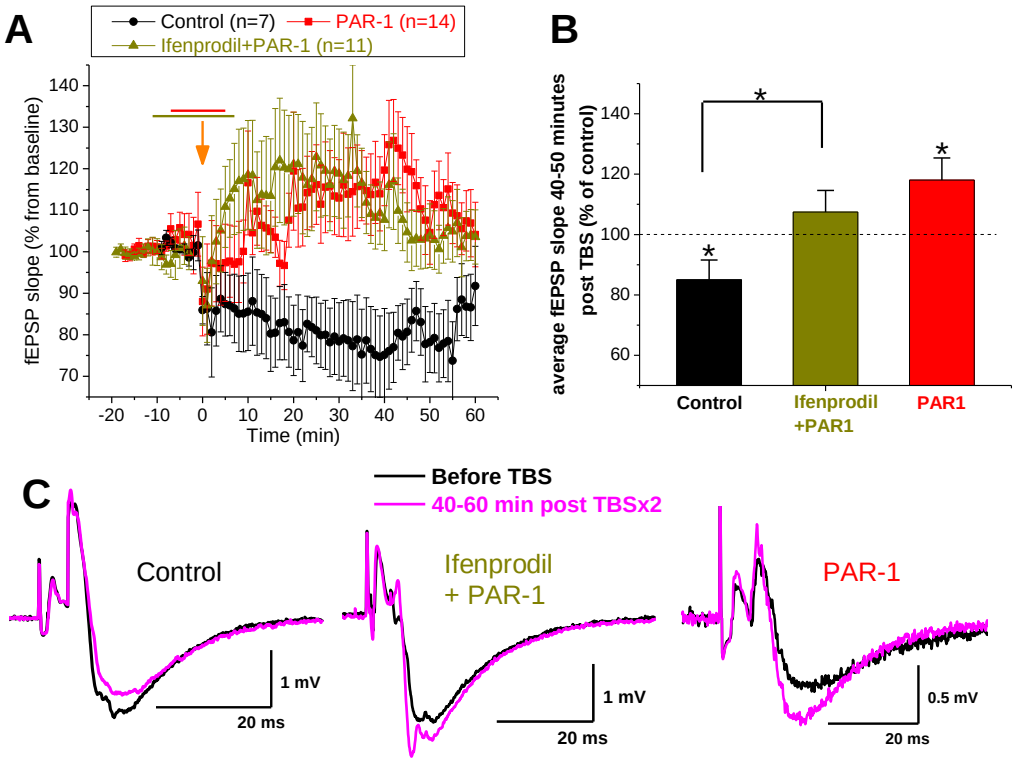

Figure 3.24. Inhibition of GluN2B-containing NMDARs decrease the size of TFLLR-mediated TBSx2 induced LTP. These recordings were performed in WT mice. **A** shows the average time-courses for TBSx2 protocol under different conditions. Orange arrow shows position of TBSx2 delivery. Dark yellow bar shows the time-span of Ifenprodil (10 μM) application. Red bar shows the time-span of TFLLR (10μM) application. TFLLR was applied 5 minutes prior to and washed out 5 minutes post TBSx2. **B** shows bar-charts representing the average % change in fEPSP 40-50 minutes post TBSx2 delivery. The average % decrease in fEPSP was -15±6.56% for TBSx2 protocol under control conditions. The average % increase in fEPSP was +7.45±7.13% for TBSx2 protocol under Ifenprodil and TFLLR. The average % increase in fEPSP was +18.07±7.30% for TBSx2 protocol under TFLLR application. Two sample independent t-test was performed between each two pairs of data. Paired t-test was performed for average % change in fEPSP from baseline. $p<0.05$, *; $p<0.01$, **. **C** shows example fEPSPs before and after TBSx2 delivery.

3.14. Summary of chapter

In this chapter evidence for release of glutamatergic and purinergic gliotransmitters via vesicular exocytosis from astrocytes in the somatosensory cortex has been provided. It was also shown that release of ATP from astrocytes could activate P2XRs on neurones. This lead to inhibition of GABAergic transmission, which in turn resulted in increase in NMDAR activity on post-synaptic neurones. It was suggested that astrocytic release of ATP contributes to LTP induction by this inhibition of GABAergic activity. It was also shown that release of glutamatergic transmission could result in the activation of extra-synaptic GluN2B-containing NMDARs on neurones. These NMDARs could contribute to LTP induction. However, it was shown that in the somatosensory cortex, astrocytic release of D-serine does not contribute to LTP induction. Please refer to Box 6 for a summary of the results of this chapter.

Box 3.6.

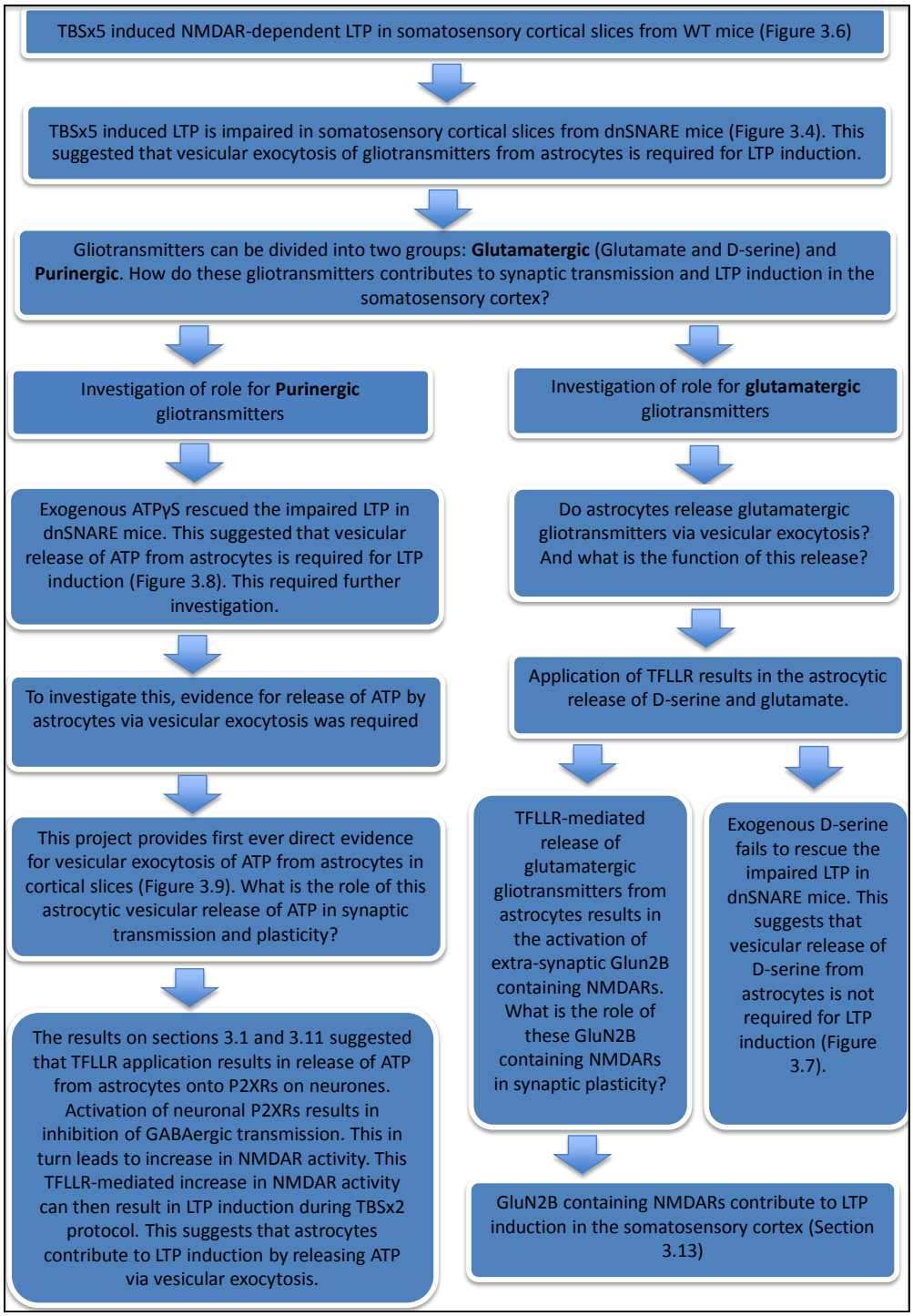
TBSx5 induced NMDAR-dependent LTP in somatosensory cortical slices from WT mice (Figure 3.6)
TBSx5 induced LTP is impaired in somatosensory cortical slices from dnSNARE mice (Figure 3.4). This suggested that vesicular exocytosis of gliotransmitters from astrocytes is required for LTP induction.
Gliotransmitters can be divided into two groups: **Glutamatergic** (Glutamate and D-serine) and **Purinergic**. How do these gliotransmitters contributes to synaptic transmission and LTP induction in the somatosensory cortex?
Investigation of role for **Purinergic** gliotransmitters
Exogenous ATPγS rescued the impaired LTP in dnSNARE mice. This suggested that vesicular release of ATP from astrocytes is required for LTP induction (Figure 3.8). This required further investigation.
To investigate this, evidence for release of ATP by astrocytes via vesicular exocytosis was required
This project provides first ever direct evidence for vesicular exocytosis of ATP from astrocytes in cortical slices (Figure 3.9). What is the role of this astrocytic vesicular release of ATP in synaptic transmission and plasticity?
The results on sections 3.1 and 3.11 suggested that TFLLR application results in release of ATP from astrocytes onto P2XRs on neurones. Activation of neuronal P2XRs results in inhibition of GABAergic transmission. This in turn leads to increase in NMDAR activity. This TFLLR-mediated increase in NMDAR activity can then result in LTP induction during TBSx2 protocol. This suggests that astrocytes contribute to LTP induction by releasing ATP via vesicular exocytosis.
Investigation of role for **glutamatergic** gliotransmitters
Do astrocytes release glutamatergic gliotransmitters via vesicular exocytosis? And what is the function of this release?
Application of TFLLR results in the astrocytic release of D-serine and glutamate.
TFLLR-mediated release of glutamatergic gliotransmitters from astrocytes results in the activation of extra-synaptic Glun2B containing NMDARs. What is the role of these GluN2B containing NMDARs in synaptic plasticity?
Exogenous D-serine fails to rescue the impaired LTP in dnSNARE mice. This suggests that vesicular release of D-serine from astrocytes is not required for LTP induction (Figure 3.7).
GluN2B containing NMDARs contribute to LTP induction in the somatosensory cortex (Section 3.13)

Chapter 4

Role for Cannabinoid Signalling during Synaptic Transmission and Plasticity in the Context of Tripartite Synapse

4.1 Motivation for studying cannabinoid signalling

Endogenous cannabinoid, or endocannabinoid (eCB), signalling in the nervous system is involved in many different functions including memory, cognition, pain perception and movement. Endocannabinoids are as widespread as other neurotransmitters such as glutamate and GABA. The density of endocannabinoid receptors (eCB-Rs) in the brain is comparable to glutamatergic and GABAergic receptors (Herkenham *et al.*, 1990). Endocannabinoid receptors can also be activated by exogenous cannabinoids. Intake of Δ^9-Tetrahydrocannabinol (Δ^9-THC), the major psychoactive component of cannabis, causes memory impairment by acting on CB1 receptors in the CNS (Kano *et al.*, 2009). Therefore, there is great interest in investigating the role of exogenous and endogenous cannabinoids in synaptic transmission and plasticity. Furthermore, CB1 receptors are present on astrocytes in addition to their neuronal localisation. Therefore, in the investigation of synaptic plasticity in the context of tripartite synapse, the role of eCBs must also be considered.

4.2 Production and release of eCBs

Neurotransmitters like glutamate and GABA are anterograde messengers. They are released from pre-synaptic neurones and diffuse to post-synaptic sites where they bind to post-synaptic receptors. eCBs act as retrograde messengers, meaning that they are synthesised and released from post-synaptic neurones and bind to receptors on pre-synaptic neurones. Endocannabinoid mediated retrograde transmission is a form of feedback mechanism to control pre-synaptic release.

Endocannabinoids are lipids and cannot be stored in vesicles. N-arachidonoylethanolamide (also called anandamide, which means inner bliss amide) was the first eCB that was identified (Devane *et al.*, 1992). The second eCB identified was 2-arachidonoylglycerol (2-AG) (Sugiura *et al.*, 1995). Anandamide (AEA) is a partial agonist of CB1 receptors. It is found at low concentrations (pmol per gram of tissue) in the brain (Pertwee *et al.*, 2010). In contrast, 2-AG is a full agonist of CB1 receptors and is present at higher concentrations (nmol per gram tissue) than anandamide in the brain (Stella *et al.*, 1997).

Endocannabinoids are produced and released from post-synaptic sites. This event is triggered either as a result of calcium elevations in post-synaptic neurones or as a result of activation of post-synaptic mGluRs (Varma *et al.*, 2001, Kim and Alger, 2010). Glutamate binding to post-synaptic mGluRs activates $G_{q/11}$, which results in Phospholipase C-β (PLC-β) activation. Alternatively, PLC-β is activated by intracellular calcium. PLC-β then hydrolyses Phosphatidylinositol 4,5-bisphosphate (PIP_2) to IP_3 and Diacylglycerol (DAG). Subsequently, Diacylglycerol lipase-α (DGL-α) uses DAG to synthesise 2-AG (Bisogno *et al.*, 2003). In mice brain, 50% of AEA production also depends on DGL-α (Gao *et al.*, 2010). However, the mechanism of this pathway is not known. Other pathways of AEA synthesis also exist.

4.3 Endocannabinoid receptors

The main eCB receptor in the CNS is called the CB1 receptor, which is a class A G-protein coupled receptor (Matsuda *et al.*, 1990). CB1 receptors are mainly localised pre-synaptically. In the hippocampus, majority of CB1 receptors are localised to pre-synaptic GABAergic interneurones (Katona *et al.*, 1999) with lower CB1 receptor localisation in glutamatergic neurones. In the cortex, CB1 receptors are also largely localised to interneurones (Hill *et al.*, 2007). However, 49% of pyramidal neurones in rat neocortex were also shown to express CB1 receptors.

4.4 Role for cannabinoids in synaptic transmission and plasticity

Activation of pre-synaptic CB1 receptors by endogenous or exogenous cannabinoids results in decrease of neurotransmitter release. This leads to depression of synaptic transmission. Some experimentally induced forms of synaptic plasticity are mediated by eCBs. These forms of synaptic plasticity are depressive and are induced pre-synaptically. Depending on the experimental protocol, they can be short term or long term.

eCB-mediated short-term depression (eCB-STD): It is believed that experimental depolarisation of post-synaptic neurones can release eCBs from these cells. These eCBs then diffuse as retrograde messengers and bind to CB1 receptors on pre-synaptic neurones. This binding results in decrease in neurotransmitter release by inhibiting voltage-gated calcium channels. During

STD, CB1 receptors are activated for only tens of seconds (Chevaleyre *et al.*, 2006). If the synapse is GABAergic, this short-term plasticity is called depolarisation–induced suppression of inhibition (DSI). If it is excitatory it is called depolarisation-induced suppression of excitation (DSE) (Pitler and Alger, 1992, Alger, 2002, Navarrete and Araque, 2010).

eCB mediated long-term depression (eCB-LTD): In the cortex and CA1 region of hippocampus, eCB LTD is induced by the same HFS/TBS protocols that induce NMDAR-dependent LTP (Chevaleyre and Castillo, 2003, Huang *et al.*, 2008). The difference is that HFS/TBS-induced eCB-LTD is induced heterosynaptically whilst NMDAR-LTP is homosynaptic. Furthermore, NMDAR-LTP depends on NMDARs and calcium elevation in post-synaptic neurones. In contrast, eCB-LTD can be induced in the absence of post-synaptic NMDAR activity and calcium elevations. The **Induction** of eCB-LTD depends on post-synaptic class I mGluRs and pre-synaptic CB1 receptors. Repetitive activation of pre-synaptic excitatory afferents (via HFS or TBS) can result in excess release of glutamate (Figure 4.1: parts 1-2). This glutamate release can activate post-synaptic mGluRs in addition to post-synaptic NMDARs (Figure 4.1 parts 3-4), thus leading to eCB synthesis via PLC activation (Figure 4.1: parts 5-6). eCBs can then diffuse to pre-synaptic neurones and activate pre-synaptic CB1 receptors, which are coupled to $G\alpha_{i/o}$ (Figure 4.1: part 7). This activation leads to reduction in adenylyl cyclase and protein kinase A activity. This leads to reduction in pre-synaptic transmitter release (Figure 4.1: part 8), which is the **expression** of eCB LTD (Chevaleyre *et al.*, 2006).

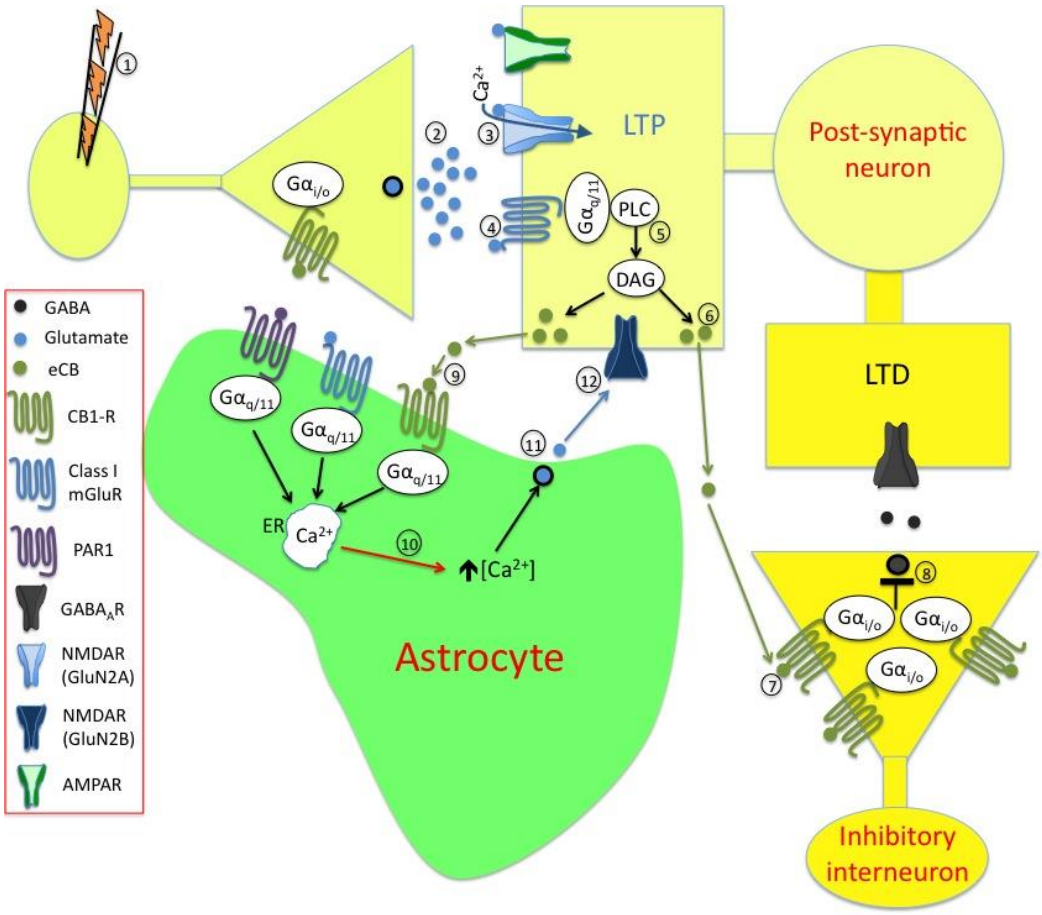

Figure 4.1. Endocannabinoid signalling in the context of tripartite synapse. Repetitive activation of pre-synaptic neurones (1) results in excess release of glutamate (2). Glutamate can bind to NMDARs (3) and result into homosynaptic LTP induction. Glutamate also activates class I mGluRs (4), which leads to PLC-mediated synthesis of eCBs (5-6). eCBS can then diffuse to pre-synaptic neurones at heterosynaptic sites where they activate pre-synaptic CB1 receptors (7). The heterosynapse can be either GABAergic or glutamatergic. In this figure, the heterosynapse has been represented as a GABAergic synapse. Pre-synaptic CB1 receptors are coupled to $G\alpha_{i/o}$, therefore their activation leads to inhibition of transmitter (in this case GABA) release (8). This leads to heterosynaptic eCB-mediated LTD. Released eCBs can also bind to CB1 receptors on astrocytes (9). In contrast to neuronal CB1 receptors, astrocytic CB1 receptors are coupled to $G\alpha_{q/11}$. Activation of astrocytic CB1 receptors leads to calcium elevation from these cells (10). This in turn leads to glutamate release from astrocytes (11), which can bind to extra-synaptic GluN2B containing NMDARs (12).

Modulation of NMDAR-dependent LTP by cannabinoid signalling: In contrast to synaptic depression, induction of NMDAR-dependent LTP does not require CB1 receptors but this does not necessarily mean that eCB signalling does not have modulatory role during NMDAR-dependent LTP induction. Studies have attempted to investigate the role of endogenous and exogenous cannabinoids during induction of NMDAR-dependent LTP. These studies will be reviewed in the following section.

As mentioned above, CB1 receptors are present on inhibitory neurones. This suggests that CB1 receptor-mediated depression of GABA release can theoretically enhance excitability and LTP induction. It has been shown that in the CA1 region of hippocampus, induction of DSI or eCB LTD at inhibitory synapses can enhance the subsequent induction of HFS-induced LTP of pyramidal neurones (Carlson *et al.*, 2002, Chevaleyre and Castillo, 2004).

The role of exogenous cannabinoid application on LTP induction has also been investigated. Different studies show different outcomes depending on the type and concentration of cannabinoid used. In CA1 region of hippocampus of 2-3 weeks old mice and rats, pre-incubation of brain slices with exogenous synthetic CB1 receptor agonists HU-210 (100 nM) or WIN55,212-2 (3-10 μM), blocked HFS induced LTP (Collins *et al.*, 1995, Misner and Sullivan, 1999). Application of 20 μM of 2-AG to slices for 20 minutes prior to HFS delivery, can also block LTP induction in the CA1 region of the hippocampus (Stella *et al.*, 1997).

In contrast to the above results, application of AEA for 30 minutes prior to delivery of HFS, does not completely block LTP (Terranova *et al.*, 1995). At AEA concentrations of 1 μM and 3 μM, LTP extent is reduced slightly but it is not blocked. At concentration of 10 μM, LTP extent is reduced further, but not completely blocked. Similarly, application of WIN55,212-2 at low concentration of 1 μM does not block LTP (Terranova *et al.*, 1995).

Application of Δ^9-THC (10-1000 pM) to CA1 region of hippocampus did not decrease the extent of LTP (Nowicky *et al.*, 1987). Interestingly, application of 10 pM of Δ^9-THC increased the duration of LTP whilst application of 1000 pM of Δ^9-THC decreased the duration of LTP.

Effect of endogenous CB1 receptor activity during LTP induction has also been investigated. These investigations have been done by either pharmacologically blocking CB1 receptors or use of CB1 receptor knockout animals. All these investigations have been carried out in CA1 region of hippocampus. Different reports have shown outcomes that are contradictory with respect to each other. Some studies have shown that application of CB1 receptor antagonist does not have any effect on LTP induction (Carlson *et al.*, 2002, Slanina *et al.*, 2005). Another study showed enhancement of *in vivo* LTP in CB1 knockout mice in comparison to WT mice (Jacob *et al.*, 2012). In contrast, there are studies that have shown complete abolishment of LTP in slices perfused with CB1 receptor antagonists (Chevaleyre and Castillo, 2003, de Oliveira Alvares *et al.*, 2006, Lin *et al.*, 2011). The reason for these contradictory results could be due to presence of CB1 receptors on both excitatory and inhibitory synapses.

All of the above-mentioned investigations of cannabinoid role during LTP induction have been performed in the hippocampus. I have only found two reports that attempted to investigate endocannabinoid role during LTP induction in the cortex. It has been shown that in the prefrontal cortex, application of WIN55,212-2 (1 μM), decreased evoked AMPAR-mediated EPSCs by acting on pre-synaptic CB1 receptors (Auclair *et al.*, 2000). Furthermore, WIN55,2212-2 application decreased the chances of LTP induction in the prefrontal cortex. In contrast, in a study in the visual cortex of young (2-3 weeks old) mice, application of WIN55,212-2 (2 μM) and AM251 (5 μM), which is a CB1 receptor antagonist, did not effect LTP induction (Huang *et al.*, 2008).

To my knowledge, there has been no study of cannabinoid role during NMDAR-dependent LTP in somatosensory cortex. Therefore, one of the objectives of my project was to investigate the role of cannabinoids in the somatosensory cortex.

4.5 Role for astrocytic CB1 receptors in synaptic transmission and plasticity

Recent reports have implicated the role of astrocytic CB1 receptors in eCB-mediated short and long-term depression. It was shown that in the CA1 region of hippocampus of 12-17 days old mice, astrocytic calcium levels were elevated by either application of various exogenous CB1 receptor agonists (AEA, WIN55,212-2 and 2-AG) or depolarisation of post-synaptic neurones (Navarrete and Araque, 2008). As CB1 receptor antagonists prevented these calcium elevations, it was suggested that CB1 receptors are localised on astrocytes. These

CB1 receptor-mediated calcium events in astrocytes were dependent on PLC activity, thereby suggesting that astrocytic CB1 receptors are coupled to $G_{q/11}$. This is in contrast to neuronal CB1 receptors, which are coupled to $G_{i/o}$. Furthermore, it was shown that calcium elevation in astrocytes, due to activation of their CB1 receptors, could result in generation of SICs in post-synaptic neurones. This suggests that CB1-receptor activation of astrocytes can result in glutamate release from these cells (Figure 4.1: parts 9-12).

The same group also showed that post-synaptic depolarisation, which usually leads to eCB mediated DSE at some excitatory synapses, also lead to short-term potentiation of some other excitatory synapses. They showed that DSE occurs at homosynaptic excitatory synapses whilst potentiation is induced at heterosynaptic synapses. They showed that these potentiation events depend on astrocytic CB1 receptors and astrocytic calcium elevations. This was in contrast to DSE induction, which depends on pre-synaptic CB1 receptors and not on calcium elevations in astrocytes. Taken together, these results suggest that eCB activation of CB1 receptors on astrocytes can result in calcium elevation in these cells. These calcium elevations can then result in glutamate release from astrocytes, leading to enhancement of glutamatergic transmission. Therefore, one can suggest that astrocytic CB1 receptors seem to act analogously to astrocytic PAR1 and mGluRs (Figure 4.1: part 9).

Can CB1-mediated activation of astrocytic glutamate release have an effect on long-term plasticity? A recent study showed that CB1 receptors on astrocytes can contribute to one form of eCB LTD in the somatosensory cortex (Min and

Nevian, 2012). As mentioned previously, delivery of HFS or TBS can induce eCB LTD at heterosynaptic synapses. However, another form of eCB dependent LTD can be induced at homosynaptic excitatory synapses in the neocortex via a Spike-timing dependent protocol (STDP). This protocol involves pairing post-synaptically evoked action potentials with pre-synaptic firing. With the correct temporal interval between pre- and post-synaptic firing, STDP can result in long-term depression of synaptic transmission. As mentioned previously, eCB LTD depends on eCB release from post-synaptic neurone, which through retrograde transport binds to pre-synaptic CB1 receptors resulting in depression of glutamate release. However, this study showed that during induction of eCB LTD, there was an increase in frequency of calcium elevations in astrocytes that were in close proximity of the LTD site (Min and Nevian, 2012). It was shown that eCB release from post-synaptic neurones could activate CB1 receptors on astrocytes, which lead to calcium elevation in these cells. This in turn resulted in release of glutamate from astrocytes. The authors showed that this astrocytic glutamate release could activate pre-synaptic NMDARs. It was suggested that activation of pre-synaptic NMDARs could decrease pre-synaptic release, presumably through calcium entry through these receptors and phosphotase activation, hence contributing to induction of LTD. To summarise, this study shows that CB1 receptors on astrocytes can result in vesicular release of glutamate in the somatosensory cortex. It also suggests that this glutamate release can contribute to induction of eCB-LTD.

The above mentioned study shows that glutamate release as a result of CB1 receptor activation of astrocytes can contribute to induction of eCB-LTD in the

somatosensory cortex. Can glutamate release as a result of CB1 receptor activation of astrocytes also contribute to induction of NMDAR-dependent LTP? As mentioned above, one study in the hippocampus showed that astrocytic glutamate release following CB1 receptor activation lead to enhancement of glutamatergic transmission and generation of SICs. Therefore, it is possible that CB1 receptor activation of astrocytes can also contribute to LTP induction.

4.6 Project Objectives and hypothesis

As mentioned above, studies have investigated the role played by cannabinoids during LTP induction. Most of these studies have been carried out in the hippocampus with only two reports in the cortex. In my project, the role of cannabinoids during synaptic transmission and LTP induction in the somatosensory cortex was investigated. The hypothesis was that cannabinoids can result in calcium elevation in astrocytes by acting on CB1 receptors on these cells. This cannabinoid-mediated calcium elevation in astrocytes can in turn result in gliotransmitter release from these cells, thereby contributing to synaptic transmission and LTP induction.

Chapter 5: Results 2

Cannabinoid receptors contribute to astroglial Ca^{2+}-signalling and synaptic plasticity in neocortex

5.1. Introduction

The objective in this part of the project was to investigate the role of endocannabinoid signalling in synaptic transmission and plasticity in the somatosensory cortex. Previous studies have shown that activation of CB1 receptors on astrocytes can result in calcium elevation in these cells (Navarrete and Araque, 2008, Min and Nevian, 2012). It was also shown that this calcium elevation results in glutamate release from astrocytes. Therefore, one can suggest that astrocytic CB1 receptors act analogously to astrocytic PAR-1 and mGluRs. It was shown in chapter 3 that application of TFLLR results in vesicular release of ATP specifically from astrocytes. If astrocytic CB1 receptors act analogously to astrocytic PAR-1, then one can suggest that application of CB1 receptor agonist should result in calcium dependent vesicular release of ATP specifically from astrocytes. Therefore, the first objective of this project was to investigate whether application of AEA can result in vesicular release of ATP from astrocytes.

The second objective of this project was to investigate the role played by endocannabinoid signalling in synaptic plasticity in the somatosensory cortex. More specifically, the aim was to investigate the role for AEA application and CB1 receptors on TBS-induced LTP. Majority of previous studies investigating role for cannabinoid signalling in LTP induction have been carried out in the hippocampus (Nowicky *et al.*, 1987, Collins *et al.*, 1995, Terranova *et al.*, 1995, Stella *et al.*, 1997, Misner and Sullivan, 1999, Chevaleyre and Castillo, 2003, de Oliveira Alvares *et al.*, 2006, Lin *et al.*, 2011) with only one report in the

prefrontal cortex (Auclair *et al.*, 2000) and one report in the visual cortex (Huang *et al.*, 2008). There is yet to be an investigation in role for cannabinoid signalling during LTP induction in the somatosensory cortex. This project will be the first ever attempt to investigate such a role for cannabinoid signalling in the somatosensory cortex.

Previous studies have shown that activation of astrocytic CB1 receptors by either application of CB1 receptor agonists or by depolarisation of post-synaptic neurones, results in calcium elevation in astrocytes (Navarrete and Araque, 2008, Min and Nevian, 2012). This CB1 receptor dependent calcium elevation in astrocytes resulted in release of glutamate from these cells. However, as was shown on chapter 3, in addition to glutamate, astrocytes can also release ATP via vesicular exocytosis. Therefore, activation of CB1 receptors on astrocytes should theoretically result in vesicular release of ATP from these cells. My objective was to investigate this notion.

Previously, my colleagues showed that activation of CB1 receptors on astrocytes in the somatosensory cortex can induce significant elevation of intracellular calcium levels in astrocytes (Rasooli-Nejad *et al.*, 2014), thereby verifying the findings of the above-mentioned reports. For this purpose, they used to two transgenic mice lines. One was the dnSNARE mice and the other was the GFAP-EGFP (GFEC) mice. GFEC mice express EGFP under the control of GFAP promoter. This means that their astrocytes express EGFP fluorescence, which helps in identifying these cells. 2-photon fluorescent microscopy was used to monitor astrocytic Ca^{2+} signalling. Calcium levels in astrocytes of dnSNARE

mice were also compared with calcium levels in astrocytes of dnSNARE wild-type littermates. They loaded astrocytes with fluorescent dyes Rhod-2AM (GFEC and dnSNARE mice) or Oregon Green BAPTA-2AM.

In baseline conditions (before application of AEA), astrocytes of all mice strains exhibited spontaneous Ca^{2+}-transients, which were more prominent in the branches (Figure 5.1a-b). The average frequency of transients per astrocyte varied in the range of 0.5-2.1 min^{-1} for all mice strains. Bath application of 500 nM AEA induced robust Ca^{2+} elevation both in the soma and branches and increased the amplitude and frequency of spontaneous Ca^{2+} transients (n=6; see Figure 5.1a-c). There was no significant difference in the action of AEA between astrocytes of different strains ($p<0.05$, two sample independent t-test; see Figure 5.1c). It has to be emphasised that, in the concentrations used, AEA selectively activates CB1 receptors. The specificity of AEA action was confirmed by inhibition with AM251, a selective antagonist of CB1 receptors. Application of AM251 (1 μM) significantly decreased the response to AEA in 5 WT and 5 dnSNARE astrocytes ($p<0.01$, paired t-test; see Figure 5.1c). These results showed that CB1 receptors can bring substantial contribution to Ca^{2+}-signalling in the neocortical astrocytes. Importantly, these data showed that expression of dnSNARE protein in astrocytes did not affect eCB-mediated calcium signalling.

Activation of CB1 receptors on astrocytes should theoretically result in vesicular release of gliotransmitters such as ATP and D-serine from these cells. To investigate this, my colleagues used microelectrode biosensors to monitor the concentration of ATP and D-serine in neocortical slices (Rasooli-Nejad *et al.*,

2014). Activation of intracellular Ca^{2+} elevation in astrocytes by 500 nM AEA induced a robust increase in the levels of extra-cellular ATP and D-serine in cortical slices from WT mice. The eCB-induced elevation in the ambient concentration of extra-cellular ATP and D-serine reached correspondingly 0.9±0.3 µM and 2.3±0.8 µM (n=6; see Figure 5.1d-e). The eCB-induced elevation in concentrations of ATP and D-serine was significantly decreased in dnSNARE-expressing mice correspondingly by 74±17% and 83±15% in comparison to WT mice ($p<0.01$, two sample t-test; see Figure 5.1d-e). These results suggested that activation of CB1 receptors on astrocytes results in calcium-dependent vesicular release of ATP and D-serine specifically from these cells. The objective of my project was to investigate the role played by this CB1-mediated calcium dependent astrocytic vesicular release in synaptic transmission and LTP induction.

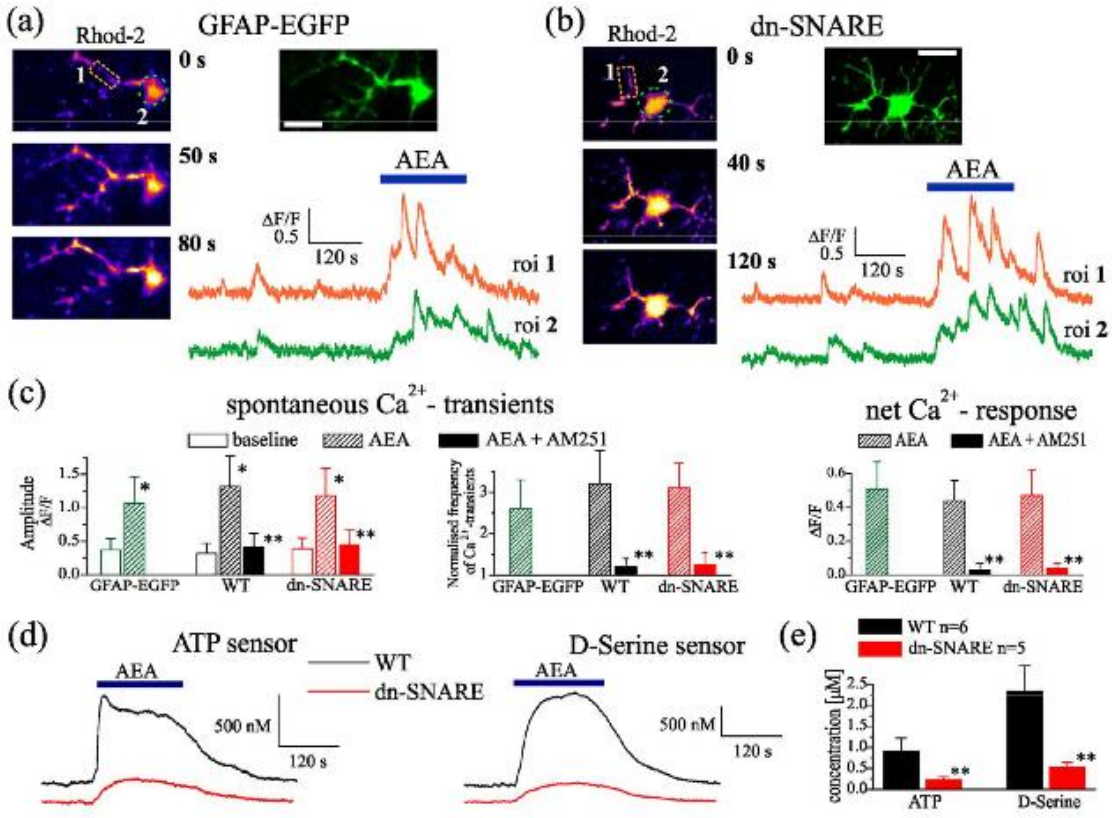

Figure 5.1. Cannabinoid receptors activate astrocytic Ca^{2+} signalling and release of gliotransmitters. a-c, Ca^{2+}-signalling activated by the bath application of 500 nM of anandamide (AEA) to neocortical slices. **a-b**, representative 2-photon images of EGFP fluorescence and pseudo-color images of Rhod-2 fluorescence recorded in the astrocytes from GFAP-EGFP **(a)** and dnSNARE **(b)** mouse during AEA application at times indicated. Scale bars are 10 μm. Graphs below show the time course of Rhod-2 fluorescence averaged over regions indicated in fluorescence image. Note marked spontaneous elevations in the Ca^{2+} level, which were enhanced by application of AEA. **c,** The pooled data on spontaneous Ca^{2+}-transients and net response to AEA recorded in astrocytes of different mice strains in control and in presence of CB1 receptor antagonist AM251 (1 μM). Data shown as mean±SD for 6 cells in control (for each strain) and 5 cells under AM251 (WT and dnSNARE). Frequency of transients (middle graph) was measured 3 min after application of AEA and was normalised to baseline value. Net response was measured with 3 min after AEA application and averaged over whole cell image. Asterisks (*) indicate statistical significance of effect of AEA on the peak amplitude of Ca^{2+}-transients, double asterisks (**) indicate significance of inhibitory effect of AM251; $p<0.01$ given by paired t-test in both cases. **d-e,** AEA activated release of ATP and D-serine in slice preparations from somatosensory cortex was detected using microelectrode biosensors. **d,** The representative responses of cortical slices of WT and dnSNARE mice to the application of 500 nM AEA were recorded using microelectrode sensors to ATP and D-serine placed in layer 2/3 of cortex. **e,** The pooled data on the peak magnitude of ATP and D-serine transients evoked by application of AEA; data shown as mean ±SD for number of experiments indicated. Two sample independent t-test was performed between WT and dnSNARE mice; **, $p<0.01$.

5.2. Application of AEA results in calcium-dependent vesicular exocytosis of ATP from astrocytes

In the introduction of this chapter it was shown that activation of CB1 receptors on astrocytes via AEA application can result in calcium dependent vesicular release of ATP from astrocytes. It was shown in chapter 3 that vesicular release of ATP from astrocytes could activate P2XRs on neurones. To investigate whether AEA application can result in vesicular release of ATP from astrocytes on to P2XRs on neurones, a "sniffer"-cell approach was used. In this approach, cortical neurones were acutely isolated via vibro-dissociation technique, which allows functional membrane receptors to be retained at the cell surface. Another benefit of this technique is the ability to retain a fraction of functional synapses, which can be verified by staining with FM1-43 and presence of miniature spontaneous synaptic currents (Figure 5.2a). Furthermore, with vibro-dissociation, not only isolated neurones are obtained but in some cases some astrocytes remain attached to the isolated neurone (Figure 5.2b-c). This retains a certain proportion of intimate contact between thin astrocytic processes and neuronal membrane. Such neuron-astrocyte "bundle" could work as a good model of glia-neuron interaction unit, enabling efficient activation of astrcoytes and direct monitoring of neuronal response. In comparison to bath application of pharamacological agents to the whole slice, the "neuron-astrocyte bundle" has an advantage of better control of drug application and lack of side-effects of massive activation of astrocyte network and poly-synaptic connections. With vibro-dissociation two "types" of dissociation preparations are possible: 1) isolated neurones with no astrocytes attached (Figure 5.2a); 2) "neuron-astrocyte

bundle" (Figure 5.2b-c). Neurones from these two preparation were patch clamped followed by application of 500 nM of AEA to investigate the vesicular release of astrocytic ATP onto neuronal P2XRs.

P2XR-mediated sEPSCs were recorded from acutely isolated neocortical neurones at membrane potential of -80 mV in the presence of CNQX (50 μM), D-APV (30 μM) and picrotoxin (100 μM). Prior to application of AEA, TFLLR (5 μM) was applied to isolated preparations to show that the effect of TFLLR on "neurone-astrocyte bundle" is similar to the effect of TFLLR application to cortical slices shown on Figure 3.2 in chapter 3. Baseline P2XR-mediated sEPSCs had an average amplitude of 9.8±2.2 pA with an average decay time constant of 8.9±1.7 ms (n=7). These values were similar to the amplitude and decay time of P2XR-mediated sEPSCs recorded from cortical slices shown on Figure 3.2. Application of TFLLR to isolated neurones with no astrocytes attached did not result in significant change in either the average amplitude or frequency of P2XR-mediated sEPSCs (Figure 5.2a and 5.2d). Further analysis of these sEPSCs showed a unimodal probability distribution in both amplitude and decay time. Application of TFLLR failed to result in the appearance of the "slow" P2XR-mediated sEPSCs (Figure 5.2a). In contrast, amplitude and decay time probability distributions of sEPSCs recorded from neurones in "neurone-astrocyte bundle" showed bimodal distributions with amplitude distributions showing peaks at 5.9±1.4 pA and 9.9±2.6 pA (n=6; see Figure 5.2b). The decay time distributions showed peaks at 8.8±1.1 ms and 15.1±2.2 ms (Figure 5.2b). Application of TFLLR to these "neurone-astrocyte bundle" resulted in a significant increase in the frequency of sEPSCs and decrease in their average

amplitude (Figure 5.2b and 5.2d). This increase in frequency and decrease in average amplitude is as a result of increase in the slower and smaller sEPSCs (Figure 5.2b). These results are similar to results showed on Figure 3.9, where application of TFLLR to cortical slices resulted in the increase in frequency of the "slow" P2XR-mediated sEPSCs. To verify that the appearance of these "slow" sEPSCs was as a result vesicular release of ATP from astrocytes, TFLLR was also applied to "neurone-astrocyte bundle" isolated from dnSNARE mice, where vesicular exocytosis is impaired selectively in astrocytes. Application of TFLLR to "neurone-astrocyte bundle" from dnSNARE mice failed to significantly change the frequency and average amplitude of P2XR-mediated sEPSCs, thereby showing that the "slow" sEPSCs were indeed due to vesicular release of ATP from astrocytes (Figure 5.2c-d). Taken together, these results confirm that "neurone-astrocyte bundle" can indeed be used as a model for glia-neuron interaction unit and that these units show similar properties to their counterparts in cortical slices.

If, as mentioned above, AEA-mediated calcium dependent vesicular release of ATP is analogous to TFLLR application, then one would expect to see the appearance of "slow" P2XR-mediated sEPSCs following AEA application. To investigate this, AEA was applied to isolated neurone preparations from WT and dnSNARE mice. Similar to TFLLR, application of AEA to isolated neurones with no attached astrocytes produced no change in the frequency or average amplitude of P2XR-mediated sEPSCs (Figure 5.2a and 5.2d). However, application of AEA to "neurone-astrocyte bundle" from WT mice resulted in a significant increase in the frequency of the "slow" sEPSCs (Figure 5.2b and

5.2d). Application of AEA to "neuron-astrocyte bundle" from dnSNARE mice did not result in change in either frequency or average amplitude of sEPSCs (Figure 5.2c and 5.2d). These results show that application of AEA can result in vesicular exocytosis of ATP from astrocytes. This ATP release from astrocytes can then activate P2XRs on neurones. This suggests that CB1 receptors on astrocytes act analogously to PAR-1 on astrocytes. This means that calcium elevations in astrocytes via either PAR-1 receptors or CB1 receptors can result in vesicular release of ATP from these cells.

The data on Figure 5.2 was obtained with collaboration with Dr Yuriy Pankratov.

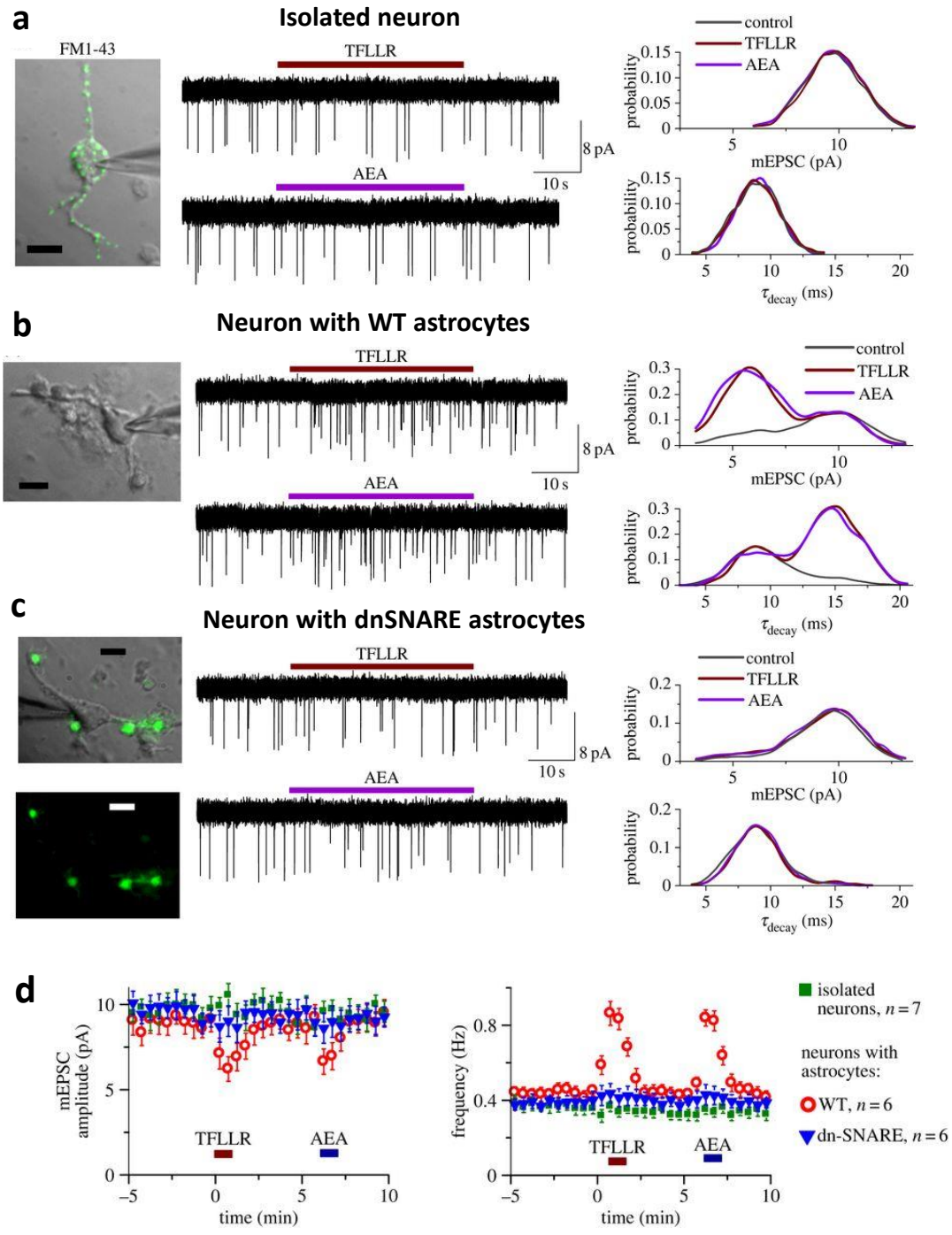

Figure 5.2. For Figure legend see next page.

Figure 5.2. Detection of ATP release from astrocytes using modified "sniffer-cell" method. a-c, whole cell P2XR-mediated sEPSCs were recorded from acutely isolated neocortical pyramidal neurones at membrane potential of -80 mV under CNQX (50 μM), D-APV (30 μM) and picrotoxin (100 μM). Astrocytes were activated by 1 min-long application of TFLLR (10 μM) and AEA (500 nM). **a**, Vibro-dissociation preparation of WT isolated neurone with no attached astrocyte. Whole-cell currents were recorded in the isolated neuron simultaneously with staining with synaptic vesicular marker FM1-43. Prior to recording, the cell was pre-incubated with 3 μM FM1-43 for 15 min, then dye was washed out for 15 min. From left to right: representative fluorescent and gradient contrast image of neuron showing punctate staining with FM1-43, the trace showing spontaneous synaptic currents and distributions of sEPSCs amplitude and decay time. **b,** Similar recordings were made from vibro-dissociation preparation of "neurone-astrocyte bundle" from WT mice. **c,** Recordings from vibro-dissociation preparation of "neurone-astrocyte bundle" from dnSNARE mice. Green fluorescence confirms the dnSNARE expression in astrocytes attached to the neuron. **d,** Time course of changes in the average amplitude and frequency of P2XR-mediated sEPSCs during TFLLR and AEA application. Dots represent values averaged over 30 seconds time window. Data shown as mean±SD for number of neurons as indicated. Difference between WT and dnSNARE mice in the effects of TFLLR and AEA on sEPSC frequency was significant at $p<0.005$ (two sample independent t-test).

The above results show that activation of CB1 receptors on astrocytes can result in calcium-dependent vesicular release of ATP from these cells. These CB1 receptors were activated by exogenous application of AEA. It would be reasonable to ask weather endogenous CBs can also activate exocytosis from cortical astrocytes. As was shown in chapter 3, HFS stimulation of neuronal afferents resulted in vesicular release of ATP from astrocytes (Figure 3.9). This ATP release resulted in the increase in frequency of "slow" P2XR-mediated sEPSCs on neurones. This effect was similar to application of TFLLR to cortical slices. If CB1 receptors on astrocytes are activated by endogenous cannabinoids during delivery of HFS to neuronal afferents, then one would expect that these receptors to contribute to calcium-dependent vesicular exocytosis of ATP from astrocytes during HFS delivery.

To investigate this, P2XR-mediated sEPSCs were recorded from neurones of layer 2/3 of cortical slices under CNQX (50 µM) and picrotoxin (100 µM) at holding voltage of -80 mV. Similar to Figure 3.10, delivery of the short HFS train caused a significant elevation in frequency of the "slow" P2XR-mediated sEPSCs (Figure 5.3b-d). However, delivery of HFS during application of AM251 (1 µM), which is an antagonist of CB1 receptors, significantly reduced the increase in frequency of "slow" P2XR-mediated sEPSCs (Figure 5.3b-d). Furthermore, delivery of HFS during application of AM251 resulted in a smaller increase in astrocytic calcium elevation (Figure 5.3a), thereby suggesting that some of the HFS-mediated calcium elevations in astrocytes are due to CB1 receptors on these cells. Other sources of calcium elevation could be due to P2XRs and NMDARs on astrocytes (Palygin *et al.*, 2010). It was shown

previously by my colleagues that application of UBP141 could selectively inhibit NMDARs on astrocytes but not NMDARs on neurones (Palygin *et al.*, 2011). As UBP141 specifically blocks GluN2C/D-containing NMDARs, it was suggested that astrocytic NMDARs consist of GluN2C/D. Therefore, UBP141 can be used as a specific antagonist of astrocytic NMDARs. To confirm the results from the previous report that other source of HFS-induced calcium elevation is due to NMDARs on astrocytes, HFS was delivered during the application of UBP141. The increase in astrocytic calcium elevation and P2XR-mediated sEPSCs were significantly less when HFS was delivered under UBP141 than when HFS was delivered in control conditions (Figure 5.4e).

Taken together, these results show that activation of neuronal afferents can result in elevation of intracellular calcium levels in astrocytes, which in turn leads to vesicular exocytosis of ATP from astrocytes. These intra-cellular calcium elevations in astrocytes are due to CB1 receptors, P2XRs and NMDARs on these cells. Therefore, these receptors allow astrocytes to "sense" neurotransmitter release from neurones, thereby allowing astrocytes to be activated in response to neuronal activity. Following activation, astrocytes can then release gliotransmitters such as ATP onto neurones. These results confirm that bidirectional communication between astrocytes and neurones is present in the somatosensory cortex.

In addition to CB1 receptors, NMDARs and P2XRs on astrocytes, it has been shown that astrocytic mGluR5 are also involved in elevation of calcium levels in astrocytes following electrical stimulation of afferent fibres (Panatier *et al.*,

2011). Therefore inhibition of mGluRs should also decrease the extent of HFS-induced astrocytic calcium elevation and P2XR-mediated sEPSCs. To investigate this, HFS was delivered during application of 10 μM of MPEP, which is a selective antagonist of mGluR5. As expected, HFS delivery during MPEP application resulted in a significantly lower increase in astrocytic calcium elevation and sEPSCs (Figure 5.4e). These results suggest that mGluR5 on astrocytes can also contribute to calcium dependent vesicular release of ATP from these cells. However, a recent study has shown that mGluR5 expression is significantly reduced in hippocampal and cortical astrocytes from mice above 2 weeks of age (Sun *et al.*, 2013). In this report it was shown that most mGluR5 were located at post-synaptic spines and dendrites of neurones. If this is the case, then how does the inihibtion of mGluRs decrease astrocytic calcium elevation and vesicular release of ATP? It has been shown that eCBs are produced and released from post-synaptic sites following activation of mGluRs on these sites (Varma *et al.*, 2001, Kim and Alger, 2010). Therefore, delivery of HFS to pre-synaptic afferents can result in release of glutamate from these neurones. Anterograde transport of glutamate can result in the activation of mGluR5 on post-synaptic neurones, thereby leading to release of eCBs from post-synaptic sites. Retrograde transport of eCBs can then activate CB1 receptors on astrocytes, thereby leading to calcium-dependent vesicular exocytosis of ATP from astrocytes. If this mechanism is true, it would explain why mGluR5 are involved in calcium elevation in astrocytes, even though these receptors are present on post-synaptic neurones. This needs to be investigated further in the future.

The results on Figure 5.3 were obtained in collaboration with Dr Yuriy Pankrotov. The results on Figures 5.2 and 5.3 have been published (Rasooli-Nejad *et al.*, 2014).

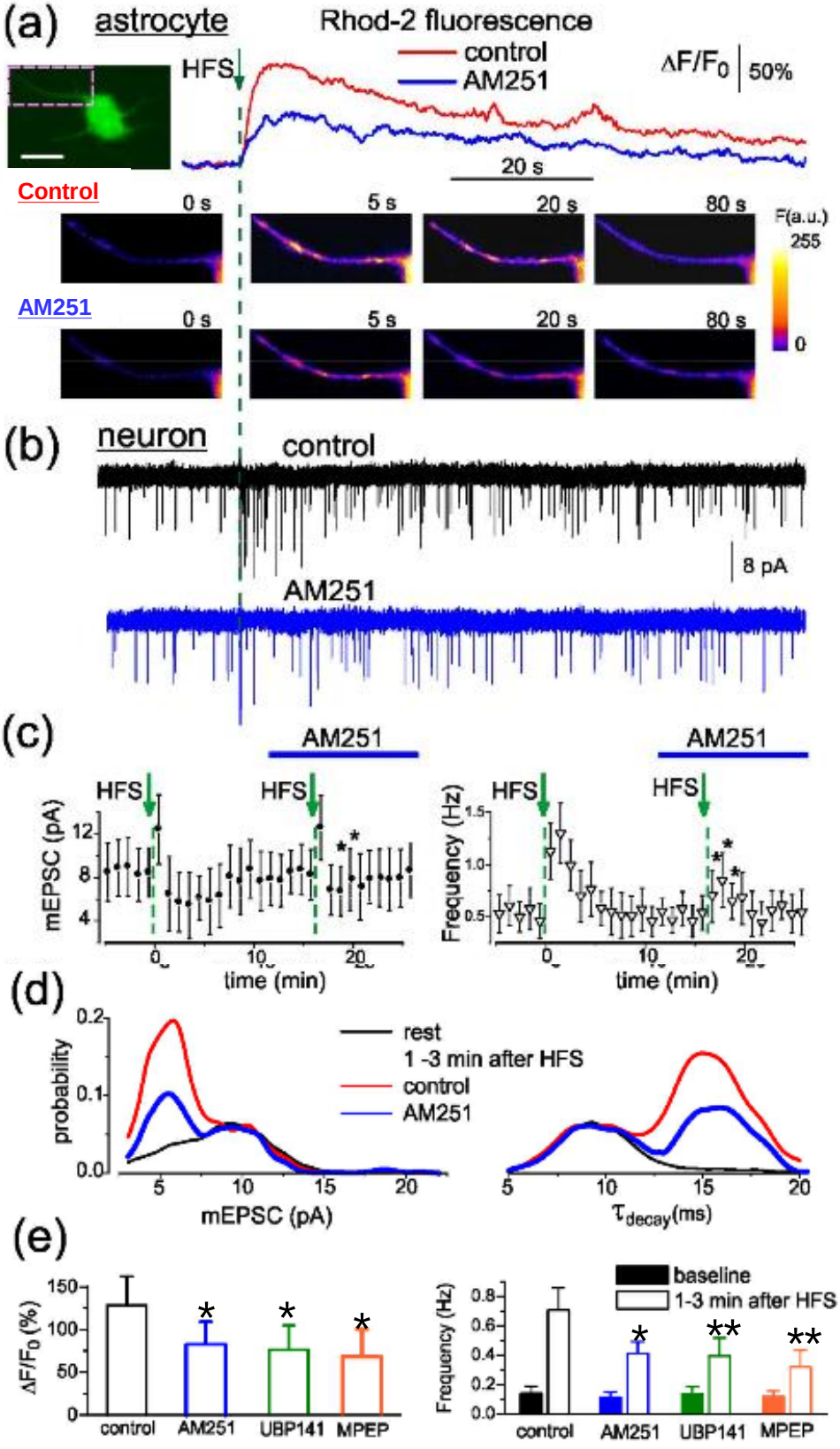

Figure 5.3. For Figure legend see next page.

Figure 5.3. Attenuation of Ca^{2+}-signalling in cortical astrocytes via inhibition of CB1 receptors inhibits the release of ATP from these cells. a, Ca^{2+} signalling was monitored in cortical astrocytes loaded with Rhod-2AM using 2-photon fluorescent microscopy. HFS was delivered at zero time to trigger Ca^{2+} elevation in the astrocyte. Graphs show the time course of Rhod-2 fluorescence averaged over a single astrocyte process indicated in the GFAP-EGFP fluorescent imgae of astrocyte (scale bar is 5 μM). The representative pseudo-colour 2-photon images, recorded at time indicated, are shown below. **b,** example P2XR-mediated sEPSC recordings from cortical neuron before and after HFS delivery under control and under application of AM251 (1 μM). P2XR-mediated sEPSCs were recorded from neurones of layer 2/3 of somatosensory cortex of WT mice. These sEPSCs were recorded at holding potential of -80 mV in the presence of picrotoxin (100 μM) and CNQX (50 μM). **c,** The average time course of HFS delivery during P2XR-mediated sEPSC recordings under control and AM251 application. Each dot shows the average amplitude and frequency of spontaneous currents recorded in 1 min time window in the pyramidal neurones; data are presented as mean±SD for 7 neurons. The asterisks (*) indicate the significant difference from the control values ($p<0.05$, paired t-test). **d,** The amplitude and decay time probability distributions of P2XR-mediated sEPSCs recorded before and during 1-3 minutes after HFS for one example recording. **e,** bar-charts show the peak magnitude of HFS-induced Ca^{2+} transients in the astrocyte and frequency of slow P2XR-mediated sEPSCs averaged within 3 min time window before (baseline) and after HFS train. Data are shown as mean±SD for following number of experiments: 7 for AM251, 6 for UBP141 and 4 for MPEP. The statistical significance of difference from the control values was as indicated. $P<0.05$, *; $p<0.01$, **.

5.3. Activation of astrocytic vesicular release with AEA contributes to TBS-induced LTP

In the previous section it was shown that application of AEA could result in calcium dependent vesicular release of ATP from astrocytes. This suggested that AEA and CB1 receptors act analogously to TFLLR and PAR-1. It was shown in chapter 3 that application of TFLLR could change the direction of TBSx2-induced synaptic plasticity from LTD to LTP. It was shown that this change from LTD to LTP was as a result of ATP release from astrocytes following application of TFLLR. If AEA acts in a similar manner to TFLLR application, then one would expect that application of AEA during TBSx2 delivery to also result in LTP induction. To investigate this, TBSx2 was delivered after 15 minutes of AEA (500 nM) application. AEA was washed out 10 minutes after delivery of TBSx2.

Delivery of TBSx2 during AEA reversed the direction of synaptic plasticity from LTD to LTP (Figures 5.4A and 5.4C). The size of this LTP, 40-50 minutes post TBSx2, was +41.3±14.4% (n=10). There was a significant difference between TBSx2 under control and TBSx2 under AEA ($p<0.01$, two sample independent t-test; see Figure 5.4D). These results suggest that application of AEA can contribute to LTP induction in a similar manner to application of TFLLR.

In chapter 3 it was shown that TFLLR could rescue LTP via vesicular exocytosis of ATP from astrocytes. It was shown that inhibition of P2XRs prevented the rescue of TBSx2-induced LTP with TFLLR, suggesting that P2XRs and hence

ATP release are involved in the rescue of LTP. In section 5.2, it was shown that application of AEA could result in release of ATP from astrocytes, thereby leading to activation of P2XRs on neurones. It was also shown that inhibition of CB1 receptors could decrease the degree of HFS-induced increase in P2XR-mediated sEPSCs. These results suggested that AEA can result in vesicular release of ATP from astrocytes and onto P2XRs on neurones. Therefore, the mechanism of rescue of LTP during TBSx2 under AEA could be similar to TFLLR i.e. depend on ATP release and activation of P2XRs. To investigate this, TBSx2 was delivered again under AEA but this time P2X receptor antagonists PPADS (10 µM) and 5-BDBD (5 µM) were perfused alongside AEA. As expected, inhibition of P2X receptors prevented rescue of LTP with AEA (Figures 5.4A and 5.4C). Delivery of TBSx2 under AEA, PPADS, 5-BDBD, resulted in a significant LTD of -23.77±9.08% ($n=13$, $p<0.05$, paired t-test; see Figure 5.4D). The size of this LTD was similar to LTD induced when TBSx2 was delivered under control (no drugs applied) conditions (Figure 5.4D). These results suggest that the LTP induced with TBSx2 under AEA application is dependent on the activity of P2XRs.

The above results show that AEA application during TBSx2 can result in LTP induction. It was suggested that this rescue of LTP is dependent on vesicular release from astrocytes. To provide evidence that this LTP rescue is indeed due to vesicular release from astrocytes, the above recordings were repeated in cortical slices in dnSNARE mice. Delivery of TBSx2 to dnSNARE cortical slices in the absence of any pharmacological agents resulted in an LTD of -25.38±15.37% ($n=8$; see Figure 5.4B-D). This TBSx2-induced LTD in

dnSNARE mice was similar in size to TBSx2 induced LTD in WT mice (Figure 5.4D). Application of AEA to dnSNARE cortical slices failed to change the direction of TBSx2-induced synaptic plasticity from LTD to LTP i.e. AEA application also resulted in an LTD (Figure 5.4B-C). The size of this LTD was -10.82±8.76% (n=11). This is in contrast to AEA application to WT mice, where a significant LTP was induced (Figures 5.4A and 5.4D).

Taken together, the results in this section suggest that AEA can contribute to TBS-induced LTP by resulting in vesicular exocytosis from astrocytes. As inhibition of P2XRs prevented this rescue of LTP, one can suggest that this rescue of LTP is due to AEA-mediated vesicular release of ATP from astrocytes.

The results on Figure 5.4 have been published (Rasooli-Nejad *et al.*, 2014).

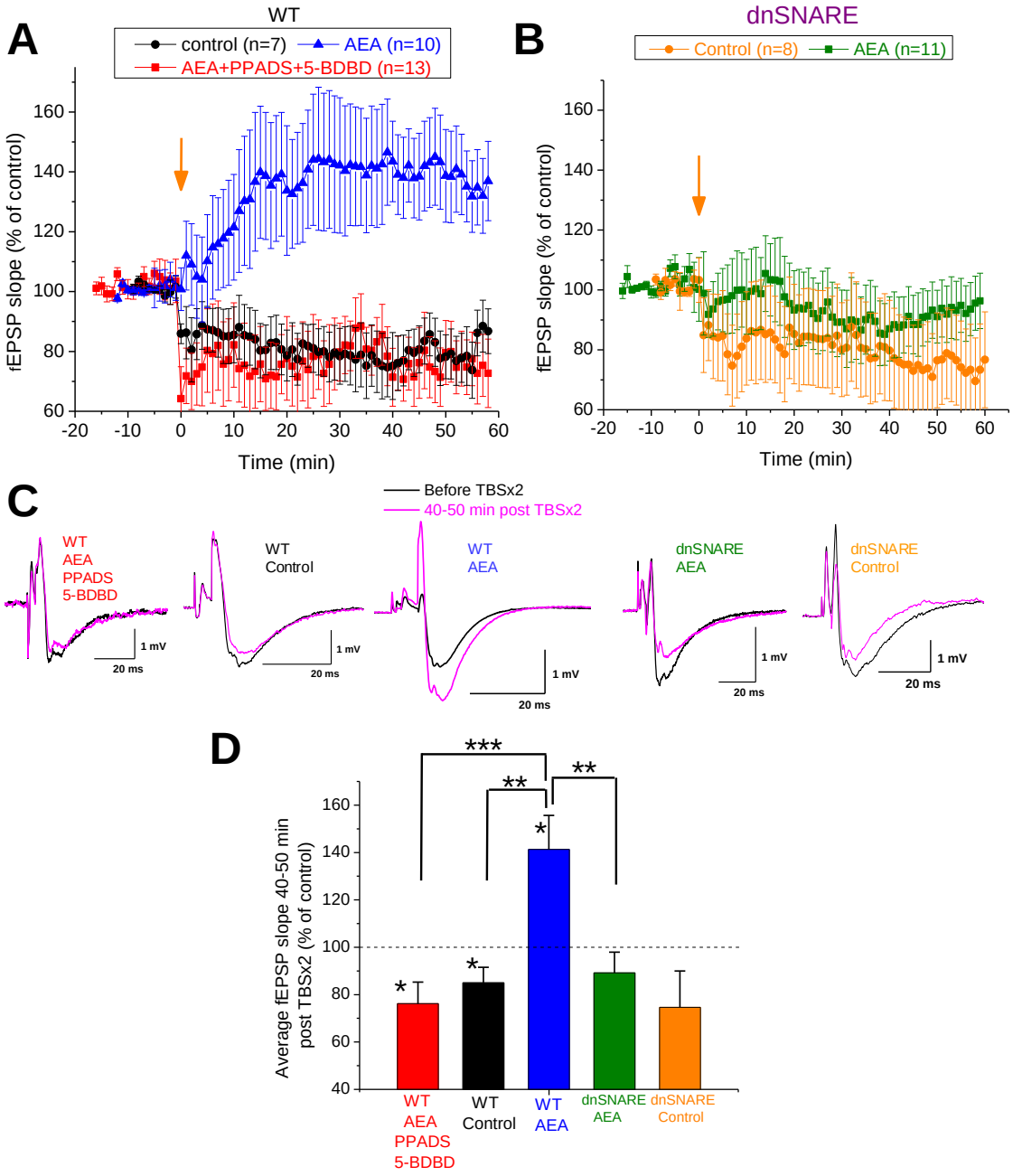

Figure 5.4. For Figure legend see next page.

Figure 5.4. AEA application can result in TBSx2-induced LTP via vesicular exocytosis. A, These recordings were performed in WT mice. The average time-courses for fEPSP recordings with TBSx2 protocol are shown. Orange arrow shows position of TBSx2 delivery. All drugs were applied 15 minutes prior to TBSx2 delivery and were washed out 10 minutes after TBSx2. **B,** shows the average time-courses for fEPSP recordings with TBSx2 in cortical slices from dnSNARE mice. **C,** shows example fEPSPs before and after TBSx2 delivery. **D**, shows bar-charts representing the average % change in fEPSP 40-50 minutes post TBSx2 delivery. For TBSx2 delivery in WT mice under AEA, PPADS, and 5-BDBD, the average % change in fEPSP was -23.77±9.08%. For TBSx2 delivery in WT mice under control conditions, the average % change in fEPSP was -15±6.56%. For TBSx2 delivery to WT mice under AEA, the average % change in fEPSP was +41.3±14.36%. For TBSx2 delivery in dnSNARE mice under AEA, the average % change in fEPSP was -10.82±8.76%. For TBSx2 delivery in dnSNARE mice under control conditions the average % increase in fEPSP was -25.38±15.37%. Two sample independent t-test was performed between each pair of data. Paired t-test was performed for average % change in fEPSP from baseline. $p<0.05$, *; $P<0.01$, **; $p<0.001$, ***.

5.4. CB1 receptors are required for induction of TBSx5-induced LTP

The results in the previous two sections showed that application of AEA could result in calcium elevation in astrocytes by binding to the CB1 receptors on these cells. It was also shown that AEA application could result in release of ATP from astrocytes. It was suggested that this release of ATP could contribute to TBS-induced LTP in the somatosensory cortex. It was also shown that inhibition of CB1 receptors with AM251 resulted in a decrease in astrocytic calcium elevation and astrocytic ATP release. As vesicular release from astrocytes is required for LTP induction, then it is possible that inhibition of CB1 receptors on astrocytes can lead to impairment of LTP induction. Previous studies, which all have been carried out in the hippocampus, have shown contradictory results. Two studies have shown that application of CB1 receptor antagonist does not have any effect on LTP induction (Carlson *et al.*, 2002, Slanina *et al.*, 2005). Another study showed enhancement of *in vivo* LTP in CB1 receptor knockout mice in comparison to WT mice (Jacob *et al.*, 2012). In contrast, three other studies have shown complete abolishment of LTP in slices perfused with CB1 receptor antagonists (Chevaleyre and Castillo, 2003, de Oliveira Alvares *et al.*, 2006, Lin *et al.*, 2011).

To investigate the role of endogenous cannabinoids on LTP induction in the somatosensory cortex, TBSx5 protocol was delivered during application of AM251. Delivery of TBSx5 during application of AM251 completely abolished LTP and actually induced a significant LTD of -26.69±5.02% (n=13, $p<0.001$,

paired t-test; see Figure 5.5). These results suggest that CB1 receptors and hence eCBs are required for LTP induction in the somatosensory cortex.

The above results suggest that CB1 receptors are required for LTP induction in the somatosensory cortex. If this is the case, then it would be interesting to see what effect application of exogenous cannabinoids has on TBSx5-induced LTP induction. As shown in the previous section, application of AEA contributed to induction of LTP with TBSx2. Therefore, one would expect an enhancement of LTP if AEA were applied during the delivery of TBSx5. However, CB1 receptors are also present on pre-synaptic sites, where they can inhibit transmitter release. Previous studies that have attempted to investigate the role of application of exogenous cannabinoids have shown contrasting results. In CA1 region of hippocampus of 2-3 weeks old mice and rats, pre-incubation of brain slices with exogenous synthetic CB1 receptor agonists HU-210 (100 nM) or WIN55,212-2 (3-10 μM), blocked HFS induced LTP (Collins *et al.*, 1995, Misner and Sullivan, 1999). Application of 20 μM of 2-AG to slices for 20 minutes prior to HFS delivery also blocked LTP induction in the CA1 region of the hippocampus (Stella *et al.*, 1997). A study in the prefrontal cortex showed that application of high concentration of WIN55,212-2 (1 mM), decreased the chances of LTP induction in the prefrontal cortex (Auclair *et al.*, 2000). In contrast, another study showed that application of AEA, for 30 minutes prior to delivery of HFS, did not completely block LTP (Terranova *et al.*, 1995). An earlier study showed that application of Δ^9-THC (10-1000 pM) to CA1 region of hippocampus did not decrease the extent of LTP (Nowicky *et al.*, 1987). In a study in the visual cortex

of young (2-3 weeks old) mice, application of WIN55,212-2 (2 μM) did not effect LTP induction (Huang *et al.*, 2008).

None of the above studies were carried out in the somatosensory cortex. To investigate the effect AEA application has on LTP induction in the somatosensory cortex, TBSx5 was delivered during application of 500 nM of AEA. Application of AEA resulted in a significant LTP of +68.78±22.11% (n=8, paired t-test, $p<0.05$; see Figure 5.5). There was no statistically significant difference between LTP with AEA and LTP in control conditions ($p<0.05$, two sample t-test; see Figure 5.5B). These results show that application of 500 nM of AEA does not have an effect on TBSx5 induced LTP in the somatosensory cortex.

The results on Figure 5.5 have been published (Rasooli-Nejad *et al.*, 2014).

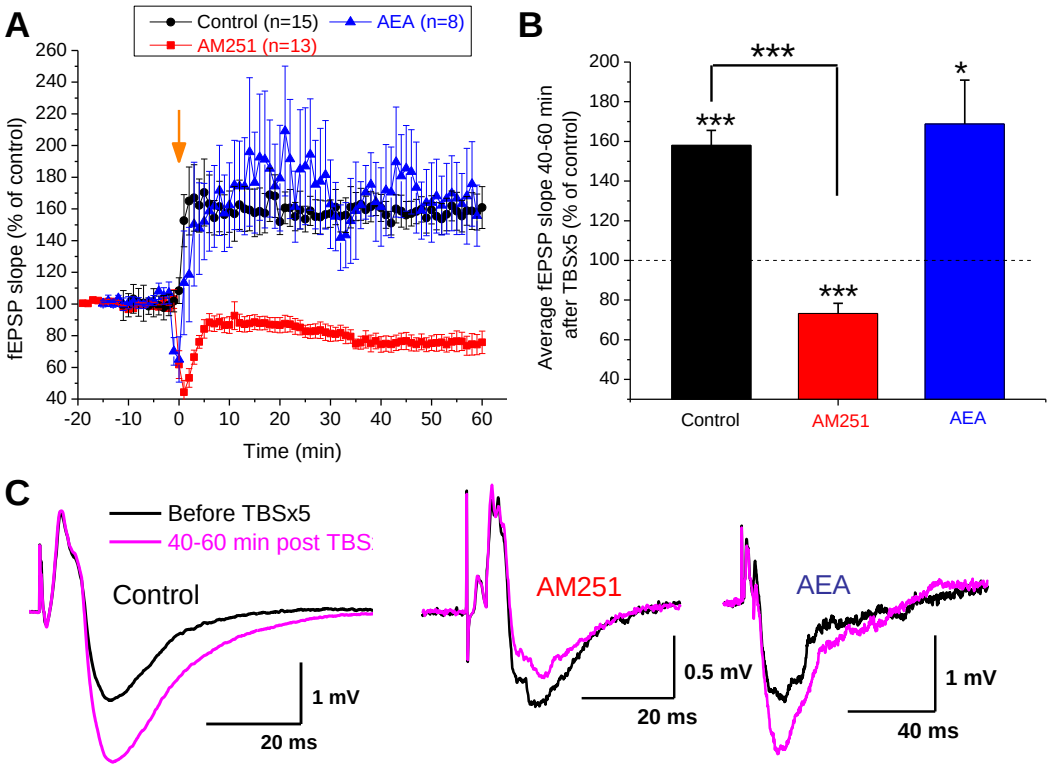

Figure 5.5. CB1 receptors are required for induction of TBSx5-induced LTP. A, These recordings were performed in WT mice. The average time-courses for fEPSP recordings during TBSx5 protocol are shown. Orange arrow shows position of TBSx5 delivery. All drugs were applied 15 minutes prior to TBSx5 delivery and were washed out 10 minutes after TBSx5. **B,** shows bar-charts representing the average % change in fEPSP 40-60 minutes post TBSx5 delivery. For TBSx5 delivery in control conditions, the average % change in fEPSP was +58±7.54%. For TBSx5 delivery under AM251 (1 µM), the average % change in fEPSP was -26.69±5.02%. For TBSx5 delivery under AEA (500 nM), the average % change in fEPSP was +68.78±22.11%. Two sample independent t-test was performed between control and AM251 data. Paired t-test was performed for average % change in fEPSP from baseline. $p<0.05$, *; $P<0.01$ **; $p<0.001$. **C,** shows example fEPSPs before and after TBSx5 delivery.

5.5. Application of AEA can increase fEPSPs by increasing vesicular release of gliotransmitters from astrocytes

As shown in the previous sections, AEA application during TBSx2 resulted in the induction of LTP. It was suggested that this rescue of LTP is due to AEA-mediated vesicular release of ATP from astrocytes onto neuronal P2XRs. It was suggested that this action of AEA is similar to TFLLR application. TFLLR application could increase the fEPSP size without delivery of TBS protocol. However, it was shown that this TFLLR mediated increase in fEPSP was not an LTP because washout of TFLLR reduced the fEPSP back to baseline value (see Figure 3.19 in chapter 3). If AEA action is similar to TFLLR, then one would expect that AEA, by binding to CB1 receptors on astrocytes and thus inducing calcium dependent release of gliotrasnmitters from these cells, to result in increase in fEPSP. However, AEA can also bind CB1 receptors on pre-synaptic sites, which results in inhibition of neurotransmitter release. This latter action could either decrease neurotransmitter release at excitatory synapses, thereby decreasing fEPSP, or decrease neurotransmitter release at inhibitory synapses, thereby increasing fEPSP. To investigate the effect of AEA on synaptic transmission in somatosensory cortex, 500 nM of AEA was applied to cortical slices during recordings of fEPSPs. Anandamide was applied subsequent to 10 minutes of baseline fEPSP recordings (Figure 5.6A). Within 2-10 minutes of AEA application, there was a significant increase of 17.18±3.78% in fEPSP ($n=10$, $p<0.01$, paired t-test; see Figures 5.6A and 5.6C). Following 10 minutes of application, AEA was washed out from the slice. Washout of AEA resulted in decrease of fEPSP back to baseline value. The average size of fEPSP following

10-20 minutes of AEA washout was 6.72±4.03% in comparison to baseline fEPSP (before AEA application) (Figures 5.6A and 5.6C). There was no significant difference between baseline fEPSP and fEPSP following AEA washout ($p<0.05$, paired t-test; see Figure 5.6C). These results suggest that similar to TFLLR application, AEA application can increase the fEPSP but that this increase is not an LTP because washout of AEA reduces the fEPSP back to baseline value.

The increase in fEPSP following AEA application can be due to two reasons: 1) fEPSP increases as a result of activation of CB1 receptors on astrcoytes, which leads to increase in vesicular release of gliotransmitters from these cells; 2) activation of CB1 receptors on pre-synaptic inhibitory neurones leads to decrease of neurotransmitter release, hence leading to increase in fEPSP. To investigate whether AEA increase in fEPSP was due to vesicular release from astrocytes, AEA (500 nM) was applied to cortical slices from dnSNARE mice. In contrast to WT mice, application of AEA to cortical slices from dnSNARE mice did not increase the fEPSP. In fact it resulted in a significant decrease of -11.97±3.77% in fEPSP ($n=7$, $p<0.05$, paired t-test; see Figure 5.6A). Washout of AEA did not bring the fEPSP back to baseline value (Figures 5.6A and 5.6C). These results suggest that AEA application to dnSNARE cortical slices results in a decrease in synaptic transmission. This decrease is an LTD because washout of AEA does not bring the fEPSP back to baseline level. These results imply that when vesicular release from astrocytes is impaired, AEA application results in decrease in synaptic transmission, presumably through decrease of transmitter release from excitatory neurons. These results also suggest that the increase in fEPSP in

WT mice following the application of AEA is as a result of AEA-mediated activation of astrocytic vesicular release.

The above data suggested that in WT mice, AEA application could increase vesicular release from gliotranmitters from astrocytes, thereby increasing fEPSP. It was also suggested that in dnSNARE mice, AEA decreases fEPSP by decreasing release of neurotransmitters from pre-synaptic sites. To investigate whether these effects are due to changes in release probability or due to post-synaptic effects, paired pulse protocol was carried out during the fEPSP recordings shown on Figure 5.6A. If PPR does not change following AEA application, then one can suggest that the change in fEPSP is due to post-synaptic changes. However, if PPR changes in response to AEA application, then one can suggest that the change in fEPSP is as a result of changes in release probability. The results of paired pulse protocol are shown on Figure 5.6D. Paired pulse protocol was carried out during control (C), following 5-10 minutes of AEA application (A), and following 10-20 minutes after AEA washout (W). Two inter-stimulus intervals were used: 50 ms and 200 ms. Example fEPSPs during paired pulse protocol with inter-stimulus interval of 50 ms are shown on Figure 5.6E. Example fEPSPs during paired pulse protocol with inter-stimulus interval of 200 ms are shown on Figure 5.6F.

Delivery of paired pulse protocol with 50 ms interval under control conditions in WT mice resulted in the second fEPSP being larger than the first fEPSP (Figure 5.6E). The average PPR across 8 experiments was 1.61±0.18 (Figure 5.6D). When AEA was applied to cortical slices from WT mice, the fEPSP increased

(Figure 5.6E). Delivery of Paired pulse protocol resulted in a significant increase in paired pulse ratio ($p<0.05$, paired t-test; see Figure 5.6D-E). The PPR under AEA was 2.21±0.25 (n=8). Washout of AEA decreased the PPR to 1.80±0.18 (n=8; see Figure 5.6D). These results suggest that the increase in fEPSP as a result of application of AEA is due to increase in release probability and not due to an increase in post-synaptic component. This is in contrast to TFLLR application, where PPR did not change, thereby suggesting that the increase in fEPSP was due to a post-synaptic component (Figure 3.19).

Delivery of paired pulse protocol with 200 ms interval under control conditions in WT mice resulted in a PPR of 1.13±0.12 (n=7; see Figures 5.6D and 5.6F). This PPR is smaller in comparison to PPR with 50 ms interval. This is as expected because increasing the interval between the two pulses (200 ms) theoretically results in a lower intra-cellular calcium levels in pre-synaptic terminals in comparison to when inter-stimulus interval is shorter at 50 ms. This means that during paired pulse protocol with 50 ms interval, there is large rise in calcium levels in pre-synaptic terminal when the second pulse is going to be delivered; this results in a larger pre-synaptic release during the second pulse, hence leading to a large PPR. However, during paired pulse protocol with 200 ms interval, the calcium rise in pre-synaptic terminals drops due to the longer interval between the two pulses; this results in a lower neurotransmitter release form pre-synaptic terminals during the delivery of the second pulse, thereby resulting in a lower PPR. Therefore the PPR with 200 ms is smaller than PPR with 50 ms interval. Application of AEA did not significantly alter the PPR with 200 ms interval (Figures 5.6D and 5.6F).

The above paired pulse protocols were repeated in cortical slices from dnSNARE mice. Under control conditions, the PPRs with 50 ms interval and 200 ms interval were significantly less in dnSNARE mice in comparison to WT mice (two sample independent t-test, $p<0.05$; see Figures 5.6D-F). This suggests that the release probability in dnSNARE mice is less than in WT mice. This drop in release probability could be due to the impairment of vesicular release of gliotrasnmitters from astrocytes.

Application of AEA to dnSNARE mice results in decrease in fEPSP (Figure 5.6E). Delivery of paired pulse protocol with 50 ms interval during AEA application in dnSNARE mice results in a significant increase in PPR ($p<0.001$, paired t-test; see Figure 5.6D). The PPR for 50 ms interval during control conditions was 1.26±0.07, whilst PPR under AEA application was 1.39±0.08 (n=7; see Figures 5.6D-E). Change in PPR with AEA application to dnSNARE cortical slices suggests that the decrease in fEPSP as a result of AEA is due to decrease in release probability.

It was shown that in WT mice application of 500 nM of AEA could increase fEPSP by increasing vesicular exocytosis from astrocytes. In contrast to this, a recent report in the CA1 region of hippocampus has shown that application of exogenous cannabinoids can result in decrease of fEPSP and can induce LTD (Han *et al.*, 2012). One possible explanation for this contradiction between my results and this report is that in my experiments a low concentration of AEA was used. To see what effect does a higher concentration of AEA has on synaptic transmission, 5 µM of AEA was applied to cortical slices from WT mice during

recording of fEPSPs. Application of 5 μM of AEA resulted in a significant drop in fEPSP of -23.18±6.74% (n=6, $p<0.05$, paired t-test; see Figure 5.6B-C). Washout of AEA did not increase the fEPSP back to baseline (Figure 5.6B-C), suggesting that the decrease in synaptic transmission was an LTD. This suggests that, in WT cortical slices, application of higher concentration (5 μM) of AEA results in decrease in synaptic transmission and LTD, whilst application of lower concentration (500 nM) of AEA results in increase in synaptic transmission.

Taken together, the results in this section show that application of 500 nM of AEA can increase fEPSP by increasing vesicular release of gliotransmitters from astrocytes.

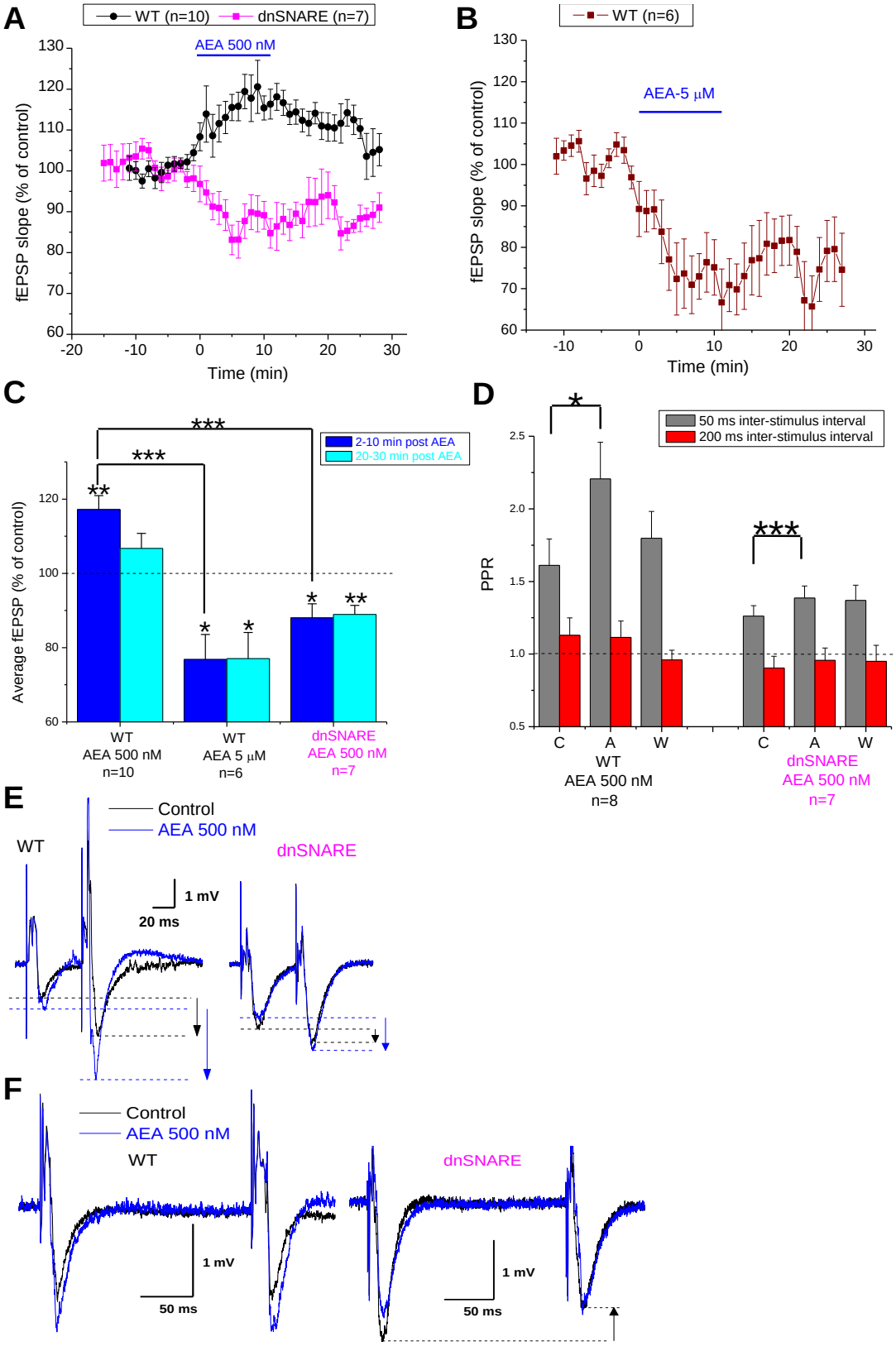

Figure 5.6. For Figure legend see next page.

Figure 5.6. Application of AEA can increase fEPSPs by increasing vesicular release of gliotransmitters from astrocytes. A, shows average time-courses for fEPSP recordings before and after application of 500 nM AEA in WT and dnSNARE mice. Blue bar shows the time-span of AEA application. **B,** shows average time-course for fEPSP recordings before and after application of 5 μM of AEA in WT mice. **C**, shows the data from **A** and **B** in form of bar-charts. Paired t-test was performed for fEPSP change from baseline. Two sample independent t-test was performed between WT and dnSNARE data. Two sample t-test was also performed between data for application of 500 nM of AEA to WT mice and data for application of 5 μM of AEA to WT mice. The statistical significant levels were as follows $p<0.05$, *; $p<0.01$, **; $p<0.001$, ***. **D**, paired pulse protocol was carried out during the fEPSP recordings shown in **A**. Paired pulse protocol was carried out under control conditions (C), 5 minutes after AEA application (A), and 15 minutes after washout of AEA (W). Two inter-stimulus intervals were used for paired pulse: 50 ms and 200 ms. For each time interval (50 and 200 ms), paired t-test was performed between control and AEA data. Furthermore, for each time interval, paired t-test was also performed between control and washout data. These t-tests were performed for both WT and dnSNARE recordings. The statistical significant levels were as follows $p<0.05$, *; $p<0.01$, **; $p<0.001$, ***. **E,** shows example fEPSP traces for 50 ms inter-stimulus interval for paired pulse protocol under control and AEA in WT and dnSNARE mice. Downward arrow indicates increase in paired pulse ratio. **F,** shows example fEPSP traces for 200 ms inter-stimulus interval for paired pulse protocol under control and AEA in WT and dnSNARE mice. Upward arrow indicated decrease in paired pulse ratio.

5.6. Application of AEA may increase NMDAR activity

In the previous sections it was shown that application of AEA could result in vesicular release of ATP from astrocytes. It was suggested that in this action, AEA acts similarly to TFLLR. However, it was shown in chapter 3 that TFLLR application could also result in release of glutamatergic gliotransmitter release from astrocytes in addition to release of ATP (see sections 3.13 and 3.14). This suggests that AEA application might also result in release of glutamatergic transmitters. One previous study in the CA1 region of the hippocampus showed that activation CB1 receptors on astrocytes results in rise in intracellular calcium levels in these cells. This in turn leads to glutamate release from astrocytes (Navarrete and Araque, 2008). To investigate whether in the somatosensory cortex, AEA application can result in enhancement of NMDAR activity, 500 nM of AEA was applied to cortical slices from WT mice during recording of evoked NMDAR EPSCs. Similar to Figure 3.24, NMDAR eEPSCs were recorded at -40 mV holding voltage under PPADS (10 µM), 5-BDBD (5 µM), picrotoxin (10 µM) and DNQX (30 µM).

Application of AEA resulted in a percentage increase of 55.14±34.61% in the average amplitude of NMDAR eEPSC (n=3). Increase in eEPSC amplitude could be either due to changes in release probability or due to post-synaptic changes. Quantal analysis was carried out to investigate whether the increase in amplitude following AEA application were due to release probability or due post-synaptic changes. Figure 5.7A shows the amplitude probability distributions for baseline NMDAR eEPSC recordings and for eEPSC recordings during application of

AEA. Binomial models of release were fitted to the data and are shown. These models are shown as grey lines on the PDFs. The parameters of the models are also given. Application of AEA resulted in an increase in probability of release (p) and maximum number of release sites (n). In contrast, there was no increase in quantal amplitude (q). This suggests that the increase in the average amplitude of NMDAR eEPSC seen as a result of AEA application is due to increase in release of glutamatergic transmitters. These are preliminary results. The next step for investigating whether this AEA-mediated increase in release of glutamatergic transmitters is as a result of vesicular release from astrocytes would be to repeat the above protocol in dnSNARE mice.

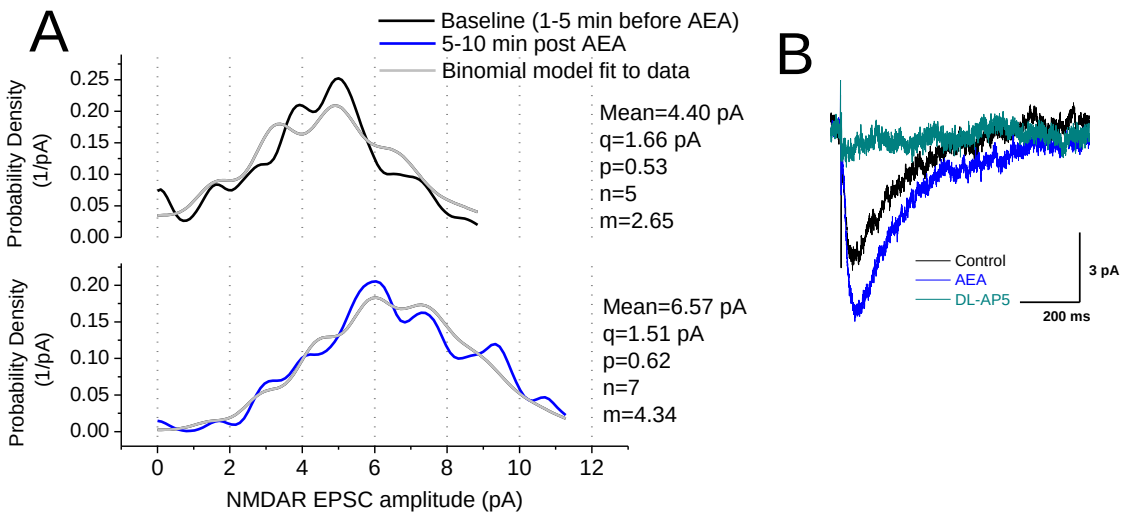

Figure 5.7. Application of AEA can increase the average amplitude of evoked NMDAR EPSCs by increasing release probability. Example of an evoked NMDAR EPSC recordings prior to and post AEA (500 nM) application. Evoked NMDAR EPSCs were recorded at -40 mV holding voltage under Picrotoxin (100 µM), PPADS (10 µM), 5-BDBD (5 µM) and DNQX (30 µM). **A**, shows the amplitude probability distribution functions for before and after AEA application. Both baseline and AEA PDFs were fitted with a binomial release model and the fit of this model to data is shown as grey lines. Model parameters are quantal amplitude (q), number of release sites (n), probability of release (p), and the average number of quanta released (m). **B,** shows example evoked NMDAR EPSCs. These example eEPSCs shown are average of 20 successive recorded eESPCs. As can be seen, DL-AP5 completely abolished the current thereby indicating that the evoked current was due to NMDAR activity.

5.7. Summary of chapter

The aim of this chapter was to investigate the role of endogenous and exogenous cannabinoids in synaptic transmission and plasticity in context of tripartite synapse. First, it was shown that AEA could elevate intracellular calcium concentrations in astrcoytes by binding to CB1 receptors on these cells. It was then shown that AEA-mediated activation of calcium elevation on astrocytes could result in release of ATP and D-serine from astrocytes via vesicular exocytosis. In addition, by using vibro-dissociation technique, it was shown that application of AEA onto isolated astrocytes resulted in vesicular release of ATP from these cells. The released ATP activated P2XRs on isolated neurones. It was also shown that delivery of HFS resulted in calcium elevation in astrocytes and vesicular release of ATP from these cells. This calcium elevation depended on CB1 receptors, thereby indicating that **endogenous** cannabinoids can activate calcium dependent vesicular release of ATP from astrocytes. This suggested that activation of astrocytes during TBS/HFS-induced LTP could involve endogenous cannabinoids. Field recordings were carried out to provide evidence for this notion. It was shown that CB1 receptors are required for the induction of LTP. It was also shown that application of AEA could induce LTP during TBSx2 protocol. This LTP induction depended on vesicular release from astrocytes and P2XRs, thereby suggesting that AEA can contribute to LTP in the somatosensory cortex by resulting in vesicular exocytosis of ATP from astrocytes.

Chapter 6: Discussion

6.1. Summary of results

The main aim of this project was to investigate the role for gliotransmitter release from astrocytes during synaptic transmission and plasticity in the somatosensory cortex. The role of cannabinoid signalling in the context of tripartite synapse was also investigated. The original findings of this project were:

- TBS-induced NMDAR-dependent LTP in the somatosensory cortex requires vesicular exocytosis of gliotransmitters from astrocytes
- Astrocytes can release ATP by calcium dependent vesicular exocytosis
- ATP release from astrocytes contributes to LTP induction in the somatosensory cortex.
- Astrocytes can release glutamatergic gliotransmitters (D-serine and glutamate) via vesicular exocytosis. Release of glutamatergic gliotransmitters results in activation of extra-synaptic GluN2B-containing NMDARs on neurones.
- GluN2B-containing NMDARs contribute to LTP induction in the somatosensory cortex.
- In the somatosensory cortex, vesicular release of D-serine from astrocytes does not contribute to LTP induction.
- Application of AEA results in calcium elevation in astrocytes of the somatosensory cortex by activating CB1 receptors on these cells. AEA-mediated calcium elevation in astrocytes leads to release of ATP and D-serine from astrocytes. This release of ATP can contribute to LTP induction

- In the somatosensory cortex, stimulation of neuronal afferent fibres leads to calcium elevation in astrocytes. This calcium elevation depends on CB1 receptors and NMDARs on astrocytes. CB1 receptor-mediated calcium elevation in astrocytes leads to release of ATP from these cells.
- In the somatosensory cortex, CB1 receptors are required for LTP induction.

6.2. Role for purinergic gliotransmitters

Previous reports had already shown that in the hippocampus and hypothalamus, vesicular release of gliotransmitters from astrocytes is required for LTP induction (Pascual *et al.*, 2005, Panatier *et al.*, 2006, Henneberger *et al.*, 2010). However, there had been no study showing the importance of vesicular exocytosis from astrocytes during LTP induction in the **somatosensory cortex**. The first original finding of this project was that, similar to hippocampus and hypothalamus, vesicular exocytosis from astrocytes is required for induction of NMDAR-dependent LTP in the somatosensory cortex. Those previous studies from hippocampus and hypothalamus had shown that ATP and D-serine are the gliotransmitters that contribute to LTP induction. For this reason, in this project, the role of these gliotransmitters in LTP induction was investigated in the somatosensory cortex. It was shown that in the somatosensory cortex, the modulation of NMDAR activity that contributes to LTP induction is not due to D-serine release from astrocytes, but due to ATP release from astrocytes.

One of the objectives of this project was to investigate the role played by vesicular release of ATP from astrocytes on synaptic transmission and plasticity.

The group of researchers who engineered the dnSNARE mice had already shown that in the CA1 region of hippocampus, vesicular release of ATP from astrocytes is required for LTP induction (Pascual *et al.*, 2005). They suggested that ATP, following release from astrocytes, is broken down into adenosine in the synapse (see Figure 6.1, steps 2-10). Increase in extracellular levels of adenosine results in increase in tonic inhibition of glutamatergic transmission during baseline activity. This means that as a result of ATP release from astrocytes, baseline glutamatergic transmission is lowered. Therefore, during delivery of HFS, there is a larger range for glutamatergic transmission to increase by. Hence, a large LTP can be induced in WT mice. However, in dnSNARE mice, vesicular release of ATP is impaired, and so less adenosine is available. This leads to a greater baseline glutamatergic transmission, which leads to a smaller range for LTP to increase by. Hence, LTP size is reduced. Basically, the idea is that astrocytes by releasing ATP can lower baseline glutamatergic activity, and therefore modulate the size of LTP. However, in contrast to this report, my results showed that in the somatosensory cortex, baseline activity is actually higher in WT mice than in dnSNARE mice (Figure 3.4). This means that the impairment of vesicular release from astrocytes results in **decrease** in baseline transmission in the somatosensory cortex. This suggests that, in contrast to hippocampus, in the somatosensory cortex, the impairment of LTP induction seen in dnSNARE mice is **not due to increase** in baseline transmission. This suggests that, in the somatosensory cortex, the impairment of LTP induction is not due to adenosine-mediated increase in glutamatergic tonic inhibition. Therefore, the mechanism of this LTP impairment must be different in the somatosensory cortex.

It was shown that application of ATPγS, which is a non-hydrolysable form of ATP, could rescue the impaired TBS-induced LTP in cortical slices from dnSNARE mice. This suggested that vesicular release of ATP from astrocytes is required for LTP induction in the somatosensory cortex. It also suggests that ATP can contribute to LTP induction without being broken down to adenosine.

To investigate how astrocytic ATP contributes to LTP induction, first evidence for calcium dependent exocytosis of ATP from astrocytes was provided (Figure 3.9). This was one the main original findings of this project. This project provided the first ever direct evidence for ATP release from astrocytes via calcium-dependent exocytosis in any region of brain. Furthermore, it was shown that release of ATP from astrocytes could activate P2XRs on neurones, which in turn lead to inhibition of phasic and tonic GABAergic transmission. This inhibition of inhibition resulted in increase in NMDAR activity (see Figure 6.1, steps 11-15). This suggested that ATP release from astrocytes can contribute to increase in NMDAR activity and hence to NMDAR-dependent LTP.

How does activation of neuronal P2XRs result in inhibition of $GABA_A$ receptors? It has been shown by my colleagues that P2XRs can inhibit $GABA_A$Rs by acting through Ca^{2+}-dependent phosphorylation by protein kinase C (Lalo *et al.*, 2014). Protein Kinase C can directly phosphorylate the intracellular loop of $GABA_A$R β subunits (Brandon *et al.*, 2000). This results in decrease in $GABA_A$ channel activity.

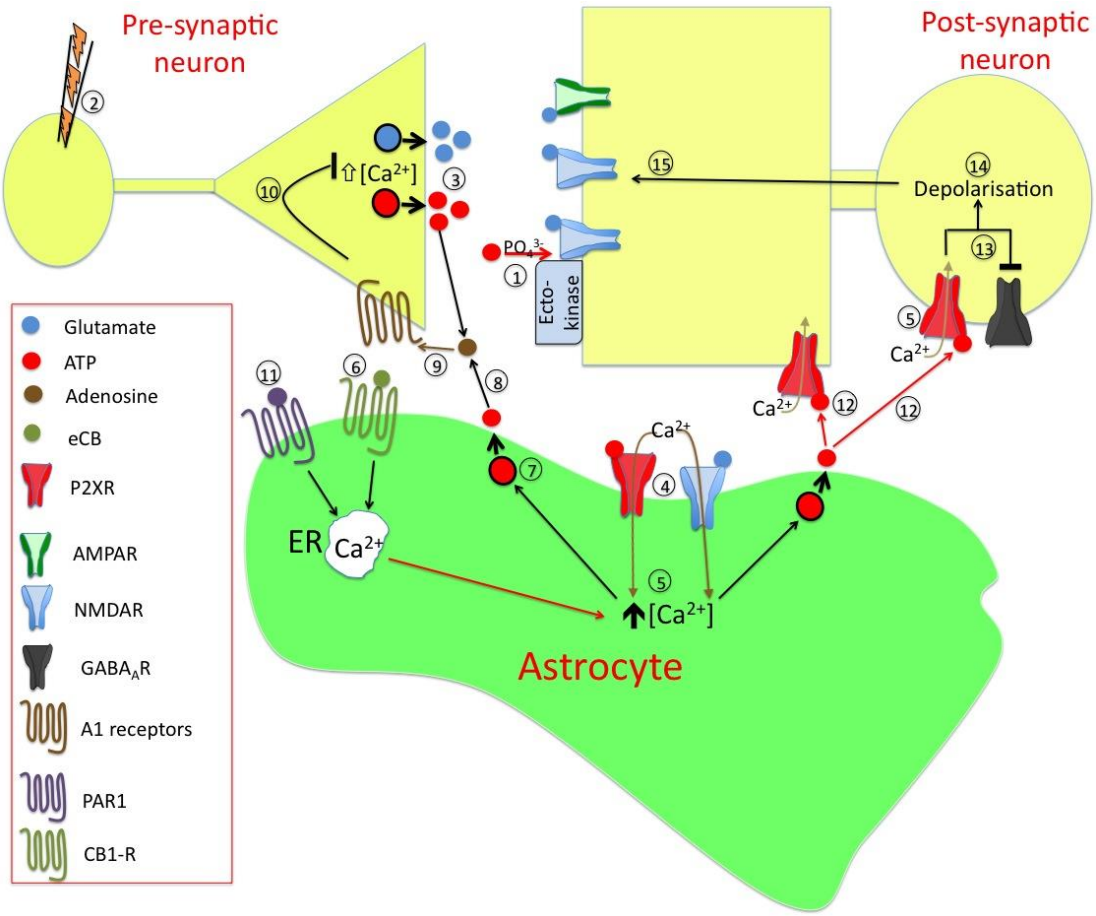

Figure 6.1. Modulation of synaptic transmission by astrocytic purinergic signalling. Previous studies have suggested different mechanisms for modulation of synaptic transmission via purinergic signalling. One mechanism suggests that ATP can enhance NMDAR activity by acting as a phosphate donor for phosphorylation by ecto-protein kinases (1). Another mechanism involves the breakdown of astrocytic ATP to adenosine: stimulation of pre-synaptic fibres (2) results in release of neurotransmitters from these fibres (3). Spillover of neurotransmitters to extra-synaptic sites results in activation of astrocytic ionotropic receptors (4). This leads to calcium elevation in astrocytes (5). Activation of CB1 receptors can also result in calcium elevation in astrocytes (6). Calcium elevation in astrocytes leads to vesicular exocytosis of ATP from these cells (7). ATP is then broken down to adenosine in the extra-cellular space (8). Adenosine can then bind to A1 receptors on pre-synaptic neurones (9) leading to a persistent tonic suppression of calcium dependent neurotransmitter release (10). In this PhD project, a different mechanism has been suggested. It was shown that following activation neuronal afferents (2) or activation of PAR-1 via TFLLR (11), vesicular release of ATP from astrocytes could lead to activation of P2XR on neurones (12). This triggers activation of protein kinase C, which results in inhibition of neuronal GABA$_A$Rs (13). This leads to increase in excitation and depolarisation (14), leading to increase in activation of post-synaptic NMDARs (15).

6.3. Role of glutamatergic transmission

In addition to vesicular exocytosis of ATP from astrocytes, this project also provides the first ever evidence for release of glutamatergic gliotransmitters (Glutamate and D-serine) from **cortical** astrocytes via **vesicular exocytosis**. It was shown that application of TFLLR could result in increase in frequency of GluN2B-dependent NMDARs sEPSCs. This increase in frequency was dependent on vesicular exocytosis of glutamate from astrocytes. The next step in this investigation would be to show that this astrocytic vesicular exocytosis of glutamatergic gliotransmitters could be induced, not only via TFLLR application, but also following stimulation of neuronal afferents of layer IV/V of cortex. Basically, the experiments on Figure 3.10 should be repeated, with the exception that that NMDAR-mediated sEPSCs should be recorded instead of P2XR-mediated sEPSCs.

It was suggested that application of TFLLR could result in vesicular release of glutamatergic gliotransmitters onto extra-synaptic GluN2B-containing NMDARs on neurons. Are both glutamate and D-serine release from astrocytes involved in this effect? Application of TFLLR resulted in increase in only the frequency of NMDAR sEPSCs but not the average amplitude. In contrast, application of exogenous D-serine resulted in an increase in **both** the average amplitude and frequency of NMDAR-mediated sEPSCs. Therefore, If D-serine were also released from astrocytes following TFLLR application, then one would expect an increase in the average amplitude of NMDAR sEPSCs. However, there was no increase in average amplitude following TFLLR application. This could suggest

that D-serine is not released by astrocytes. However, the preliminary data obtained by my colleagues by using microelectrode biosensors suggest that D-serine is indeed released by astrocytes via vesicular exocytosis following application of TFLLR. Therefore, it seems that D-serine is released by astrocytes but its release does not increase the average amplitude of NMDAR sEPSCs. There could be two possible scenarios.

(i) In the first scenario, application of TFLLR could result in the release of endogenous D-serine from astrocytes onto extra-synaptic GluN2B-containing NMDARs, leading to the full opening of these NMDARs. This would in turn lead to increase in detection of these NMDAR-mediated sEPSCs and so increase in frequency of these sEPSCs. As these GluN2B-containing extra-synaptic NMDARs have lower amplitude than GluN2A-containing synaptic NMDARs, their activation results in a decrease in the average amplitude of sEPSCs. It is possible that when D-serine is released from astrocytes, it only binds to extra-synaptic NMDARs. In contrast, it is possible that when exogenous D-serine is applied, it results in **global** activation of NMDARs, leading to opening of both synaptic and extra-synaptic NMDARs, thereby leading to an increase in **both** the average amplitude and frequency of sEPSCs.

(ii) The idea of the second scenario comes from a study from the CA1 region of hippocampus, where it was shown that D-serine acts on synaptic and not extra-synaptic NMDARs (Papouin *et al.*, 2012). Therefore, it is possible that the D-serine released from astrocytes following application of TFLLR, acts only on synaptic NMDARs and not extra-synaptic GluN2B-containing NMDARs. In this

scenario, it is possible that activation of extra-synaptic GluN2B-containing NMDARs depends **solely** on glutamate release from astrocytes and not D-serine release. Again, as these extra-synaptic NMDARs have lower amplitude than synaptic GluN2A-containing NMDARs, their activation results in decrease in average amplitude of NMDAR sEPSCs. Activation of extra-synaptic NMDARs could occlude the effect of endogenous D-serine on synaptic NMDARs, thereby preventing increase in the average amplitude of sEPSCs. To investigate whether D-serine released by cortical astrocytic acts on extra-synaptic NMDARs would be an area for future investigation.

It has been shown that in the CA1 region of hippocampus, calcium elevation in astrocytes, either spontaneously or as a result of application of agonists of PAR-1 or mGluR5, can result in generation of neuronal GluN2B-dependent SICs (Fellin *et al.*, 2004, Shigetomi *et al.*, 2008). However, in my recordings of sEPSCs from cortical slices, no SICs were seen. The GluN2B-dependent SICs have average amplitude of 100 pA (Fellin *et al.*, 2004). In contrast, the GluNB-dependent NMDARs from my recordings have average amplitude of 4 pA (see Figure 3.20). Due to the large amplitude of SICs, it has been suggested that SICs cannot be generated as a result of release from SLMVs (SLMVs are the same size as synaptic vesicles; approximately 30-40 nm in diametre). Therefore, it has been suggested that SICs are probably due to astrocytic release from full fusion of vesicles that are 300 nm or larger (Fellin *et al.*, 2004, Kang *et al.*, 2013). The presence of these large vesicles has been shown in the hippocampus (Kang, Peng et al. 2013). However, to my knowledge, there is yet no evidence for presence of such large vesicles in the cortex. The absence of SICs in my recordings from the

somatosensory cortex suggests that these large vesicles are perhaps absent in the somatosensory cortex. Therefore, the small GluN2B-dependent sEPSCs observed following application of TFLLR are probably due to release from astrocytic SLMVs. However, it is also possible that such large vesicles are also present in the cortex; the generation of the small GluN2B-dependent sEPSCs could be due a kiss and run release mechanism from the larger vesicles where only a fraction of the vesicular content is release into extra-synaptic space. The nature of astrocytic vesicles in the cortex is another area for future investigation.

It was shown that in the somatosensory cortex, GluN2B-containing NMDARs contribute to LTP induction (Figure 3.23). As was mentioned above, release of glutamate from astrocytes can activate extra-synaptic GluN2B-containing NMDARs. However, release of glutamate from astrocytes is not the only glutamate source for activation GluN2B-containing NMDARs. During recordings of spontaneous NMDAR sEPSCs shown on Figure 3.20, prior to application of TFLLR, there is no or very few GluN2B-dependent NMDARs sEPSCs. This is because during spontaneous activity (i.e. when afferent fibres are not stimulated) neuronal release of glutamate mainly activates synaptic NMDARs (Dalby and Mody, 2003). This means that during spontaneous activity, there is no spillover of glutamate onto extra-synaptic sites. However, during stimulation of afferent fibres (e.g. during recordings of fEPSPs and TBS delivery), glutamate released from neurones can theoretically spillover from synapse onto extra-synaptic sites, where it can activate GluN2B-containing NMDARs. This means that the source of glutamate that activates extra-synaptic GluN2B-containing NMDARs need necessarily not be astrocytic; it could also be

due to neuronal glutamate spillover from synapses. Are the GluN2B-containing NMDARs that contribute to LTP induction activated by spillover of neuronal glutamate or does astrocytic release of glutamate on these NMDARs also contribute to LTP induction? The results on Figure 3.24, where TFLLR was delivered during TBSx2 delivery, suggested that the release of glutamate from astrocytes onto GluN2B-containing NMDARs does not contribute to LTP induction. This suggests that, similar to D-serine, glutamate release from astrocytes does not make a major contribution to LTP induction.

If the numbers of GluN2B subunits decrease during development, then how do GluN2B containing NMDARs contribute to LTP induction? Studies have attributed this to interaction of GluN2B with CaMK-II. Following activation, CaMK-II can remain locked in active conformation by interacting with the C-terminal of GluN2B subunits (Strack and Colbran, 1998, Bayer *et al.*, 2001). This interaction seems to be important, as one study showed that over-expression of the C-terminal of GluN2B, which blocked the interaction of this subunit with CamK-II, resulted in decrease in size of HFS-induced LTP in the CA1 region of hippocampus of 3-4 months old mice (Zhou *et al.*, 2007). This showed that GluN2B subunits contribute to LTP induction via their interaction with CaMK-II.

It has been suggested that rapid uptake of glycine by GlyT-1 prevents saturation of NMDARs, enabling D-serine to act as the primary co-agonist for modulating NMDAR activity (Fossat *et al.*, 2011, Henneberger *et al.*, 2013). As it is the general consensus that astrocytes are the main source of D-serine, it is suggested

that astrocytic D-serine release can modulate NMDAR activity and hence LTP. However, in this project it was it was shown that vesicular release of D-serine from astrocytes is not required for LTP induction in the somatosensory cortex. This was in contrast to studies from the hippocampus and hypothalamus, where D-serine release from astrocytes contributed to the induction of LTP (Panatier *et al.*, 2006, Henneberger *et al.*, 2010). This suggests that in the somatosensory cortex, either the modulation of NMDAR is mainly through glycine and not D-serine or that D-serine is indeed involved in modulation of NMDARs but the source of this D-serine is neuronal and not astrocytic. A group of researchers showed that in the cortex, D-serine was mainly localised to neurones and that cortical neurones can release D-serine via non-vesicular mechanism (Kartvelishvily *et al.*, 2006, Rosenberg *et al.*, 2010). Based on these results it has been suggested that astrocytes are the site for the production of L-serine, which is a precursor for D-serine. Astrocytes then release L-Serine into extra-cellular space, where it can be taken up by neurones. Neurons can then convert L-serine to D-serine (Wolosker, 2011). This means that neurones can both store and release D-serine. Therefore, it is possible that in the cortex, D-serine is indeed involved in modulation of NMDAR activity but the source of D-serine is neuronal and not astrocytic. This could explain the reason as to why in this project it was shown that vesicular release of D-serine from astrocytes is not involved in LTP induction. It could be that the level of D-serine released from neurones is sufficient in modulating NMDAR activity. Therefore the release of D-serine from astrocytes does not contribute further to NMDAR activity and LTP induction. In the future, the potential role of endogenous **neuronal** D-serine in synaptic transmission and plasticity should be investigated.

A recent study has shown that calcium elevations in cultured astrocytes as a result of TFLLR application results in glutamate release not by vesicular exocytosis but via bestrophin-1 channels (Woo *et al.*, 2012). In contrast to this report, the results shown on Figure 3.22 clearly show that in the absence of vesicular exocytosis, TFLLR application does not lead to release of glutamate. Therefore release from bestrophin-1 channels is unlikely in slice preparations from somatosensory cortex. It is possible that the release of glutamate from bestrophin-1 channels could be due to astrocytes in cultured preparation and not in astrocytes from slices.

A disadvantage of using TFLLR to selectively mediate astrocytic release is that PAR1 receptors are also present on neurons. Even though it has been shown by my colleagues and other research groups (Lee *et al.*, 2007, Lalo *et al.*, 2014) that TFLLR application specifically activates calcium elevation in astrocytes and not neurones, the other potenial effects of TFLLR as a result of activation of neuronal PAR1 receptors cannot be ruled out. This means that TFLLR, as a pharmacological agent which leads to PAR1-mediated intracellular calcium elevation, is selective for astrocytes, but it is not necessarilly selective for astroctyes over neurones as a pharmacological agent that activates PAR1 receptors in **general**. Recently, a group of researchers have used a genetic approach to address this problem (Agulhon *et al.*, 2013). They enginnered a transgenic mice line called GFAP-human M3 Muscarinic receptor (hM3Dq) that expresses a G_q GPCR called hM3Dq DREADD (Designer Receptors Exclusively Activated by Designer Drugs) selectively in GFAP positive glial cells. This receptor cannot be activated by endogenous GPCR ligands and can only be

activated via an inert pharmacological ligand called Clozapine-N-Oxide (CNO). These researchers showed that application of CNO selectively activates calcium elevation in astrocytes and not neurons. This DREADD approach is a superior method to TFLLR application and future investigation for selective activation of astrocytic calcium elevation should utiliswe this approach.

6.4. Role for endocannabinoid signalling in the context of tripartite synapse

Previous studies had shown that activation of CB1 receptors on astrocytes could result in calcium-dependent release of **glutamate** form these cells (Navarrete and Araque, 2010, Min and Nevian, 2012). In this PhD project it was shown that activation of CB1 receptors on astrocytes could also result in calcium dependent vesicular release of **ATP** from these cells.

Calcium elevations in astrocytes can occur either spontaneously or as a result of activation of their receptors. Activation of neuronal afferents leads to release of neurotransmitters such as glutamate and ATP. These neurotransmitters can then spillover onto extra-synaptic sites, where they can activate receptors on astrocytes. This leads to calcium-dependent exocytosis from astrocytes. This is why when HFS is delivered to afferent neurones there is a large increase in frequency of calcium-dependent exocytosis of ATP from astrocytes (Figures 3.9 and 5.3). Previous reports had shown that the astrocytic receptors that induce calcium elevations are mGluR5 (Fellin *et al.*, 2004, Panatier *et al.*, 2011). However, a recent report suggested that mGluR5 is only expressed on astrocytes

of mice that are less than 2 weeks old (Sun *et al.*, 2013). This report suggested that receptors other than mGluR5 must be involved in elevation of calcium levels in astrocytes. The work performed in this PhD project and the previous work carried out by my colleagues has shown that P2XRs and NMDARs are involved in calcium elevation in astrocytes following delivery of HFS to neuronal afferents (Palygin *et al.*, 2010). In addition to the involvement of NMDARs and P2XRs in calcium elevation in astrocytes, it was shown that CB1 receptors are also involved in calcium elevation in astrocytes (Figure 5.3). It was suggested that release of glutamate from afferent neurones could activate mGluR5 on post-synaptic neurones. This in turn can result in production and release of endogenous cannabinoids from post-synaptic neurons. These cannabinoids can then activate CB1 receptors on astrocytes, thereby leading to calcium elevations in these cells.

It has been shown that not all calcium elevations in astrocytes result in release of gliotransmitters or result in changes in synaptic plasticity (Shigetomi *et al.*, 2008, Agulhon *et al.*, 2010). However, the results in this PhD project clearly show that CB1 receptors, PAR-1 and NMDARs are all involved in calcium-dependent vesicular exocytosis of ATP and that this release results in modulation of synaptic plasticity.

The data in this PhD project showed that inhibition of CB1 receptors with AM251 could result in complete abolishment of TBSx5-induced LTP. There are two possible mechanisms for this outcome. The first mechanism can be attributed to CB1 receptors on astrocytes. Inhibition of CB1 receptors on

astrocytes results in decrease in calcium dependent vesicular release of ATP from astrocytes. As vesicular release of ATP from astrocytes is required for LTP induction, inhibition of CB1 receptors results in impairment of LTP induction. This mechanism is also supported by the data showing that application of 500 nM of AEA can result in increase in fEPSP and can contribute to induction of LTP (Figures 5.4 and 5.6). The other possible mechanism for the impairment of TBSx5-induced LTP with AM251 could be due to CB1 receptors on inhibitory neurons. It has been reported by a previous study that constitutive eCB release from post-synaptic hippocampal neurones can result in tonic inhibition of GABA release (Neu *et al.*, 2007). In this study, application of AM251 to slices from CA1 region of hippocampus lead to an increase in GABA release. When BAPTA was used in the post-synaptic cell, the tonic eCB inhibition was abolished. These results suggested that post-synaptic cells constitutively release eCBs, which bind to GABAergic pre-synaptic CB1 receptors, thereby leading to tonic decrease in GABA release. Furthermore, another study has shown that inhibition of GABA release from pre-synaptic neurones via eCBs can facilitate LTP induction in excitatory neurones (Carlson *et al.*, 2002). Therefore, it is possible that during application of AM251, CB1 receptors on GABAergic pre-synaptic neurons are inhibited, thereby leading to increase in GABAergic transmission, which leads to decrease in excitation. This decrease in excitation can theoretically result in impairment of LTP induction following delivery of TBS or HFS protocol.

What has been discussed above suggests that inhibition of CB1 receptors results in **impairment** of LTP by increasing GABA release. However, if CB1 receptors on GABAergic pre-synaptic neurones were continuously inhibited, then one

would expect a decrease in baseline glutamatergic transmission. If baseline glutamatergic transmission decreases, there is a possibility that there is a larger extent for glutamatergic transmission to increase by during the induction of LTP. Therefore, a smaller stimulation is required for LTP induction i.e. the LTP threshold becomes smaller (ABS curve from Figure 1.2 shifts to the left). If this latter scenario is the case, then inhibition of CB1 receptors on pre-synaptic GABAergic neurones should result in **enhancement** of LTP during delivery of TBS or HFS. This suggests that inhibition of CB1 receptors on GABAergic neurones can result in either enhancement or impairment of LTP. This could explain why different studies show different outcomes when delivering HFS/TBS during inhibition of CB1 receptors. Three studies reported that when slices are incubated with CB1 receptor antagonists, LTP induction is completely abolished (Chevaleyre and Castillo, 2003, de Oliveira Alvares *et al.*, 2006, Lin *et al.*, 2011). These are in agreement with the results in this PhD project. In contrast, in another study where HFS was delivered to hippocampal slices from CB1 receptor KO mice, enhancement of LTP was reported (Jacob *et al.*, 2012). It could be that with CB1 receptor KO mice there is a **continuous** increase in GABAergic transmission and hence a persistent decrease in baseline glutamatergic transmission, thereby resulting a decrease in LTP threshold. In contrast, with application of antagonists of CB1 receptor, GABAergic CB1 receptors are inhibited for a **short-time** interval and so there is no shift in the LTP threshold. In this case, the inhibition of GABAergic CB1 receptors can yield in a "temporary" decrease in excitation that results in impairment of LTP induction.

The discussion above suggests two possible ways in which cannabinoids can modulate LTP induction: (1) via CB1 receptors on GABAergic pre-synaptic neurones. (2) via CB1 receptors on astrocytes. However, there exists a third possible way in which cannabinoids can contribute to LTP induction: (3) via CB1 receptors on glutamatergic pre-synaptic neurones. Activation of these CB1 receptors can result in decrease in release of glutamate from pre-synaptic terminals. It has been shown that application of exogenous cannabinoids can decrease excitatory synaptic transmission. Application of 2 μM of synthetic cannabinoid agonist WIN55,212-2 can decrease evoked AMPA EPSC amplitude in slices from hippocampus and cortex (Schlicker and Kathmann, 2001, Kawamura *et al.*, 2006). In several studies it has been shown that application of exogenous cannabinoids can result in impairment of HFS-induced LTP (Collins *et al.*, 1995, Stella *et al.*, 1997, Misner and Sullivan, 1999). This has been attributed to the reduction in glutamate release as a result of activation of CB1 receptors. However, as was mentioned above, activation of CB1 receptors on GABAergic neurons and activation of CB1 receptors on astrocytes should result in enhancement of LTP. In fact, it has been shown that there is a significantly higher expression of CB1 receptors on GABAergic neurons than glutamatergic neurons (Katona *et al.*, 1999, Hill *et al.*, 2007). Therefore, one would expect an enhancement in LTP induction rather than impairment of LTP. If this is the case, then why do most studies show impairment?

The synthetic CB1 receptor agonist WIN55212-2 can inhibit IPSCs at low concentrations (EC_{50} of 0.24 μM) whilst it can inhibit EPSCs at higher concentrations (EC_{50} of 2.01 μM) in the CA1 region of the hippocampus (Hajos

et al., 2001). The latter outcome has been attributed to TRPV1 channels. It has been shown that exogenous cannabinoids are involved in activation of Transient receptor potential vanilloid type 1 (TRPV1) channels. Activation of TRPV1 channels can lead to LTD by resulting in internalisation of posy-synaptic AMPA receptors (Chavez *et al.*, 2010). Therefore, it seems that at lower concentrations of CB1 agonists, mainly inhibitory synapses are inhibited because there are more CB1 receptors on GABAergic neurones. However, with increase in concentration of CB1 receptor agonists, excitatory neurones also show depression, mainly through activation of TRPV1 channels by cannbinoids. This could explain why in this PhD project, application of 5 μM of AEA to WT cortical slices resulted in depression of fEPSPs whilst application of 500 nM of AEA resulted in increase in fEPSP (Figure 5.6). The depression in fEPSP with 5 μM of AEA is probably due to TRPV1 channels. The increase in fEPSP with 500 nM of AEA is either due to activation of CB1 receptors on astrocytes or due to activation of CB1 receptors on GABAergic pre-synaptic neurones. However, application of 500 nM of AEA to cortical slices from dnSNARE mice resulted in depression of fEPSP, suggesting that the increase in fEPSP in WT mice is due to CB1 receptors on astrocytes.

Another area of endocannabinoid research open for future investigations involves the research in different roles for the two different eCBs. It is not known why neurones release two types of eCBs. It has been shown that anandamide and 2-AG induce different physiological effects *in vivo* (Alger and Kim, 2011) but how neurones utilise these two different eCBs differently to induce these effects is not

known. Future studies should investigate whether endogenous AEA and 2-AG have different effects on different LTP/LTD protocols.

In a recent finding it was shown that *in vivo* application of exogenous cannabinoids resulted in LTD of excitatory transmission in CA1 region of hippocampus (Han *et al.*, 2012). They showed that this LTD was due to decrease in AMPAR activity. As mentioned above, previous studies had suggested that this decrease in AMPAR activity is due to decrease in release of glutamate from excitatory pre-synaptic neurones as a result of activation of CB1 receptors on these cells. However, this study, by using specific neuronal and astrocytic CB1 receptor knockout mice, showed that the LTD was dependent on astrocytic CB1 receptors and not on neuronal CB1 receptors. They showed that activation of CB1 receptors on astrocytes could result in glutamate release from these cells. They showed that the glutamate released from astrocytes could activate post-synaptic NMDARs, which in turn lead to AMPAR endocytosis and LTD. It is possible that the AMPAR endocytosis observed in this report is due to activity of TRPV1 channels and not NMDAR channels. The authors did not investigate this possibility. Nonetheless, the importance of this report is the finding that astrocytes can release glutamate on post-synaptic NMDARs. For future investigations, these mice can be used to distinguish between the effect of astrocytic CB1 receptors and neuronal CB1 receptors.

In this PhD project, the effect of AEA application on NMDAR activity in the somatosensory cortex was also investigated. It was shown that application of AEA could indeed increase NMDAR activity (Figure 5.7). However, more

experiments are required to show that this increase in NMDAR activity is as a result of vesicular exocytosis from astrocytes. For this purpose, cortical slices from dnSNARE mice should be used. Furthermore, evidence should be provided showing that the release of glutamate from astrocytes is dependent on activation of CB1 receptors on these cells. For this purpose, AM251 can be applied during recordings of NMDAR eEPSCs. However, to provide stronger support that the release of glutamate from astrocytes are due to astrocytic CB1 receptors, the above-mentioned transgenic mice line where CB1 receptors are specifically knocked out in astrocytes should be used.

To summarise the above discussion, endocannabinoids can modulate synaptic transmission and plasticity with the following 5 mechanisms:

(1) By acting on CB1 receptors on presynaptic glutamatergic neurones, eCBs can decrease synaptic transmission (Figure 6.2: steps 1-4), thereby contributing to LTD induction or impairment of LTP induction of excitatory transmission.

(2) Activation of CB1 receptors on astrocytes can result in release of glutamate from these cells. The released glutamate can activate NMDARs on pre-synaptic neurones, leading to decrease in release of glutamate from neurones via an unknown mechanism (Figure 6.2: steps 5-9). The decrease in glutamate release results in depression of synaptic transmission (Min and Nevian, 2012).

(3) Activation of TRPV1 channels by cannabinoids can result in AMPAR endocytosis leading to LTD (Figure 6.2: steps 10-11).

(4) Cannabinoids can inhibit GABAergic transmission by activating CB1 receptors on pre-synaptic neurones (Figure 6.2: steps 12-13). This leads to increase in excitation, which can result in modulation of LTP.

(5) Cannabinoids can increase release of gliotransmitters from astrocytes by acting on CB1 receptors on these cells. Release of transmitters such as glutamate and ATP onto post-synaptic receptors can increase excitability and LTP (Figure 6.2: steps 14-16).

Results from previous studies show evidence for mechanisms (1) to (4). The importance of the research in this PhD project is that it shows that mechanism (5) should also be considered when investigating role for endocannabinoid signalling.

It is believed that smoking cannabis impairs learning and memory by acting on CB1 receptors (Kano *et al.*, 2009). How do exogenous cannabinoids impair memory by acting on CB1 receptors? i.e. how do mechanisms (1) to (5) result in impairment of memory?

Depression of synaptic transmission refers to changes that lead to weakening of synaptic transmission, whilst potentiation refers to changes that lead to strengthening of synaptic transmission. It is the general consensus that LTP is associated with formation of memory whilst LTD is associated with impairment of memory. This reasoning comes from pioneering observations that

manipulations that block LTP also significantly impair performances in learning and memory related tasks (Martin *et al.*, 2000). This suggests that when potentiation of synaptic transmission and plasticity is observed, it is associated with enhancement of memory; whilst when depression is observed, it is associated with impairment of memory. If this reasoning is to be accepted then it suggests that mechanisms (1) to (4) result in impairment of learning and memory because the outcome of all these mechanisms is decrease in release of transmitters and hence depression of synaptic transmission. This implies that mechanism (5), which results in increase in transmission, cannot be associated with cannabinoid-induced impairment of memory, thereby suggesting that mechanisms (1) to (4) might be the more likely mechanisms for explaining the reason for impairment of memory following intake of exogenous cannabinoids. However, just because research shows that blocking of LTP results in impairment of memory does not necessarily mean that potentiation can be linearly associated with memory formation or that depression can be linearly associated with memory impairment. This is actually a misunderstanding. In fact it is has been suggested that both potentiation and depression of synaptic transmission are required for formation of new memories. It has been suggested that "correct processing of memory-related information should be dependent on defining the salience of information to be encoded, a process that requires not only potentiation of synaptic strength but also depression" (Costenla *et al.*, 2010). I believe this misunderstanding is the reason as to why there has been no investigation of an **increase** in excitation following the action of endogenous or exogenous cannabinoids. To my knowledge this PhD project provides the first evidence for such an effect. This reasoning should be kept in mind not just for

research in role of cannabinoids in synaptic transmission and plasticity, but for all research that associates *in vitro* and *in vivo* synaptic plasticity with learning and memory tasks.

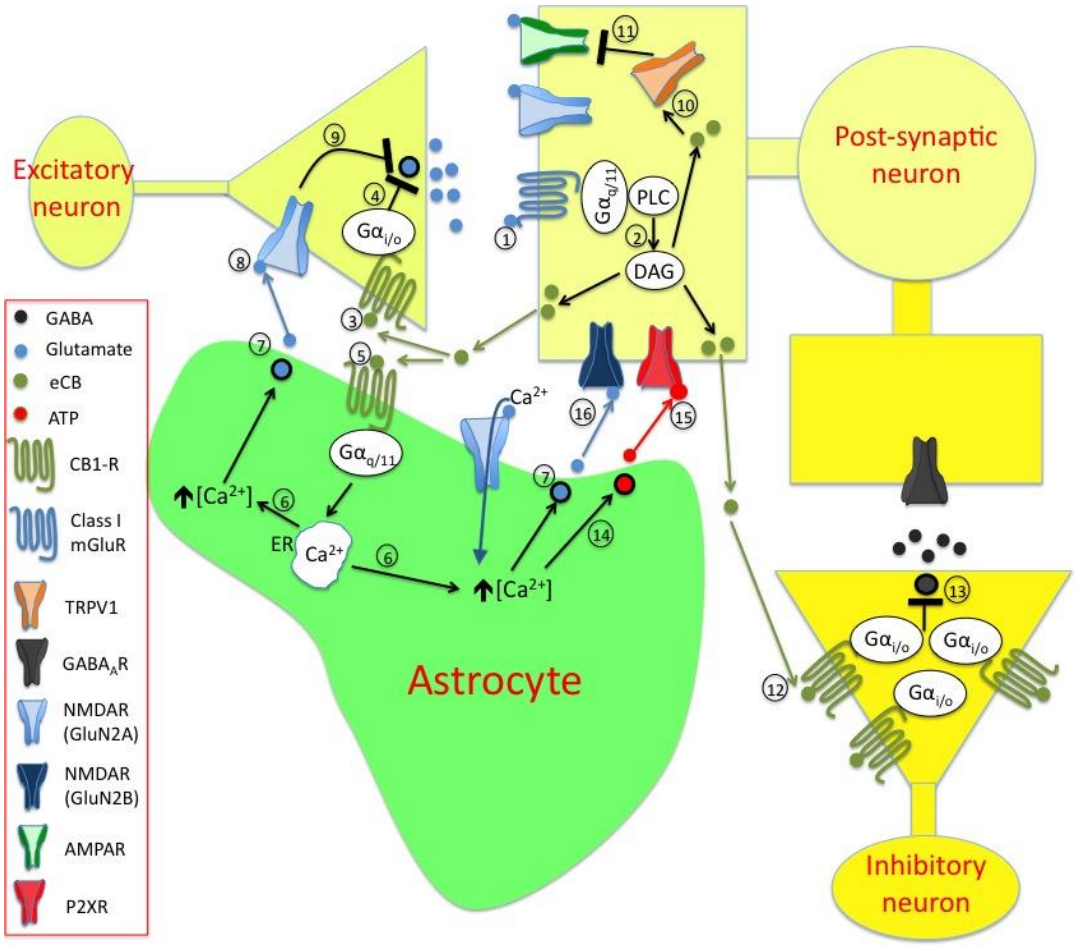

Figure 6.2. Endocannabinoids can modulate synaptic transmission by different mechanisms. Mechanism (1): Activation of class I mGluRs (1) leads to PLC-mediated synthesis of eCBs (2). eCBS can then diffuse to pre-synaptic glutamatergic neurones where they activate pre-synaptic CB1 receptors (3). Pre-synaptic CB1 receptors are coupled to $G\alpha_{i/o}$, therefore their activation leads to inhibition of glutamate release (4). **Mechanism (2):** eCBs can also activate CB1 receptors on astrocytes (5). In contrast to neuronal CB1 receptors, astrocytic CB1 receptors are coupled to $G\alpha_{q/11}$. Activation of astrocytic CB1 receptors leads to calcium elevation in these cells (6). This results in glutamate release from astrocytes (7), which can bind to pre-synaptic NMDARs (8). This leads to decrease in glutamate release via an unknown mechanism (9). **Mechanism (3):** eCBs like AEA can also remain intracellularly where they can activate TRPV1 channels (10). Activation of TRPV1 channels can result in endocytosis of AMPARs via activation of calcineurin (11). **Mechanism (4):** Released eCBs can also diffuse to pre-synaptic GABAergic neurones where they can activate CB1 receptors on these cells (12). This leads to inhibition of GABA release (13). **Mechanism (5):** Activation of CB1 receptors on astrocytes (5) can result in calcium dependent vesicular release of ATP from astrocytes (14). The released ATP can then activate P2XRs in neurones (15). Glutamate release from astrocytes can activate GluN2B-containing NMDARs on post-synaptic sites (16).

6.5. Conclusion

The primary role of astrocyte is to isolate individual synapses so that neurotransmitter release from one synapse does not spillover into another synapse i.e. glutamate spilled over from synaptic transmission is transported into the astrocytes. This isolation of synaptic transmission allows for precise spatial and temporal information processing (Nedergaard and Verkhratsky, 2012). However, as was shown in this PhD project, another function of astrocytes is to release gliotransmitters onto extra-synaptic sites. This suggests that astrocytic gliotransmitters modulate synaptic transmission not by directly effecting synaptic transmission by specific local gliotransmitter release but by exerting a less specific control by release onto extra-synaptic sites. This means that astrocytes can allow for rapid and precise synaptic transmission by isolating synapses and at the same time modulate synaptic transmission by releasing gliotransmitters onto less specific extra-synaptic sites.

This project provides evidence for calcium dependent vesicular exocytosis of glutamate, ATP and D-serine from astrocytes. This direct evidence is in the form of electrophysiological recordings. However, as was mentioned in the first chapter, vesicular exocytosis from neurones requires the presence of certain proteins involved in the exocytosis mechanism. The presence of only some of the proteins involved in exocytosis has been shown in astrocytes. These are VGLUT1/2, VAMP2 and VAMP3 (Bezzi *et al.*, 2004, Martineau *et al.*, 2013). If, as the results in this project show, astrocytes are capable of calcium-dependent vesicular exocytosis, then the presence of all the proteins involved in exocytosis

must be shown in astrocytes. Therefore, in future investigations, attempts should be made to provide evidence for other proteins involved in exocytosis in astrocytes. If future investigations fail to provide such evidence, then it is possible that in dnSNARE mice, the expression of cytosolic portion of VAMP2 specifically in astrocytes is affecting other release mechanisms that are non-exocytotic. If this were the case, then it is possible that vesicular exocytosis does not occur in astrocytes. However, even if this possibility was the case, it is clear that the results in this project show that gliotransmitters are released from slice preparation via calcium-dependent mechanism.

References

Aguado, F., Espinosa-Parrilla, J. F., Carmona, M. A. and Soriano, E. (2002). Neuronal activity regulates correlated network properties of spontaneous calcium transients in astrocytes in situ. *J Neurosci.* **22**(21), 9430-9444.

Agulhon, C., Boyt, K. M., Xie, A. X., Friocourt, F., Roth, B. L. and McCarthy, K. D. (2013). Modulation of the autonomic nervous system and behaviour by acute glial cell Gq protein-coupled receptor activation in vivo. *J Physiol.* **591**(Pt 22), 5599-5609.

Agulhon, C., Fiacco, T. A. and McCarthy, K. D. (2010). Hippocampal short- and long-term plasticity are not modulated by astrocyte Ca2+ signaling. *Science.* **327**(5970), 1250-1254.

Agulhon, C., Petravicz, J., McMullen, A. B., Sweger, E. J., Minton, S. K., Taves, S. R., Casper, K. B., Fiacco, T. A. and McCarthy, K. D. (2008). What is the role of astrocyte calcium in neurophysiology? *Neuron.* **59**(6), 932-946.

Alger, B. E. (2002). Retrograde signaling in the regulation of synaptic transmission: focus on endocannabinoids. *Prog Neurobiol.* **68**(4), 247-286.

Alger, B. E. and Kim, J. (2011). Supply and demand for endocannabinoids. *Trends Neurosci.* **34**(6), 304-315.

Amzica, F. and Neckelmann, D. (1999). Membrane capacitance of cortical neurons and glia during sleep oscillations and spike-wave seizures. *J Neurophysiol.* **82**(5), 2731-2746.

Andersen, P. (1980). Participating neurones and mechanisms underlying theta activity in unanaesthetized rabbits. *Prog Brain Res.* **54**, 371-380.

Andrienzen, W. (1893). On a system of fibre-like cells surrounding the blood vessels of the brain of man and mammals and its physiological significance. *Int Monatsschr Anat Physiol.* **10**, 532-540.

Arai, T., Miklossy, J., Klegeris, A., Guo, J. P. and McGeer, P. L. (2006). Thrombin and prothrombin are expressed by neurons and glial cells and accumulate in neurofibrillary tangles in Alzheimer disease brain. *J Neuropathol Exp Neurol.* **65**(1), 19-25.

Araque, A., Li, N., Doyle, R. T. and Haydon, P. G. (2000). SNARE protein-dependent glutamate release from astrocytes. *J Neurosci.* **20**(2), 666-673.

Araque, A., Parpura, V., Sanzgiri, R. P. and Haydon, P. G. (1999). Tripartite synapses: glia, the unacknowledged partner. *Trends Neurosci.* **22**(5), 208-215.

Araque, A., Sanzgiri, R. P., Parpura, V. and Haydon, P. G. (1998). Calcium elevation in astrocytes causes an NMDA receptor-dependent increase in the frequency of miniature synaptic currents in cultured hippocampal neurons. *J Neurosci.* **18**(17), 6822-6829.

Artola, A. and Singer, W. (1993). Long-term depression of excitatory synaptic transmission and its relationship to long-term potentiation. *Trends Neurosci.* **16**(11), 480-487.

Auclair, N., Otani, S., Soubrie, P. and Crepel, F. (2000). Cannabinoids modulate synaptic strength and plasticity at glutamatergic synapses of rat prefrontal cortex pyramidal neurons. *J Neurophysiol.* **83**(6), 3287-3293.

Ayalon, G. and Stern-Bach, Y. (2001). Functional assembly of AMPA and kainate receptors is mediated by several discrete protein-protein interactions. *Neuron.* **31**(1), 103-113.
Bai, D., Zhu, G., Pennefather, P., Jackson, M. F., MacDonald, J. F. and Orser, B. A. (2001). Distinct functional and pharmacological properties of tonic and quantal inhibitory postsynaptic currents mediated by gamma-aminobutyric acid(A) receptors in hippocampal neurons. *Mol Pharmacol.* **59**(4), 814-824.
Banke, T. G. and Traynelis, S. F. (2003). Activation of NR1/NR2B NMDA receptors. *Nat Neurosci.* **6**(2), 144-152.
Barria, A., Muller, D., Derkach, V., Griffith, L. C. and Soderling, T. R. (1997). Regulatory phosphorylation of AMPA-type glutamate receptors by CaM-KII during long-term potentiation. *Science.* **276**(5321), 2042-2045.
Baude, A., Nusser, Z., Roberts, J. D., Mulvihill, E., McIlhinney, R. A. and Somogyi, P. (1993). The metabotropic glutamate receptor (mGluR1 alpha) is concentrated at perisynaptic membrane of neuronal subpopulations as detected by immunogold reaction. *Neuron.* **11**(4), 771-787.
Baxter, A. W., Choi, S. J., Sim, J. A. and North, R. A. (2011). Role of P2X4 receptors in synaptic strengthening in mouse CA1 hippocampal neurons. *Eur J Neurosci.* **34**(2), 213-220.
Bayer, K. U., De Koninck, P., Leonard, A. S., Hell, J. W. and Schulman, H. (2001). Interaction with the NMDA receptor locks CaMKII in an active conformation. *Nature.* **411**(6839), 801-805.
Bergeron, R., Meyer, T. M., Coyle, J. T. and Greene, R. W. (1998). Modulation of N-methyl-D-aspartate receptor function by glycine transport. *Proc Natl Acad Sci U S A.* **95**(26), 15730-15734.
Bergersen, L. H., Morland, C., Ormel, L., Rinholm, J. E., Larsson, M., Wold, J. F., Roe, A. T., Stranna, A., Santello, M., Bouvier, D., Ottersen, O. P., Volterra, A. and Gundersen, V. (2012). Immunogold detection of L-glutamate and D-serine in small synaptic-like microvesicles in adult hippocampal astrocytes. *Cereb Cortex.* **22**(7), 1690-1697.
Bergles, D. E. and Jahr, C. E. (1998). Glial contribution to glutamate uptake at Schaffer collateral-commissural synapses in the hippocampus. *J Neurosci.* **18**(19), 7709-7716.
Bezzi, P., Gundersen, V., Galbete, J. L., Seifert, G., Steinhauser, C., Pilati, E. and Volterra, A. (2004). Astrocytes contain a vesicular compartment that is competent for regulated exocytosis of glutamate. *Nat Neurosci.* **7**(6), 613-620.
Bienenstock, E. L., Cooper, L. N. and Munro, P. W. (1982). Theory for the development of neuron selectivity: orientation specificity and binocular interaction in visual cortex. *J Neurosci.* **2**(1), 32-48.
Bisogno, T., Howell, F., Williams, G., Minassi, A., Cascio, M. G., Ligresti, A., Matias, I., Schiano-Moriello, A., Paul, P., Williams, E. J., Gangadharan, U., Hobbs, C., Di Marzo, V. and Doherty, P. (2003). Cloning of the first sn1-DAG lipases points to the spatial and temporal regulation of endocannabinoid signaling in the brain. *J Cell Biol.* **163**(3), 463-468.
Bliss, T. V. and Lomo, T. (1973). Long-lasting potentiation of synaptic transmission in the dentate area of the anaesthetized rabbit following stimulation of the perforant path. *J Physiol.* **232**(2), 331-356.

Borden, L. A., Smith, K. E., Hartig, P. R., Branchek, T. A. and Weinshank, R. L. (1992). Molecular heterogeneity of the gamma-aminobutyric acid (GABA) transport system. Cloning of two novel high affinity GABA transporters from rat brain. *J Biol Chem.* **267**(29), 21098-21104.
Bramham, C. R., Torp, R., Zhang, N., Storm-Mathisen, J. and Ottersen, O. P. (1990). Distribution of glutamate-like immunoreactivity in excitatory hippocampal pathways: a semiquantitative electron microscopic study in rats. *Neuroscience.* **39**(2), 405-417.
Brandon, N. J., Delmas, P., Kittler, J. T., McDonald, B. J., Sieghart, W., Brown, D. A., Smart, T. G. and Moss, S. J. (2000). GABAA receptor phosphorylation and functional modulation in cortical neurons by a protein kinase C-dependent pathway. *J Biol Chem.* **275**(49), 38856-38862.
Brunig, I., Scotti, E., Sidler, C. and Fritschy, J. M. (2002). Intact sorting, targeting, and clustering of gamma-aminobutyric acid A receptor subtypes in hippocampal neurons in vitro. *J Comp Neurol.* **443**(1), 43-55.
Burnashev, N. (1996). Calcium permeability of glutamate-gated channels in the central nervous system. *Curr Opin Neurobiol.* **6**(3), 311-317.
Burnstock, G. (1972). Purinergic nerves. *Pharmacol Rev.* **24**(3), 509-581.
Bushong, E. A., Martone, M. E., Jones, Y. Z. and Ellisman, M. H. (2002). Protoplasmic astrocytes in CA1 stratum radiatum occupy separate anatomical domains. *J Neurosci.* **22**(1), 183-192.
Buzsaki, G. (1986). Hippocampal sharp waves: their origin and significance. *Brain Res.* **398**(2), 242-252.
Cahoy, J. D., Emery, B., Kaushal, A., Foo, L. C., Zamanian, J. L., Christopherson, K. S., Xing, Y., Lubischer, J. L., Krieg, P. A., Krupenko, S. A., Thompson, W. J. and Barres, B. A. (2008). A transcriptome database for astrocytes, neurons, and oligodendrocytes: a new resource for understanding brain development and function. *J Neurosci.* **28**(1), 264-278.
Cai, Z., Schools, G. P. and Kimelberg, H. K. (2000). Metabotropic glutamate receptors in acutely isolated hippocampal astrocytes: developmental changes of mGluR5 mRNA and functional expression. *Glia.* **29**(1), 70-80.
Caraiscos, V. B., Elliott, E. M., You-Ten, K. E., Cheng, V. Y., Belelli, D., Newell, J. G., Jackson, M. F., Lambert, J. J., Rosahl, T. W., Wafford, K. A., MacDonald, J. F. and Orser, B. A. (2004). Tonic inhibition in mouse hippocampal CA1 pyramidal neurons is mediated by alpha5 subunit-containing gamma-aminobutyric acid type A receptors. *Proc Natl Acad Sci U S A.* **101**(10), 3662-3667.
Carlson, G., Wang, Y. and Alger, B. E. (2002). Endocannabinoids facilitate the induction of LTP in the hippocampus. *Nat Neurosci.* **5**(8), 723-724.
Castro-Alamancos, M. A., Donoghue, J. P. and Connors, B. W. (1995). Different forms of synaptic plasticity in somatosensory and motor areas of the neocortex. *J Neurosci.* **15**(7 Pt 2), 5324-5333.
Chavez, A. E., Chiu, C. Q. and Castillo, P. E. (2010). TRPV1 activation by endogenous anandamide triggers postsynaptic long-term depression in dentate gyrus. *Nat Neurosci.* **13**(12), 1511-1518.
Chen, N. H., Reith, M. E. and Quick, M. W. (2004). Synaptic uptake and beyond: the sodium- and chloride-dependent neurotransmitter transporter family SLC6. *Pflugers Arch.* **447**(5), 519-531.

Chen, X., Wang, L., Zhou, Y., Zheng, L. H. and Zhou, Z. (2005). "Kiss-and-run" glutamate secretion in cultured and freshly isolated rat hippocampal astrocytes. *J Neurosci.* **25**(40), 9236-9243.
Chevaleyre, V. and Castillo, P. E. (2003). Heterosynaptic LTD of hippocampal GABAergic synapses: a novel role of endocannabinoids in regulating excitability. *Neuron.* **38**(3), 461-472.
Chevaleyre, V. and Castillo, P. E. (2004). Endocannabinoid-mediated metaplasticity in the hippocampus. *Neuron.* **43**(6), 871-881.
Chevaleyre, V., Takahashi, K. A. and Castillo, P. E. (2006). Endocannabinoid-mediated synaptic plasticity in the CNS. *Annu Rev Neurosci.* **29**, 37-76.
Clayton, D. A., Mesches, M. H., Alvarez, E., Bickford, P. C. and Browning, M. D. (2002). A hippocampal NR2B deficit can mimic age-related changes in long-term potentiation and spatial learning in the Fischer 344 rat. *J Neurosci.* **22**(9), 3628-3637.
Cobb, S. R., Buhl, E. H., Halasy, K., Paulsen, O. and Somogyi, P. (1995). Synchronization of neuronal activity in hippocampus by individual GABAergic interneurons. *Nature.* **378**(6552), 75-78.
Coco, S., Calegari, F., Pravettoni, E., Pozzi, D., Taverna, E., Rosa, P., Matteoli, M. and Verderio, C. (2003). Storage and release of ATP from astrocytes in culture. *J Biol Chem.* **278**(2), 1354-1362.
Collins, D. R., Pertwee, R. G. and Davies, S. N. (1995). Prevention by the cannabinoid antagonist, SR141716A, of cannabinoid-mediated blockade of long-term potentiation in the rat hippocampal slice. *Br J Pharmacol.* **115**(6), 869-870.
Colquhoun, D., Jonas, P. and Sakmann, B. (1992). Action of brief pulses of glutamate on AMPA/kainate receptors in patches from different neurones of rat hippocampal slices. *J Physiol.* **458**, 261-287.
Contreras, J. E., Sanchez, H. A., Eugenin, E. A., Speidel, D., Theis, M., Willecke, K., Bukauskas, F. F., Bennett, M. V. and Saez, J. C. (2002). Metabolic inhibition induces opening of unapposed connexin 43 gap junction hemichannels and reduces gap junctional communication in cortical astrocytes in culture. *Proc Natl Acad Sci U S A.* **99**(1), 495-500.
Cornell-Bell, A. H., Finkbeiner, S. M., Cooper, M. S. and Smith, S. J. (1990). Glutamate induces calcium waves in cultured astrocytes: long-range glial signaling. *Science.* **247**(4941), 470-473.
Costenla, A. R., Cunha, R. A. and de Mendonca, A. (2010). Caffeine, adenosine receptors, and synaptic plasticity. *J Alzheimers Dis.* **20 Suppl 1**, S25-34.
Cotrina, M. L., Lin, J. H., Alves-Rodrigues, A., Liu, S., Li, J., Azmi-Ghadimi, H., Kang, J., Naus, C. C. and Nedergaard, M. (1998). Connexins regulate calcium signaling by controlling ATP release. *Proc Natl Acad Sci U S A.* **95**(26), 15735-15740.
Coughlin, S. R. (1994). Protease-activated receptors start a family. *Proc Natl Acad Sci U S A.* **91**(20), 9200-9202.
Crepel, V., Panenka, W., Kelly, M. E. and MacVicar, B. A. (1998). Mitogen-activated protein and tyrosine kinases in the activation of astrocyte volume-activated chloride current. *J Neurosci.* **18**(4), 1196-1206.

Cubelos, B., Gimenez, C. and Zafra, F. (2005). Localization of the GLYT1 glycine transporter at glutamatergic synapses in the rat brain. *Cereb Cortex.* **15**(4), 448-459.
D'Antoni, S., Berretta, A., Bonaccorso, C. M., Bruno, V., Aronica, E., Nicoletti, F. and Catania, M. V. (2008). Metabotropic glutamate receptors in glial cells. *Neurochem Res.* **33**(12), 2436-2443.
Dalby, N. O. and Mody, I. (2003). Activation of NMDA receptors in rat dentate gyrus granule cells by spontaneous and evoked transmitter release. *J Neurophysiol.* **90**(2), 786-797.
Davies, C. H., Davies, S. N. and Collingridge, G. L. (1990). Paired-pulse depression of monosynaptic GABA-mediated inhibitory postsynaptic responses in rat hippocampus. *J Physiol.* **424**, 513-531.
Davies, C. H., Starkey, S. J., Pozza, M. F. and Collingridge, G. L. (1991). GABA autoreceptors regulate the induction of LTP. *Nature.* **349**(6310), 609-611.
Dawson, G. R., Maubach, K. A., Collinson, N., Cobain, M., Everitt, B. J., MacLeod, A. M., Choudhury, H. I., McDonald, L. M., Pillai, G., Rycroft, W., Smith, A. J., Sternfeld, F., Tattersall, F. D., Wafford, K. A., Reynolds, D. S., Seabrook, G. R. and Atack, J. R. (2006). An inverse agonist selective for alpha5 subunit-containing GABAA receptors enhances cognition. *J Pharmacol Exp Ther.* **316**(3), 1335-1345.
de Oliveira Alvares, L., Genro, B. P., Vaz Breda, R., Pedroso, M. F., Da Costa, J. C. and Quillfeldt, J. A. (2006). AM251, a selective antagonist of the CB1 receptor, inhibits the induction of long-term potentiation and induces retrograde amnesia in rats. *Brain Res.* **1075**(1), 60-67.
Deng, Q., Terunuma, M., Fellin, T., Moss, S. J. and Haydon, P. G. (2011). Astrocytic activation of A1 receptors regulates the surface expression of NMDA receptors through a Src kinase dependent pathway. *Glia.* **59**(7), 1084-1093.
Devane, W. A., Hanus, L., Breuer, A., Pertwee, R. G., Stevenson, L. A., Griffin, G., Gibson, D., Mandelbaum, A., Etinger, A. and Mechoulam, R. (1992). Isolation and structure of a brain constituent that binds to the cannabinoid receptor. *Science.* **258**(5090), 1946-1949.
Dingledine, R., Borges, K., Bowie, D. and Traynelis, S. F. (1999). The glutamate receptor ion channels. *Pharmacol Rev.* **51**(1), 7-61.
Dudek, S. M. and Bear, M. F. (1992). Homosynaptic long-term depression in area CA1 of hippocampus and effects of N-methyl-D-aspartate receptor blockade. *Proc Natl Acad Sci U S A.* **89**(10), 4363-4367.
Dunwiddie, T. V., Diao, L. and Proctor, W. R. (1997). Adenine nucleotides undergo rapid, quantitative conversion to adenosine in the extracellular space in rat hippocampus. *J Neurosci.* **17**(20), 7673-7682.
Dunwiddie, T. V. and Hoffer, B. J. (1980). Adenine nucleotides and synaptic transmission in the in vitro rat hippocampus. *Br J Pharmacol.* **69**(1), 59-68.
Edwards, F. A., Konnerth, A. and Sakmann, B. (1990). Quantal analysis of inhibitory synaptic transmission in the dentate gyrus of rat hippocampal slices: a patch-clamp study. *J Physiol.* **430**, 213-249.
Egan, T. M., Samways, D. S. and Li, Z. (2006). Biophysics of P2X receptors. *Pflugers Arch.* **452**(5), 501-512.

Ehmsen, J. T., Ma, T. M., Sason, H., Rosenberg, D., Ogo, T., Furuya, S., Snyder, S. H. and Wolosker, H. (2013). D-serine in glia and neurons derives from 3-phosphoglycerate dehydrogenase. *J Neurosci.* **33**(30), 12464-12469.
Eichenbaum, H. (2000). A cortical-hippocampal system for declarative memory. *Nat Rev Neurosci.* **1**(1), 41-50.
Erb, L., Liao, Z., Seye, C. I. and Weisman, G. A. (2006). P2 receptors: intracellular signaling. *Pflugers Arch.* **452**(5), 552-562.
Erisir, A. and Harris, J. L. (2003). Decline of the critical period of visual plasticity is concurrent with the reduction of NR2B subunit of the synaptic NMDA receptor in layer 4. *J Neurosci.* **23**(12), 5208-5218.
Erreger, K., Dravid, S. M., Banke, T. G., Wyllie, D. J. and Traynelis, S. F. (2005). Subunit-specific gating controls rat NR1/NR2A and NR1/NR2B NMDA channel kinetics and synaptic signalling profiles. *J Physiol.* **563**(Pt 2), 345-358.
Fastbom, J., Pazos, A. and Palacios, J. M. (1987). The distribution of adenosine A1 receptors and 5'-nucleotidase in the brain of some commonly used experimental animals. *Neuroscience.* **22**(3), 813-826.
Fellin, T., Halassa, M. M., Terunuma, M., Succol, F., Takano, H., Frank, M., Moss, S. J. and Haydon, P. G. (2009). Endogenous nonneuronal modulators of synaptic transmission control cortical slow oscillations in vivo. *Proc Natl Acad Sci U S A.* **106**(35), 15037-15042.
Fellin, T., Pascual, O., Gobbo, S., Pozzan, T., Haydon, P. G. and Carmignoto, G. (2004). Neuronal synchrony mediated by astrocytic glutamate through activation of extrasynaptic NMDA receptors. *Neuron.* **43**(5), 729-743.
Fiacco, T. A., Agulhon, C. and McCarthy, K. D. (2009). Sorting out astrocyte physiology from pharmacology. *Annu Rev Pharmacol Toxicol.* **49**, 151-174.
Fossat, P., Turpin, F. R., Sacchi, S., Dulong, J., Shi, T., Rivet, J. M., Sweedler, J. V., Pollegioni, L., Millan, M. J., Oliet, S. H. and Mothet, J. P. (2011). Glial D-Serine Gates NMDA Receptors at Excitatory Synapses in Prefrontal Cortex. *Cereb Cortex.*
Frenguelli, B. G., Potier, B., Slater, N. T., Alford, S. and Collingridge, G. L. (1993). Metabotropic glutamate receptors and calcium signalling in dendrites of hippocampal CA1 neurones. *Neuropharmacology.* **32**(11), 1229-1237.
Fujii, S. (2004). ATP- and adenosine-mediated signaling in the central nervous system: the role of extracellular ATP in hippocampal long-term potentiation. *J Pharmacol Sci.* **94**(2), 103-106.
Furukawa, H., Singh, S. K., Mancusso, R. and Gouaux, E. (2005). Subunit arrangement and function in NMDA receptors. *Nature.* **438**(7065), 185-192.
Gao, Y., Vasilyev, D. V., Goncalves, M. B., Howell, F. V., Hobbs, C., Reisenberg, M., Shen, R., Zhang, M. Y., Strassle, B. W., Lu, P., Mark, L., Piesla, M. J., Deng, K., Kouranova, E. V., Ring, R. H., Whiteside, G. T., Bates, B., Walsh, F. S., Williams, G., Pangalos, M. N., Samad, T. A. and Doherty, P. (2010). Loss of retrograde endocannabinoid signaling and reduced adult neurogenesis in diacylglycerol lipase knock-out mice. *J Neurosci.* **30**(6), 2017-2024.

Golgi, C. (1885). Sulla fina anatomia degli organi centrali del sistema nervoso. *riv sper fremiat med leg alienazioni ment* **11**, 72-123.
Gordon, G. R., Baimoukhametova, D. V., Hewitt, S. A., Rajapaksha, W. R., Fisher, T. E. and Bains, J. S. (2005). Norepinephrine triggers release of glial ATP to increase postsynaptic efficacy. *Nat Neurosci.* **8**(8), 1078-1086.
Goutagny, R., Jackson, J. and Williams, S. (2009). Self-generated theta oscillations in the hippocampus. *Nat Neurosci.* **12**(12), 1491-1493.
Green, J. D. and Arduini, A. A. (1954). Hippocampal electrical activity in arousal. *J Neurophysiol.* **17**(6), 533-557.
Groc, L., Heine, M., Cognet, L., Brickley, K., Stephenson, F. A., Lounis, B. and Choquet, D. (2004). Differential activity-dependent regulation of the lateral mobilities of AMPA and NMDA receptors. *Nat Neurosci.* **7**(7), 695-696.
Groc, L., Heine, M., Cousins, S. L., Stephenson, F. A., Lounis, B., Cognet, L. and Choquet, D. (2006). NMDA receptor surface mobility depends on NR2A-2B subunits. *Proc Natl Acad Sci U S A.* **103**(49), 18769-18774.
Guastella, J., Nelson, N., Nelson, H., Czyzyk, L., Keynan, S., Miedel, M. C., Davidson, N., Lester, H. A. and Kanner, B. I. (1990). Cloning and expression of a rat brain GABA transporter. *Science.* **249**(4974), 1303-1306.
Hajos, N., Ledent, C. and Freund, T. F. (2001). Novel cannabinoid-sensitive receptor mediates inhibition of glutamatergic synaptic transmission in the hippocampus. *Neuroscience.* **106**(1), 1-4.
Halassa, M. M., Fellin, T. and Haydon, P. G. (2007). The tripartite synapse: roles for gliotransmission in health and disease. *Trends Mol Med.* **13**(2), 54-63.
Hamilton, N., Vayro, S., Kirchhoff, F., Verkhratsky, A., Robbins, J., Gorecki, D. C. and Butt, A. M. (2008). Mechanisms of ATP- and glutamate-mediated calcium signaling in white matter astrocytes. *Glia.* **56**(7), 734-749.
Hamilton, N. B. and Attwell, D. (2010). Do astrocytes really exocytose neurotransmitters? *Nat Rev Neurosci.* **11**(4), 227-238.
Han, J., Kesner, P., Metna-Laurent, M., Duan, T., Xu, L., Georges, F., Koehl, M., Abrous, D. N., Mendizabal-Zubiaga, J., Grandes, P., Liu, Q., Bai, G., Wang, W., Xiong, L., Ren, W., Marsicano, G. and Zhang, X. (2012). Acute cannabinoids impair working memory through astroglial CB1 receptor modulation of hippocampal LTD. *Cell.* **148**(5), 1039-1050.
Hartlage-Rubsamen, M., Zeitschel, U., Apelt, J., Gartner, U., Franke, H., Stahl, T., Gunther, A., Schliebs, R., Penkowa, M., Bigl, V. and Rossner, S. (2003). Astrocytic expression of the Alzheimer's disease beta-secretase (BACE1) is stimulus-dependent. *Glia.* **41**(2), 169-179.
Hayashi, Y., Shi, S. H., Esteban, J. A., Piccini, A., Poncer, J. C. and Malinow, R. (2000). Driving AMPA receptors into synapses by LTP and CaMKII: requirement for GluR1 and PDZ domain interaction. *Science.* **287**(5461), 2262-2267.
Henneberger, C., Bard, L., King, C., Jennings, A. and Rusakov, D. A. (2013). NMDA receptor activation: two targets for two co-agonists. *Neurochem Res.* **38**(6), 1156-1162.
Henneberger, C., Papouin, T., Oliet, S. H. and Rusakov, D. A. (2010). Long-term potentiation depends on release of D-serine from astrocytes. *Nature.* **463**(7278), 232-236.

Herkenham, M., Lynn, A. B., Little, M. D., Johnson, M. R., Melvin, L. S., de Costa, B. R. and Rice, K. C. (1990). Cannabinoid receptor localization in brain. *Proc Natl Acad Sci U S A.* **87**(5), 1932-1936.
Hertz, L. and Zielke, H. R. (2004). Astrocytic control of glutamatergic activity: astrocytes as stars of the show. *Trends Neurosci.* **27**(12), 735-743.
Hill, E. L., Gallopin, T., Ferezou, I., Cauli, B., Rossier, J., Schweitzer, P. and Lambolez, B. (2007). Functional CB1 receptors are broadly expressed in neocortical GABAergic and glutamatergic neurons. *J Neurophysiol.* **97**(4), 2580-2589.
Hirase, H., Qian, L., Bartho, P. and Buzsaki, G. (2004). Calcium dynamics of cortical astrocytic networks in vivo. *PLoS Biol.* **2**(4), E96.
Hollenberg, M. D., Saifeddine, M., al-Ani, B. and Kawabata, A. (1997). Proteinase-activated receptors: structural requirements for activity, receptor cross-reactivity, and receptor selectivity of receptor-activating peptides. *Can J Physiol Pharmacol.* **75**(7), 832-841.
Hollmann, M. and Heinemann, S. (1994). Cloned glutamate receptors. *Annu Rev Neurosci.* **17**, 31-108.
Hua, Y. and Scheller, R. H. (2001). Three SNARE complexes cooperate to mediate membrane fusion. *Proc Natl Acad Sci U S A.* **98**(14), 8065-8070.
Huang, Y., Yasuda, H., Sarihi, A. and Tsumoto, T. (2008). Roles of endocannabinoids in heterosynaptic long-term depression of excitatory synaptic transmission in visual cortex of young mice. *J Neurosci.* **28**(28), 7074-7083.
Ievglevskyi, O., Palygin, O., Kondratskaya, E., Grebenyuk, S. and Krishtal, O. (2012). Modulation of ATP-induced LTP by cannabinoid receptors in rat hippocampus. *Purinergic Signal.* **8**(4), 705-713.
Illes, P. and Alexandre Ribeiro, J. (2004). Molecular physiology of P2 receptors in the central nervous system. *Eur J Pharmacol.* **483**(1), 5-17.
Jacob, W., Marsch, R., Marsicano, G., Lutz, B. and Wotjak, C. T. (2012). Cannabinoid CB1 receptor deficiency increases contextual fear memory under highly aversive conditions and long-term potentiation in vivo. *Neurobiol Learn Mem.* **98**(1), 47-55.
Jahn, R. and Scheller, R. H. (2006). SNAREs--engines for membrane fusion. *Nat Rev Mol Cell Biol.* **7**(9), 631-643.
Jourdain, P., Bergersen, L. H., Bhaukaurally, K., Bezzi, P., Santello, M., Domercq, M., Matute, C., Tonello, F., Gundersen, V. and Volterra, A. (2007). Glutamate exocytosis from astrocytes controls synaptic strength. *Nat Neurosci.* **10**(3), 331-339.
Junge, C. E., Lee, C. J., Hubbard, K. B., Zhang, Z., Olson, J. J., Hepler, J. R., Brat, D. J. and Traynelis, S. F. (2004). Protease-activated receptor-1 in human brain: localization and functional expression in astrocytes. *Exp Neurol.* **188**(1), 94-103.
Kang, N., Peng, H., Yu, Y., Stanton, P. K., Guilarte, T. R. and Kang, J. (2013). Astrocytes release D-serine by a large vesicle. *Neuroscience.* **240**, 243-257.
Kano, M., Ohno-Shosaku, T., Hashimotodani, Y., Uchigashima, M. and Watanabe, M. (2009). Endocannabinoid-mediated control of synaptic transmission. *Physiol Rev.* **89**(1), 309-380.

Kartvelishvily, E., Shleper, M., Balan, L., Dumin, E. and Wolosker, H. (2006). Neuron-derived D-serine release provides a novel means to activate N-methyl-D-aspartate receptors. *J Biol Chem.* **281**(20), 14151-14162.
Katona, I., Sperlagh, B., Sik, A., Kafalvi, A., Vizi, E. S., Mackie, K. and Freund, T. F. (1999). Presynaptically located CB1 cannabinoid receptors regulate GABA release from axon terminals of specific hippocampal interneurons. *J Neurosci.* **19**(11), 4544-4558.
Katsuki, H., Nonaka, M., Shirakawa, H., Kume, T. and Akaike, A. (2004). Endogenous D-serine is involved in induction of neuronal death by N-methyl-D-aspartate and simulated ischemia in rat cerebrocortical slices. *J Pharmacol Exp Ther.* **311**(2), 836-844.
Kawamura, Y., Fukaya, M., Maejima, T., Yoshida, T., Miura, E., Watanabe, M., Ohno-Shosaku, T. and Kano, M. (2006). The CB1 cannabinoid receptor is the major cannabinoid receptor at excitatory presynaptic sites in the hippocampus and cerebellum. *J Neurosci.* **26**(11), 2991-3001.
Khakh, B. S., Burnstock, G., Kennedy, C., King, B. F., North, R. A., Seguela, P., Voigt, M. and Humphrey, P. P. (2001). International union of pharmacology. XXIV. Current status of the nomenclature and properties of P2X receptors and their subunits. *Pharmacol Rev.* **53**(1), 107-118.
Khakh, B. S. and North, R. A. (2012). Neuromodulation by extracellular ATP and P2X receptors in the CNS. *Neuron.* **76**(1), 51-69.
Kim, J. and Alger, B. E. (2010). Reduction in endocannabinoid tone is a homeostatic mechanism for specific inhibitory synapses. *Nat Neurosci.* **13**(5), 592-600.
Kimelberg, H. K. (2004). Increased release of excitatory amino acids by the actions of ATP and peroxynitrite on volume-regulated anion channels (VRACs) in astrocytes. *Neurochem Int.* **45**(4), 511-519.
Kirkwood, A. and Bear, M. F. (1994). Hebbian synapses in visual cortex. *J Neurosci.* **14**(3 Pt 2), 1634-1645.
Kirkwood, A. and Bear, M. F. (1994). Homosynaptic long-term depression in the visual cortex. *J Neurosci.* **14**(5 Pt 2), 3404-3412.
Kirkwood, A., Dudek, S. M., Gold, J. T., Aizenman, C. D. and Bear, M. F. (1993). Common forms of synaptic plasticity in the hippocampus and neocortex in vitro. *Science.* **260**(5113), 1518-1521.
Komatsu, Y., Fujii, K., Maeda, J., Sakaguchi, H. and Toyama, K. (1988). Long-term potentiation of synaptic transmission in kitten visual cortex. *J Neurophysiol.* **59**(1), 124-141.
Lalo, U., Andrew, J., Palygin, O. and Pankratov, Y. (2009). Ca2+-dependent modulation of GABAA and NMDA receptors by extracellular ATP: implication for function of tripartite synapse. *Biochem Soc Trans.* **37**(Pt 6), 1407-1411.
Lalo, U., Palygin, O., Rasooli-Nejad, S., Andrew, J., Haydon, P. G. and Pankratov, Y. (2014). Exocytosis of ATP from astrocytes modulates phasic and tonic inhibition in the neocortex. *PLoS Biol.* **12**(1), e1001747.
Lalo, U., Pankratov, Y., Kirchhoff, F., North, R. A. and Verkhratsky, A. (2006). NMDA receptors mediate neuron-to-glia signaling in mouse cortical astrocytes. *J Neurosci.* **26**(10), 2673-2683.
Lalo, U., Pankratov, Y., Wichert, S. P., Rossner, M. J., North, R. A., Kirchhoff, F. and Verkhratsky, A. (2008). P2X1 and P2X5 subunits form

the functional P2X receptor in mouse cortical astrocytes. *J Neurosci.* **28**(21), 5473-5480.
Lalo, U., Rasooli-Nejad, S. and Pankratov, Y. (2014). Exocytosis of gliotransmitters from cortical astrocytes: implications for synaptic plasticity and ageing.
Lansman, J. B., Hess, P. and Tsien, R. W. (1986). Blockade of current through single calcium channels by Cd2+, Mg2+, and Ca2+. Voltage and concentration dependence of calcium entry into the pore. *J Gen Physiol.* **88**(3), 321-347.
Larson, J., Wong, D. and Lynch, G. (1986). Patterned stimulation at the theta frequency is optimal for the induction of hippocampal long-term potentiation. *Brain Res.* **368**(2), 347-350.
Le, K. T., Villeneuve, P., Ramjaun, A. R., McPherson, P. S., Beaudet, A. and Seguela, P. (1998). Sensory presynaptic and widespread somatodendritic immunolocalization of central ionotropic P2X ATP receptors. *Neuroscience.* **83**(1), 177-190.
Lee, C. J., Mannaioni, G., Yuan, H., Woo, D. H., Gingrich, M. B. and Traynelis, S. F. (2007). Astrocytic control of synaptic NMDA receptors. *J Physiol.* **581**(Pt 3), 1057-1081.
Lee, H. K., Kameyama, K., Huganir, R. L. and Bear, M. F. (1998). NMDA induces long-term synaptic depression and dephosphorylation of the GluR1 subunit of AMPA receptors in hippocampus. *Neuron.* **21**(5), 1151-1162.
Lerner, D. J., Chen, M., Tram, T. and Coughlin, S. R. (1996). Agonist recognition by proteinase-activated receptor 2 and thrombin receptor. Importance of extracellular loop interactions for receptor function. *J Biol Chem.* **271**(24), 13943-13947.
Lester, R. A., Clements, J. D., Westbrook, G. L. and Jahr, C. E. (1990). Channel kinetics determine the time course of NMDA receptor-mediated synaptic currents. *Nature.* **346**(6284), 565-567.
Li, D., Herault, K., Silm, K., Evrard, A., Wojcik, S., Oheim, M., Herzog, E. and Ropert, N. (2013). Lack of evidence for vesicular glutamate transporter expression in mouse astrocytes. *J Neurosci.* **33**(10), 4434-4455.
Li, D., Ropert, N., Koulakoff, A., Giaume, C. and Oheim, M. (2008). Lysosomes are the major vesicular compartment undergoing Ca2+-regulated exocytosis from cortical astrocytes. *J Neurosci.* **28**(30), 7648-7658.
Lin, Q. S., Yang, Q., Liu, D. D., Sun, Z., Dang, H., Liang, J., Wang, Y. X., Chen, J. and Li, S. T. (2011). Hippocampal endocannabinoids play an important role in induction of long-term potentiation and regulation of contextual fear memory formation. *Brain Res Bull.* **86**(3-4), 139-145.
Lisman, J., Malenka, R. C., Nicoll, R. A. and Malinow, R. (1997). Learning mechanisms: the case for CaM-KII. *Science.* **276**(5321), 2001-2002.
Liu, L., Wong, T. P., Pozza, M. F., Lingenhoehl, K., Wang, Y., Sheng, M., Auberson, Y. P. and Wang, Y. T. (2004). Role of NMDA receptor subtypes in governing the direction of hippocampal synaptic plasticity. *Science.* **304**(5673), 1021-1024.
Liu, T., Sun, L., Xiong, Y., Shang, S., Guo, N., Teng, S., Wang, Y., Liu, B., Wang, C., Wang, L., Zheng, L., Zhang, C. X., Han, W. and Zhou, Z. (2011). Calcium triggers exocytosis from two types of organelles in a single astrocyte. *J Neurosci.* **31**(29), 10593-10601.

Liu, X. B., Murray, K. D. and Jones, E. G. (2004). Switching of NMDA receptor 2A and 2B subunits at thalamic and cortical synapses during early postnatal development. *J Neurosci.* **24**(40), 8885-8895.
Lu, J., Helton, T. D., Blanpied, T. A., Racz, B., Newpher, T. M., Weinberg, R. J. and Ehlers, M. D. (2007). Postsynaptic positioning of endocytic zones and AMPA receptor cycling by physical coupling of dynamin-3 to Homer. *Neuron.* **55**(6), 874-889.
Macrides, F., Eichenbaum, H. B. and Forbes, W. B. (1982). Temporal relationship between sniffing and the limbic theta rhythm during odor discrimination reversal learning. *J Neurosci.* **2**(12), 1705-1717.
Maggio, N., Shavit, E., Chapman, J. and Segal, M. (2008). Thrombin induces long-term potentiation of reactivity to afferent stimulation and facilitates epileptic seizures in rat hippocampal slices: toward understanding the functional consequences of cerebrovascular insults. *J Neurosci.* **28**(3), 732-736.
Maienschein, V., Marxen, M., Volknandt, W. and Zimmermann, H. (1999). A plethora of presynaptic proteins associated with ATP-storing organelles in cultured astrocytes. *Glia.* **26**(3), 233-244.
Malenka, R. C. and Bear, M. F. (2004). LTP and LTD: an embarrassment of riches. *Neuron.* **44**(1), 5-21.
Malenka, R. C., Kauer, J. A., Perkel, D. J., Mauk, M. D., Kelly, P. T., Nicoll, R. A. and Waxham, M. N. (1989). An essential role for postsynaptic calmodulin and protein kinase activity in long-term potentiation. *Nature.* **340**(6234), 554-557.
Martin, S. J., Grimwood, P. D. and Morris, R. G. (2000). Synaptic plasticity and memory: an evaluation of the hypothesis. *Annu Rev Neurosci.* **23**, 649-711.
Martineau, M., Shi, T., Puyal, J., Knolhoff, A. M., Dulong, J., Gasnier, B., Klingauf, J., Sweedler, J. V., Jahn, R. and Mothet, J. P. (2013). Storage and uptake of D-serine into astrocytic synaptic-like vesicles specify gliotransmission. *J Neurosci.* **33**(8), 3413-3423.
Matsuda, L. A., Lolait, S. J., Brownstein, M. J., Young, A. C. and Bonner, T. I. (1990). Structure of a cannabinoid receptor and functional expression of the cloned cDNA. *Nature.* **346**(6284), 561-564.
Mayer, M. L. (2006). Glutamate receptors at atomic resolution. *Nature.* **440**(7083), 456-462.
Mayer, M. L. and Armstrong, N. (2004). Structure and function of glutamate receptor ion channels. *Annu Rev Physiol.* **66**, 161-181.
Mayer, M. L., Westbrook, G. L. and Guthrie, P. B. (1984). Voltage-dependent block by Mg2+ of NMDA responses in spinal cord neurones. *Nature.* **309**(5965), 261-263.
Min, R. and Nevian, T. (2012). Astrocyte signaling controls spike timing-dependent depression at neocortical synapses. *Nat Neurosci.* **15**(5), 746-753.
Misner, D. L. and Sullivan, J. M. (1999). Mechanism of cannabinoid effects on long-term potentiation and depression in hippocampal CA1 neurons. *J Neurosci.* **19**(16), 6795-6805.
Miya, K., Inoue, R., Takata, Y., Abe, M., Natsume, R., Sakimura, K., Hongou, K., Miyawaki, T. and Mori, H. (2008). Serine racemase is

predominantly localized in neurons in mouse brain. *J Comp Neurol.* **510**(6), 641-654.
Monyer, H., Burnashev, N., Laurie, D. J., Sakmann, B. and Seeburg, P. H. (1994). Developmental and regional expression in the rat brain and functional properties of four NMDA receptors. *Neuron.* **12**(3), 529-540.
Mothet, J. P., Pollegioni, L., Ouanounou, G., Martineau, M., Fossier, P. and Baux, G. (2005). Glutamate receptor activation triggers a calcium-dependent and SNARE protein-dependent release of the gliotransmitter D-serine. *Proc Natl Acad Sci U S A.* **102**(15), 5606-5611.
Navarrete, M. and Araque, A. (2008). Endocannabinoids mediate neuron-astrocyte communication. *Neuron.* **57**(6), 883-893.
Navarrete, M. and Araque, A. (2010). Endocannabinoids potentiate synaptic transmission through stimulation of astrocytes. *Neuron.* **68**(1), 113-126.
Nedergaard, M. and Verkhratsky, A. (2012). Artifact versus reality--how astrocytes contribute to synaptic events. *Glia.* **60**(7), 1013-1023.
Nett, W. J., Oloff, S. H. and McCarthy, K. D. (2002). Hippocampal astrocytes in situ exhibit calcium oscillations that occur independent of neuronal activity. *J Neurophysiol.* **87**(1), 528-537.
Neu, A., Foldy, C. and Soltesz, I. (2007). Postsynaptic origin of CB1-dependent tonic inhibition of GABA release at cholecystokinin-positive basket cell to pyramidal cell synapses in the CA1 region of the rat hippocampus. *J Physiol.* **578**(Pt 1), 233-247.
Nolte, C., Matyash, M., Pivneva, T., Schipke, C. G., Ohlemeyer, C., Hanisch, U. K., Kirchhoff, F. and Kettenmann, H. (2001). GFAP promoter-controlled EGFP-expressing transgenic mice: a tool to visualize astrocytes and astrogliosis in living brain tissue. *Glia.* **33**(1), 72-86.
North, R. A. (2002). Molecular physiology of P2X receptors. *Physiol Rev.* **82**(4), 1013-1067.
Nowicky, A. V., Teyler, T. J. and Vardaris, R. M. (1987). The modulation of long-term potentiation by delta-9-tetrahydrocannabinol in the rat hippocampus, in vitro. *Brain Res Bull.* **19**(6), 663-672.
Oh, M. C. and Derkach, V. A. (2005). Dominant role of the GluR2 subunit in regulation of AMPA receptors by CaMKII. *Nat Neurosci.* **8**(7), 853-854.
Olah, M. E. and Stiles, G. L. (1995). Adenosine receptor subtypes: characterization and therapeutic regulation. *Annu Rev Pharmacol Toxicol.* **35**, 581-606.
Overstreet, L. S., Jones, M. V. and Westbrook, G. L. (2000). Slow desensitization regulates the availability of synaptic GABA(A) receptors. *J Neurosci.* **20**(21), 7914-7921.
Oya, M., Kitaguchi, T., Yanagihara, Y., Numano, R., Kakeyama, M., Ikematsu, K. and Tsuboi, T. (2013). Vesicular nucleotide transporter is involved in ATP storage of secretory lysosomes in astrocytes. *Biochem Biophys Res Commun.* **438**(1), 145-151.
Palygin, O., Lalo, U. and Pankratov, Y. (2011). Distinct pharmacological and functional properties of NMDA receptors in mouse cortical astrocytes. *Br J Pharmacol.* **163**(8), 1755-1766.

Palygin, O., Lalo, U., Verkhratsky, A. and Pankratov, Y. (2010). Ionotropic NMDA and P2X1/5 receptors mediate synaptically induced Ca2+ signalling in cortical astrocytes. *Cell Calcium.* **48**(4), 225-231.
Panatier, A., Theodosis, D. T., Mothet, J. P., Touquet, B., Pollegioni, L., Poulain, D. A. and Oliet, S. H. (2006). Glia-derived D-serine controls NMDA receptor activity and synaptic memory. *Cell.* **125**(4), 775-784.
Panatier, A., Vallee, J., Haber, M., Murai, K. K., Lacaille, J. C. and Robitaille, R. (2011). Astrocytes are endogenous regulators of basal transmission at central synapses. *Cell.* **146**(5), 785-798.
Pangrsic, T., Potokar, M., Stenovec, M., Kreft, M., Fabbretti, E., Nistri, A., Pryazhnikov, E., Khiroug, L., Giniatullin, R. and Zorec, R. (2007). Exocytotic release of ATP from cultured astrocytes. *J Biol Chem.* **282**(39), 28749-28758.
Pankratov, Y., Lalo, U., Castro, E., Miras-Portugal, M. T. and Krishtal, O. (1999). ATP receptor-mediated component of the excitatory synaptic transmission in the hippocampus. *Prog Brain Res.* **120**, 237-249.
Pankratov, Y., Lalo, U., Krishtal, O. and Verkhratsky, A. (2002). Ionotropic P2X purinoreceptors mediate synaptic transmission in rat pyramidal neurones of layer II/III of somato-sensory cortex. *J Physiol.* **542**(Pt 2), 529-536.
Pankratov, Y., Lalo, U., Krishtal, O. and Verkhratsky, A. (2003). P2X receptor-mediated excitatory synaptic currents in somatosensory cortex. *Mol Cell Neurosci.* **24**(3), 842-849.
Pankratov, Y., Lalo, U., Krishtal, O. A. and Verkhratsky, A. (2009). P2X receptors and synaptic plasticity. *Neuroscience.* **158**(1), 137-148.
Pankratov, Y., Lalo, U., Verkhratsky, A. and North, R. A. (2006). Vesicular release of ATP at central synapses. *Pflugers Arch.* **452**(5), 589-597.
Pankratov, Y., Lalo, U., Verkhratsky, A. and North, R. A. (2007). Quantal release of ATP in mouse cortex. *J Gen Physiol.* **129**(3), 257-265.
Pankratov, Y. V. and Krishtal, O. A. (2003). Distinct quantal features of AMPA and NMDA synaptic currents in hippocampal neurons: implication of glutamate spillover and receptor saturation. *Biophys J.* **85**(5), 3375-3387.
Pankratov, Y. V., Lalo, U. V. and Krishtal, O. A. (2002). Role for P2X receptors in long-term potentiation. *J Neurosci.* **22**(19), 8363-8369.
Papouin, T., Ladepeche, L., Ruel, J., Sacchi, S., Labasque, M., Hanini, M., Groc, L., Pollegioni, L., Mothet, J. P. and Oliet, S. H. (2012). Synaptic and extrasynaptic NMDA receptors are gated by different endogenous coagonists. *Cell.* **150**(3), 633-646.
Parpura, V., Basarsky, T. A., Liu, F., Jeftinija, K., Jeftinija, S. and Haydon, P. G. (1994). Glutamate-mediated astrocyte-neuron signalling. *Nature.* **369**(6483), 744-747.
Parpura, V., Fang, Y., Basarsky, T., Jahn, R. and Haydon, P. G. (1995). Expression of synaptobrevin II, cellubrevin and syntaxin but not SNAP-25 in cultured astrocytes. *FEBS Lett.* **377**(3), 489-492.
Pascual, O., Casper, K. B., Kubera, C., Zhang, J., Revilla-Sanchez, R., Sul, J. Y., Takano, H., Moss, S. J., McCarthy, K. and Haydon, P. G. (2005). Astrocytic purinergic signaling coordinates synaptic networks. *Science.* **310**(5745), 113-116.

Pavlides, C., Greenstein, Y. J., Grudman, M. and Winson, J. (1988). Long-term potentiation in the dentate gyrus is induced preferentially on the positive phase of theta-rhythm. *Brain Res.* **439**(1-2), 383-387.
Pertwee, R. G., Howlett, A. C., Abood, M. E., Alexander, S. P., Di Marzo, V., Elphick, M. R., Greasley, P. J., Hansen, H. S., Kunos, G., Mackie, K., Mechoulam, R. and Ross, R. A. (2010). International Union of Basic and Clinical Pharmacology. LXXIX. Cannabinoid receptors and their ligands: beyond CB(1) and CB(2). *Pharmacol Rev.* **62**(4), 588-631.
Petralia, R. S. (2012). Distribution of extrasynaptic NMDA receptors on neurons. *ScientificWorldJournal.* **2012**, 267120.
Petralia, R. S., Wang, Y. X., Hua, F., Yi, Z., Zhou, A., Ge, L., Stephenson, F. A. and Wenthold, R. J. (2010). Organization of NMDA receptors at extrasynaptic locations. *Neuroscience.* **167**(1), 68-87.
Phillis, J. W., Song, D. and O'Regan, M. H. (1997). Inhibition by anion channel blockers of ischemia-evoked release of excitotoxic and other amino acids from rat cerebral cortex. *Brain Res.* **758**(1-2), 9-16.
Pin, J. P., Galvez, T. and Prezeau, L. (2003). Evolution, structure, and activation mechanism of family 3/C G-protein-coupled receptors. *Pharmacol Ther.* **98**(3), 325-354.
Pitler, T. A. and Alger, B. E. (1992). Postsynaptic spike firing reduces synaptic GABAA responses in hippocampal pyramidal cells. *J Neurosci.* **12**(10), 4122-4132.
Proctor, W. R. and Dunwiddie, T. V. (1987). Pre- and postsynaptic actions of adenosine in the in vitro rat hippocampus. *Brain Res.* **426**(1), 187-190.
Rasooli-Nejad, S., Palygin, O., Lalo, U. and Pankratov, Y. (2014). Cannabinoid receptors contribute to astroglial Ca(2)(+)-signalling and control of synaptic plasticity in the neocortex. *Philosophical transactions of the Royal Society of London. Series B, Biological sciences.* **369**(1654), 20140077.
Redman, S. (1990). Quantal analysis of synaptic potentials in neurons of the central nervous system. *Physiol Rev.* **70**(1), 165-198.
Roche, K. W., O'Brien, R. J., Mammen, A. L., Bernhardt, J. and Huganir, R. L. (1996). Characterization of multiple phosphorylation sites on the AMPA receptor GluR1 subunit. *Neuron.* **16**(6), 1179-1188.
Romano, C., Sesma, M. A., McDonald, C. T., O'Malley, K., Van den Pol, A. N. and Olney, J. W. (1995). Distribution of metabotropic glutamate receptor mGluR5 immunoreactivity in rat brain. *J Comp Neurol.* **355**(3), 455-469.
Rosenberg, D., Artoul, S., Segal, A. C., Kolodney, G., Radzishevsky, I., Dikopoltsev, E., Foltyn, V. N., Inoue, R., Mori, H., Billard, J. M. and Wolosker, H. (2013). Neuronal D-serine and glycine release via the Asc-1 transporter regulates NMDA receptor-dependent synaptic activity. *J Neurosci.* **33**(8), 3533-3544.
Rosenberg, D., Kartvelishvily, E., Shleper, M., Klinker, C. M., Bowser, M. T. and Wolosker, H. (2010). Neuronal release of D-serine: a physiological pathway controlling extracellular D-serine concentration. *Faseb J.* **24**(8), 2951-2961.
Rubio, M. E. and Soto, F. (2001). Distinct Localization of P2X receptors at excitatory postsynaptic specializations. *J Neurosci.* **21**(2), 641-653.

Rusakov, D. A. and Kullmann, D. M. (1998). Extrasynaptic glutamate diffusion in the hippocampus: ultrastructural constraints, uptake, and receptor activation. *J Neurosci.* **18**(9), 3158-3170.
Sakimura, K., Kutsuwada, T., Ito, I., Manabe, T., Takayama, C., Kushiya, E., Yagi, T., Aizawa, S., Inoue, Y., Sugiyama, H. and et al. (1995). Reduced hippocampal LTP and spatial learning in mice lacking NMDA receptor epsilon 1 subunit. *Nature.* **373**(6510), 151-155.
Sans, N., Petralia, R. S., Wang, Y. X., Blahos, J., 2nd, Hell, J. W. and Wenthold, R. J. (2000). A developmental change in NMDA receptor-associated proteins at hippocampal synapses. *J Neurosci.* **20**(3), 1260-1271.
Schell, M. J., Brady, R. O., Jr., Molliver, M. E. and Snyder, S. H. (1997). D-serine as a neuromodulator: regional and developmental localizations in rat brain glia resemble NMDA receptors. *J Neurosci.* **17**(5), 1604-1615.
Schlicker, E. and Kathmann, M. (2001). Modulation of transmitter release via presynaptic cannabinoid receptors. *Trends Pharmacol Sci.* **22**(11), 565-572.
Schmitt, L. I., Sims, R. E., Dale, N. and Haydon, P. G. (2012). Wakefulness affects synaptic and network activity by increasing extracellular astrocyte-derived adenosine. *J Neurosci.* **32**(13), 4417-4425.
Seri, B., Garcia-Verdugo, J. M., McEwen, B. S. and Alvarez-Buylla, A. (2001). Astrocytes give rise to new neurons in the adult mammalian hippocampus. *J Neurosci.* **21**(18), 7153-7160.
Shavit, E., Michaelson, D. M. and Chapman, J. (2011). Anatomical localization of protease-activated receptor-1 and protease-mediated neuroglial crosstalk on peri-synaptic astrocytic endfeet. *J Neurochem.* **119**(3), 460-473.
Shigetomi, E., Bowser, D. N., Sofroniew, M. V. and Khakh, B. S. (2008). Two forms of astrocyte calcium excitability have distinct effects on NMDA receptor-mediated slow inward currents in pyramidal neurons. *J Neurosci.* **28**(26), 6659-6663.
Shigetomi, E., Tong, X., Kwan, K. Y., Corey, D. P. and Khakh, B. S. (2012). TRPA1 channels regulate astrocyte resting calcium and inhibitory synapse efficacy through GAT-3. *Nat Neurosci.* **15**(1), 70-80.
Sieghart, W. and Sperk, G. (2002). Subunit composition, distribution and function of GABA(A) receptor subtypes. *Curr Top Med Chem.* **2**(8), 795-816.
Sigel, E. and Steinmann, M. E. (2012). Structure, function, and modulation of GABA(A) receptors. *J Biol Chem.* **287**(48), 40224-40231.
Silva, A. J., Stevens, C. F., Tonegawa, S. and Wang, Y. (1992). Deficient hippocampal long-term potentiation in alpha-calcium-calmodulin kinase II mutant mice. *Science.* **257**(5067), 201-206.
Sim, J. A., Chaumont, S., Jo, J., Ulmann, L., Young, M. T., Cho, K., Buell, G., North, R. A. and Rassendren, F. (2006). Altered hippocampal synaptic potentiation in P2X4 knock-out mice. *J Neurosci.* **26**(35), 9006-9009.
Slanina, K. A., Roberto, M. and Schweitzer, P. (2005). Endocannabinoids restrict hippocampal long-term potentiation via CB1. *Neuropharmacology.* **49**(5), 660-668.
Stell, B. M., Brickley, S. G., Tang, C. Y., Farrant, M. and Mody, I. (2003). Neuroactive steroids reduce neuronal excitability by selectively enhancing

tonic inhibition mediated by delta subunit-containing GABAA receptors. *Proc Natl Acad Sci U S A.* **100**(24), 14439-14444.
Stella, N., Schweitzer, P. and Piomelli, D. (1997). A second endogenous cannabinoid that modulates long-term potentiation. *Nature.* **388**(6644), 773-778.
Stern-Bach, Y., Bettler, B., Hartley, M., Sheppard, P. O., O'Hara, P. J. and Heinemann, S. F. (1994). Agonist selectivity of glutamate receptors is specified by two domains structurally related to bacterial amino acid-binding proteins. *Neuron.* **13**(6), 1345-1357.
Stout, C. E., Costantin, J. L., Naus, C. C. and Charles, A. C. (2002). Intercellular calcium signaling in astrocytes via ATP release through connexin hemichannels. *J Biol Chem.* **277**(12), 10482-10488.
Strack, S. and Colbran, R. J. (1998). Autophosphorylation-dependent targeting of calcium/ calmodulin-dependent protein kinase II by the NR2B subunit of the N-methyl- D-aspartate receptor. *J Biol Chem.* **273**(33), 20689-20692.
Stricker, C. and Redman, S. (1994). Statistical models of synaptic transmission evaluated using the expectation-maximization algorithm. *Biophys J.* **67**(2), 656-670.
Striggow, F., Riek-Burchardt, M., Kiesel, A., Schmidt, W., Henrich-Noack, P., Breder, J., Krug, M., Reymann, K. G. and Reiser, G. (2001). Four different types of protease-activated receptors are widely expressed in the brain and are up-regulated in hippocampus by severe ischemia. *Eur J Neurosci.* **14**(4), 595-608.
Suadicani, S. O., Brosnan, C. F. and Scemes, E. (2006). P2X7 receptors mediate ATP release and amplification of astrocytic intercellular Ca2+ signaling. *J Neurosci.* **26**(5), 1378-1385.
Sugiura, T., Kondo, S., Sukagawa, A., Nakane, S., Shinoda, A., Itoh, K., Yamashita, A. and Waku, K. (1995). 2-Arachidonoylglycerol: a possible endogenous cannabinoid receptor ligand in brain. *Biochem Biophys Res Commun.* **215**(1), 89-97.
Sun, W., McConnell, E., Pare, J. F., Xu, Q., Chen, M., Peng, W., Lovatt, D., Han, X., Smith, Y. and Nedergaard, M. (2013). Glutamate-dependent neuroglial calcium signaling differs between young and adult brain. *Science.* **339**(6116), 197-200.
Terranova, J. P., Michaud, J. C., Le Fur, G. and Soubrie, P. (1995). Inhibition of long-term potentiation in rat hippocampal slices by anandamide and WIN55212-2: reversal by SR141716 A, a selective antagonist of CB1 cannabinoid receptors. *Naunyn Schmiedebergs Arch Pharmacol.* **352**(5), 576-579.
Tian, G. F., Azmi, H., Takano, T., Xu, Q., Peng, W., Lin, J., Oberheim, N., Lou, N., Wang, X., Zielke, H. R., Kang, J. and Nedergaard, M. (2005). An astrocytic basis of epilepsy. *Nat Med.* **11**(9), 973-981.
Tovar, K. R. and Westbrook, G. L. (1999). The incorporation of NMDA receptors with a distinct subunit composition at nascent hippocampal synapses in vitro. *J Neurosci.* **19**(10), 4180-4188.
Tsai, G. and Coyle, J. T. (2002). Glutamatergic mechanisms in schizophrenia. *Annu Rev Pharmacol Toxicol.* **42**, 165-179.

Tuominen, H. J., Tiihonen, J. and Wahlbeck, K. (2005). Glutamatergic drugs for schizophrenia: a systematic review and meta-analysis. *Schizophr Res.* **72**(2-3), 225-234.
Ushkaryov, Y. A., Petrenko, A. G., Geppert, M. and Sudhof, T. C. (1992). Neurexins: synaptic cell surface proteins related to the alpha-latrotoxin receptor and laminin. *Science.* **257**(5066), 50-56.
Valtschanoff, J. G., Burette, A., Wenthold, R. J. and Weinberg, R. J. (1999). Expression of NR2 receptor subunit in rat somatic sensory cortex: synaptic distribution and colocalization with NR1 and PSD-95. *J Comp Neurol.* **410**(4), 599-611.
Van Horn, M. R., Sild, M. and Ruthazer, E. S. (2013). D-serine as a gliotransmitter and its roles in brain development and disease. *Front Cell Neurosci.* **7**, 39.
Varma, N., Carlson, G. C., Ledent, C. and Alger, B. E. (2001). Metabotropic glutamate receptors drive the endocannabinoid system in hippocampus. *J Neurosci.* **21**(24), RC188.
Verkhratsky, A. and Kirchhoff, F. (2007). Glutamate-mediated neuronal-glial transmission. *J Anat.* **210**(6), 651-660.
Volterra, A. and Meldolesi, J. (2005). Astrocytes, from brain glue to communication elements: the revolution continues. *Nat Rev Neurosci.* **6**(8), 626-640.
Vorobjev, V. S. (1991). Vibrodissociation of sliced mammalian nervous tissue. *J Neurosci Methods.* **38**(2-3), 145-150.
Wall, M. J. and Dale, N. (2013). Neuronal transporter and astrocytic ATP exocytosis underlie activity-dependent adenosine release in the hippocampus. *J Physiol.* **591**(Pt 16), 3853-3871.
Wallraff, A., Odermatt, B., Willecke, K. and Steinhauser, C. (2004). Distinct types of astroglial cells in the hippocampus differ in gap junction coupling. *Glia.* **48**(1), 36-43.
Walz, W. (2000). Role of astrocytes in the clearance of excess extracellular potassium. *Neurochem Int.* **36**(4-5), 291-300.
Wang, D., Cui, Z., Zeng, Q., Kuang, H., Wang, L. P., Tsien, J. Z. and Cao, X. (2009). Genetic enhancement of memory and long-term potentiation but not CA1 long-term depression in NR2B transgenic rats. *PLoS One.* **4**(10), e7486.
Wang, H. and Reiser, G. (2003). Thrombin signaling in the brain: the role of protease-activated receptors. *Biol Chem.* **384**(2), 193-202.
Watanabe, J., Beck, C., Kuner, T., Premkumar, L. S. and Wollmuth, L. P. (2002). DRPEER: a motif in the extracellular vestibule conferring high Ca2+ flux rates in NMDA receptor channels. *J Neurosci.* **22**(23), 10209-10216.
Wei, W., Zhang, N., Peng, Z., Houser, C. R. and Mody, I. (2003). Perisynaptic localization of delta subunit-containing GABA(A) receptors and their activation by GABA spillover in the mouse dentate gyrus. *J Neurosci.* **23**(33), 10650-10661.
Wilhelm, A., Volknandt, W., Langer, D., Nolte, C., Kettenmann, H. and Zimmermann, H. (2004). Localization of SNARE proteins and secretory organelle proteins in astrocytes in vitro and in situ. *Neurosci Res.* **48**(3), 249-257.
Wolosker, H. (2011). Serine racemase and the serine shuttle between neurons and astrocytes. *Biochim Biophys Acta.* **1814**(11), 1558-1566.

Woo, D. H., Han, K. S., Shim, J. W., Yoon, B. E., Kim, E., Bae, J. Y., Oh, S. J., Hwang, E. M., Marmorstein, A. D., Bae, Y. C., Park, J. Y. and Lee, C. J. (2012). TREK-1 and Best1 channels mediate fast and slow glutamate release in astrocytes upon GPCR activation. *Cell.* **151**(1), 25-40.
Xiang, Z., Bo, X., Oglesby, I., Ford, A. and Burnstock, G. (1998). Localization of ATP-gated P2X2 receptor immunoreactivity in the rat hypothalamus. *Brain Res.* **813**(2), 390-397.
Yamada, J., Furukawa, T., Ueno, S., Yamamoto, S. and Fukuda, A. (2007). Molecular basis for the GABAA receptor-mediated tonic inhibition in rat somatosensory cortex. *Cereb Cortex.* **17**(8), 1782-1787.
Yao, Y. and Mayer, M. L. (2006). Characterization of a soluble ligand binding domain of the NMDA receptor regulatory subunit NR3A. *J Neurosci.* **26**(17), 4559-4566.
Ye, Z. C., Wyeth, M. S., Baltan-Tekkok, S. and Ransom, B. R. (2003). Functional hemichannels in astrocytes: a novel mechanism of glutamate release. *J Neurosci.* **23**(9), 3588-3596.
Yuzaki, M. and Mikoshiba, K. (1992). Pharmacological and immunocytochemical characterization of metabotropic glutamate receptors in cultured Purkinje cells. *J Neurosci.* **12**(11), 4253-4263.
Zhang, Q., Fukuda, M., Van Bockstaele, E., Pascual, O. and Haydon, P. G. (2004). Synaptotagmin IV regulates glial glutamate release. *Proc Natl Acad Sci U S A.* **101**(25), 9441-9446.
Zhang, Q., Pangrsic, T., Kreft, M., Krzan, M., Li, N., Sul, J. Y., Halassa, M., Van Bockstaele, E., Zorec, R. and Haydon, P. G. (2004). Fusion-related release of glutamate from astrocytes. *J Biol Chem.* **279**(13), 12724-12733.
Zhao, M. G., Toyoda, H., Lee, Y. S., Wu, L. J., Ko, S. W., Zhang, X. H., Jia, Y., Shum, F., Xu, H., Li, B. M., Kaang, B. K. and Zhuo, M. (2005). Roles of NMDA NR2B subtype receptor in prefrontal long-term potentiation and contextual fear memory. *Neuron.* **47**(6), 859-872.
Zhou, Y., Takahashi, E., Li, W., Halt, A., Wiltgen, B., Ehninger, D., Li, G. D., Hell, J. W., Kennedy, M. B. and Silva, A. J. (2007). Interactions between the NR2B receptor and CaMKII modulate synaptic plasticity and spatial learning. *J Neurosci.* **27**(50), 13843-13853.
Zimmermann, H. and Braun, N. (1999). Ecto-nucleotidases--molecular structures, catalytic properties, and functional roles in the nervous system. *Prog Brain Res.* **120**, 371-385.